Resurgence in Deformed Integrable Models

Lucas Schepers

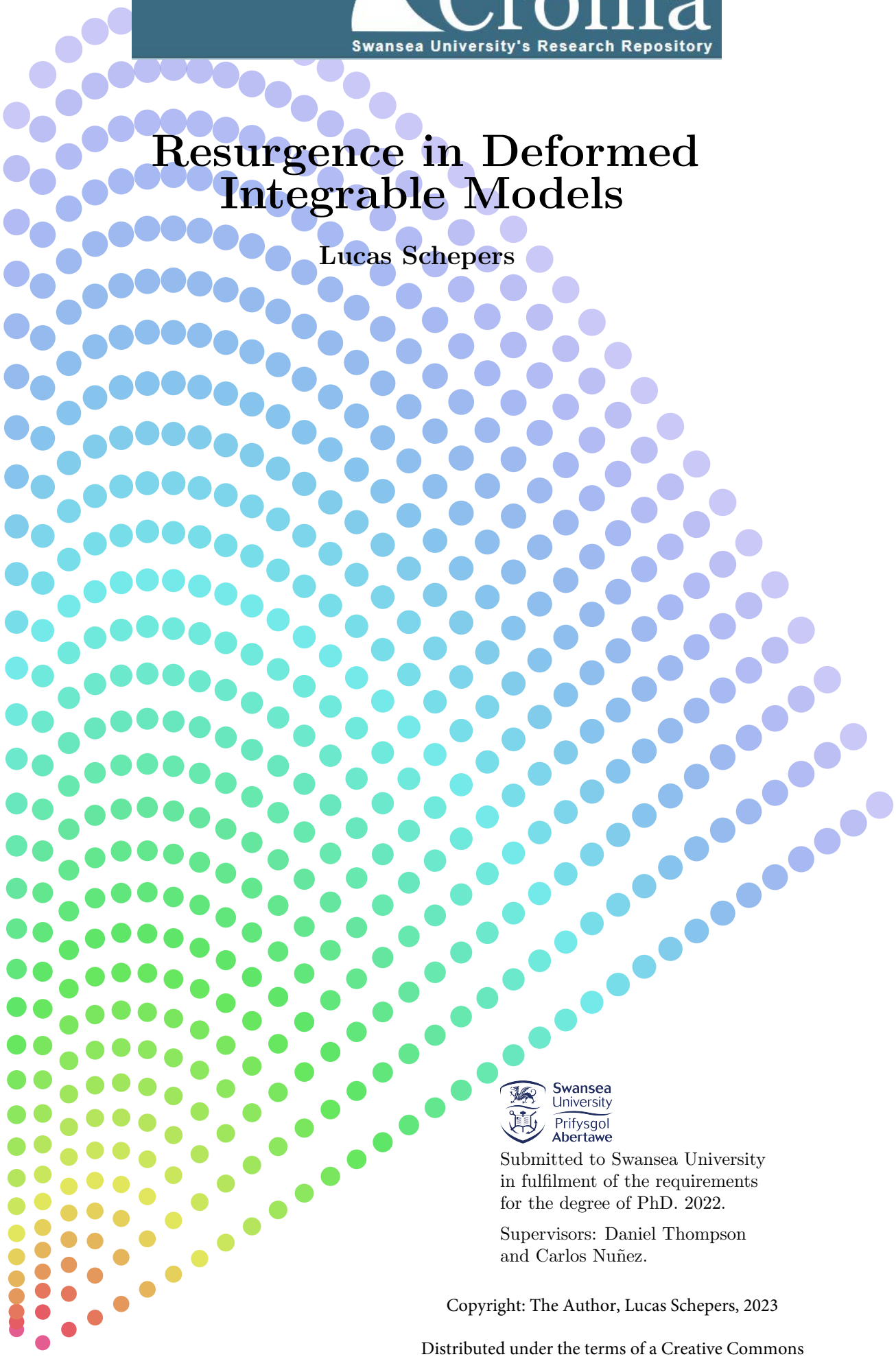

Swansea University
Prifysgol Abertawe

Submitted to Swansea University in fulfilment of the requirements for the degree of PhD. 2022.

Supervisors: Daniel Thompson and Carlos Nuñez.

To much perseverance

Abstract

Resurgence has been shown to be a powerful and even necessary technique to understand many physical system. The study of perturbative methods in general quantum field theories is hard, but progress is often possible in reduced settings, such as integrable models. In this thesis, we study resurgent effects in integrable deformations of two-dimensional σ-models in two settings.

First, we study the integrable bi-Yang-Baxter deformation of the $SU(2)$ principal chiral model (PCM) and find finite action uniton and complex uniton solutions. Under an adiabatic compactification on an S^1, we obtain a quantum mechanical system with an elliptic Lamé-like potential. We perform a perturbative calculation of the ground state energy of this quantum mechanical system to large orders obtaining an asymptotic series. Using the Borel-Padé technique, we determine that the locations of branch cuts in the Borel plane match the values of the uniton and complex uniton actions. Therefore, we can match the non-perturbative contributions to the energy with the uniton solutions which fractionate upon adiabatic compactification. An off-shoot of the WKB analysis, is to identify the quadratic differential of this deformed PCM with that of an $\mathcal{N} = 2$ Seiberg-Witten theory. This can be done either as an $N_f = 4$ $SU(2)$ theory or as an elliptic $SU(2) \times SU(2)$ quiver theory. The mass parameters of the gauge theory are given in terms of the bi-Yang-Baxter deformation parameters.

Second, we perform a perturbative expansion of the thermodynamic Bethe ansatz (TBA) equations of the $SU(N)$ λ-model with WZW level k in the presence of a chemical potential. This is done with its exact S-matrix and the recently developed techniques [1, 2] using a Wiener-Hopf decomposition, which involve a careful matching of bulk and edge ansätze. We determine the asymptotic expansion of this series and compute its renormalon ambiguities in the Borel plane. The analysis is supplemented by a parallel solution of the TBA equations that results in a transseries. The transseries comes with an ambiguity that is shown to precisely match the Borel ambiguity. It is shown that the leading IR renormalon vanishes when k is a divisor of N.

Contents

Foreword

The task of computing exactly the values of observables in an interacting theory is typically, and certainly in the absence of simplifications provided by supersymmetry or integrability, a difficult problem. Perturbation theory may be the only viable recourse to this and indeed can be capable of making predictions of astonishing accuracy [3, 4]. However, a fundamental limitation of such approaches is that the resulting perturbative series will often have a radius of convergence of zero. Commonly, we consider some coupling constant $z = g^2$, and perform perturbation theory around $z \approx 0$ for some observable $\mathcal{O}$:

$$\mathcal{O}(z) = \sum_{n=0}^{\infty} a_n z^n \,, \tag{1}$$

where a_n will go like $n! A^{-n}$ with $A > 0$ for a very general class of systems. In quantum field theories, the origin of this can sometimes be anticipated from the factorial growth of the number of Feynman diagrams with the order of perturbation theory. This was first argued by Dyson [5], see also [6–8]. However, not only the number of Feynman diagrams can cause divergences. Sometimes, a particular sequence of diagrams can be identified that is responsible for a divergence. Such divergences are called renormalons [9, 10]. If divergence of asymptotic series is such a common phenomenon, the question arises what meaning – if any – should be ascribed to formal asymptotic perturbative expansions?

Starting with pioneering work of Dingle, Bogomolny and Zinn-Justin [11–13], it has become clear that actually far from being meaningless, a great deal of information is actually deeply encoded in the asymptotic expansion. For instance, a growth $a_n = n!(A)^{-n}$ indicates that the theory contains a non-perturbative object (instanton, renormalon, uniton etc) that enters with an action $S_{\text{instanton}} = \frac{A}{2}$. In this scenario, the use of Borel resummation of the perturbative series leads to ambiguities if $A > 0$. Crucially however, this ambiguity can be precisely cancelled by the inclusion of a leading order contribution arising from the non-perturbative saddle.

Now sub-leading, in $\frac{1}{n}$, contributions to a_n encode information about fluctuations around this non-perturbative saddle. With sufficient dedication one could then establish, from the perturbative saddle alone, that the perturbation series around the non-perturbative saddle will itself typically be asymptotic with a growth indicative of further non-perturbative sectors. Ambiguities in resummation here will be cancelled by a higher

non-perturbative sector. These ideas are further explored for an audience not familiar with high-energy physics in the Section "Resurgence for Laymen". It is explained with more mathematical depth in Chapter 1.

The cancellations behave in a very specific way. The perturbative sector saddle [0] is void of any instantons, but receives contributions from instanton-anti-instanton events $[\mathcal{I}\bar{\mathcal{I}}]$ and their higher order cousins $[\mathcal{I}^n\bar{\mathcal{I}}^n]$. The single instanton $[\mathcal{I}]$ is to interact with the members of its conjugacy class $\{[\mathcal{I}^{n+1}\bar{\mathcal{I}}^n]\}$. This information is also often captured using the "resurgence triangle" [14, 15]. Two instanton configurations that cancel each other's ambiguities are said to be in the same sector and are hence put in the same of column of the resurgence triangle.

This leads to the idea of resurgence; that deeply encoded in the perturbative expansion lies all the non-perturbative information. Physical observables appropriately combine contributions from the perturbative sector and relevant non-perturbative sectors into a *transseries* in such a fashion that all ambiguities are cancelled. The relative weighting of the contributions to the transseries can undergo discrete jumps as z is varied - this is the Stokes jump phenomenon.

In the context of quantum mechanics, the interrelation between Borel resummation and the Stokes phenomenon are crucial in the understanding of the WKB approximation. The study of asymptotic series in this context commenced with the seminal work of Bender and Wu [16] and was further expanded on by Voros [17] and Silverstone [18]. On a higher level, Stokes jumps of 'Voros symbols' are encoded by the Delabaere-Dillinger-Pham [19] formula. This information can be visualised by understanding the mutations of Stokes graphs [20–23] (detailed in Sections 1.2.3 and 3.3.4). Algebraically, we can capture this information using a Stokes automorphism.

However, modern physics has attempted to stretch the application of these techniques to wider settings in QFTs. The celebrated work by Gaiotto, Moore and Neitzke [24, 25], connects the very same information to the wall-crossing phenomena in $\mathcal{N} = 2$ four-dimensional gauge theories. The ideas of resurgence have by now been applied beyond quantum mechanics, to include string theory, gauge theory, Kondo Problems, hydrodynamics and matrix models [14, 26–41]. This sampling of works inevitably does not do justice to the large body of work on this topic and we recommend the reader to consult the review articles of [42–45] both for their pedagogical presentation and wider bibliography.

It is the aim of this thesis to bring more models into the fold of resurgent analysis. The setting of general QFT still proves to be a very hard one, and many of the papers cited above employ some sort of reduction to a simpler system where more traction can be gained. One area where a particularly high level of understanding has been achieved is that of 2d integrable models, which shall be the theatre of this thesis. This field of study is properly introduced in Chapter 2.

In Chapter 3, we consider a two parameter deformation of such an integrable model, the bi-Yang-Baxter model, which is discussed at more length in Section 2.2. A technique was developed by [46, 47] in which the 2d model is adiabatically reduced to a 1d quantum

mechanics through a twisted boundary condition. We show that the 2d model exhibits some finite action classical solutions called *(complex) unitons*. It is shown how a WKB analysis of the 1d QM recovers the finite action of these unitons. This makes it tempting to think of unitons as the 2d analogue of the 1d instantons. Moreover, we show how the potential can be related to $\mathcal{N} = 2$ Seiberg-Witten curves.

In Chapter 4 we take a different approach. We continue the work of [1, 2, 48, 49] (see also the recent papers [50–59]) and study the thermodynamic Bethe ansatz (TBA) equations of the integrable models which depend on the exact S-matrix. We study the scattering of a particular particle in the presence of a chemical potential. Our model of choice here is the λ-deformed model which is discussed in Section 2.3. This model is particularly interesting as it is asymptotically a conformal field theory (CFT) and such models were not previously investigated in this context. In this model we obtain a perturbative series through careful comparison of an 'edge' and a 'bulk' regime. We derive an asymptotic expansion of this series and find its ambiguities. A separate, but related solution to the same problem was developed using Wiener-Hopf decomposition techniques [49]. This alternative solution gives a transseries with a built-in ambiguity. We perform this computation in the case of the λ-model and show that the two ambiguities match. This mirrors the well-known ambiguity cancellation [12, 13] in a 2d setting.

Acknowledgements

In the first place, my gratitude extends to Dan, who gave me not only the chance to embark on this project, but without whose mentor-ship, guidance and encouragement this thesis would have fallen flat on many more occasions.

Secondly, I would like to thank S. Prem Kumar, Saskia Demulder and Giacomo Piccinini for useful conversations on this and related topics, as well as my other collaborators Leonardo Santilli, Carlos Nuñez, Andrea Legramandi and Mohammad Akhond. I am supported by The Royal Society through grant RGF\R1 \180087 Generalised Dualities, Resurgence and Integrability.

In addition, I wish to thank my other friends in the UK. I thank Mohammad for being an animated speaker and Karol for being a supportive listener. Freya for being a dreamer and Laura for bringing just the right amount of crazy into my life. Lewis for indulging my curiosity of mathematical and philosophical puzzles, Andrea for being both my oldest and my youngest friend, Ricardo for his laugh. And many more, Ali, Astrid, David, Dawid, Giacomo, John, Luke, Neil, Marika, Kostas, Robin, Ryan, Sergio, Shaun, Stefano, Will and Zsolt all receive thanks for making Swansea a colourful, lively and friendly place. Glenn and Carla have set an early example of how to be a successful and healthy PhD student.

An old adage dictates that those who have been friends for longer than seven years never part ways. Although Johann, Kerrewin and Marnix have joined this club only as of late, I am confident that our stimulating friendship will not violate this wisdom. Jonas, Matt and Thomas: thank you for teaching me how friendship can be dynamic, yet taken for granted so easily, that it appears static. The final words of gratitude go towards my parents whose enduring and unconditional support predates this project by many years. Without them, I would not have been so lucky to be on this path.

Lastly, this thesis would have been much more miserable without the reinvigorating divinity of the late Beethoven string quartets as performed by the Brodsky Quartet, as well as the energising venom of the Shostakovich string quartets brilliantly brought to life by the Fitzwilliam Quartet. Honourable mentions go towards the Glazunov string quartes, the piano works by Scriabin, the string quartets by Hindemith, string music by Bartók and frankly all chamber music by Brahms, Debussy, Dvořák, Franck, Mendelssohn, Ravel, Saint-Saëns, Schubert, Sibelius, Smetana and Poulenc.

The picture on the front is an adaptation of Figure 4.1.

Declaration of Authorship

I declare that:

1. This work has not previously been accepted in substance for any degree and is not being concurrently submitted in candidature for any degree.

2. This thesis is the result of my own investigations, except where otherwise stated. Other sources are acknowledged by footnotes giving explicit references. A bibliography is appended. In particular, the thesis is based on the following publications:

   > Lucas Schepers and Daniel C. Thompson. 'Resurgence in the bi-Yang-Baxter model'. *Nucl. Phys. B* 964 (2021), p. 115308. DOI: 10.1016/j.nuclphysb.2021.115308. arXiv: 2007.03683 [hep-th]
   >
   > Lucas Schepers and Daniel C. Thompson. 'Asymptotics in an Asymptotic CFT' (Jan. 2023). arXiv: 2301.11803 [hep-th]

   These papers have been incorporated in Chapters 3 and 4 of these thesis, respectively. In addition, the Foreword and Section 2.2 are based on the first paper.

3. I hereby give consent for my thesis, if accepted, to be available for photocopying and for inter-library loan, and for the title and summary to be made available to outside organisations.

4. The University's ethical procedures have been followed and, where appropriate, that ethical approval has been granted.

Signed: Lucas Schepers
Date: 30 September 2022

Resurgence for Laymen

This Section is written for a wider, non-scientific audience to give a small teaser of what this thesis is about. I will assume the reader is familiar with basic calculus (differentation and integration of basic functions and basic algebraic manipulations), but no specific technical knowledge is required.

First, I will introduce what perturbation theory is, followed by a discussion of perturbation theory in a physics context. I will then explain how perturbation theory in a double well potential causes problems, before finishing off with a discussion of how resurgence can alleviate the problem.

Perturbation Theory

Suppose you have an equation you know how to solve. For example,

$$x^2 - 1 = 0\,. \tag{2}$$

This has the solutions $x_1 = 1$ and $x_2 = -1$, but we shall focus on the positive solution here. Now, let's suppose we have an equation that looks a lot like it, but has an extra term, for example

$$x^2 + ax - 1 = 0\,. \tag{3}$$

If you remember how to solve quadratic equation, then this still an equation we can solve exactly. However, let's for a moment forget about the quadratic formula. Instead, we will assume that a is a very small number, like $\frac{1}{100}$. In that case, the Equation (3) looks a lot like Equation (2).

The basic idea of perturbation theory is to exploit this similarity. We know that if $a = 0$, then $x = 1$ is a solution to Equation (3). As such, we might expect that if a is a very small number, that $x = 1$ is *almost* a solution to (3). Let's try to be a bit more systematic and propose

$$x_1 = 1 + Xa\,. \tag{4}$$

This is a guess of what the solution might look like, but we do not know yet what the number X is going to be.[1] We just know that if a is small, that x_1 is very close to 1.

[1] Such an educated guess is in physics also called an *ansatz*, which is German for a beginning, or an attempt.

Let us substitute our guess (4) into (3):

$$\begin{aligned} x^2 + ax - 1 &= (1 + Xa)^2 + a(1 + Xa) - 1 \\ &= 1 + 2Xa + X^2a^2 + a + Xa^2 - 1 \\ &= a(2X + 1) + a^2(X^2 + X) \\ &\approx (2X + 1)a\,. \end{aligned} \tag{5}$$

In the calculation I have sorted the expression powers of a. I have done this because if a is a very small number, then a^2 is an even smaller. In the last line, I have thus done something strange: I have removed the a^2 term because it is smaller than the a term and therefore not as important. If we now wish to solve $x^2 + ax - 1 = 0$, we should set $2X + 1 = 0$, which is satisfied by $X = -\frac{1}{2}$. This gives us an approximate solution to Equation (3):

$$x_1 \approx 1 - \frac{1}{2}a\,. \tag{6}$$

Let us now check how good our guess is. If you remember how to solve quadratic Equations, like (3), you would find that

$$x_1 = -\frac{a}{2} + \sqrt{1 + \frac{a^2}{4}}, \qquad x_2 = -\frac{a}{2} - \sqrt{1 + \frac{a^2}{4}}\,. \tag{7}$$

We will then use the special formula

$$\begin{aligned} \sqrt{1 + y} &= 1 + \frac{1}{2}y - \frac{1}{8}y^2 + \frac{1}{16}y^3 + \ldots \\ &\approx 1 + \frac{1}{2}y\,, \end{aligned} \tag{8}$$

for the case $y = \frac{a^2}{4}$. If we apply this to our exact solution (7), we get that

$$x_1 = 1 - \frac{a}{2} + \frac{a^2}{8} \approx 1 - \frac{a}{2}\,, \tag{9}$$

which is exactly what we found in Equation (6)!

But what if I had wanted to make a better approximation? Well, we could have gone back to Equation (4), and instead make a slightly more sophisticated guess $x_1 = 1 + Xa + Ya^2$. Because a^2 is smaller than a, we call this term with Y *sub-leading*. Because a^2 is so much smaller, it does not contribute as much to the solution as the term with X. However, we could still substitute it back into the solution (3). If we would then look at the term proportional to a^2, and set it to 0, we would find that $Y = \frac{1}{8}$, as was predicted by Equation (9)!

To summarise, the basic approach of perturbation theory is

1. Start with a difficult equation that has a term in it which is very small.

2. Solve the difficult equation when the small term is completely gone. This should hopefully be easier.

3. Make a guess for the full solution as the sum of the solution of the previous step, and a small correction.

4. Put the guess back into the difficult equation and find out precisely what the small correction is.

5. Write down the approximate solution with the small correction.

The formula used in Equation (8) is a special case of a technique called the Taylor series. We start with a function $f(x)$ that is sufficiently nice[2]. Its n^{th} derivative I will denote as $f^{(n)}(x) \equiv \left(\frac{d}{dx}\right)^n f(x)$. If we want to calculate the function close to zero, that is $x \approx 0$, we have the formula

$$f(x) = f(0) + f'(0)x + \frac{1}{2!}f''(0)x^2 + \frac{1}{3!}f^{(3)}(0)x^3 + \ldots + \frac{1}{n!}f^{(n)}(0)x^n + \ldots\,, \tag{10}$$

The formula (8) is the case $f(y) = \sqrt{1+y}$ for the Taylor series (10). It turns out, that when we do perturbation theory to many orders, so we consider terms $a, a^2, a^3, \ldots$, the solution we find is precisely the Taylor series of the *exact* solution. The power of perturbation theory is that we can use the technique in a lot of cases where the main equation is too difficult. That is why we first consider it in the case where some part is very small. However, if we consider more and more corrections, we will get closer and closer to the real answer: the exact solution to the difficult problem.

Divergences

Unfortunately, this is not where the story of perturbation theory ends. It turns out that for many problems in physics, making increasingly precise approximations causes certain problems. A reason for this is that often we have to solve differential equations rather than algebraic equations such as (2). A differential equation is an equation for a function rather than for a number. Typically, the equation involves one or more derivatives of the function that is being solved for. An example is $\frac{d}{dx}y(x) = y(x)$ which has solution $y(x) = Ae^x$, for any constant A.

Suppose we are calculating the solution of some differential equation using perturbation theory, like we did with Equation (6), and the successive terms go like this:

$$x = 1 + a + 2a^2 + 6a^3 + 24a^4 + 120a^5 + \ldots + n!a^n + \ldots\,. \tag{11}$$

Let us look at the quantity $b_n = n!a^n$ and how it grows as n becomes bigger, as it does when we make more precise approximations. To do this, we compare consecutive terms:

$$\frac{b_{n+1}}{b_n} = \frac{(n+1)!a^{n+1}}{n!a^n} = an\,. \tag{12}$$

[2] 'sufficiently nice' is what mathematicians say when they do not want to engage with details of precise conditions.

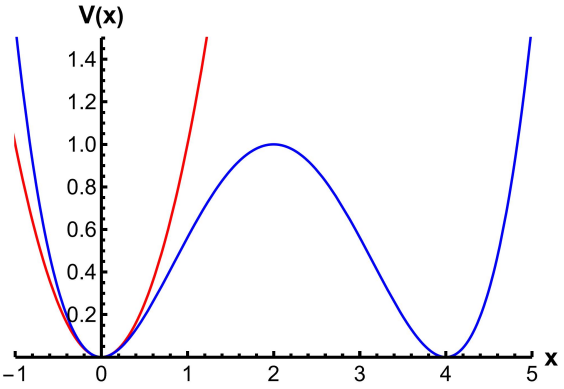

Figure 1: The harmonic oscillator potential $V(x) = x^2$ is drawn is red, and the double well potential $V(x) = x^2(1 - x/4)^2$ is drawn is blue. We see that the two potentials share a minimum at $x = 0$, but the double well has a second minimum at $x = 4$.

We are assuming a is a small number, so for any fixed value of n, the quantity an is also small. However, in principle we could make a lot of better approximations and then n could be arbitrarily big. This would mean that b_{n+1} is a lot larger than b_n. However, if we want a better approximation to x, we had better hoped that b_n is very small for large n so that the extra approximations do not change the result. If the extra terms b_n at large n are sufficiently small, we would obtain a *convergent* sequence for x. However, we have just argued that the sum (11) becomes large, therefore it is not convergent: it is *divergent*.

An example where this problem occurs is when we study the ground state energy of a quantum mechanical particle in a double well potential. This is described by the Schrödinger equation, which is a differential equation. The ground state energy is simply the scenario in which the particle has the least amount of energy possible. The double well potential has been drawn in Figure 1, and shows two possible minima for the particle. The ground state of a particle, where it has little energy, is determined such that the particle is trapped in one of the two minima. A particle trapped in a potential with just one minima (also drawn in Figure 1), also called the *harmonic oscillator*, is easily solved. This is the base case of step 2 of the plan for perturbation theory outlined above. We can then do the perturbation theory by considering the double well potential as a small change compared to the single well potential.

However, the method is only partially successful because we obtain a divergent sequence similar to the one outlined above. The theory of resurgence has been developed to remedy this problem. We will not go into mathematical detail here, but instead refer to Chapter 1. However, we can give a sketch of where the solution lies. A classical particle with low energy would be trapped in the well, as it would not have enough energy to overcome the barrier separating the two minima. However, a quantum mechanical particle is not bound to these rules as strictly as it can exhibit *quantum tunnelling*. This means that its wave function extends into regions where it is classically forbidden because it does not have enough energy. As such, a quantum mechanical particle feels

the existence of the second minimum more strongly. Even more, it can suddenly appear in the other minimum. If a particle behaves like this, it is called an *instanton*.

It turns out that such instanton effect manifest in the system by virtue of an $e^{-1/x}$-function. This function is particularly nasty as it does not have a well-defined Taylor series (10). Because our perturbation theory was meant to calculate the Taylor series, it makes perfect sense that it would not be sensitive to $e^{-1/x}$-like instanton effects! The central claim of *resurgence* is that these instanton-like effects, which are conventionally not picked up by perturbation theory, are still hiding somewhere in the series (11). The price we have to pay, however, is that we can only find these instanton-like effect by computing many terms (at least twenty or thirty, but ideally hundreds) of the perturbation theory, which is difficult. However, using these instanton effects, we can also remedy the apparent divergence of the perturbative series.

Chapter 1

Introduction to Resurgence

This first Chapter shall serve to survey the landscape of resurgence and, secondly, will be introducing some techniques to analyse asymptotic series. We will be expanding on the qualitative introduction of resurgence in the foreword and fill in the mathematical details. Reflecting the more mathematical nature of this Section, we shall sometimes be using the theorem-lemma-proof style of writing.

In Section 1.1, we will start with reviewing the techniques of Borel transforms and Borel re-summations which are at the centre of resurgent analysis. Section 1.2 is devoted to the more physical setting of WKB approximations. This will show us a more geometric picture of the problem with Stokes lines and saddle points. Section 1.3 expands on the WKB approach by considering a particular type of WKB problem, the *uniform WKB* which is well-studied [15]. In Section 1.4, we discuss a particular example, the Airy equation, at length. In Section 1.5, we consider another physical example, the Sine-Gordon equation, and demonstrate on a practical level the techniques discussed before.

1.1 Borel Techniques

As a starter let us recall some basic techniques developed first over a 100 hundred years ago by Emile Borel [62]. The material is quite well-known, but, at the same time, it is crucial for the remainder of the thesis. In fact, the exact examples discussed in this Section shall prove relevant in real physical systems, such as those in Sections 4.2.5 and 3.3.3.

1.1.1 Borel Transformations

Let us set some conventions and write $\tilde{\phi}(z)$ for an asymptotic expansion around $z = \infty$:

$$\tilde{\phi}(z) = \sum_{n=0}^{\infty} a_n z^{-n-1}. \tag{1.1}$$

I will generally assume that a_n grows factorially. This means $\tilde{\phi}(z)$ is generically not convergent and for the moment we shall think of it as a formal power series. The goal of the resurgence programme is in fact to extract from this data a meaningful well-defined function. The Borel transformations of $\tilde{\phi}(z)$ is defined as an expansion around $\zeta = 0$:

$$\hat{\phi}(\zeta) = \mathcal{B}(\tilde{\phi}(z)) = \sum_{n=0}^{\infty} \frac{a_n}{n!} \zeta^n \,, \tag{1.2}$$

with the same coefficients a_n.

Example 1. Consider the following asymptotic expansion for $a \in \mathbb{R}$

$$\tilde{\phi}(z) = \sum_{n=0}^{\infty} \frac{\Gamma(n+a)}{\Gamma(a) A^n} z^{-n-1} = \sum_{n=0}^{\infty} \frac{a_{(n)}}{A^n} z^{-n-1}, \tag{1.3}$$

where $a_{(n)}$ is the Pochhammer symbol. The Borel transformation is given by

$$\hat{\phi}(\zeta) = \mathcal{B}(\tilde{\phi}(z)) = \frac{1}{(1-\zeta/A)^a}, \tag{1.4}$$

which can be confirmed by Taylor expanding $\hat{\phi}(\zeta)$. We thus see that removing the factorial growth of the asymptotic expansion has created a holomorphic function around the origin. However, it does exhibit a singularity at $\zeta = A$. If a is an integer we are simply dealing with a pole. If a is not an integer, there is a branch cut singularity.

In this section, I will try to consistently denote asymptotic expansions as $\tilde{\phi}(z)$ and their Borel transformation as $\hat{\phi}(\zeta)$. Firstly, we observe that the Borel transformation is a linear operator on formal power series. Often we will need to understand how an operation on a function $\tilde{\phi}(z)$ will translate to an operation on its Borel transform $\hat{\phi}(\zeta)$, or the other way around. A good summary of this is found in Table 1 of Dorigoni [42]. The most important example is discussed in the following proposition:

Proposition 2. Taking the product of two functions $\tilde{\phi}_1(z)$, $\tilde{\phi}_2(z)$ corresponds to taking the convolution of the Borel transforations. That is, if $\tilde{\phi}_3(z) = \tilde{\phi}_1(z)\tilde{\phi}_2(z)$, then

$$\hat{\phi}_3(\zeta) = (\hat{\phi}_1 * \hat{\phi}_2)(\zeta) = \int_0^{\zeta} dw \; \hat{\phi}_1(w)\hat{\phi}_2(\zeta - w). \tag{1.5}$$

Proof. Let the asymptotic expansions be given by

$$\begin{aligned} \tilde{\phi}_1(z) &= \sum_{n=0}^{\infty} a_n z^{-n-1}, \\ \tilde{\phi}_2(z) &= \sum_{n=0}^{\infty} b_n z^{-n-1}. \end{aligned} \tag{1.6}$$

It follows that

$$\tilde{\phi_1}(z)\tilde{\phi_2}(z) = \sum_{n=0}^{\infty} c_n z^{-n-1}, \qquad c_n = \sum_{\substack{p+q=n-1 \\ p,q\geq 0}} a_q b_p. \tag{1.7}$$

For the convolution we see that

$$\begin{aligned}
(\hat{\phi_1} * \hat{\phi_2})(z) &= \sum_{n,m\geq 0}^{\infty} \frac{a_n b_m}{n!m!} \int_0^{\zeta} d\omega\, \omega^n (\omega - \zeta)^m \\
&= \sum_{n,m\geq 0}^{\infty} \frac{a_n b_m}{n!m!} B(n+1, m+1)\zeta^{n+m+1} \\
&= \sum_{n,m\geq 0}^{\infty} \frac{a_n b_m}{(n+m)!} \zeta^{n+m+1} \\
&= \sum_{n=0}^{\infty} \frac{c_n}{n!}\zeta^n,
\end{aligned} \tag{1.8}$$

Here, the coefficients c_n are given precisely by Equation (1.7), and we have used the integral form of the Euler-Beta function [1] $B(n,m) = \frac{\Gamma(n)\Gamma(m)}{\Gamma(n+m)}$. We can thus conclude that indeed

$$\mathcal{B}(\tilde{\phi_1}\tilde{\phi_2}) = \hat{\phi_1} * \hat{\phi_2} \tag{1.10}$$

■

Among Borel transforms $\hat{\phi}(\zeta)$, the convolution product $*$ given by Equation (1.5) plays an analogous role to the multiplication product among expansion $\tilde{\phi}(z)$. Therefore, $\tilde{\phi}(z)$ is sometimes refereed to as living in the *multiplicative model*, and $\hat{\phi}(\zeta)$ as living in the *convolutive model*. The precise algebraic structure of these models is further discussed in [42, 45, 63].

1.1.2 Borel Resummations

Given an asymptotic expansion $\tilde{\phi}(z)$ and its Borel transform $\hat{\phi}(\zeta) = \mathcal{B}(\tilde{\phi}(z))$, I will define the Borel resummation as[2]

$$S_\theta \tilde{\phi}(z) = \int_0^{e^{i\theta}\infty} \hat{\phi}(\zeta) e^{-\zeta z} d\zeta\,. \tag{1.11}$$

The significance of the Borel resummation is demonstrated in the next Example.

Remark 3. Let us closely study what happens for $S_0\tilde{\phi}(z)$ when we consider the expan-

[1] The Euler-Beta function can be given as an integral representation by

$$B(x,y) = z^{-x-y-1} \int_0^z dw\, w^{y-1}(z-w)^{x-1}. \tag{1.9}$$

[2] Essentially, if $\theta = 0$, the Borel resummation is the Laplace transform of its Borel transformation.

sions (1.1) and (1.2) for $z \to \infty$:

$$\begin{aligned} S_0\tilde{\phi}(z) &= \int_0^\infty d\zeta\ \hat{\phi}(\zeta) e^{-\zeta z} \\ &= \sum_{n=0}^\infty \int_0^\infty d\zeta\ \frac{a_n}{n!}\zeta^n e^{-\zeta z} \qquad \text{choose } s = \zeta z \\ &= \sum_{n=0}^\infty \frac{a_n}{n!} z^{-n-1} \int_0^\infty ds\ s^n e^{-s} \\ &= \sum_{n=0}^\infty \frac{a_n}{n!} z^{-n-1}\Gamma(n+1) \\ &= \tilde{\phi}(z)\,. \end{aligned} \tag{1.12}$$

In other words, we retrieve the original expansion. However, although the original expansion may be divergent, the Borel transform need not be, and its holomorphicity in certain regions may tell us something about the analytic structure of $\tilde{\phi}(z)$.

The Borel resummations are well defined under the assumption that $\hat{\phi}(\zeta)$ is well defined along the integration contour. This is the original motivation for introducing a non-zero θ in Equation (1.11) as it allows to probe further into the complex plane of the expansion parameter. If $\hat{\phi}(\zeta)$ has a singularity or a branch cut in the direction θ, it may be advantageous to define lateral Borel resummation, that is, we shall integrate just above and just below the singular direction:

$$S_{\theta^\pm} := S_{\theta \pm \epsilon}\,, \tag{1.13}$$

where we take ϵ to be small. Of particular interest is the contour $S_{\theta^+} - S_{\theta^-}$ that lets us study the discontinuity around the simple pole or branch cut. The next two examples will form the core archetypes that will return in Chapters 3 and 4.

Example 4. Let us re-visit Example 1 and compute the discontinuity $S_{\theta^+} - S_{\theta^-}$. First, we will write the Borel transform as $\hat{\phi} = \exp[-\log(1-\zeta/A)a]$. Observe that there is no ambiguity,

$$\hat{\phi}(\zeta + i\epsilon) - \hat{\phi}(\zeta - i\epsilon) = 0\,,$$

if $\zeta < A$. In the case $\zeta > A$, we use the fact that for a positive real number x, the logarithm has a discontinuity given by $\log(-x \pm i\epsilon) = \log(x) \pm i\pi$ which leads to

$$\hat{\phi}(\zeta + i\epsilon) - \hat{\phi}(\zeta - i\epsilon) = 2i(\zeta/A - 1)^{-a}\sin(a\pi)\,, \quad \zeta > A\,. \tag{1.14}$$

This discontinuity vanishes for integer a because there is no branch cut in this case.

Calculating the Borel resummation of this yields

$$\begin{aligned}(S_+ - S_-)\tilde{\phi}(z) &= \int_0^\infty \Big[\hat{\phi}(\zeta + i\epsilon) - \hat{\phi}(\zeta - i\epsilon)\Big] e^{-z\zeta} \\ &= \int_A^\infty 2i(\zeta/A - 1)^{-a} \sin(a\pi) d\zeta \\ &= 2iA^a \sin(a\pi) e^{-Az} \int_0^\infty e^{-xz} x^{-a} dx \\ &= \frac{2\pi i}{\Gamma(a)} A^a z^{-1+a} e^{-Az}\,, \qquad a \notin \mathbb{Z}\,.\end{aligned} \tag{1.15}$$

In the case that $a = 1$, we find that $\hat{\phi}(\zeta)$ has a simple pole. In this case we can evaluate the later Borel resummation by selecting the residue. This leads to

$$(S_+ - S_-)\tilde{\phi}(z) = 2\pi i A e^{-Az}\,, \tag{1.16}$$

which is incidentally the $a = 1$ case of Equation (1.15).

Example 5. Let us briefly discuss the case of a cut in the Borel plane on the negative real axis. We start with a perturbative series for $A > 0$

$$\tilde{\phi}(z) = \sum_{n=0}^\infty \frac{\Gamma(n+a)}{\Gamma(a)(-A)^n} z^{-n-1}\,, \tag{1.17}$$

which has a Borel transform

$$\hat{\phi}(\zeta) = \mathcal{B}(\tilde{\phi}(z)) = \sum_{n=0}^\infty \frac{\Gamma(n+a)}{\Gamma(a)\Gamma(n+1)(-A)^n} \zeta^n = (1 + \zeta/A)^{-a}\,, \tag{1.18}$$

that has a cut along $\zeta \in (-\infty, -A)$. The Borel discontinuity across this cut is given by

$$\hat{\phi}(\zeta - i\epsilon) - \hat{\phi}(\zeta + i\epsilon) = 2i(-\zeta/A - 1)^{-a} \sin(a\pi)\,, \quad \zeta < -A\,. \tag{1.19}$$

The borel re-summation of the contour of interest is thus given by

$$\begin{aligned}(S_{\pi+\epsilon} - S_{\pi-\epsilon})\tilde{\phi}(z) &= \int_0^{-\infty} \Big[\hat{\phi}(\zeta - i\epsilon) - \hat{\phi}(\zeta + i\epsilon)\Big] e^{-\zeta/z} d\zeta \\ &= \frac{2\pi i A^a}{\Gamma(a)} (-z)^{-1+a} e^{Az}\,.\end{aligned} \tag{1.20}$$

Remark 6. More generally, one may consider series that grow more wildly. A series is called a q-Gevrey series if it grows like

$$\tilde{\phi}(z) \sim \sum_{k=0}^\infty (k!)^q z^{-k} \tag{1.21}$$

In that case we define a sum in the q-Borel plane by

$$\hat{\phi}(s)_q \sim \sum_{k=0}^{\infty} s^k. \tag{1.22}$$

The Borel resummation is obtained by applying q inverse Laplace transforms. The case $q = 1$ retrieves the original Borel plane which has been explored above. However, it is good to note that higher Gevrey-degree series may appear in physics. A paper by Cavalcanti [64] explores a set of diagrams obtained by concatenating cat eye diagrams in a massless scalar $\lambda\phi^4/4!$-theory that give a $(n!)^3$ renormalon contribution. By introducing the k-Borel transform, constructed by dividing out $(n!)^k$, we can say that the 3-Borel transform has singularities, or that the expansion has singularities in the 3-Borel plane.

Remark 7. Suppose we have an asymptotic expansion $\tilde{\phi}(z)$, its Borel transformation $\hat{\phi}(\zeta)$ which is singular in the direction θ and we want to evaluate $(S_{\theta+} - S_{\theta-})\tilde{\phi}(z)$. However, let us assume we do not have a closed form for $\hat{\phi}(\zeta)$, either because the expansion is not one that is known, or because it is difficult to compute the coefficients a_n. This means that $\hat{\phi}(\zeta)$ is a polynomial, hence holomorphic which means that the closed loop integral $(S_{\theta+} - S_{\theta-})\tilde{\phi}(z)$ is trivial. To combat this situation, it may be advantageous to artificially introduce poles and approximate $\hat{\phi}(\zeta) = \sum_{k=0}^{n} \frac{a_k}{k!}\zeta^k$ by a rational function

$$\mathrm{PD}_n\hat{\phi}(\zeta) := \frac{\sum_{k=0}^{n/2} p_k\zeta^k}{\sum_{k=0}^{n/2} q_k\zeta^k}\,, \tag{1.23}$$

called the *Padé Approximant*[3]. We fix $q_0 = 1$ while the other coefficients q_k, p_k are fixed by requiring that in the Taylor series approximation[4]

$$\mathrm{PD}_n\hat{\phi}(\zeta) - \hat{\phi}(\zeta) = \mathcal{O}(\zeta^{n+1})\,. \tag{1.24}$$

1.1.3 Stokes Automorphism

When the borel transformation has singularities along a direction θ, we expect jumps as we cross this line. These effects may be conveniently captured by the lateral Borel transformations (1.13). I will repackage this in terms of the Stokes automorphism $\mathfrak{S}_\theta$, which is defined by the following equation:

$$S_{\theta+} = S_{\theta-} \circ (\mathfrak{S}_\theta). \tag{1.25}$$

[3]Really what I have presented is the *diagonal* Padé Approximant, which is where the orders of the polynomials in the denominator and the numerator are equal. In general, one may use a set-up in which these are not the same.

[4]One particularly pleasing behaviour of the Padé-approximant is that applying it to the Taylor approximation of a rational polynomial, returns the original rational polynomial. Concretely, if

$$r(x) = \frac{\sum_{k=0}^{n/2} p_k\zeta^k}{\sum_{k=0}^{n/2} q_k\zeta^k}$$

is a rational polynomial and $\tilde{r}(x) = \sum_{k=0}^{n} b_k x^k$ is its Taylor series at n^{th}-order, then $\mathrm{PD}_n\tilde{r}(x) = r(x)$.

I will define the discontinuity as $\mathrm{Disc}_\theta = \mathrm{Id} - \mathfrak{S}_\theta$. In other words,

$$S_{\theta^+} - S_{\theta^-} = -S_{\theta^-} \circ \mathrm{Disc}_\theta. \tag{1.26}$$

However, with abuse of language, we will often refer to $S_{\theta^+} - S_{\theta^-}$ as the discontinuity. A more thorough first principles approach to the Stokes automorphism can be carried out using Alien calculus which Appendix 1.A is devoted to. However, in this thesis we shall be more concerned with physical origins of Stokes automorphism as they appear for example in WKB approximations.

1.2 WKB Analysis

We will now shift gears and turn to the question of how to obtain perturbative series in quantum mechanics. The main tool for this is WKB analysis, which we will discuss below. The key take-away is that when we study the resurgent structure of a WKB problem, we can interpret the Stokes automorphism in a geometrical sense as a topological change of the paths of steepest ascent. This translates the algebraic and analytic problem of the previously discussion into a more geometric picture.

Similar to analyses as presented in [23] Section 2 and [43] Appendix B, I will here discuss the connection between WKB analysis in ordinary quantum mechanics and stokes phenomena. Ordinary WKB approximation is an approximation in the $\hbar \to 0$, meaning quantum fluctuations are small. In the exact WKB method we shall also consider non-perturbative contributions in $\hbar$.

1.2.1 WKB Ansatz

Consider the time-independent Schrödinger equation for a wavefunction $\Psi(q)$ in a potential[5] $V(q)$ with a mass $m = 1$.

$$E\Psi(q) = \left(\frac{-\hbar^2}{2}\frac{\partial^2}{\partial q^2} + V(q)\right)\Psi(q). \tag{1.27}$$

Let $p(q) = \sqrt{2(E - V(q))}$ be the semiclassical momentum, hence the turning points are now the zeroes of $p(q)$. We may now write the Schrödinger Equation (1.27) as

$$\hbar^2 \frac{\partial^2}{\partial q^2}\Psi(q) + p^2(q)\Psi(q) = 0. \tag{1.28}$$

[5] In this section, I will try to make all dependencies on $\hbar$ explicit. I should thus warn that in general one may consider the case where the potential $V(q)$ also depends on $\hbar$. In this case one can consider a general potential of the form $\mathbb{V}(q,\hbar) = \sum_{n=1}^{\infty} \hbar^n V_n(q)$. Such is done by Iwaki and Nakanishi [23], but because we want to study the system to leading order in $\hbar$, I will not make the generalisation here. A particular example with such a quantum deformed potential is studied by [65]

Proposition 8. The ansatz

$$\Psi(q) = \exp\left(\frac{i}{\hbar}\int_{q_0}^{q} dz\, S(z,\hbar)\right) \tag{1.29}$$

will solve Equation (1.28) if the function $S(z,\hbar)$ satisfies the Ricatti Equation[6]

$$S^2(z,\hbar) - i\hbar S'(z,\hbar) = p^2(z). \tag{1.30}$$

Proof. First compute derivatives of the wave function (1.29):

$$\Psi'(q) = \frac{i}{\hbar}S(q,\hbar)\Psi(q), \tag{1.31}$$

$$\Psi''(q) = \frac{i}{\hbar}S'(q,\hbar)\Psi(q) + \left(\frac{i}{\hbar}S(q,\hbar)\right)^2\Psi(q). \tag{1.32}$$

Therefore, assuming Equation (1.30),

$$\hbar^2\frac{\partial^2}{\partial q^2}\Psi(q) + p^2(q)\Psi(q) = \left[\hbar^2\left(\frac{i}{\hbar}S'(q,\hbar) - \frac{1}{\hbar^2}S^2(q,\hbar)\right) + p^2(q)\right]\Psi(q) = 0. \tag{1.33}$$

■

We shall think of $S(q,\hbar)$ as a power series in $\hbar$:

$$S(z,\hbar) = \sum_{k=0}^{\infty}\hbar^k S_k(z). \tag{1.34}$$

The terms $S_k(z)$ are fixed by the requirement that $S(z,\hbar)$ solves Equation (1.30) order by order in $\hbar$, leading to the following recursion relation [43]:

$$\begin{aligned} S_0(q) &= \pm p(q). \\ S_n(q) &= \frac{1}{2S_0}\left(iS'_{n-1}(q) - \sum_{k=1}^{n-1}S_k(q)S_{n-k}(q)\right). \end{aligned} \tag{1.35}$$

Definition 9. Define the solutions $S^+(q)$ and $S^-(q)$ of Equation (1.30) as those that behave as $S^\pm(q) = \pm p(q) + \mathcal{O}(\hbar)$ to leading order in $\hbar$. Define the odd and the even part as

$$\begin{aligned} S_{\text{even}}(q,\hbar) &= \frac{1}{2}\left(S^+(q,\hbar) - S^-(q,\hbar)\right) \\ S_{\text{odd}}(q,\hbar) &= \frac{1}{2}\left(S^+(q,\hbar) + S^-(q,\hbar)\right) \end{aligned} \tag{1.36}$$

[6] Here the prime on the function $S(q,\hbar)$ denote a derivative with respect to the first variable z (or later q).

Proposition 10. $S_{\text{even}}(z,\hbar)$ and $S_{\text{odd}}(z,\hbar)$ are related by

$$S_{\text{odd}}(z,\hbar) = \frac{i\hbar}{2}\frac{\partial}{\partial z}\log S_{\text{even}}(z,\hbar). \tag{1.37}$$

Proof. Firstly, we see that $S^{\pm}(z,\hbar) = S_{\text{odd}}(z,\hbar) \pm S_{\text{even}}(z,\hbar)$. Plugging $S^{\pm}(z,\hbar)$ into Equation (1.30), yields two equations. Taking their difference and re-writing gives

$$S_{\text{odd}}(z,\hbar) = \frac{i\hbar}{2S_{\text{even}}(z,\hbar)}\frac{\partial}{\partial z}S_{\text{even}}(z,\hbar)\,, \tag{1.38}$$

which is equivalent to Equation (1.37). ■

Proposition 11. S_{even} only contains even powers of $\hbar$ and S_{odd} only contains odd powers of $\hbar$.

Proof. First, we need to prove that $S_n^+ = (-1)^{n+1}S_n^-$. This can be done easily by using the principle of strong induction and the recursion relation (1.35). It follows that $S_{\text{even},n} = \frac{1}{2}(S_n^+ - S_n^-)$ and $S_{\text{odd},n} = \frac{1}{2}(S_n^+ + S_n^-)$ vanish for n odd and n even, respectively. ■

The two solutions $S^{\pm}(z,\hbar)$ give rise to two solutions $\Psi^{\pm}(z,\hbar)$ for the wave function. Substituting Equation (1.37) into Equation (1.29) gives

$$\begin{aligned}\Psi^{\pm}(q) &= \exp\left(\frac{i}{\hbar}\int_{q_0}^{q} dz\,(S_{\text{odd}}(z,\hbar) \pm S_{\text{even}}(z,\hbar))\right)\\ &= \exp\left(\frac{-1}{2}\int_{q_0}^{q} dz\,\partial_z(\log S_{\text{even}}(z,\hbar))\right)\exp\left(\pm\frac{i}{\hbar}\int_{q_0}^{q} dz\,S_{\text{even}}(z,\hbar)\right)\\ &= [S_{\text{even}}(q,\hbar)]^{-1/2}\exp\left(\pm\frac{i}{\hbar}\int_{q_0}^{q} dz\,S_{\text{even}}(z,\hbar)\right).\end{aligned} \tag{1.39}$$

Computing this expression order by order in $\hbar$ will give what is conventionally known as the WKB solutions. However, if we wish to compute the integral over paths of stationary phase in complex z-plane, i.e. paths of steepest ascend which are also known as thimbles, we may encounter Stokes phenomena as the coupling constants change. This is where we can see the source of the resurgent phenomena in the WKB method, which will be discussed in more detail below.

Remark 12. Often, one will immediately transition to an ansatz of the form $\Psi(q) = U(q,h)^{-1/2}\exp\left(i\hbar^{-1}\int dq\,U(q,\hbar)\right)$. In this case, we need to demand that $U(q,\hbar)$ satisfies a modified Ricatti equation:

$$U(q,\hbar)^2 - p(q)^2 = \hbar^2 U(q,\hbar)^{1/2}\frac{d^2}{dq^2}(U(q,\hbar)^{-1/2}) \tag{1.40}$$

This approach is for example taken in [17] or [15]. However, in this case we should remember we can still solve the Ricatti equation by expanding $U(q,\hbar) = \sum_{n=0}^{\infty}\hbar^{2n}S_{2n}(q)$, where the $S_n(q)$ can be computed recursively using Equation (1.35).

1.2.2 WKB as a Semi-Classical Limit

In this section we shall show how one can obtain the WKB approximation up to leading order from the action formalism. Consider a classical path $x_c(t)$ starting at $x_c(t_0) = x_0$, with momentum $p_c = \partial_t x_c(t)$ The action for the path going from (t_0, x_0) to (t, x) is given by[7]

$$\begin{aligned}\mathcal{S}(x,t) &= \int_{t_0}^{t} dt \left[\frac{(p_c(t))^2}{2m} - V(x_c(t))\right] \\ &= \int_{t_0}^{t} dt \left[\frac{(p_c(t))^2}{m} - \left(\frac{(p_c(t))^2}{2m} + V(x_c(t))\right)\right] \\ &= \int_{t_0}^{t} dt \frac{dx_c(t)}{dt} p_c(t) - \int_{t_0}^{t} dt\ E \\ &= \int_{x_0}^{x} dx\ p_c(x) - E(t - t_0).\end{aligned} \tag{1.41}$$

Define

$$T(x,t) = \int_{x_0}^{x} dx\ p_c(x), \tag{1.42}$$

hence

$$\frac{\partial T(x,t)}{\partial x} = p_c(x), \qquad \frac{\partial T(x,t)}{\partial E} = t - t_0. \tag{1.43}$$

The quantum path integral is obtained by integrating the exponent of the classical action over all possible paths:

$$\int \mathcal{D}[x(t)] e^{\frac{i}{\hbar}\mathcal{S}(x,t)}. \tag{1.44}$$

In the semi-classical limit, we know that the leading contribution comes from paths that extremise the action. Such classical paths have phases that add constructively. If we connect to Proposition 8 by taking an ansatz for $S(x,t)$ by setting

$$T(q,t) = \int_{q_0}^{q} dz S(z,\hbar), \qquad \text{i.e.} \quad p_c(q) = \frac{\partial T}{\partial q} = S(q,\hbar), \tag{1.45}$$

we essentially are considering the contribution of the classical path. To leading order in $\hbar$, the ansatz (1.45) solves the Ricatti equation (1.30), which reproduces the result given by Equation (1.35) that $S_0(q) = \pm p(q)$. The crux is that we may understand the WKB method as an approximation around the classical path.

1.2.3 Stokes Curves

Let us go back to the WKB solution Equation (1.29):

$$\Psi(q) = [S_{\text{even}}(q,\hbar)]^{-1/2} \exp\left(\frac{i}{\hbar}\int_{\gamma} dz\, S_{\text{even}}(z,\hbar)\right). \tag{1.46}$$

[7] Please note that this action $\mathcal{S}(x,t)$ is different from the ansatz $S(z,\hbar)$ from the previous section.

In this section, we shall more carefully consider the types of possible integration paths γ. Although I have not been explicit about this before, really we should think of $p_c(q)$ as a complex valued function of the complex variable q. With this in mind, let P_0 denote the roots of the complex function $p_c(q)$, which I will also refer to as *(classical) turning points*, for they denote the boundary between classically allowed and classically forbidden regions. The poles of $p_c(q)$ will be denoted by P_∞. In both cases, we may also consider what happens as $q \to \infty$ which may be a pole or a root. In other words, I am considering q as a variable on the Riemann sphere $\mathbb{CP}^1$. Finally, we let let $P := P_0 \cup P_\infty$.

In particular, we will consider paths of stationary phase, in other words we demand that the imaginary part of the exponent is constant (with respect to q):

$$\mathrm{Re}\left(\int^q dz\ p_c(z) \right) = \text{constant}, \tag{1.47}$$

up to the leading order $p_c(z)$ of $S(z, \hbar)$. Employing the terminology of [23] we will call paths that satisfy (1.47) *trajectories*. We may also consider paths that start at a turning point $a \in P_0$ in which case Equation (1.47) becomes

$$\mathrm{Re}\left(\int_a^q dz\ p_c(z) \right) = 0. \tag{1.48}$$

These trajectories are called *Stokes curves* or *Stokes trajectories*. The *Stokes graph* is graph whose vertex set is P and whose edges are the Stokes curves. The interiors of the faces of the Stokes graphs are called *Stokes regions*.

Remark 13. The paths that satisfy (1.47) are also known as paths of *steepest ascent* (or descent depending on orientation). Assume $z(t)$ is a path through a complex space with a constant imaginary part. Therefore

$$\partial_t \mathrm{Re}(z(t)) = \partial_t z(t) - i\partial_t \mathrm{Im}(z(t)) = \partial_t z(t).$$

Use the freedom in parametrisation of t of the path $z(t)$ to choose a path that is traversed at constant speed. In other words $|\partial_t z(t)| = \text{constant}$, hence $\partial_t \partial_t \mathrm{Re}(z(t)) = 0$, which means $z(t)$ is a path of steepest ascent or descent.

Example 14. Around a simple turning point $q_0 \in P_0$, we may write

$$p_c^2(q) = 2(E - V(q)) \approx a(q - q_0) + \dots \tag{1.49}$$

to leading order. In effect, this means we are considering the Schrödinger equation

$$\psi'' + a(q - q_0)\psi = 0. \tag{1.50}$$

After a transformation of q this is known as the Airy equation, which will be studied in detail in Section 1.4. For now, let us consider the Stokes curves of $(p_c(z))^2 = -z$. The

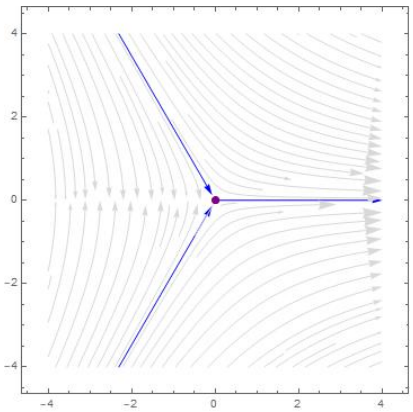

Figure 1.1: Stokes trajectories around a simple pole $(p_c(q))^2 = -q$ in the complex q-plane. The root is the purple dot and together with the pole at infinity (not displayed due to logistical concerns) and the blue lines they form the Stokes graph. Note there is a branch cut along the negative real axis.

only root is found at $z = 0$, so let us compute

$$\int_0^q p_c(z)\, dz = i\frac{2}{3}z^{3/2}\Big|_0^q = i\frac{2}{3}q^{3/2}. \tag{1.51}$$

Write $q = re^{i\theta}$. Hence imposing Equation (1.48) gives $\frac{3}{2}\theta = n\pi$ for some $n \in \mathbb{Z}$. Taking $\theta \in [0, 2\pi)$ gives three possibilities: $\theta = 0, \frac{2}{3}\pi, \frac{4}{3}\pi$, see also Figure 1.1.

Example 15. Here we will take a look the stokes trajectories of $(p_c(q))^2 = -\frac{a^2}{q^2}$ for some nonzero $a \in \mathbb{C}$. This potential has no turning points and is as such is a little pathological. It falls outside the assumptions of [23] and is thus considered purely for pedagogical reasons. I will normalise integration cycles by taking $z = 1$ as starting point, hence

$$\int_1^q p_c(z)\mathrm{d}z = \int_1^q i\frac{a}{z}dz = ia\ln q. \tag{1.52}$$

Recall that $\ln q = \log(|q|) + i\,\mathrm{Arg}\, q$. If $a \in \mathbb{R}$, then condition (1.48) is satisfied by $\mathrm{Arg}\, q = \text{constant}$. If $a \in i\mathbb{R}$, then condition (1.48) is satisfied by $|q| = \text{constant}$. If a is not on the real or the imaginary axis, some combination of the argument and the norm of q must be constant which leads to Stokes trajectories spiralling in and out of the singularity, see figure 1.2. Often one chooses a normalisation such that the integral (1.52) vanishes which leads to a zero of the action.

The vocabulary of [23] prescribes the following:

(i) A *generic trajectory* flows into P_∞ at both ends.

(ii) A *saddle trajectory* is a trajectory that flows into P_0 at both ends.

(iii) A *Separating trajectory* flows on one end into P_0 and on other end into P_∞.

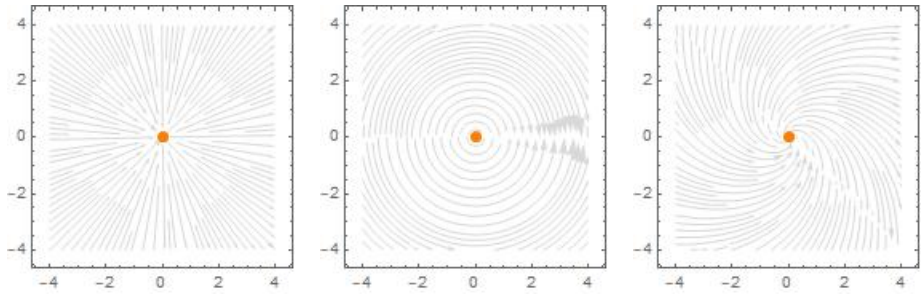

(a) $a = 1$ (b) $a = i$ (c) $a = i + 1$

Figure 1.2: Stokes trajectories of $(p_c(q))^2 = -\frac{a^2}{q^2}$ for several values of a.

(iv) A *closed trajectory* is simply a closed curve that does not intersect with P.

Critically, trajectories cannot flow towards local maxima, because these are forbidden per the maximum modulus principle of holomorphic functions. We can subdivide saddle trajectories into ones that flow into distinct point in P_0 and those that flow into the same point, respectively called *regular saddle trajectories* and *degenerate saddle trajectories*. It follows from the definition that a Stokes curve is either a saddle trajectory or a separating trajectory.

In this section I will assume that there is at most 1 saddle trajectory in the Stokes graph. It is a lemma proven by [23] that under this assumption all trajectories can be classified as one of the trajectories (i)-(iv).

1.2.4 Borel Resummation

Let us take a look at the WKB solutions (1.39)

$$\Psi(q) = [S_{\text{even}}(q,\hbar)]^{-1/2} \exp\left(\frac{i}{\hbar}\int_\gamma dz\, S_{\text{even}}(z,\hbar)\right). \tag{1.53}$$

through another set of glasses: we should recall that $S_{\text{even}}(z,\hbar) = \sum_{n=0}^{\infty} \hbar^{2n} S_{2n}(z)$ is a power series of even powers of $\hbar$. Carrying these powers of $\hbar$ through the integral we see that in the exponent of Equation (1.53) there is only one term with negative power of $\hbar$, which is equal to the classical path integral $\frac{i}{\hbar}T(z,t)$ – see Equation (1.45). It is a well known fact in real analysis that the function $f(x) = e^{-1/x}$ does not have a well-defined Taylor series at $x = 0$. This is an indication that a power series of Equation (1.53), the resulting series is divergent and we shall need to perform a Borel resummation in $\hbar$.

In Section 1.1.2, I did not only define the Borel resummation along the real axis, but in fact we can define Borel resummations along any direction θ (assuming summability). Instead of choosing a non-zero angle θ, we can equivalently consider the system where we perform a Borel resummation along $\theta = 0$, but with $\hbar \to \hbar e^{-i\theta}$ [23, 45]. This then

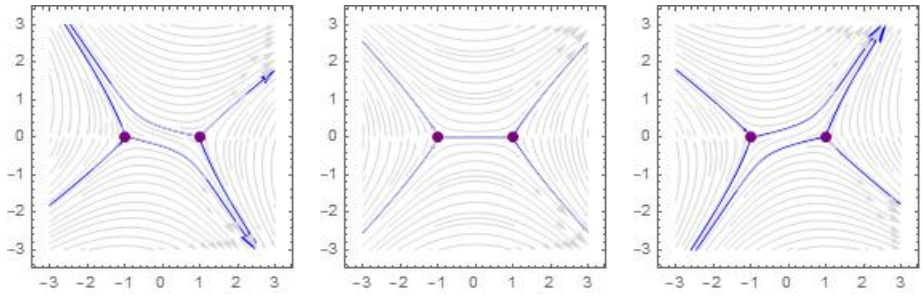

(a) $\theta = -\pi/10$ (b) $\theta = 0$ (c) $\theta = +\pi/10$

Figure 1.3: Here, we demonstrate the Stokes phenomenon by considering the classical momentum $(p_c(q))^2 = e^{i\theta}(q-1)(q+1)$. This is equivalent to considering a classical momentum $(p_c(q))^2 = (q-1)(q+1)$, but performing a Borel resummation along the θ direction. Again, the purple dot indicates the roots $q = \pm 1$ and the blue lines are the Stokes curves. We can clearly see that there a unique (regular) saddle trajectory when $\theta = 0$, but that the topology of the Stokes graph changes discontinuously as we vary θ.

amounts to considering trajectories with

$$\mathrm{Im}\left(e^{i\theta}\int_a^q dz\; p_c(z)\right) = 0. \tag{1.54}$$

These trajectories are the *Stokes curve in the direction* θ, which form the Stokes graph $G_\theta[p_c(q)]$ in direction θ.

Given a system with classical momentum $p_c(q)$, we we will consider a situation for which the Stokes graph G_{θ_0} has precisely 1 saddle trajectory. Furthermore, we assume there exists some ϵ such that G_θ, where $\theta \in (\theta_0 - \epsilon, \theta_0 + \epsilon)$ has a saddle trajectory only if $\theta = \theta_0$. In other words, if $\theta \in (\theta_0 - \epsilon, \theta_0) \cup (\theta_0, \theta_0 + \epsilon)$, then G_θ does not have a saddle trajectory. Hence, as θ varies over $(\theta_0 - \epsilon, \theta_0 + \epsilon)$, the topology of the corresponding Stokes graph can change. This is what is known as the *Stokes phenomenon* or the *mutation* of Stokes graph and is at the core of much of this field. An archetypical example of this can be seen in Figure 1.3.

Iwaki and Nakanishi [23] give a number of technical theorems about Borel resummability which I will here summarise. To be precise, we will be considering the Borel resummability of the power series expansion of

$$\exp\left(\frac{i}{\hbar}\int_\gamma dz\, S_{\mathrm{reg}}(z,\hbar)\right), \tag{1.55}$$

where $S_{\mathrm{reg}} = S_{\mathrm{even}} - S_0$, to extract the regular part of the exponent. The first proposition states that if we integrate over a path that is contained in $D \cup \{p\}$ for a single Stokes region D and a pole $p \in P_\infty$, the WKB solution is resummable. In particular such a path cannot cross any Stokes curves. However, if we consider a path that crosses a separating trajectory, we can deform the path such that it crosses through the pole, thus paths that cross separating trajectories are also resummable. A further corollary stipulates

that if we integrate along paths in a Stokes graph that is free of saddle trajectories, the solutions are Borel resummable everywhere. Given some θ_1, θ_2, a final proposition states that if we integrate along a curve whose endpoints do not lie on a Stokes curve for all $\theta \in [\theta_1, \theta_2]$ and for these values of θ the path never crosses or touches a Stokes curve, then the Borel resummations of the WKB solutions in the θ_1 and θ_2 are identical.

1.3 Uniform WKB

In this Section I will be mostly be following the approach taken by Dunne and Ünsal [15] (see also [66–69] and [70]), which provides an alternative way of understanding the WKB approach. Their approach applies to any potential with locally harmonic degenerate vacua. That is, a minimum that looks like $V(x) = x^2 + \mathcal{O}(x^3)$. Such quantum mechanics include the well-studied double well (DW) and sine-gordon (SG) potentials

$$\begin{aligned} V_{\mathrm{DW}}(x) &= x^2(1+gx)^2\,, \\ V_{\mathrm{SG}}(x) &= \frac{1}{g^2}\sin^2(gx)\,. \end{aligned} \tag{1.56}$$

The main advantage of their approach is that it provides a systematic approach to understanding transseries terms in the expansion. Moreover, they are able to show "strong resurgence", in the sense that **all** non-perturbative information is contained within the perturbative expansion.

In this section I will discuss the solutions and in particular the energy levels of the double well system. Although I will not prove all the results in detail, the purpose of this Section is rather to illustrate their techniques and results. Let us start with the Schrödinger equation (1.27). We start by re-writing the problem by using $g^2 = \frac{\hbar^2}{2}$ and $\frac{1}{g^2}V(q) = V(y)$, so that now we solve

$$-g^4\partial_y^2\Psi(y) + V(y)\Psi(y) = g^2 E\Psi(y). \tag{1.57}$$

We make a slight modification to standard WKB ansatz (1.29) by making instead the ansatz

$$\Psi(y) = \frac{D_\nu(\frac{1}{g}u(y))}{\sqrt{u'(y)}}, \tag{1.58}$$

where u plays an analogous role previously performed by $\int S$. $D_\nu(z)$ is the parabolic cylinder function which satisfies the harmonic oscillator problem, with energy $E = \nu + 1/2$:

$$\partial_z^2 D_\nu(z) + \left(\nu + \frac{1}{2} - \frac{z^2}{4}\right)D_\nu(z) = 0 \tag{1.59}$$

For the ansatz (1.58) to solve Equation (1.57), we need to demand the following Ricatti

equation is satisfied

$$g^2 E + \frac{1}{4}(u')^2 u^2 - g^2(\nu + \frac{1}{2})(u')^2 - \frac{g^4}{2}\left(\frac{u''}{(u')^{3/2}}\right)'(u')^{1/2} - V(y) = 0. \tag{1.60}$$

Here the prime naturally denotes a derivative with respect to y. We follow the now standard method of making perturbative expansions in g^2:

$$\begin{aligned} E(\nu, g^2) &= \sum_{k=1}^{\infty} g^{2k} E_k(\nu) \\ u(y) &= \sum_{k=1}^{\infty} u_k(y) g^{2k}. \end{aligned} \tag{1.61}$$

We will determine the functions $u_n(y)$ and $E_n(\nu)$ by plugging the expansions back into (1.60) and solving it order by order in g^2. For example, at zeroth order we find the equation

$$u_0^2 (u_0')^2 = 4V. \tag{1.62}$$

With this, we may solve for u_0

$$(u_0(y))^2 = \int_0^y dy \sqrt{V(y)}\,. \tag{1.63}$$

In the $g^2 \to 0$ limit, we have that ν is almost an integer. To be precise, we can write the $\nu(N, g^2) = N + \delta\nu(N, g^2)$ and we consider the expansion

$$E(\nu, g^2) = E(\nu = N, g^2) + \delta\nu \left(\frac{\partial E}{\partial \nu}\right)\Big|_{\nu=N} + \mathcal{O}((\delta\nu)^2)\,. \tag{1.64}$$

Here, $E(\nu = N, g^2)$ is the usual perturbative expansion in Rayleigh-Schrödinger perturbation theory. In this same $g^2 \to 0$ limit, using[8] $D_\nu(y) = y^\nu e^{-y^2/4}$, leads to the usual non-perturbative term of the WKB [71]

$$\psi(y) = \exp\left(-\frac{(u_0)^2}{4g^2}\right)\,. \tag{1.67}$$

Another crucial step in the uniform WKB is the setting of a global boundary condition. The goal of this is to relate separate vacua. By connecting the separate vacua,

[8] To see this approximation for the parabolic cylinder function, we could use the following asymptotic series [15]:

$$D_\nu(z) \approx z^\nu e^{-z^2/4} F_1(z^2) + \frac{\sqrt{2\pi}}{\Gamma(-\nu)} e^{\pm i\pi\nu} z^{-1-\nu} e^{z^2/4} F_2(z^2), \tag{1.65}$$

with

$$\begin{aligned} F_1(z^2) &= \sum_{k=0}^{\infty} \frac{1}{k!} \frac{\Gamma(k - \nu/2)\Gamma(k + (1-\nu)/2)}{\Gamma(-\nu/2)\Gamma((1-\nu)/2)} \left(\frac{-2}{z^2}\right)^k, \\ F_2(z^2) &= \sum_{k=0}^{\infty} \frac{1}{k!} \frac{\Gamma(k + (1+\nu)/2)\Gamma(k + 1 + \nu/2)}{\Gamma((\nu+1)/2)\Gamma(1 + \nu/2)} \left(\frac{2}{z^2}\right)^k. \end{aligned} \tag{1.66}$$

we can construct resurgent relations. The precise boundary condition depends on the model being studied. This global boundary condition can be shown [15] to be similar to the quantisation conditions set by ZJJ [72, 73].

In the case of the SG potential, we impose a global boundary condition based on the periodicity of the potential

$$\Psi(\theta + L) = e^{i\alpha}\Psi(\theta), \tag{1.68}$$

where L is the periodicity and $\alpha \in [0, \pi]$ is the Bloch angle. In addition we demand a Bloch condition that relates the values of the wave function at some midpoint of the potential θ_{midpoint}.

In the case of the double well potential, the system is symmetric around $y = -1/2$ the midpoint potential energy barier. We can thus impose a condition on the wavefunction at this point. If the wavefunction is even (respectively odd) around $y = -1/2$, we may impose $\Psi(-1/2) = 0$ (respectively $\Psi'(-1/2) = 0$). This situation for example corresponds to the ground state (respectively the first excited state). We may now limit the problem to the domain $-1/2 \leq y \leq \infty$ with a Dirichlet (respectively Neumann) boundary condition at $y = -1/2$ and a Dirichlet boundary condition at $y = \infty$ and symmetrically extend to the other well.

It is possible to use the uniform WKB ansatz to determine the precise asymptotic form for $E_n^{S_I}$. The procedure is detailed in [15] but we shall give a brief overview here. Expanding the boundary condition in terms of $\nu = N + \delta\nu + (\delta\nu)^2 + \dots$ allows us to determine $\delta\nu$ in terms of g^2. The setting of global boundary conditions shows that $\delta\nu$ is a series expansion of an instanton fugacity $\xi = \frac{2S_I}{\pi g^2} e^{-S_I/g^2}$, where $S_I^{\text{DW}} = \frac{1}{6}$ and $S_I^{\text{SG}} = 2$ are the instanton actions. These are related to the global boundary conditions through $S = \frac{1}{2}(u_0(y_{\text{midpoint}})^2$. This can be used to compute the N^{th} energy level

$$E(v, g^2) = E(\nu = N, g^2) + \delta\nu \left[\frac{\partial E(\nu, g^2)}{\partial \nu}\right]_{\nu=N} + \mathcal{O}((\delta\nu)^2)\,. \tag{1.69}$$

The first ambiguity of $E(v, g^2)$, at order ξ^2, is the imaginary part of $\delta\nu \left[\frac{\partial E(v,g^2)}{\partial \nu}\right]_{\nu=N}$. As this lies thus in the instanton-anti-instanton section, we write this as

$$\text{Im}\left(\delta\nu \frac{\partial E(\nu, g^2)}{\partial \nu}\right)_{\nu=N} = \pm\xi^2 \left(a_0^{I\bar{I}} + a_1^{I\bar{I}} g^2 + \mathcal{O}(g^4)\right) \tag{1.70}$$

By considering dispersion relations at the ground state[9],

$$\begin{aligned} E_k(N=0) &= \oint_{\mathcal{C}} \frac{E(N=0, g^2)}{(g^2)^{k+1}} d(g^2) \\ &= \frac{1}{i\pi} \int_0^{+\infty} \frac{\text{Disc}_0 E(N=0, g^2)}{(g^2)^{k+1}} d(g^2)\,, \end{aligned} \tag{1.71}$$

[9] $\mathcal{C}$ denotes a counter-clockwise closed contour around $g^2 = 0$. The first equality is simply a restatement of (3.42) using Cauchy's theorem. Next we deform the contour up and down the positive real axis and around infinity to obtain the second equality.

for the coefficients $\mathcal{E}_k(N=0)$, it is possible to determine an asymptotic form [15]

$$E_n(N=0) = -\frac{2}{\pi}\frac{n!}{(2S_I)^n}\left(a_0^{I\bar{I}} + a_1^{I\bar{I}}\frac{2S_I}{n} + \mathcal{O}(k^{-2})\right). \tag{1.72}$$

This gives the leading late order (large n) behaviour of the perturbative expansion of the ground series.

1.4 Airy Function

As a foundational exercise, in this section we discuss at some length the Airy function with a particular eye towards asymptotic expansions and resurgence. The Airy function is a nice example because all the resummations are completely known. This material is covered in for example [44, 74, 75] and similar toy functions are studied in [46, 76].

Although Airy's original area of application of this function was optics [77], it is interesting to note that a generalised "matrix Airy function" has been studied by Kontsevich [78] and Witten [79, 80] in the context of intersection numbers of stable classes on the moduli space of curves.

The Airy function $Z(\kappa)$ is described by a differential equation

$$Z''(\kappa) - \kappa Z(\kappa) = 0. \tag{1.73}$$

In integral form this can be formulated as

$$Z(\kappa) = \int_\gamma dz\, e^{-S(z)}, \qquad S(z) = -\kappa z + z^3/3\,, \tag{1.74}$$

where we shall in the next Section try to be a bit more precise as to the nature of the path γ.

1.4.1 Saddle Points

Equation (1.74) will only solve Equation (1.73) if the boundary terms of the integral vanish. However, we are free to choose a path. This freedom shall be used to integrate over paths of steepest ascent only (see Section 3.3). The saddle points can be found by solving $\frac{dS}{dz} = 0$ which will yield

$$z_\pm = \pm\sqrt{\kappa} \tag{1.75}$$

The saddle point can be connected by a stokes line if when $\operatorname{Im} S(z_+) = \operatorname{Im} S(z_-)$ which gives $\operatorname{Arg}\kappa = \frac{2\pi n}{3}$ for $n \in \mathbb{N}$. For these values of κ there is a thimble that passes through both points. If we cross a stokes line by moving $\theta := \operatorname{Arg}\kappa$, the thimbles that go through the points $z_\pm$ discontinuously switch its asymptotic direction.

Let us try to solve Equation (1.73) with a (single!) instanton ansatz:

$$Z(\kappa) = e^{-\frac{1}{2}A\kappa^{\alpha}}\kappa^{\beta}\sum_{l=0}^{\infty} a_l \kappa^{-\alpha l} \tag{1.76}$$

After reparametrising some of the dummy variables ($l \to l-1$ or $l \to l-2$), substituting into the differential equations yields

$$\begin{aligned} e^{-\frac{1}{2}A\kappa^{\alpha}}\kappa^{\beta}\kappa^{2\alpha-2}\Big\{ & \sum_{l=0}^{\infty} \frac{\alpha^2}{4} A^2 a_l \kappa^{-\alpha l} \\ & - \Big(\frac{\alpha}{2}(\alpha-1)A + A\alpha\beta\Big)\sum_{l=1}^{\infty} a_{l-1}\kappa^{-\alpha l} \\ & + \beta(\beta-1)\sum_{l=2}^{\infty} a_{l-2}\kappa^{-\alpha l} \\ & - \alpha A \sum_{l=2}^{\infty} a_{l-1}(-\alpha(l-1))\kappa^{-\alpha l} \\ & + 2\beta\sum_{l=3}^{\infty} a_{l-2}(-\alpha(l-2))\kappa^{-\alpha l} \\ & + \sum_{l=3}^{\infty} a_{l-2}(-\alpha(l-2))(-\alpha(l-2)-1)\kappa^{-\alpha l}\Big\} \\ & - \kappa Z(\kappa) = 0\,. \end{aligned} \tag{1.77}$$

To solve this equation, all terms involving summations with a_{l-1} or a_{l-2} need to vanish, leaving only the first and the last line to cancel each other. However, I will start by matching the overall exponents of κ: this is done by demanding $2\alpha - 2 = 1$, hence $\alpha = 3/2$. To match the overall coefficients we will need that $\alpha^2 A^2/4 = 1$, hence $A_{\pm} = \pm A$, $A = 4/3$. Of the ensuing lines, the second one is the only one to contribute a factor of $\kappa^{-\alpha}$ (since the other summations start at $l = 2$ or higher). Therefore, it is necessary to demand $\frac{\alpha}{2}(\alpha-1)A + A\alpha\beta = 0$, which gives $\beta = -1/4$. The remaining lines give a recursion relation that will need to be satisfied:

$$a_n = \frac{a_{n-1}}{An}\Big[\frac{5}{36} + n(n-1)\Big], \tag{1.78}$$

which is solved by

$$a_n := A^{-n}\frac{1}{2\pi n!}\Gamma(n+5/6)\Gamma(n+1/6). \tag{1.79}$$

It is easy to see that this indeed satisfies the recursion relation. Again, I note that the coefficients diverge factorially for large n behaviour: $a_n \propto A^{-n}n!$.

Remark 16. Although, it may not look like it at first sight, the coefficients (1.79) are actually rational numbers. For example, $a_0 = 1$ and $a_1 = 5/48$. (The reason for this are special properties of the gamma functions, such as $\Gamma(x)\Gamma(1-x) = \pi/\sin(\pi x)$.)

Remark 17. In Section 1.2, we discussed how the Airy function can be obtained as a

WKB approximation around a turning point with a classical momentum $p_c(\kappa) = \kappa$. To be precise, we will also need to set $\hbar = i$ in the WKB approach. In this formalism we can calculate the non-perturbative part:

$$\int_0^\kappa S_0(z)dz = \pm \int_0^\kappa p_c(z)dz = \frac{2}{3}\kappa^{3/2}, \tag{1.80}$$

which agrees precisely with the exponential factors found using the above transseries ansatz. Furthermore, using formula (1.35), we can compute that $S_1(z) = \frac{i}{4z}$, hence its contribution to the wavefunction is

$$\exp\left(\int^q iS_1(z)\right) = \exp\left(\frac{-1}{4}\log(q)\right) = q^{-1/4}, \tag{1.81}$$

which precisely reproduces $\beta = -1/4$. The higher order of $S(z)$ will contribute only higher orders of $x = q^{-3/2}$ Performing a series expansion around $x \approx 0$ will yield a series with coefficients in $\mathbb{Q}$, which agree precisely with those of Equation (1.79). A numerical computation of this is presented in Appendix 1.B.2.

1.4.2 Borel Analysis

If we take into account the two choices in the transseries $A_\pm = \pm A$ above, a general solution to the equation (1.73) be a combination of the form

$$Z(\kappa) = AZ_-(\kappa) + BZ_+(\kappa), \tag{1.82}$$

where A and B are constants to be fixed by boundary conditions and

$$Z_\pm = \frac{1}{\sqrt{2\pi}\kappa^{1/4}} e^{\pm\frac{1}{2}A\kappa^{3/2}}\Phi_\pm(\kappa)\,. \tag{1.83}$$

The perturbative sectors are given by

$$\Phi_\pm(\kappa) = \sum_{n=0}^{\infty} a_n^\pm \kappa^{-\frac{3}{2}n}, \tag{1.84}$$

where

$$a_n^\pm = \mp(\pm 1)^n a_n, \tag{1.85}$$

and the coefficients a_n are given by Equation (1.79). Traditionally, the function $Z_-(\kappa)$ has been called the Airy function $Ai(\kappa)$ whereas $Z_+(\kappa)$ is the "Bairy" function $Bi(\kappa)$. It is at this stage natural to work in the variable $z = \kappa^{3/2}$. If one takes away the constant a_0,

$$\tilde{\Phi}_\pm = \Phi_\pm \pm a_0, \tag{1.86}$$

the Borel transforms are known in closed form and are given by[10]

$$\mathcal{B}(\tilde{\Phi}_{\pm})(s) = -\frac{5}{48}\,{}_2F_1(7/6, 11/6, 2|\pm s/A). \tag{1.87}$$

This hypergeometric function has a branch cut singularity at $s = \pm A$. Around the singularity it takes a special form [44]:

$$\mathcal{B}(\tilde{\phi}_{\pm})(s)|_{s\simeq\pm A} = \frac{i}{2\pi i(s \mp A)} + i\mathcal{B}(\tilde{\phi}_{\mp})(s \mp A)\frac{\log(s \mp A)}{2\pi i} \tag{1.88}$$

This means that upon crossing the stokes lines, we pick up terms related to the other sector. We can capture this information in terms of the Stokes automporphism from Section 1.1.3. However, the Alien calculus developed in Appendix 1.A very naturally applies to Equation (1.88) as well. The Alien calculus attempts to isolate the discontinuity of the Borel resummation of individual singularities in the Borel plane. In terms of Alien derivatives we have

$$\Delta_{\pm A}\Phi_{\pm} = -i\Phi_{\mp}. \tag{1.89}$$

In all other cases the Alien derivative vanishes. We can hence also conclude the Stokes factors are given by $S_{\pm} = -i$. The technology presented in Appendix 1.A was developed to quantify these statements. We calculate the Stokes automorphism and the alien derivative as [44]:

$$\begin{aligned} \mathfrak{S}_0\Phi_+ &= \Phi_+ - ie^{-Az}\Phi_- & \mathfrak{S}_0\Phi_- &= \Phi_- \\ \mathfrak{S}_\pi\Phi_- &= \Phi_- - ie^{Az}\Phi_+ & \mathfrak{S}_\pi\Phi_+ &= \Phi_+. \end{aligned} \tag{1.90}$$

Hence the discontinuities are given by

$$\begin{aligned} \mathrm{Disc}_0\Phi_+ &= ie^{-Az}\Phi_- \\ \mathrm{Disc}_\pi\Phi_- &= ie^{Az}\Phi_+ \end{aligned} \tag{1.91}$$

Remark 18. Referring back to the WKB approach of this problem as in Remark 17, choosing $p_c(q) = \sqrt{q}$ reproduces the series Φ_+, whereas $p_c(q) = -\sqrt{q}$ gives Φ_-. We may thus understand that the solutions Φ_+ and Φ_- correspond to solutions with different orientations of the potentials, which is the same thing as living on a different sheet of the Riemann surface.

1.4.3 Large Order Relations and Resurgence

In this section I will show how one can relate the coefficients of one sector to the other sector. We see that the coefficients at large n in one sector are related to those at small n in the other sector. In this section I will work in the variable $x = z^{-1} = \kappa^{-3/2}$, following [44]. Start by writing down Cauchy's theorem away from the discontinuity for

[10] Here the variable s is the variable in the Borel plane, a role which in Section 1.1 was fulfilled by ζ.

Φ_+:

$$\Phi_+(x) = \frac{1}{2\pi i} \oint_{C_x} dw \frac{\Phi_+(w)}{w-x}. \tag{1.92}$$

Here, the contour C_w is a small circle around w traversed counter-clockwise. I shall blow up the contour to infinity where the function is not singular. Along θ we integrate along the discontuinity, hence

$$\Phi_+(x) = -\frac{1}{2\pi i} \int_0^\infty dw \frac{\mathrm{Disc}_0 \Phi_+}{w-x}. \tag{1.93}$$

The minus sign in simply due to the definiton (1.26). We shall now employ Equation (1.91), and plug in the asymptotic expansions for $\Phi_\pm$ (1.84).

$$\begin{aligned} \sum_{n=0}^\infty a_n^+ x^n &= -\frac{1}{2\pi} \int_0^\infty \frac{dw}{w-x} e^{-A/w} \sum_{k=0}^\infty a_k^- w^k \\ &= -\frac{1}{2\pi} \int_0^\infty dw \sum_{l=0}^\infty x^l \sum_{k=0}^\infty e^{-A/w} a_k^- w^{k-l-1}, \end{aligned} \tag{1.94}$$

By comparing powers of x, we must conclude that

$$\begin{aligned} a_n^+ &= -\frac{1}{2\pi} \int_0^\infty \sum_{k=0}^\infty dw\ a_k^- w^{k-l-1} e^{-A/w} \\ &= -\frac{1}{2\pi} \sum_{k=0}^\infty a_k^- \Gamma(n-k) A^{k-n} \\ &= -\frac{\Gamma(n)}{2\pi A^n} \sum_{k=0}^\infty a_k^- A^k \prod_{j=1}^k \frac{1}{n-j}\,. \end{aligned} \tag{1.95}$$

In the second line I have used

$$\int_0^\infty e^{-A/w} w^{k-l-1} dw = \Gamma(l-k) A^{k-l}\,. \tag{1.96}$$

$\Gamma(n-k)$ has been rewritten into $\Gamma(n)$ removing excessive factors. We can now rewrite the sum as Taylor series in the variable n^{-1}:

$$a_n^+ \sim -\frac{i\Gamma(n)}{2\pi i A^n} \sum_{k=0}^\infty \frac{c_k}{n^k} \tag{1.97}$$

The coefficients a_n^- and A have been repackaged into c_n. For the first few coefficients we have $c_0 = a_0^-$, $c_1 = Aa_1^-$, $c_2 = Aa_1^- + A^2 a_2^-$ and $c_3 = Aa_1^- + 3A^2 a_2^- + A^3 a_3^-$. From Equation (1.97) we can hence also see how the coefficients of different sectors are related. Should n be chosen large, on the LHS we relate the Φ_+ sector at high order to the Φ_- on the RHS at small orders (because the first terms dominate more easily for large n). The fact that the asymptotic expansion in one perturbative sector may contain information about other sectors is called *resurgence*.

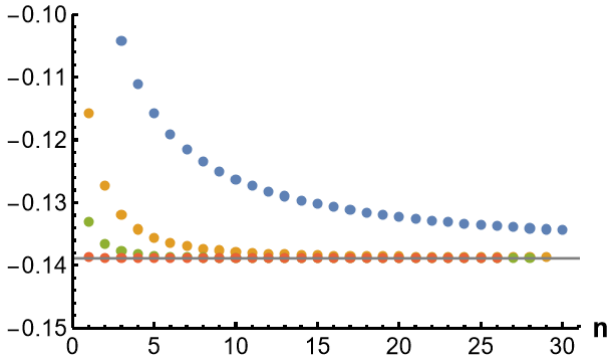

Figure 1.4: We compute the left hand side of Equation (1.100) for $m = 3$ - given by the blue dots. It is shown that the it converges to $b_3 = -\frac{5}{36}$. The first, second and fourth Richardson Transformations are given respectively in orange, green and red.

In Equation (1.97), we have used the value of the Stokes constant $S_+ = -i$. If this information is not at our disposal we may still try to extract information from the large-order relations by considering the series

$$\frac{A}{n}\frac{a^+_{n+1}}{a^+_n} = \frac{\sum_{k=0}^{\infty} c_k/(n+1)^k}{\sum_{k=0}^{\infty} c_k/n^k}. \tag{1.98}$$

We shall perform the same trick and re-expand in the variable n^{-1}:

$$\frac{A}{n}\frac{a^+_{n+1}}{a^+_n} = \sum_{k=0}^{\infty} \frac{b_k}{n^k}. \tag{1.99}$$

To find b_k we will need knowledge of $c_0, \ldots, c_k$. In particular, $b_0 = 1$, $b_1 = 0$, $b_2 = -\frac{c_1}{c_0}$, $b_3 = \frac{1}{c_0^2}(c_0c_1 + c_1^2 - 2c_0c_2)$ Taking the large n limit of Equation (1.99), we easily see the right hand side converges to b_0. However, with knowledge of $b_0, \ldots, b_{m-1}$ it is also easy to create a series that converges to b_m:

$$n^m\left(\frac{A}{n}\frac{a^+_{n+1}}{a^+_N} - \sum_{k=0}^{m-1}\frac{b_k}{n^k}\right) = \sum_{k=m}^{\infty}\frac{b_k}{n^{k-m}} = b_m + \frac{b_{m+1}}{n} + \ldots. \tag{1.100}$$

The point here is that, even without knowledge of the Stokes constant, we can compute large n limits of the left hand side of Equation (1.100) using a^+_n. On the other side, knowing just a few coefficients a^-_n we can predict its limit. For example, this should predict[11] that the left hand side of Equation (1.100) converges to $= -\frac{5}{36}$. This is verified, using the Richardson Transformation - see Remark 19 below, in Figure 1.4.

Remark 19. There is a trick to accelerate convergence of series such as the RHS of Equation (1.100) called the Richardson Transformation. To explain this let us start with

[11] The series b_b seems to have the simple behaviour $b_n = (-1)^n \frac{5}{36}$ for $n \geq 2$.

a series

$$s(n) = \sum_{k=0}^{\infty} \frac{s_k}{n^k}, \tag{1.101}$$

which is convergent as $n \to \infty$. Following [44], define the N-Richardson $R_s(n, N)$ transformation of the series s as

$$\begin{aligned} R_s(n, 0) &= s(n), \\ R_s(n, N) &= R_s(n+1, N-1) + \frac{n}{N}\Big(R_s(n+1, N-1) - R_s(n, N-1)\Big). \end{aligned} \tag{1.102}$$

I have written some simple stand-alone code that converts a sequence of numbers in Mathematica into its Richardson transform, and conveniently plots it. This code is widely applicable and given in Appendix 1.B.1.

Proposition 20. One will see that in the large n expansion $R_s(n, N)$ has no terms proportional to $\frac{1}{n}, \ldots, \frac{1}{n^N}$, i.e. it takes the following form:

$$s_0 + \frac{s'_{N+1}}{n^{N+1}} + \frac{s'_{N+2}}{n^{N+2}} + \ldots \tag{1.103}$$

where s'_{N+k} are some new coefficients that depend linearly on $s_N, \ldots, s_{N+k}$.

1.5 Practical Resurgence: The Sine-Gordon Potential

To contrast the previous Section, where we made heavy use of closed form expression for the perturbative expansions that enabled precise and exact situations, in this Section we take a different approach. We shall start with relative naivety and study the coefficients of a perturbative series. We demonstrate how to analyse this and find the leading terms in an asymptotic expansion.

The setting for this Section shall be QM mechanics with the Sine-Gordon potential, briefly mentioned in Section 1.3. A more general version of this model shall be found in the analysis of the bi-Yang-Baxter model in Chapter 3. This model is more completely treated in [34, 46], but we shall give a basic analysis here.

$$V(x) = \frac{1}{g^2} \sin^2(gx)\,. \tag{1.104}$$

We use the package [81] to compute the perturbative series for energy of the ground state of this model:

$$E_0 = \frac{1}{2} - \frac{1}{8}g^2 - \frac{1}{32}g^4 - \frac{3}{128}g^6 - \frac{53}{2048}g^8 + \mathcal{O}(g^{10}) = \sum_{n=0}^{\infty} a_n g^{2n}\,. \tag{1.105}$$

The first 100 terms (to order g^{200}) of this series are easily obtained on a laptop in under 20 seconds. Relying on the package, the code to compute this sequence, as well as the

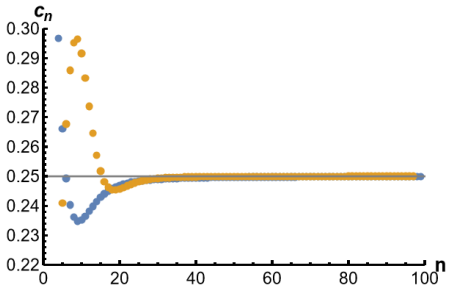

Figure 1.5: We consider the series c_n in blue, its second Richardson transformation, in orange. It clearly converges to $\frac{1}{2S} = \frac{1}{4}$, in grey.

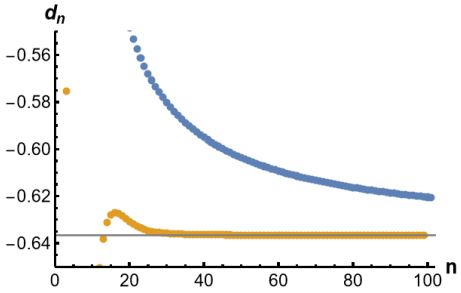

Figure 1.6: We consider the series d_n in blue, its second Richardson transformation, in orange. It clearly converges to $A = -\frac{2}{\pi}$, in grey.

code to analyse its asymptotics, is very simple. I have given it in Appendix 1.B.3. To find the location of its Borel pole we define $b_n = \frac{a_{n+1}}{a_n}$ and $c_n = b_{n+1} - b_n$. If we had an asymptotic series $a_n \sim A(2S)^{-n}\Gamma(n+1)$, as one could expect from Equation (1.72), then c_n should thus converge to $\frac{1}{2S}$. This convergence is shown in Figure 1.5 and indicates that $S = 2$, which is precisely the instanton action of the Sine-Gordon model.

To determine the overall coefficient A, we simply compute the series $d_n = \frac{a_n}{(2S)^{-n}\Gamma(n)}$. The convergence of this series is shown in Figure 1.6 and indicates that $A = -\frac{2}{\pi}$. Now that we know the leading behaviour of this series, we can subtract it and define $e_n = a_n + \frac{2}{\pi 4^n}\Gamma(n+1)$. In figure 1.7, we show that the sub-leading behaviour is given by $e_n \approx \frac{5}{\pi 4^n}\Gamma(n)$.

Combining these numerical results gives an asymptotic expansion which matches that of the literature [15]

$$a_n = -\frac{2}{\pi}\frac{\Gamma(n+1)}{4^n}\left(1 - \frac{5}{2}\frac{1}{n} + \mathcal{O}(n^{-2})\right). \tag{1.106}$$

To avoid the $\frac{1}{n}$ divergence, we define a new asymptotic series that removes the constant part

$$\tilde{\phi}(g^2) = \sum_{n=1}^{\infty} a_n g^{2n} = \sum_{n=0}^{\infty} a_{n=1} g^{2n+2} \equiv \sum_{n+0}^{\infty} b_n g^{2n+2} \tag{1.107}$$

This is a relatively simple asymptotic expansion that falls in the category that was

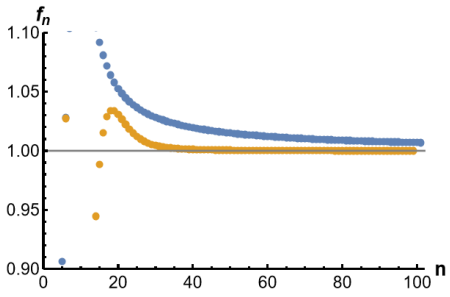

Figure 1.7: We define the series $f_n = \frac{e_n}{5\pi^{-1}4^{-n}\Gamma(n)}$ and show it converges to 1. Colours as in 1.6 and 1.5

discussed in Examples 4 and 1. We simplify adapt it to $a = 2$, $A = 4$ and $g^2 = z^{-1}$ for the leading term, and $a = 1$ for the sub-leading term. We conclude that

$$(S_+ - S_-)\,\tilde{\phi}(g^2) = -\frac{i}{4}\frac{1}{g^2}e^{-4/g^2}\left(1 - 10g^2 + \mathcal{O}(g^4)\right) . \tag{1.108}$$

1.A Alien Calculus

In this Appendix, we will discuss some of the more mathematical inquiries into the structure of the Stokes automorphism. However, for the remainder of the thesis, this Section shall not be immediately invoked and as such it thus serves more as a foundational exercise.

The field of study of resurgent function was found by Écalle [82], but this section shall mostly draw from the notation of Dorigoni [42]. We shall introduce the framework of *alien calculus* to consider general power series $\hat{\phi}(z)$. By considering their Borel transformations around its singularities, we uncover, and make precise their rich analytic structure.

1.A.1 Alien Derivatives

Whereas the stokes automorphism $\mathfrak{S}_\theta$ captures the full information as we cross a stokes line θ, the alien derivative will tell us about the contribution of the individual singularities that lie on the stokes line. Denote the set of singularities along the direction θ by Sing_θ. We may now introduce operators called alien derivatives Δ_ω as

$$\mathfrak{S}_\theta = \exp\left(\sum_{\omega\in\text{sing}_\theta} e^{-\omega z}\Delta_\omega\right). \tag{1.109}$$

At this stage it is unclear why we should refer to the operator Δ_ω as a derivation. Firstly, I would like to draw an analogy to the momentum operator, which is also a derivation and upon exponentiation generates translations. In the same spirit we may treat the

alien derivative. Furthermore, it satisfies the Leibniz rule of differentiation[12], which in a simple case will be demonstrated in Example 22.

Example 21. In this example we look at the simple case in which the Borel transform $\hat{\phi}(\zeta)$ of $\tilde{\phi}(z)$ has a single simple singularity at $\zeta = \omega$:

$$\hat{\phi}(\zeta) = \frac{a}{2\pi i(\zeta - \omega)} + \frac{\hat{\psi}(\zeta - \omega)}{2\pi i} \log(\zeta - \omega) + f(\zeta - w), \tag{1.110}$$

where $\hat{\psi}$ and f are holomorphic around the origin. In fact, an asymptotic expansion $\tilde{\phi}(z)$ is said to be a *simple resurgent function* precisely if its Borel transform $\hat{\phi}(\zeta)$ *locally* around a singularity can be put in form as in Equation (1.110). Let us first focus on what happens if $\hat{\phi}(\zeta)$ is globally of the form as in Equation (1.110).

$\hat{\psi}(\zeta)$ is naturally the Borel transform of some other function $\tilde{\psi}(z)$. We will study the singular structure around $\theta := \mathrm{Arg}(w) = 0$ by looking at the lateral resumations. By changing variable to $\zeta' = \zeta - \omega$, I may conclude [13]to evaluate the logarithmic integral.

$$(S_{\theta^+} - S_{\theta^-})\tilde{\phi}(z) = -ae^{-\omega z} - e^{-\omega z} \int_0^\infty d\zeta'\, e^{-z\zeta'} \hat{\psi}(\zeta'). \tag{1.112}$$

The first term picks up a minus sign because the contour given by $S_{\theta^+} - S_{\theta^-}$ is clockwise. When there is only one singularity in the direction θ, Equation (1.109) simplifies heavily. Plugging this into (1.25), gives

$$(S_{\theta^+} - S_{\theta^-})\tilde{\phi}(z) = S_{\theta^-}(e^{-\omega z}\Delta_\omega \tilde{\phi}(z)) \tag{1.113}$$

Comparing Eqations (1.112) and (1.113) will give us the alien derivative:

$$\Delta_\omega \tilde{\phi}(z) = -a - \tilde{\psi}(z). \tag{1.114}$$

Example 22. This example is taken from [44] and [42] and is to demonstrate the Leibniz rule in a simple example. Let

$$\hat{\phi}_1(\zeta) = \frac{a}{2\pi i(\zeta - \omega)}, \qquad \hat{\phi}_2(\zeta) = \frac{b}{2\pi i(\zeta - \omega)}, \tag{1.115}$$

where a, b, ω are non-zero parameters. Looking back to the previous example it is easy to see that

$$\Delta_\omega \tilde{\phi}_1 = -a, \qquad \Delta_\omega \tilde{\phi}_2 = -b. \tag{1.116}$$

[12]By the Leibniz rule of differentiation we mean that $\frac{d}{dx}(f(x)g(x)) = \left(\frac{d}{dx}f(x)\right)g(x) + f(x)\left(\frac{d}{dx}g(x)\right)$.

[13]Here I have used

$$\frac{1}{2\pi i}\int_\gamma f(z)\log(z)dz = -\int_0^\infty f(z)dz \tag{1.111}$$

To calculate $\Delta_\omega(\tilde{\phi}_1\tilde{\phi}_2)$ we must transition to the convolutive algebra:

$$\begin{aligned}\mathcal{B}(\tilde{\phi}_1\tilde{\phi}_2)(\zeta) = (\hat{\phi}_1 * \hat{\phi}_2)(\zeta) &= \frac{ab}{(2\pi i)^2}\int_0^\zeta d\xi\ \frac{1}{\xi-\omega}\frac{1}{\zeta-\omega-\xi} \\ &= \frac{ab}{(2\pi i)^2}\frac{1}{\zeta-2\omega}\int_0^\zeta d\xi\Big(\frac{1}{\xi-\omega}+\frac{1}{\zeta-\xi-\omega}\Big) \\ &= \frac{ab}{(2\pi i)^2(\zeta-2\omega)}2[\log(\zeta-\omega)-\log(-\omega)]\end{aligned} \tag{1.117}$$

The factor of 2 arises because the integrals coincidentally take the same value. We find that the convolution exhibits a simple pole at $\zeta = 2\omega$ and a logarithmic singularity at $\zeta = \omega$. To find $\Delta_\omega(\tilde{\phi}_1\tilde{\phi}_2)$ we must focus on the latter singularity, hence I will write

$$\mathcal{B}(\tilde{\phi}_1\tilde{\phi}_2)(\zeta) = \hat{\psi}(\zeta)\frac{\log(\zeta-\omega)}{2\pi i}, \tag{1.118}$$

where

$$\hat{\psi}(\zeta) = \frac{2ab}{2\pi i(\zeta-\omega)}. \tag{1.119}$$

Incidentally,

$$\hat{\psi}(\zeta) = b\hat{\phi}_1(\zeta) + a\hat{\phi}_2(\zeta) \tag{1.120}$$

Because performing a Borel transformation is linear, we are free to change from the convolutive model $\hat{\phi}(\zeta)$ to the multiplicative model $\tilde{\phi}(z)$ in Equation (1.120). I shall now use Example 21 on Equation (1.118):

$$\begin{aligned}\Delta_\omega(\tilde{\phi}_1\tilde{\phi}_2)(z) &= -\tilde{\psi}(z) \\ &= -b\tilde{\phi}_1(z) - a\tilde{\phi}_2(z) \\ &= (\Delta_\omega\tilde{\phi}_1(z))\tilde{\phi}_2(z) + \tilde{\phi}_1(z)(\Delta_\omega\tilde{\phi}_2(z)).\end{aligned} \tag{1.121}$$

In this simple example, we have thus verified the Leibniz rule of differentiation. It is also worth discussing the singularity at $\zeta = 2\omega$. If we were to apply the Leibniz rule to $\tilde{\phi}_1\tilde{\phi}_2$, we would find $\Delta_{2\omega}(\tilde{\phi}_1\tilde{\phi}_2) = 0$ because $\tilde{\phi}_{1,2}$ do not have singularities at $\zeta = 2\omega$. However, Equation (1.117) clearly indicates a singulary. This does not show any inconsistencies: it just shows that to study a singularity we must include all possible ways to get there. In the present case

$$\Delta_\omega\Delta_\omega(\tilde{\phi}_1\tilde{\phi}_2)(z) = -\Delta_\omega\tilde{\psi}(z) = 2ab \neq 0. \tag{1.122}$$

Example 23. This neat example is taken from [36] and shows how it possible to construct the Stokes automorphism from alien derivatives. Consider the following asymptotic expansion:

$$\tilde{\phi}(z) = \sum_{n=0}^{\infty}\frac{n!}{(n+1)A^n}z^{-n-1}. \tag{1.123}$$

Its Borel transform is given by

$$\hat{\phi}(\zeta) = -\frac{A}{\eta}\log(1 - s/A). \tag{1.124}$$

This can be rewritten as

$$\hat{\phi}(\zeta) = -\hat{\psi}(\zeta - A)\log(\zeta - A) + \log(-A)\frac{A}{s}, \tag{1.125}$$

with

$$\hat{\psi}(\zeta) = \frac{A}{\zeta + A}. \tag{1.126}$$

Hence, we can use our previous result of simple resurgent functions as in Example 21 and conclude that

$$\Delta_A\tilde{\phi}(z) = 2\pi i\hat{\psi}(z). \tag{1.127}$$

Moreover, using Example 1, we can deduce that

$$\tilde{\psi}(z) = \sum_{n=0}^{\infty}\frac{n!}{(-A)^n}z^{-n-1}. \tag{1.128}$$

We can even go on to compute the Stokes automorphism. Let us again place the singularity on the positive real axis: $\theta = \mathrm{Arg}(A) = 0$. Observe that the Borel transformation has only one singularity along this direction. Therefore higher power of the alien derivative vanish. Thus, using the definition of the Stokes automorphism:

$$\mathfrak{S}_0\tilde{\phi}(z) = \tilde{\phi}(z) + 2\pi i e^{-Az}\tilde{\psi}(z) \tag{1.129}$$

This behaviour is very typical for what one tends to see in resurgent analyses. If the singularity $A \in \mathbb{R}_{>0}$ is on the real line, the ambiguity is imaginary and exponentially suppressed.

1.A.2 Bridge Equation

In practice, one will need a clever way to find the alien derivatives to allow us to calculate the Stokes automorphism and hence the discontinuity. An important tool to this end is finding and solving the Bridge equation which will relate the alien derivates and the ordinary derivatives $\partial_z = \frac{\partial}{\partial z}$ and $\partial_\sigma = \frac{\partial}{\partial \sigma}$. In this section we focus on the case of a 1-parameter transseries, meaning we only consider 1 symbol that is non-perturbative in the perturbative parameter.

We shall start by observing that ∂_z commutes with $S_{\theta^\pm}$. From Equation (1.25) it is clear that $S_{\theta^+} = S_{\theta^-}\mathfrak{S}_\theta$, hence

$$S_{\theta^-}\mathfrak{S}_\theta\partial_z = S_{\theta^+}\partial_z = \partial_z S_{\theta^+} = \partial_z S_{\theta^-}\mathfrak{S}_\theta = S_{\theta^-}\partial_z\mathfrak{S}_\theta. \tag{1.130}$$

Therefore, ∂_z commutes with $\mathfrak{S}_\theta$. Define the pointed alien derivative as

$$\dot{\Delta}_w \tilde{\phi}(z) = e^{-wz} \Delta_w \tilde{\phi}(z). \tag{1.131}$$

Written in terms of pointed alien derivative Equation (1.109) becomes

$$\mathfrak{S}_\theta = \exp\Big(\sum_{w \in \mathrm{Sing}_w} \dot{\Delta}_w \Big), \tag{1.132}$$

hence ∂_z commutes with $\dot{\Delta}_w$. Imagine $\mathcal{F}(z, \sigma)$ is some transseries solution to an ODE. Because ∂_σ and $\dot{\Delta}_w$ commute with ∂_z, applying them to the ODE ensures that $\partial_\sigma \mathcal{F}$ and $\dot{\Delta}_w \mathcal{F}$ solve the same ODE (which may be different from the initial one). This means they must be proportional. This statement is better known as the bridge equation:

$$\dot{\Delta}_w \mathcal{F} = A_w(\sigma) \partial_\sigma \mathcal{F}, \tag{1.133}$$

where $A_w(\sigma)$ is a complex number and in general a power series in σ:

$$A_w(\sigma) = \sum_{n=0}^{\infty} A_n^{(w)} \sigma^n. \tag{1.134}$$

The coefficients A_w^k can be identified as the Stokes constants, also known as Stokes coefficients or Stokes multipliers.

Example 24. Let us study the Bridge equation for a single parameter transseries $\mathcal{F}(z, \sigma) = \sum_{l=0}^{\infty} \sigma^l F_l(z)$ which might look like

$$\dot{\Delta}_w \mathcal{F}(z, \sigma) = S_1 \partial_\sigma \mathcal{F}(z, \sigma), \tag{1.135}$$

for a single Stokes constant S_1. Next, suppose there is only a single singularity in the Stokes direction $\theta = \arg(w)$. Consequently

$$\mathfrak{S}_\theta \mathcal{F}(z, \sigma) = \exp(S_1 \partial_\sigma) \mathcal{F}(z, \sigma) = \mathcal{F}(z, \sigma + S_1). \tag{1.136}$$

Let us now study an extended example, which in many ways functions as the archetype for resurgence: the instanton ansatz. For concreteness, one might consider the Ricatti equation for some $a > 0$

$$\frac{\partial f}{\partial z} - af + \frac{1}{z^2} f^2 + \frac{1}{z} = 0. \tag{1.137}$$

It can be shown [42] that we may expect singularities of the solution at $-na$ for $n \geq 1$, hence we can solve this equation by taking an Ansatz of the form

$$\mathcal{F}(z, \sigma) = \sum_{l=0}^{\infty} \sigma^l F^{(l)}(z), \qquad F^{(l)}(z) = e^{-laz} \phi_l(z), \tag{1.138}$$

where ϕ_l is a formal power series in z^{-1}. σ is a resurgence parameter to keep track of the orders of the different instanton sectors. Applying Δ_{na} and ∂_σ to Equation (1.137), gives respectively

$$\begin{aligned} \partial_z(\Delta_{na} f) - a(\Delta_{na} f) + \frac{2}{z^2} f(\Delta_{na} f) = 0 \\ \partial_z(\partial_\sigma f) - a(\partial_\sigma f) + \frac{2}{z^2} f(\partial_\sigma f) = 0 \end{aligned} . \tag{1.139}$$

Note that $\Delta_{na} \frac{1}{z} = 0$ because $\frac{1}{z}$ is not singular around $z = na$. We can thus see explicitly that $\Delta_{na} f$ and $\partial_\sigma f$ satisfy the same ODE, so that they must be proportional and we can posit the bridge equation:

$$\dot{\Delta}_{na} \mathcal{F}(z, \sigma) = A_{na}(\sigma) \partial_\sigma \mathcal{F}(z, \sigma), \qquad A_{na}(\sigma) = \sum_{k=0}^{\infty} A_k^{(n)} \sigma^k. \tag{1.140}$$

Plugging in Equation (1.138) yields

$$\sum_{l=0}^{\infty} \Delta_{na} \sigma^l e^{-(n+l)az} \phi_l(z) = \sum_{l=0}^{\infty} \sum_{k=0}^{\infty} A_k^{(n)}(l) \sigma^{k+l-1} e^{-laz} \phi_l(z). \tag{1.141}$$

Matching powers of e^{az} yields

$$\Delta_{na} \sigma^l \phi_l(z) = \sum_{k=0}^{\infty} A_k^{(n)}(l+n) \sigma^{k+l+n-1} \phi_{l+n}(z). \tag{1.142}$$

Next, we must demand that the power of σ match on both sides, hence we need only the contribution for $k = 1 - n$. This gives the bridge equation[14]:

$$\Delta_{na} \phi_l(z) = A_{1-n}^{(n)}(l+n) \phi_{l+n}(z). \tag{1.143}$$

Because $A_k^{(n)}$ is defined only for $k \geq 0$ we must chose $n \leq 1$. We may define the Stokes constants as $A_n := A_{1-n}^{(n)}$ and since the instanton action is $S_0 = a$ we can connect with Equation 6.21 from [42] and Equation 4.10 from [44]:

$$\Delta_{na} \phi_k(z) = A_n(n+k) \phi_{n+k}(z) \quad \text{for} \quad n \leq 1 \tag{1.144}$$

Or, in other words

$$\dot{\Delta}_{na} \mathcal{F}(z, \sigma) = A_{na}(\sigma) \partial_\sigma \mathcal{F}(z, \sigma), \qquad A_{na}(\sigma) = A^n \sigma^{1-n} \quad \text{for} \quad n \leq 1. \tag{1.145}$$

For completion, it should be mentioned that in the above equation we set $\phi_i(z) = 0$ if $i < 0$. Because the alien derivative Δ_{na} vanishes for $n > 1$, the computation of the

[14] An observant reader may have noticed that the derivation of the bridge equation was dependent on the transseries ansatz Equation (1.138), but not directly on the Ricatti equation(1.137). This means that, for example, the MIS model (See [44] Section 4 for an introduction of the MIS model and refences therein.) which has the same transseries ansatz, has structurally the same bridge equation. However, the Stokes constants A_n are model-dependent.

Stokes automorphism along the positive real axis simplifies:

$$\mathfrak{S}_0 = \exp\left(\sum_{l=1}^{\infty} e^{-laz}\Delta_{la}\right) = \exp(e^{az}\Delta_a) = 1 + e^{az}\Delta_a + \frac{1}{2}e^{2az}\Delta_a^2 + \dots. \tag{1.146}$$

By using Equation (1.143) k times, we find

$$\Delta_a^k \phi_n = A_1^k \prod_{i=1}^{k}(n+i)\phi_{n+k} = A_1^k \binom{n+k}{n}\phi_{n+k}. \tag{1.147}$$

Therefore

$$\mathfrak{S}_0\phi_n = \sum_{k=0}^{\infty} A_1^k e^{-kaz}\binom{n+k}{n}\phi_{n+k}. \tag{1.148}$$

We can even compute the action of the Stokes automorphism on the whole transseries:

$$\begin{aligned}
\mathfrak{S}_0\mathcal{F}(z,\sigma) &= \sum_{l=0}^{\infty}\sigma^l e^{-laz}\mathfrak{S}_0\phi_l(z) \\
&= \sum_{l=0}^{\infty}\sum_{k=0}^{\infty}\sigma^l e^{-(l+k)az}A_1^k\binom{n+k}{n}\phi_{n+k} \\
&= \sum_{l=0}^{\infty}(\sigma + A_1)^l e^{-laz}\phi_l \\
&= \mathcal{F}(z,\sigma+A_1)
\end{aligned} \tag{1.149}$$

Remark 25. The bridge equations is also interesting on a conceptual level as it shows first signs of *resurgence*. This can be seen in the sense that action of the alien derivative returns data which was already present in the transseries. Hence, the non-perturbative ambiguities which are associates with the Stokes jump (as codified by the alien derivatives) depend on other properties of the original function. This can already be seen in Equation (1.133), but it is even more evident in the bridge equation (1.143) for the instanton transseries. It shows that alien derivatives (and thus the Stokes automorphism) connect different sectors of the transseries with each other.

So far, we have only considered the ambiguity along the positive real axis. Along the negative real axis we encounter a more difficult situation, since there are infinitely many non-vanishing alien derivatives Δ_{na} for $n \leq -1$. In this direction we find for the

Stokes automorphism

$$\begin{aligned}\mathfrak{S}_\pi &= \exp\Big(\sum_{l=1}^{\infty} e^{laz}\Delta_{-la}\Big)\\ &= 1 + e^{az}\Delta_{-a} + e^{2az}(\Delta_{-2a} + \frac{1}{!}\Delta_{-a}^2)+\\ &\quad + e^{3az}(\Delta_{-3a} + \frac{1}{2!}(\Delta_{-a}\Delta_{-2a} + \Delta_{-2a}\Delta_{-a}) + \frac{1}{3!}\Delta_{-a}^3) + \dots\\ &= 1 + \sum_{m=1}^{\infty} e^{maz}\sum_{k=1}^{n}\frac{1}{k!}\sum_{\substack{l_1,\dots,l_k\geq 1\\ \sum_{i=1}^k l_i = k}}\prod_{i=1}^{k}\Delta_{-l_i A}\end{aligned} \tag{1.150}$$

It should be noted that the order of the product

$$\prod_{i=1}^{k}\Delta_{-l_i a} = \Delta_{-l_1 a}\cdot\Delta_{-l_2 a}\cdot\ldots\cdot\Delta_{-l_k a} \tag{1.151}$$

is relevant because alien derivatives at different singularities do not commute. Let us act with the stokes automorphism on the asymptotic expansions and use the bridge equation (1.143) and find [36, 83]:

$$\mathfrak{S}_\pi\phi_n = \phi_n + \sum_{m=1}^{\infty} e^{maz}\sum_{k=1}^{n}\frac{1}{k!}f(n,k)\phi_{n-k}, \tag{1.152}$$

where I have isolated a numerical factor

$$\begin{aligned}f(n,k) &= \sum_{\substack{l_1,\dots,l_k\geq 1\\ \sum_{i=1}^k l_i = k}}\prod_{i=1}^{k}A_{-l_i}(n-\sum_{j=1}^{i}l_j)\\ &= \sum_{\gamma\in\Gamma(k,l)}\prod_{j=1}^{k}(n-\gamma_j)S_{-d\gamma_j}.\end{aligned} \tag{1.153}$$

Here the summation is over k-partitions of l: $\Gamma(k,l) = \{\gamma_i\in\mathbb{Z} : 0 = \gamma_0 \leq \ldots \leq \gamma_k \leq l\}$. The transitions to the second line is performed by setting $\gamma_i = l_i - l_{i-1}$ and $\gamma_0 = 0$. Moreover, I have defined $d\gamma_j = \gamma_j - \gamma_{j-1}(= l_j)$.

1.B Numerics

1.B.1 Richardson Transformation

The following modular block of code take in a sequence of numbers that one expects to converge and calculates its Richardson transforms

```
RichardsonDat[SerDat_, Rorders_] := Module[{rt, RTDat, TotDat},
    rt[s_, n_, m_] := rt[s, n, m] =
        rt[s, n + 1, m - 1] + n/m (rt[s, n + 1, m - 1] - rt[s, n, m - 1]);
```

```
    rt[s_, n_, 0] := SerDat[[n]];
    RTDat[m_] := Table[rt[SerDat, n, m], {n, 1, Length[SerDat] - m}];
    TotDat = Table[RTDat[Rorders[[i]]], {i, 1, Length[Rorders]}]
];
```

Notice that the recursive definition as implemented here saves the results for first Richardson Transformation and uses it for the second, which is used for the third , etc. This is important with recursive definition as otherwise this coefficients are calculated multiple times causing inefficiencies. However, in many circumstances the goal is to create plot or compute the final value of its convergence. This done using another simple function

```
PlotRTDataGuess[Data_, Orders_, Guess_, OptionsPattern[ListPlot]] :=
Module[{lp, line},
  lp = ListPlot[Data, PlotRange -> OptionValue[PlotRange]];
  line = Plot[Guess, {t, 0, 2 + (Data[[1]] // Length)}];
  Show[line, lp,
    PlotRange -> {{0, (Data[[1]] // Length)}, {0.8 Guess, 1.2 Guess}}]
]
```

When experimenting, and one does not wish to gain a quick insight, one can use

```
QuickRT[ListDat_] := Module[{MyDat},
  MyDat = RichardsonDat[ListDat, {0, 1, 2, 3}];
  {MyDat[[-1, -1]], PlotRTDataGuess[MyDat, {0, 1, 2, 3},
    MyDat[[-1, -1]]]}
]
```

To gain more control over the exact presentation, the following code was used to generate the plots of this thesis

```
PlotRT[ListDat_, Orders_, Guess_, ypltrange_, yaxislabel_] :=
 Module[{RTDat, lineplt, listplt},
  RTDat = RichardsonDat[ListDat, Orders];
  lineplt = Plot[Guess, {t, 0, 2 + (ListDat // Length)},
    PlotStyle -> {Gray}];
  listplt = ListPlot[RTDat,
    PlotRange -> {{0, 1 + Length@ListDat}, ypltrange},
    PlotStyle -> Directive[PointSize[0.02]],
    AxesStyle -> Directive[Thick, Black],
    TicksStyle -> Directive[Thick, Black, Larger],
    AxesLabel -> {Style["n", 16, Bold, Black],
        Style[yaxislabel, 16, Bold, Black]},
    AxesOrigin -> {0, ypltrange[[1]]}];
  Show[ listplt, lineplt]
]
```

1.B.2 Airy Function

In this appendix I present the code that produced Figure 1.4. Our first task shall be to convert the coefficients a_k^- into the coefficients c_k which in turn need to be converted to coefficients b_k:

```
rhs[n_, end_] := Sum[am[i] A^i Product[1/(n - r),
    {r, 1, i}], {i, 0, end}]
c[k_] := SeriesCoefficient[rhs[1/x, k], {x, 0, k}]
series[n_, k_] := Sum[c[i] n^(-i), {i, 0, k}]
b[k_] := SeriesCoefficient[
  series[m + 1, k]/series[m, k], {m, Infinity, k}]
```

We will furthermore need the following details:

```
A = 4/3;
a[n_] := N[1/(2 Pi) A^(-n)
    Gamma[n + 5/6] Gamma[n + 1/6]/n!];
ap[n_] := -a[n]
am[n_] := (-1)^n a[n]
```

To obtain Figure 1.4 one runs

```
f[n_] := ap[n + 1] A/(ap[n] n)
approx3[n_] := (f[n] - b[0] - b[2]/n^2) n^3
dat = N@Table[approx3[n], {n, 1, 30}];

PlotRT[dat, {0, 1, 2, 4}, -5/36, {-0.15, -0.1}, "␣"]
```

Here, `f[n]` is the LHS of Equation (1.99), `approx[n]` is the LHS of Equation (1.100) for $m = 2$, `s[n]` is the RHS of Equation (1.100) and `srt` is its 5-Richardson transformation.

1.B.3 Sine-Gordon Potential

For the plots of Section 1.5, I used the BenderWu package [81]

```
Needs["BenderWu`"]

Coefs = BWProcess@BenderWu[1/2 Sin[x]^2, x, 0, 100];
```

To find the convergence of the action 1.5 it is simply

```
difs = Differences@Ratios@N@Coefs;
QuickRT@difs
```

For Figure 1.6, one needs

```
f[n_] := (1/4)^n Gamma[n + 1]
Asymp = Table[f[n], {n, 0, Length@Coefs - 1}];
QuickRT@N[Coefs/Asymp]
```

And lastly for Figure 1.7:

```
subcoefs = N[Coefs + 2/Pi Asymp];
g[n_] := (2/Pi) (5/2) (1/4)^n Gamma[n]
SubAsymp = Table[g[n], {n, 0, Length@Coefs - 1}];
QuickRT[subcoefs/SubAsymp]
```

Chapter 2

Integrable Sigma Models

2.1 Integrability

This Chapter shall serve to introduce the models that will be discussed for the remainder of the thesis. We will be considering 2d models and discuss their integrable structures. In particular, some of these models may be considered σ-models with a particular target space.

In this first Section we shall focus on these integrable structures. In Section 2.2, we shall discuss in more depth a 2-parameter deformation of one of these models, called the *Yang-Baxter deformation*, that preserves the integrable structure of its parent. This shall form the basis of Chapter 3 in which we discuss certain instanton-like solutions of this model which will feature some resurgent aspects. Section 2.3, we consider the λ-deformed σ-model which will be extensively studied in Chapter 4. However, in this analysis we shall also be relying on the S-matrix of the model. The study of S-matrices of integrable models is particularly rich and is discussed in Section 2.4.

As a last stop before discussing the integrable structure of these models, let us briefly introduce the types of models that shall be discussed.

The most well-studied integrable models include the $SU(N)$ Gross-Neveu (GN) model, the $SU(N)$ principal chiral model (PCM) and the $O(N)$ vector model. Of all these models, the exact S-matrix is known which establishes the quantum and classical integrability of these models. We will give a brief introduction and definition. As all the models to follow are defined on a two-dimensional world-sheet, we generically parameterise their space-time coordinates by (t, x). The $SU(N)$ GN is a theory of N Majorana fermions ψ

$$S_{GN} = \frac{1}{\mathsf{t}} \int d^2x \left[i\bar{\psi} \cdot \partial\!\!\!/ \psi + \frac{\mathsf{t}^2}{8} (\bar{\psi} \cdot \psi)^2 \right]. \tag{2.1}$$

For a Lie group G, we can define the principal chiral model as a theory of a G-valued

field g. Typically, we will take $G = SU(N)$.

$$S_{PCM} = \frac{1}{2\pi \mathsf{t}} \int d^2x \, \mathrm{Tr} \left(\partial_\mu g \partial^\mu g^{-1} \right) . \tag{2.2}$$

The $O(N)$ vector model consists of a set of fields n valued in $\mathbb{R}^N$ constrained by $|n| = 1$ with an action

$$S_{O(N)} = \frac{1}{2\mathsf{t}} \int d^2x \, \partial_\mu n \partial^\mu n \, . \tag{2.3}$$

These theories are similar in the sense that the key input parameters include a coupling parameter t^2 and a size of the global symmetry group N. Moreover, all these theories are asymptotically free, which means their large energy scale dynamics can be studied perturbatively. At low energies, it is known these theories develop a mass gap. This is all to say, that despite their somewhat artificial 2d construction, they exhibit many of the features associated with 4d Yang-Mills theory.

For an extensive review of classical Liouville integrability in Hamiltonian systems and 2d integrable models we refer the reader to the lecture notes [84–88]. However, we will highlight some aspects here relevant to the remainder of the thesis.

Let us first introduce classical Liouville integrability of a finite dimensional system. Here we take the viewpoint of a classical phase space M endowed with a Poisson bracket[1]. A distinguished function $H : M \to \mathbb{R}$ on the phase space plays the role of the Hamiltonian and governs time evolution for other functions $F, G : M \to \mathbb{R}$ on the phase space. Such functions are thus said to be a *conserved charge* (also called *integral of motion*) if they satisfy

$$\frac{d}{dt} F := \{F, H\} = 0 \, . \tag{2.4}$$

Finding such conserved charges is not always easy but constitutes the main task of enquiries into integrable systems. Noether's theorem guarantees that any global symmetry of the system will generate such a conserved charge. However, some conserved charges are generated by symmetries that are not manifest from the on-set.

More generally from (2.4), two functions F, G on the phase space are said to be *in involution* (or *involutive*) if they satisfy $\{F, G\} = 0$. A $2n$-dimensional system is then said to be *Liouville integrable* if there exist n independent conserved charges F_k that are all mutually in involution. Rather than studying its equations of motions, integrable systems may be solved using some integrals and auxiliary equations. Moreover,

[1] In a $2n$-dimensional phase space, one might choose canonical variables q_i, p_i with $i = 1, \ldots, n$. The Poisson bracket for arbitary functions $F, G : M \to \mathbb{R}$ is given by

$$\{F, G\} = \frac{\partial F}{\partial q_i} \frac{\partial G}{\partial p_i} - \frac{\partial G}{\partial q_i} \frac{\partial F}{\partial p_i} \, .$$

The canonical coordinates satisfy $\{q_i, p_j\} = \delta_{ij}$ and $\{p_i, p_j\} = \{p_i, p_j\} = 0$. The Poisson bracket is anti-symmetric and satisfies the Jacobi relation.

A more general approach might be taken through endowing the phase space with a symplectic form ω, which is a closed, non-degenerate 2-form. In terms of the canonical coordinates it is given by $\omega = dq_i \wedge dp_i$. The non-degeneracy means that for any 1-form β, we can find a unique vector field V_β such that $i_{V_\beta}(\omega) = \beta$. We use this to define for any function F the vector field $X_F = X_{dF}$. The Poisson bracket is then given in terms of the inner product $\{f, g\} = \omega(X_f, X_g) = (i_{X_f}\omega)(X_g)$.

integrability is generally associated with an absence of chaos.

However, for this thesis we shall be interested in integrability in the (Quantum) Field Theory setting. As Field Theories have an infinite number of degrees of freedom, this means we will need to construct an infinite number of involutive conserved charges. We will first consider the classical integrability of these models before moving to the quantum (S-matrix) integrability in Section 2.4.

Although we shall restrict ourselves to 2d integrable models, it is good to note that integrability also exists in higher dimensional models. In particular, there is a lot of evidence of integrability in $\mathcal{N} = 4$ YM theory in 4d - for reviews see [89, 90] and references therein. Although its integrable structure, through Heisenberg spin chains, is different from the one that applies to 2d models, its holographic dual $AdS_5 \times S^5$ is again integrable as a σ-model.

Finally, we will now turn to the discussion of integrability in 2d QFTs. The motto shall be the same as in the finite dimensional case. However, because our systems now exhibits infinitely many degrees of freedom, our goal shall be to construct infinitely many conserved charges.

The main object of interest is the *Lax connection* $L(z) = L_x(z)dx + L_t(z)dt$ which is a matrix-valued 1-form that depends on a spectral parameter z. Recall that (t, x) are the coordinates on the world-sheet. We require that the Lax connection satisfies a zero curvature condition

$$dL(z) - L(z) \wedge L(z) = 0\,, \tag{2.5}$$

or concretely

$$\partial_t L_x(z) - \partial_x L_t(z) + [L_x(z), L_t(z)] = 0\,. \tag{2.6}$$

In addition, we demand that the zero-curvature condition of the Lax connection encodes the equations of motion and any Bianchi identities of the system. We will use the Lax connection to construct a *Lax pair*. Its construction is not unlike that of a Wilson line. The flatness of the Lax connection guarantees that the construction is invariant under continuous transformations. We compactify a spatial direction by imposing a boundary condition $\phi(x + L) = \phi(x)$ for all the fields and construct the Wilson line around the spatial S^1 defined by

$$\begin{aligned} T(z) &= \overleftarrow{P} \exp \int_0^L L_x(z)\,, \\ M(z) &= L_t(z)\big|_{x=0}\,. \end{aligned} \tag{2.7}$$

Notice that the Lax still depends on t, it satisfies

$$\frac{d}{dt} T(z) = [M(z), T(z)]\,. \tag{2.8}$$

This allow us to define a set of conserved charges

$$F_k = \mathrm{Tr}(T(z)^k)\,. \tag{2.9}$$

The crucial point is that these charges are conserved for any value of the spectral parameter. Hence expanding around a particular value of the spectral parameter yields an infinite tower of conserved charges.

To guarantee that these conserved charges are in involution one requires the construction of a *classical r-matrix*. To explain its role we employ a tensor product notion where we take tensor product of the algebra in which the Lax pair lives. We use a subscript notation letting $A_1 = A \otimes \mathbf{1}$ and $A_2 = \mathbf{1} \otimes A$ and $r_{12} = r^{ij} t_i \otimes t_j$, where t_i are generators of the Lie algebra. Using this tensor notation for $T(z)$ in Equation (2.7), we introduce T_1 and T_2. The classical r-matrix then satisfies

$$\{T_1(z_1), T_2(z_2)\} = [r_{12}(z_1 - z_2), T_1(z_1) \otimes T_2(z_2)]\,. \tag{2.10}$$

Moreover, the classical r-matrix is anti-symmetric $r_{12}(z) = -r_{12}(-z)$ and satisfies the *classical Yang-Baxter equation*

$$[r_{12}, r_{23}] + [r_{12}, r_{13}] + [r_{13}, r_{23}] = 0\,, \tag{2.11}$$

where I have abbreviated $r_{ij} = r_{ij}(z_i - z_j)$. A large portion of the study of integrable systems in fact through the different types of solutions of classical r-matrices and their classifications - see [86] and references therein.

In sections 2.2 and 2.3 we shall review two such integrable models in more detail. The two models discussed will then form the main topic of investigation in Chapters 3 and 4 respectively. In Section 2.4 we will review some aspect of quantum integrability with a focus towards those models treated more in depth.

2.2 Bi-Yang-Baxter Deformed PCM

In this section we shall review some basic properties of the principal chiral model (PCM) and the Yang-Baxter (YB) deformations.

2.2.1 Lagrangian

The action of the undeformed PCM is

$$S_{PCM} = \frac{1}{2\pi \mathfrak{t}} \int d^2\sigma\, \mathscr{L}[g]\,, \quad \mathscr{L}[g] = \mathrm{Tr}\big(g^{-1}\partial_+ g g^{-1}\partial_- g\big)\,. \tag{2.12}$$

Here, g is a map from the world-sheet into a group manifold G. The integral is over some world-sheet, which is spanned by light cone coordinates $\sigma_\pm = \frac{1}{2}(t \pm x)$. We will later transition to a Euclidean signature with holomorphic coordinates $z = \frac{1}{2}(t + ix)$ and $\bar{z} = \frac{1}{2}(t - ix)$. Derivatives with respect to light cone coordinates are denoted respectively by $\partial_\pm$. Note that $\partial_\pm g$ lives in the tangent space and is a Lie algebra $\mathfrak{g}$ valued form such that $g^{-1}\partial_\pm g$ is the pull back to the world sheet of the Maurer-Cartan one-form.

We will be considering a system with a bi-Yang-Baxter deformation. To define this

theory we introduce the Yang-Baxter operator R, which satisfies the modified Yang-Baxter equation

$$[RA, RB] - R([RA, B] + [A, RB]) = [A, B]\,, \quad \forall A, B \in \mathfrak{g}\,. \tag{2.13}$$

Studies of the solutions to this Equation have been conducted by [91, 92]. The existence of the operator R implies that we can define a new Lie bracket which satisfies the Jacobi identity and is anti-symmetric (i.e. it defines a homomorphism of Lie algebras)

$$[A, B]_R := [RA, B] + [A, RB]\,. \tag{2.14}$$

In this paper, we will specialise to the special case $G = SU(2)$ and we choose a basis $t_i = \frac{1}{\sqrt{2}}\sigma_i$ of the algebra. A concrete solution for the Yang-Baxter operator can then be given by [87, 93, 94]

$$R = \begin{pmatrix} 0 & -1 & 0 \\ 1 & 0 & 0 \\ 0 & 0 & 0 \end{pmatrix}. \tag{2.15}$$

Furthermore, we let $\mathrm{Ad}_g(u) = gug^{-1}$ denote the adjoint operator and we define $R^g = \mathrm{Ad}_{g^{-1}} \circ R \circ \mathrm{Ad}_g$. The action with deformation parameters η and ζ, which we sometimes combine into $\chi_\pm = \zeta \pm \eta$, is given by

$$S_{\zeta,\eta} = \frac{1}{2\pi\mathfrak{t}} \int d^2\sigma\, \mathscr{L}[g]\,, \quad \mathscr{L}[g] = \mathrm{Tr}\left(g^{-1}\partial_+ g \frac{1}{1 - \eta R - \zeta R^g} g^{-1}\partial_- g \right). \tag{2.16}$$

We will use the shorthand notations

$$\begin{aligned} R_\pm &= g^{-1}\partial_\pm g \\ O_\pm &= (1 \pm \eta R \pm \zeta R^g)^{-1}, \\ J_\pm &= \mp O_\pm R_\pm, \end{aligned} \tag{2.17}$$

so that the Lagrangian could be compactly understood as

$$\mathscr{L} = \mathrm{Tr}(R_+ J_-). \tag{2.18}$$

Moreover, we find the field equations can be formulated as [95]

$$\partial_+ J_- + \partial_- J_+ + \eta[J_-, J_+]_R = 0. \tag{2.19}$$

Under a $(t, x) \to (t, -x)$ transformation on the world sheet, $\partial_\pm \to \partial_\mp$. In addition we get a minus sign appearing from the metric and lastly $R \to -R$. We can therefore see that the following Action is equivalent

$$S_{\eta,\zeta} = -\frac{1}{2\pi\mathfrak{t}} \int dz^2\, \mathrm{Tr}(R_- J_+). \tag{2.20}$$

In other words, $O_- = O_+^T$. The sign that comes with this dual description is the reason for including a sign in the definition of the current J_+ in (2.17).

2.2.2 Classical Lax Structure

Klimčík showed in [96] first that the 1-parameter Yang-Baxter deformed model (i.e. the case where $\zeta = 0$) was integrable, before showing in [95] the integrability of the 2-parameter deformation. They found the following Lax pair with spectral parameter, λ,

$$L_\pm(\lambda) = \eta(R - i)J_\pm + \frac{\left(2i\eta \pm (1 + \eta^2 - \zeta^2)\right)}{\lambda \pm 1} J_\pm \,, \tag{2.21}$$

which satisfies a zero-curvature condition

$$\partial_+ L_-(\lambda) - \partial_- L_+(\lambda) + [L_-(\lambda), L_+(\lambda)] = 0 \,, \qquad \forall \lambda \in \mathbb{C} \,. \tag{2.22}$$

This condition both follows from and implies the equation of motions and the Bianchi identity corresponding to the action (2.16).

2.2.3 The Critical Line

As already noted by Klimčík [95], the above formulation hides a certain symmetry between η and ζ. In particular, when $\eta = \zeta \equiv \varkappa$, a situation that we shall refer to as the *critical line*, there is a restoration of a $g \to g^{-1}$ symmetry. Using the definitions of Ad_g and R^g, it is easy to verify the Lagrangian for the action (2.16), can be written in two equivalent ways. Either it can be written in terms of left invariant forms, $g^{-1}\partial_\pm g$, as

$$\mathscr{L}^L_{\zeta,\eta}[g] = \mathrm{Tr}\left(g^{-1}\partial_+ g \frac{1}{1 - \eta R - \zeta R^g} g^{-1}\partial_- g \right) , \tag{2.23}$$

or else in terms of right invariant forms, $\partial_\pm g g^{-1}$, as

$$\mathscr{L}^L_{\zeta,\eta}[g] = \mathscr{L}^R_{\zeta,\eta}[g] := \mathrm{Tr}\left(\partial_+ g g^{-1} \frac{1}{1 - \eta R^{g^{-1}} - \zeta R} \partial_- g g^{-1} \right) . \tag{2.24}$$

However, if we perform the transformation $g \to g^{-1}$ of the left acting Lagrangian, we see that

$$\mathscr{L}^L_{\zeta,\eta}[g^{-1}] = \mathrm{Tr}\left(\partial_+ g g^{-1} \frac{1}{1 - \eta R - \zeta R^{g^{-1}}} \partial_- g g^{-1} \right) = \mathscr{L}^R_{\eta,\zeta}[g] = \mathscr{L}^L_{\eta,\zeta}[g] \,. \tag{2.25}$$

Therefore we see that along the critical line $\mathscr{L}^L_{\varkappa,\varkappa}[g^{-1}] = \mathscr{L}^L_{\varkappa,\varkappa}[g]$. This enhanced symmetry has profound effects on the physics, and we shall revisit this scenario many times in the rest of the paper. We shall see in particular that the perturbative structure changes discontinuously on and off the critical line.

The critical line also has a second important feature: the $SU(2)$ model on the critical line $\eta = \zeta$ is equivalent to the single parameter η-deformation of the sigma-model on S^3 viewed as a coset $SO(4)/SO(3)$ following the construction in [97, 98]. This is quite

useful since it allows the current study, restricted to the critical line, to have relevance to the behaviour of the deformations of general η-deformed cosets, and potentially to the full η-deformation of the $AdS_5 \times S^5$ string.

The case of $\eta = -\zeta$, which we describe as the co-critical line, will be discussed shortly in the context of the $SU(2)$ model.

2.2.4 Classical Symmetries

The undeformed PCM Lagrangian with group G has a global $G_L \times G_R$ symmetry acting as $g \mapsto h_L g h_R$. The two deformations break this symmetry down to an abelian subgroup. We shall not be going into depth on the topic of quantum algebras. However, it is good to know, that the breaking of the classical symmetry is augmented by non-local charges that furnish a Possion-bracket realisation of the q-deformed quantum group $\mathcal{U}_{q_L}(\mathfrak{g}) \times \mathcal{U}_{q_R}(\mathfrak{g})$. For the single parameter Yang-Baxter, or η-deformation, for which only G_L is q-deformed and G_R is preserved, this was demonstrated first in the context of $G = SU(2)$ in [99] and shown in general [100]. The quantum group structure in the case of two-deformation parameters studied here was described in [97]. Although beyond the current scope, it would be remiss not to mention that Lagrangian descriptions exist for quantum group deformed symmetries of the full $AdS_5 \times S^5$ superstring viewed as a $\mathbb{Z}_4$ graded super-coset [98]. Here q is real, but somewhat parallel to this have been the construction of q a root-of-unity integrable deformations of the $AdS_5 \times S^5$ superstring [101] which extend the bosonic λ-deformations introduced in [102].

Let us study this in detail for $G = SU(2)$ in Minkowskian signature. We will parametrise the group element through Euler angles by

$$g = \begin{pmatrix} \cos(\theta) e^{i\phi_1} & i \sin(\theta) e^{i\phi_2} \\ i \sin(\theta) e^{-i\phi_2} & \cos(\theta) e^{-i\phi_1} \end{pmatrix} , \tag{2.26}$$

where θ, ϕ_1 and ϕ_2 are fields taking values in $[0, \pi]$, $[0, \pi]$ and $[0, 2\pi]$ respectively. Under the $U(1)_L \times U(1)_R$ action $\delta g = \epsilon_L t_3 \cdot g + \epsilon_R g \cdot t_3$, such that $\delta\phi_1 + \delta\phi_2 = \epsilon_L$ and $\delta\phi_1 - \delta\phi_2 = \epsilon_R$.

The charges are then given by

$$\mathfrak{Q}^3_{L/R} = \int d^\sigma \mathrm{j}^3_{L/R} , \tag{2.27}$$

with

$$\begin{aligned} \mathrm{j}^3_L &= \frac{1}{\Delta(\theta)} \left(-\eta \sin(2\theta)\theta' + \cos(\theta)^2 a_+(\theta)\dot{\phi}_1 + \sin(\theta)^2 a_-(\theta)\dot{\phi}_2 \right) , \\ \mathrm{j}^3_R &= -\frac{1}{\Delta(\theta)} \left(\zeta \sin(2\theta)\theta' + \cos(\theta)^2 b_+(\theta)\dot{\phi}_1 + \sin(\theta)^2 b_-(\theta)\dot{\phi}_2 \right) , \end{aligned} \tag{2.28}$$

the corresponding currents. Here primes and dots denote spatial and temporal derivat-

ives respectively and for convenience we have defined

$$\begin{aligned} a_{\pm}(\theta) &= \zeta^2 + \eta(\zeta \pm \eta)\cos(2\theta) \pm \zeta\eta + 1\,, \\ b_{\pm}(\theta) &= \zeta(\zeta \pm \eta)\cos(2\theta) + \zeta\eta \pm \eta^2 \pm 1\,, \\ \Delta(\theta) &= \zeta^2 + \eta^2 + 1 + 2\zeta\eta\cos(2\theta)\,. \end{aligned} \tag{2.29}$$

We will later return to these Noether currents when we perform a twisted reduction of the theory.

Whilst these $U(1)$ currents define the only *local* Noether charges $\mathfrak{Q}^3_{L/R}$, a crucial property of these models [100] is that they exhibit some non-local conserved charges $\mathfrak{Q}^{\pm}_{L/R}$ which furnish the algebra under Poisson brackets

$$\begin{gathered} \{\mathfrak{Q}^+_{L/R}, \mathfrak{Q}^-_{L/R}\} = i\frac{q_{L/R}^{\mathfrak{Q}^3} - q_{L/R}^{-\mathfrak{Q}^3}}{q_{L/R} - q_{L/R}^{-1}}\,, \quad \{\mathfrak{Q}^{\pm}_{L/R}, \mathfrak{Q}^3_{L/R}\} = \pm i\mathfrak{Q}^{\pm}_{L/R}\,, \\ q_L = \exp\frac{2\pi}{\sigma_\zeta}\,, \quad q_R = \exp\frac{2\pi}{\sigma_\eta}\,, \end{gathered} \tag{2.30}$$

where $\sigma_{\eta,\zeta}$ are given by Equation (2.36). In this way the full $G_L \times G_R$ symmetry is recovered, but deformed to have the structure of (a classical version of) a quantum group.

2.2.5 Maillet Algebra, Twist Function and Classical Symmetries

To understand how the above charge algebra arises it is useful to consider the gauge transformed Lax

$$\tilde{L}_{\pm}(\lambda) = gL_{\pm}g^{-1} + \partial_{\pm}gg^{-1}\,, \tag{2.31}$$

from which we define its spatial component $\tilde{L} \equiv \tilde{L}_+ - \tilde{L}_-$, for which we will compute its Maillet algbera (we work here with the "right" Lax). We employ the same Tensor notation as in the end of Section 2.1.

$$\begin{aligned} \{\tilde{L}_1(x_1,\lambda_1), \tilde{L}_2(x_2,\lambda_2)\} = [r_{12}(\lambda_1,\lambda_2), \tilde{L}_1(x_1,\lambda_1)]\delta_{12} - [r_{21}(\lambda_2,\lambda_1), \tilde{L}_2(x_1,\lambda_1)]\delta_{12} \\ -(r_{12}(\lambda_1,\lambda_2) + r_{21}(\lambda_2,\lambda_1))\partial_1\delta_{12}\,, \end{aligned} \tag{2.32}$$

where r_{12} is the classical r-matrix. The term proportional to the Delta function is the non-ultra local piece.

Here the Lax is not of the form in which the r_{12} is prescribed by a twist function, indeed r_{12} in the above has non-trivial dependence on the canonical coordinates, although it can be thought of as a gauge fixing of a Lax that does have a twist function.

The non-ultra local piece however is independent of coordinates and special features are present at locations where $\lambda_1 = \lambda_2 = \lambda^\star$ such that the non-ultra local piece vanishes.

In the case at hand we have

$$(r_{12}(\lambda_1,\lambda_2)+r_{21}(\lambda_2,\lambda_1)) = f(\lambda_1,\lambda_2)\sum_i T_i\otimes T_i + g(\lambda_1,\lambda_2)\sum_i T_i\otimes R(T_i) \qquad (2.33)$$

with

$$\begin{aligned} f(\lambda_1,\lambda_2) &= \frac{4\pi\mathsf{t}\left(\zeta^2-(\eta+i\lambda_1)(\eta+i\lambda_2)\right)\left(\left(\zeta^2+1\right)(\lambda_1+\lambda_2)-\eta\left(\eta(\lambda_1+\lambda_2)+2i\left(\lambda_1\lambda_2+1\right)\right)\right)}{\left(\lambda_1^2-1\right)\left(\lambda_2^2-1\right)} \\ g(\lambda_1,\lambda_2) &= \frac{4\pi\mathsf{t}\zeta\left(\lambda_1-\lambda_2\right)\left(\left(\zeta^2+1\right)(\lambda_1+\lambda_2)+\eta^2\left(-(\lambda_1+\lambda_2)\right)-2i\eta\left(\lambda_1\lambda_2+1\right)\right)}{\left(\lambda_1^2-1\right)\left(\lambda_2^2-1\right)} \end{aligned} \qquad (2.34)$$

for which the special values $\lambda_1=\lambda_2=\lambda_\pm^\star=i(\eta\mp\zeta)$ are such that $f=g=0$.

We evaluate now the Lax at these special points to discover

$$\tilde{L}(x,\lambda_\pm^\star) = \mp 2i\alpha_L \mathrm{j}_L^3(x)T_3 + 4\alpha_L \mathrm{j}_L^\pm(x)T_\pm \qquad (2.35)$$

such that we recover the currents entering in the above. The flatness of the Lax at these values of the spectral parameter allows one to establish the conservation laws that lead to the dressed currents $\mathfrak{J}^\pm$.

2.2.6 RG Equations

The sigma-model is renormalisable in the couplings t,η,ζ with RG invariants [103],

$$\sigma_\eta = \frac{1}{\mathsf{t}\eta}\,, \qquad \sigma_\zeta = \frac{1}{\mathsf{t}\zeta}\,, \qquad (2.36)$$

and a non trivial flow[2] (at one-loop)

$$\frac{d}{d\log\mu}\mathsf{t} = -\frac{1}{2}\mathsf{t}^2(1+(\eta+\zeta)^2)(1+(\eta-\zeta)^2)\,, \qquad (2.37)$$

whose parametric solution is given by

$$\log\mu/\mu_0 = \frac{\sigma_\zeta+\sigma_\eta}{2}\arctan\left(\frac{\sigma_\eta\sigma_\zeta\mathsf{t}}{\sigma_\zeta+\sigma_\eta}\right) - \frac{\sigma_\zeta-\sigma_\eta}{2}\arctan\left(\frac{\sigma_\eta\sigma_\zeta\mathsf{t}}{\sigma_\zeta-\sigma_\eta}\right)\,. \qquad (2.38)$$

There is a single real fixed point at the origin $\mathsf{t}=\eta=\zeta=0$ but in the complex plane there are lines of fixed points

$$\eta+\zeta=\pm i\,, \quad \eta-\zeta=\pm i\,. \qquad (2.39)$$

The critical line is preserved by the RG flow and, analytically continued, intersects these at a special fixed point

$$\eta=\zeta=\frac{i}{2}\,. \qquad (2.40)$$

[2]Here we are presenting the result for $SU(2)$ but the change to $SU(N)$ simply introduces a factor of the the quadratic Casimir on the right hand side of the flow.

To understand the significance of the RG flows and the imaginary fixed points it is helpful to consider the case of the $SU(2)$ model. The analysis of [97] makes three important observations relevant to us.[3] The bi-Yang-Baxter Lagrangian can be viewed as a non-linear sigma model in a target space equipped with a pure gauge B-field and metric given by

$$\begin{aligned} ds^2 = \frac{1}{1+\chi_+^2(1-r^2)+\chi_-^2 r^2}\Bigg[\frac{dr^2}{1-r^2} + (1-r^2)(1+\chi_+^2(1-r^2)d\phi_2^2 \\ +r^2(1+\chi_-^2 r^2)d\phi_1^2 + 2\chi_-\chi_+ r^2(1-r^2)d\phi_1 d\phi_2\Bigg], \end{aligned} \tag{2.41}$$

in which we have used the Euler angles of Equation (2.26) and defined $r = \sin\frac{\theta}{2}$. The first observation is that demanding that the metric be regular and real allows not only $\chi_\pm = \zeta \pm \eta \in \mathbb{R}$ but also pure imaginary[4] $\chi_\pm = ik_\pm$ with $\mid k_\pm \mid < 1$.

Next we can see from the metric that there is, in addition to the $\mathbb{Z}_2$ action $g \to g^{-1}$ with $\eta \leftrightarrow \zeta$, a second $\mathbb{Z}_2$ invariance

$$\theta \to \theta + \pi\,, \quad \phi_1 \to \phi_2\,, \quad \phi_2 \to \phi_1\,, \quad (\zeta,\eta) \to (\zeta,-\eta)\,. \tag{2.42}$$

In the case of real parameters, which we will mostly consider here, this allows us to restrict our attention to $\eta \in \mathbb{R}^+$. Note also that this transformation maps the critical $\eta = \zeta$ line to the co-critical $\eta = -\zeta$ line.

Finally, and most remarkably, along the imaginary RG fixed points, the target space geometry coincides[5] with that of an $SU(1,1)/U(1)$ gauged WZW CFT together with a free $U(1)$ boson. The interpretation of this fixed point is the same on the critical line[6] (which recall matches the η-deformation of S^3 viewed as a coset) at the point $\eta = \zeta = \frac{i}{2}$. When considered in the context of the η-deformation of the $AdS_3 \times S^3$ superstring, the same limit of imaginary deformation parameter is shown to give rise to the Pohlmeyer reduced theory by [104].

Although outside of our present concerns, we note that when the bi-Yang-Baxter deformation is combined with an appropriate AdS_3 factor and RR fields, it has been given a supergravity embedding [105].

2.3 λ-Deformations

Although the λ-deformed theories have been around for a long time [106–108], it is only more recently that they have received more attention. Although the early works were computationally hard, and even then only applied to an $SU(2)$ case, it is the construction

[3] We thank Ben Hoare for communications on these points.

[4] In general such imaginary parameters would result in an imaginary two-form, but in the SU(2) case this two-form is pure gauge.

[5] With $\chi_\pm = ik_\pm$ this limit is obtained by setting $k_- = 1$ and shifting $\Phi \to \Phi' + k_+\Psi$, such that Ψ parameterises the free $U(1)$ factor.

[6] Even if η and ζ are complexified, we will refer to $\eta = \zeta$ as the critical *line* in the complex sense, rather than the critical plane.

of Sfetsos [102] that shed more light on the theory in a more general case. There is now a quantum group structure understanding of the theory, we know its S-matrix and it seems to lead to consistent world-sheet theory at the quantum level [101, 109, 110]. Moreover, its RG-flow equation is known [111–113]

At its heart, the λ-model provides an integrable interpolation between the conformal WZW-model [114] and the non-abelian T-Duality of the PCM. The non-abelian T-dual of a theory, despite its abelian cousin, is not a true duality of the string theory. However, it does provide a way to generate new super-gravity backgrounds and has been very successful as such [115–117]. In this spirit, it was also that the λ-model was understood as a super-gravity with RR-fluxes [118]. In fact as was shown by a series of papers [103, 119–122], the λ-model is the (analytically continued) non-abelian T-dual of the Yang-Baxter deformed PCM.

First we sketch the construction of the non-abelian T-dual of the PCM using the Buscher procedure [123]. We start with the action of the PCM (2.2)[7][8]

$$S_{\text{PCM}}[g] = -\frac{1}{4\pi\mathfrak{t}} \int d^2\sigma \, \text{Tr}\left(g^{-1}\partial_+ g g^{-1}\partial_- g \right) \tag{2.43}$$

and upgrade the left symmetry $g \to hg$ to a gauge symmetry. This means we introduce a gauge field A and we upgrade the derivative to a covariant derivative $d \to D = d + A$. The gauged PCM has an action

$$S_{\text{gPCM}}[g, A] = -\frac{1}{4\pi\mathfrak{t}} \int d^2\sigma \, \text{Tr}\left(g^{-1} D_+ g g^{-1} D_- g \right) \tag{2.44}$$

We thus obtain a local symmetry $g \to h^{-1}g$ and $A \to h^{-1}dh + h^{-1}Ah$. To fix the gauge symmetry, we demand that the connection of the gauge field is flat (i.e. the gauge field is pure gauge). This is implemented by introducing a Lagrange-multiplier gauge field ν and adding a term $-\text{Tr}(\nu F_{+-})$ to the Lagrangian. Integrating out the field ν enforces that the field strength F_{+-} vanishes and we recover the original PCM after gauge-fixing $g = 1$. However, if instead we integrate out the gauge fields A, after gauge fixing $g = 1$, we obtain the non-abelian T-dual. In this picture, the field ν becomes the fundamental field.

We will now review the construction by [102] which is a modification of the Buscher procedure. We will specialise to the case of $SU(N)$ PCM. A more recent introduction to the topic, in the context of non-abelian T-duality was provided by [88]. The key modification is that instead of adding a Lagrange multiplier term, we add a gauged

[7] We use the same light cone coordinates $\sigma_\pm = \frac{1}{2}(t \pm x)$ as in Section 2.2.1. Derivatives with respect to light cone coordinates are denoted by $\partial_\pm$.

[8] In the literature, one typically uses κ instead of r. However, we will reserve the symbol κ for a different purpose.

WZW term. Recall that the WZW model is given by

$$S_{\mathrm{WZW},k}[g] = -\frac{k}{2\pi}\int_\Sigma d^2\sigma\ \mathrm{Tr}\left(g^{-1}\partial_\mu g g^{-1}\partial^\mu g\right) - \frac{ik}{6\pi}\int_{M_3} H$$
$$H = \mathrm{Tr}\left(g^{-1}dg\right)^3 . \tag{2.45}$$

Here g is extended to a 3-manifold M_3 with boundary $\partial(M_3) = \Sigma$. It is possible to extend this map because the homotopy group $\pi_2(G)$ is trivial for any compact Lie group G. However, there is not a a unique extension. To ensure that the model does not depend on the choice of extension, we use that the path integral is invariant under a phase shift $S \to S + 2n\pi i$ for integers n (thus explaining the need for the i in the action of the WZW term). As an example, we take $\Sigma = S^2$ and $M_3 = B$ its interior. If we had two topologically different extensions $g, \tilde{g}$ (with 3-forms $H, \tilde{H}$), the difference of their actions could be defined on two copies of B with the boundaries identified, which is homeomorphic to S^3. Letting $\hat{H}$ be that extension onto S^3, we have that

$$\frac{i}{2\pi}k\left(\int_B H - \int_B \tilde{H}\right) = \frac{ik}{2\pi}\int_{S^3}\hat{H} = 2\pi i n k$$

The maps are hence characterised by $\pi_3(G) = \mathbb{Z}$. The 3-form H is integral, and a different extensions gives a contribution of $2\pi nk$ to the action. The path integral is thus single valued if $k \in \mathbb{Z}$.

We will consider the diagonal symmetry $g \to h^{-1}gh$ and gauge it [124, 125]. This leads to an action $S_{\mathrm{gWZW},k}[g, A]$. To construct the λ-model we combine a gauged PCM and a gauged WZW model like

$$S_{\lambda,k}[g, \tilde{g}, A] = S_{\mathrm{gPCM}}[\tilde{g}, A] + S_{\mathrm{gWZW}}[g, A] \tag{2.46}$$

Notice that the two models are coupled through the fact that they are gauged by the *same gauge field*. The procedure is concluded by gauge fixing $\tilde{g} = 1$ and integrating out the gauge field A using its on-shell values as was done to construct the non-abelian T-dual. The on-shell values of the gauge field are given by

$$A_+ = \lambda(1 - \lambda\mathrm{Ad}_g)^{-1}R_+ , \qquad A_- = -\lambda(1 - \lambda\mathrm{Ad}_{g^{-1}})^{-1}L_- , \tag{2.47}$$

where we defined $R_\pm = \partial_\pm g g^{-1}$ and $L_\pm = g^{-1}\partial_\pm g$. The operator Ad_g, as in Section 2.2.1, is the adjoint action $\mathrm{Ad}_g(T_a) = gT_a g^{-1}$. The namesake of the model λ is given by

$$\lambda = \frac{k}{k + \mathsf{t}^{-1}} . \tag{2.48}$$

Integrating out the gauge field then yields the action

$$S_{\lambda,k}[g] = S_{\mathrm{WZW},k}[g] + \frac{k\lambda}{\pi}\int_\Sigma R_+^a(1 - \lambda\mathrm{Ad}_g)^{-1}L_-^a , \tag{2.49}$$

The equations of motion can be stated as

$$\partial_{\pm} A_{\mp} = \pm[A_+, A_-]\,. \tag{2.50}$$

Here $A_\pm$ is the value of the gauge field in terms of g obtained by integrating out the gauge field (2.47). The equations can re-cast by introducing a Lax connection

$$L_\pm(z) = -\frac{2}{1+\lambda}\frac{A_\pm}{1\mp z}\,, \tag{2.51}$$

with zero curvature [102, 110]

$$\partial_+ L_-(z) - \partial_- L_+(z) + [L_-(z), L_+(z)] = 0\,, \qquad \forall z \in \mathbb{C}\,. \tag{2.52}$$

This gives an integrable structure to the λ-deformed model.

The parameter λ given by Equation (2.48) varies from 0 to 1 and we shall now discuss what happens in each of those limits. We will now study its flow under RG. The β-equation of the $SU(N)$-model is known to all orders in λ, but leading in $\frac{1}{k}$ and is given by [111–113]

$$\mu\frac{d\lambda}{d\mu} = \beta(\lambda) = -\frac{2N}{k}\left(\frac{\lambda}{1+\lambda}\right)^2\,. \tag{2.53}$$

Let us study what happens in the limit as $\lambda \to 0$ and $\lambda \to 1$.

In the case of $\lambda \to 1$, we can achieve this by taking $k \to \infty$. If the group element is expanded as $g = 1 + \frac{i}{k} g^a t_a$, the action $S_{\text{gWZW},k}$ reduces to the Lagrange multiplier term $-\operatorname{Tr}(\nu F_{+-})$. This recovers the Buscher procedure described above. Hence, in this limit, we recover the non-abelian T-dual of the PCM. This limit constitutes the IR limit of the model.

In the $\lambda \to 0$, or $k \ll r^2$, we obtain an action

$$S_{\lambda,k}[g] = S_{\text{WZW},k}[g] + \lambda \int R^a_+ L^a_- + \mathcal{O}(\lambda^2)\,, \tag{2.54}$$

which can be understood as a current-current deformation of the WZW model. However, it is not a marginal deformation, but marginally relevant as it moves away from the WZW theory located in the UV. This makes it different from the marginal current-current deformations considered by [126]. In the quantum theory, the dimensionless parameter λ is dimensionally transmuted into a mass gap mediated through a cut-off Λ.

2.4 Scattering Kernels

In this Section we study the scattering matrices of integrable sigma models. The study of such S-matrices is a rich field. We shall start be revising some of the background material of S-matrices in integrable sigma models before discussing some specific models. We shall be relatively brief here as these S-matrices are familiar in the literature. However, we will be more elaborate in the discussion of the S-matrix of the bi-Yang-Baxter model

since this has not been found in the literature before.

We will consider a massive particle in 2 dimensions with Lorentzian momenta p_0, p_1 defined in terms of a rapidity θ given by

$$p_0 = m\cosh\theta, \qquad p_1 = m\sinh\theta\,. \tag{2.55}$$

The S-matrix bootstrap programme, initiated by the seminal work of Zamolodchikov and Zamoldchikov [127], is a way of establishing a unique form of an S-matrix that is compatible with *factorised scattering*; integrable models have no particle production or annihilation and thus n-body scattering can be obtained as a sequence of 2-body scattering processes. The most famous requirement of the 2-body S-matrix is that is satisfies the quantum Yang-Baxter equation[9]

$$S_{12}(\theta_1-\theta_2)S_{23}(\theta_2-\theta_3)S_{31}(\theta_3-\theta_1) = S_{31}(\theta_3-\theta_1)S_{23}(\theta_2-\theta_3)S_{12}(\theta_1-\theta_2) \tag{2.56}$$

Here S_{12} is a schematic notation for the S-matrix in which particle 1 and 2 are scattered. In general we consider that particles lie in some multiplets of global symmetries and so that the two-particle scattering matrix has entries S_{ij}^{kl} in which i,j label the incoming flavour and k,l the outgoing.

Further physical constraints are placed on the S-matrix namely:

- Analyticity: the S-matrix should be an analytic function of (the complexified) rapidity variable with poles along $0 \leq \operatorname{Im}\theta < \pi$ associated to bound states.
- Hermitian Analyticity: $S_{ij}^{kl}(\theta^*)^* = S_{kl}^{ij}(-\theta)$
- Real Unitarity: $\sum_{kl} S_{ij}^{kl}(\theta)S_{mn}^{kl}(\theta)^* = \delta_{im}\delta_{jn}$ for $\theta \in \mathbb{R}$
- Crossing Symmetry: $S_{ij}^{kl}(i\pi-\theta) = S_{\bar{kl}}^{i\bar{j}}(\theta)$. This stems from interchanging s and t channel diagrams which rotates space and time directions by a $\frac{\pi}{2}$ angle.

On the subject of determining the S-matrix using the above constraints we can recommend the lecture notes [128, 129].

However, in Chapter 4, we shall consider the scattering of only 1 type of particle. This is achieved by introducing a chemical potential that freezes all other particles and selects only a distinguished particular particle. In this case, the scattering "matrix" reduces to a simple phase factor $S(\theta)$ that governs transmission and reflection. It shall prove useful in this case to define the scattering kernel of this reduced S-matrix by

$$K(\theta) = \frac{1}{2\pi i}\frac{d}{d\theta}\log S(\theta)\,, \tag{2.57}$$

[9] In [86], it is shown how one recover the classical Yang-Baxter equation (2.11) by expanding $S_{12}(z) = f(z)(1+\epsilon r_{12}(z))$ and enforcing quantum Yang-Baxter equation at second order in ϵ.

and its Fourier transform[10]

$$K(\omega) = \int_{-\infty}^{\infty} d\theta\, e^{i\omega\theta} K(\theta)\,. \tag{2.60}$$

In the case of this reduced S-matrix, the hermition analyticity can be stated simply as saying $S(-\theta) = S(\theta)^{-1}$. The consequence of this is that the function $K(\theta)$ is symmetric, and hence so is $K(\omega)$.

Lastly, it shall prove useful to write the Fourier transform of the scattering Kernel as a Wiener-Hopf (WH) decomposition

$$1 - K(\omega) = \frac{1}{G_+(\omega)G_-(\omega)}\,, \tag{2.61}$$

where $G_+(\omega)$ is analytic in the Upper Half Plane (UHP) and $G_-(\omega) = G_+(-\omega)$. This does not fully determine the functions $G_\pm(\omega)$. In particular we may multiply them by a factor of $e^{\rho(\omega)}$ for any odd function $\rho(\omega)$. We shall fix the function $\rho(\omega)$ by demanding that $G_+(\omega)$ has polynomially asymptotic behaviour in the large ω limit[11]. We can also fix the normalisation by setting $G_+(2is) = 1 + \mathcal{O}\left(\frac{1}{s}\right)$.

On a technical level, the WH decomposition is typically obtained by repeatedly using Euler's reflections formula $\Gamma(z)\Gamma(1-z) = \frac{\pi}{\sin \pi z}$. This can be rewritten as either $\Gamma(1+i\alpha z)\Gamma(1-i\alpha z) = \frac{\alpha\pi z}{\sinh(\pi\alpha z)}$ or $\Gamma(\frac{1}{2}+i\alpha z)\Gamma(\frac{1}{2}-i\alpha z) = \frac{\pi}{\cosh(\pi\alpha z)}$. Because $\Gamma(z)$ only has poles along the negative real axis, we know that $\Gamma(1-i\alpha z)$ is analytic on the UHP if α is positive. We take care of absolute value-functions by writing $\frac{|\omega|}{\omega} = \mathrm{sgn}(\omega) = \frac{\omega}{\sqrt{\omega^2}}$, which is decomposed according to $\sqrt{\omega^2} = \sqrt{i\omega}\sqrt{-i\omega}$.

In Chapter 4, it shall become clear that the quantity $G_+(\omega)$ is the key-ingredient of many of the computations. That is why in this section we will be presenting not only the S-matrix of the relevant models, but also the WH-decomposition $G_+(\omega)$.

We will now present several models and their scattering kernel. We start with the Sine-Gordon model in Section 2.4.1, before moving to the PCM in Section 2.4.2, which requires a block that scatters particles in the fundamental representation of an $SU(N)$ symmetry. Similar to how the Sine-Gordon model breaks a classical $SU(2)$ symmetry symmetry in favour of a quantum group symmetry, the $A(N)$ Toda model in Section 2.4.3 breaks a classical $SU(N)$-symmetry and generates a quantum group symmetry. The $SU(2)$ bi-Yang-Baxter model studied by Fateev [130] is presented in Section 2.4.4 and consists of two Sine-Gordon blocks. The $SU(N)$ bi-Yang-Baxter is then constructed

[10] There is an alternative way to encode the information in Equations (2.57) and (2.60) that is common in the literature. We represent the S-matrix as

$$S(\theta) = \exp\left[i\pi - 2i\int_0^\infty d\omega \frac{\sin(\omega\theta)}{\omega}\left(R(\omega) - 1\right)\right], \tag{2.58}$$

where $R(\omega) = 1 - K(\omega)$. This representation makes it natural to compute the kernel as

$$K(\theta) = \frac{1}{2\pi i}\frac{d}{d\theta}\log S(\theta) = \delta(\theta) - \frac{1}{\pi}\int_0^\infty d\omega \cos(\omega\theta) R(\omega)\,. \tag{2.59}$$

[11] To be precise, we mean large in the UHP.

from two $A(N)$ blocks in Section 2.4.5. Finally, we present a scattering Kernel of the λ-model in Section 2.4.6 which will be important in Chapter 4.

2.4.1 Sine-Gordon Scattering

The classical sine-Gordon Lagrangian density is given as

$$\mathcal{L} = \frac{1}{\gamma}\left(\frac{1}{2}(\partial_\mu u)^2 - m^2(1-\cos u)\right) . \tag{2.62}$$

The equations of motion are classically integrable and contain soliton ($\mathfrak{s}$) and conjugate soliton ($\bar{\mathfrak{s}}$) solutions. The soliton (anti-soliton) interpolates from the vacuum $u = 0$ to $u = 2\pi$ at late times ($u = 2\pi$ to $u = 0$) and are according classified by a topological charge $\mathcal{I}$ such that $\mathcal{I}[\mathfrak{s}] = 1$ and $\mathcal{I}[\bar{\mathfrak{s}}] = -1$.

Interest in the quantum Sine-Gordon theory was ignited by the role it plays as a bosonised version of the massive Thirring model (the theory of Dirac fermions with a $(\bar{\psi}\gamma^\mu\psi)^2$ Fermi interaction) [131, 132]. At the quantum level the fundamental excitations are the soliton and anti-soliton for which the S-matrix was obtained in the original work of Zamolodchikov and Zamolodchikov [127].

An alternative derivation of this S-matrix by Bernard and LeClair [133] makes evident the connection to the underlying quantum group symmetry of the theory, and thus will make direct contact with the bi-Yang-Baxter deformation shortly to be considered. By considering the quantum (Euclidean) Sine-gordon theory as a relevant perturbation of a free compact boson Φ of radius $\hat{\beta}^{-1}$, Bernard and LeClair construct a set of *non-local* conserved charges $Q_\pm$ and $\bar{Q}_\pm$. The resulting soliton-soliton scattering phase to be written as

$$\begin{aligned} S_\gamma^{SG} &= \exp\left[i\int_{-\infty}^{\infty}\frac{d\omega}{2\omega}\frac{\sin(\theta\omega)\sinh(\pi(\gamma-1)\omega/2)}{\cosh(\pi\omega/2)\sinh(\pi\gamma\omega/2)}\right] \\ &= \exp\left[i\int_{-\infty}^{\infty}\frac{d\omega}{2\omega}\sin(\theta\omega)\left(1-\coth(\pi\gamma\omega/2)\tanh(\pi\omega/2)\right)\right] . \end{aligned} \tag{2.63}$$

This representation facilitates the computation of the Kernel $K_\gamma^{SG}(\theta) = \frac{1}{2\pi i}d_\theta \log S_\gamma^{SG}$ whose Fourier transform is given as

$$1 - K_\gamma^{SG}(\omega) = \frac{1}{2}\left(1+\coth(\pi\gamma\omega/2)\tanh(\pi\omega/2)\right) \tag{2.64}$$

Its WH-decomposition (2.61) is the given by

$$G_+(\omega) = e^{\rho(\omega)}\left(\frac{1+\gamma}{2\gamma}\right)^{\frac{1}{2}}\frac{B(\frac{-i\omega}{2},\frac{-i\omega}{2})}{B(\frac{-i\omega}{2},\frac{-i\gamma\omega}{2}))}, \tag{2.65}$$

where $B(a,b) = \Gamma(a)\Gamma(b)/\Gamma(a+b)$ is the Euler Beta and $\rho(\omega)$ is any odd function. To fix $\rho(\omega)$ we demand that in the large s-limit we have polynomial behaviour $G_+(2is) = 1 + \frac{a_1}{s} + \mathcal{O}\left(\frac{1}{s^2}\right)$. This is achieved with $\rho = \alpha\omega$ and $\alpha = -\frac{1}{2}i(\gamma\log(\gamma) - (\gamma+1)\log(\gamma+$

$1) + \log(4)$).

An important feature to keep in mind is that, in contrast to the $SU(N)$ invariant block that enters in the PCM, this scattering kernel is *fermionic* which means that $\Phi(s) = G_+(2is)$ admits and expansion around $s = 0$ that is a regular polynomial in integer powers of s (i.e. no $\sqrt{s}$ factors) and there are no logs appearing in the expansion.

2.4.2 PCM Model

Suppose that we consider any theory (not the PCM) in which the fundamental states lie in the fundamental representation of $SU(N)$. The solution to the factorised scattering equation is known to be [129, 134–136]

$$\tilde{S}(\theta) = \left(P^+ + \frac{\mathrm{x} - 1/N}{\mathrm{x} + 1/N} P^-\right) S_{11}(\theta) \ , \tag{2.66}$$

where $\mathrm{x} = i\theta/(2\pi)$, $P^\pm = \frac{1}{2}(1 \pm P)$ are projectors on the symmetric and anti-symmetric and

$$S_{11}(\theta) = \frac{\Gamma\left(1 + \mathrm{x}\right)\Gamma\left(\frac{1}{N} - \mathrm{x}\right)}{\Gamma\left(1 - \mathrm{x}\right)\Gamma\left(\frac{1}{N} + \mathrm{x}\right)} \ . \tag{2.67}$$

For the PCM, which has a global $SU(N)_L \times SU(N)_R$ symmetry, the S-matrix is given by the tensor product of two copies of the above $SU(N)$ block

$$\mathbb{S}(\theta) = X(\theta)\tilde{S}(\theta) \otimes \tilde{S}(\theta) \, , \tag{2.68}$$

where

$$X_{1,1}(\theta) = -\frac{\sin(\pi(\frac{1}{N} - \mathrm{x}))}{\sin(\pi(\frac{1}{N} + \mathrm{x}))} = -\frac{\Gamma(\frac{1}{N} + \mathrm{x})\Gamma(1 - \frac{1}{N} - \mathrm{x})}{\Gamma(\frac{1}{N} - \mathrm{x})\Gamma(1 - \frac{1}{N} + \mathrm{x})} \ , \tag{2.69}$$

is an additional dressing factor that is placed by hand to ensure the correct pole structure of the S-matrix. At a technical level this factor removes a double zero in the symmetric channel on *the physical strip*[12], which is given by $0 \leq \mathrm{Im}(\theta) \leq \pi$. The vanishing of such double zeros is suggested to be a general requirement of an integrable S-matrix.

There is a rich structure of (heavier) bound states forming anti-symmetric tensor representations of $SU(N) \times SU(N)$ whose S-matrices are determined by fusion [129]. However, such states are not important for the concerns of our future TBA analysis which requires only the fundamental. In fact, with the appropriate choice of chemical potential we need only consider the symmetric channel S-matrix entry

$$\begin{aligned} \mathbb{S}(\theta) &= X_{1,1}(\theta) S_{11}(\theta)^2 \\ &= -\frac{\Gamma(1 + \mathrm{x})^2 \Gamma(1 - \mathrm{x} - \Delta)\Gamma(\Delta - \mathrm{x})}{\Gamma(1 - \mathrm{x})^2 \Gamma(1 + \mathrm{x} - \Delta)\Gamma(\Delta + \mathrm{x})} \, , \end{aligned} \tag{2.70}$$

where we defined $\Delta = \frac{1}{N}$. This was first found in [137].

[12] The physical strip is the region in the rapidity variable θ to which all values of the centre of mass energy $s = 4m^2 \cosh^2 \frac{\theta}{2}$ are mapped. It is thus somewhat of a misnomer as many regions of the physical strip correspond to unphysical processes.

It follows form the definition of the of the Fourier transform (2.57) and (2.60) that

$$1 - K(\omega) = 2\text{csch}(\pi|\omega|)\sinh(\Delta\pi|\omega|)\sinh(\pi(1-\Delta)|\omega|) \tag{2.71}$$

Its Wiener-Hopf decomposition (2.61) is given by

$$1 - K(\omega) = \frac{1}{G_+(\omega)G_-(\omega)}\,, \quad G_-(\omega) = G_+(-\omega)\,, \tag{2.72}$$

with

$$G_+(\omega) = \frac{e^{i\omega((1-\Delta)\log(1-\Delta)+\Delta\log(\Delta))}\Gamma(1-i(1-\Delta)\omega)\Gamma(1-i\Delta\omega)}{\sqrt{2\pi(1-\Delta)\Delta}\sqrt{-i\omega}\Gamma(1-i\omega)} \tag{2.73}$$

2.4.3 $A(N)$ Affine Toda

The classical affine $\mathfrak{sl}(N)$ Toda theory can be thought of as a generalisation of the sin(e/h)-Gordon theory where the fundamental field $\phi(x,t)$ is an $N-1$ weight-vector obeying the wave equation

$$\Box\phi = -\frac{m^2}{\tilde{\beta}}\sum_{j=1}^{n}\alpha_j e^{\tilde{\beta}\alpha_j\cdot\phi}\,, \tag{2.74}$$

where α_j for $j = 1\ldots N-1$ are simple roots and α_N is the affine root. We consider the case where $\tilde{\beta} = i\beta$ is pure - imaginary. In analogy to the sine-Gordon, this admits classical kink soliton solutions interpolating between $x \to \pm\infty$ constant vacua solutions $\phi = \frac{2\pi}{\beta}w$ for w a vector in the weight lattice Λ^*. The solitons are classified by a topological charge

$$\mathcal{I} = \frac{\beta}{2\pi}\int_{-\infty}^{\infty} dx\partial_x\phi \in \Lambda^*\,. \tag{2.75}$$

The one-soliton multiplet consists of solutions

$$\phi = \frac{i}{\beta}\sum_{j=1}^{N}\alpha_j\log\left[1+\exp\left(\sigma(x-vt)+\xi+\frac{2\pi ia}{N}j\right)\right]\,, \tag{2.76}$$

and the topological charges are governed by the choices for the values of ξ and fill out the weights of the a^{th} fundamental representation. The classical mass of these solitons is found to be $M_a = \frac{4mN}{\beta^2}\sin(\frac{\pi a}{N})$ and even though the theory is complex the masses are real. Now just as the sine-Gordon theory displays a $\mathcal{U}_q(\widehat{\mathfrak{sl}2})$ symmetry it is natural to expect this generalisation also encodes a quantum group symmetry. Indeed, in [138], such an S-matrix representing soliton scattering was conjectured and shown to match in the semi-classical limit the result coming from WKB quantisation.

The S-matrix for transmission of non-identical particles is given by [138]

$$S_{ik\to ki}=\prod_{j=1}^{\infty}\frac{\Gamma\left(\frac{j-1}{N\lambda}-\mathrm{x}-\frac{1}{N}\right)\Gamma\left(\frac{j-1}{N\lambda}+\mathrm{x}+1\right)\Gamma\left(\frac{j}{N\lambda}-\mathrm{x}+\frac{1}{N}\right)\Gamma\left(\frac{j}{N\lambda}+\mathrm{x}+1\right)}{\Gamma\left(\frac{j-1}{N\lambda}-\mathrm{x}\right)\Gamma\left(\frac{j}{N\lambda}-\mathrm{x}\right)\Gamma\left(\frac{j}{N\lambda}+\mathrm{x}+\frac{1}{N}+1\right)\Gamma\left(\frac{j-1}{N\lambda}+\mathrm{x}-\frac{1}{N}+1\right)}\,, \tag{2.77}$$

where we again used $\mathrm{x}=i\theta/(2\pi)$, $P^{\pm}=\frac{1}{2}(1\pm P)$. λ is related to the quantum group parameter by is related to the quantum group parameter by $q=e^{-i\pi\lambda}$. The S-matrix for identical particles, most relevant to our discussion, is dressed by

$$S_{ii\to ii}=\frac{\sin(\pi\lambda(1+N\mathrm{x}))}{\sin(\pi\lambda N\mathrm{x})}S_{ik\to ki} \tag{2.78}$$

Next we use the Weierstrass representation of the pre-factor to express, with $\gamma=\lambda^{-1}$,

$$S_{ii\to ii}=\prod_{j=1}^{\infty}\frac{\Gamma\left(\mathrm{x}+\frac{(j-1)\gamma}{N}+1\right)\Gamma\left(\mathrm{x}+\frac{j\gamma}{N}\right)}{\Gamma\left(\mathrm{x}+\frac{(j-1)\gamma}{N}-\frac{1}{N}+1\right)\Gamma\left(\mathrm{x}+\frac{j\gamma}{N}+\frac{1}{N}\right)}\,/\,(\mathrm{x}\leftrightarrow-\mathrm{x})\,, \tag{2.79}$$

The Fourier transform is given by taking Log's and invoking the integral representation of the Γ-function,

$$\log\Gamma(z+1)=\int_0^{\infty}\frac{dt}{t}e^{-t}\left(z-\frac{1-e^{-zt}}{1-e^{-t}}\right)\,,\mathrm{Re}(z+1)>0\,, \tag{2.80}$$

which yields

$$\mathcal{S}=\exp\left[-2i\int_0^{\infty}d\omega\frac{\sin(\omega\theta)}{\omega}\frac{\sinh\left(\frac{\pi\omega}{N}\right)\sinh\left(\frac{\pi\omega(-\gamma+N-1)}{N}\right)}{\sinh(\pi\omega)\sinh\left(\frac{\pi\gamma\omega}{N}\right)}\right] \tag{2.81}$$

For the case of $N=2$ the above reduces to the Sine-Gordon soliton-soliton scattering S-matrix and associated kernel.

Analogously to Equations (2.59) and (2.58) we can extract $K(\omega)$ from (2.81) as

$$\begin{aligned}1-K(\omega)&=1+\frac{\sinh(\pi\Delta|\omega|)\sinh((1-\Delta-\gamma\Delta)\pi|\omega|)}{\sinh(\pi|\omega|)\sinh(\pi\gamma\Delta|\omega|)}\\&=\frac{\sinh((1+\gamma)\pi\Delta\omega)\sinh(\pi(1-\Delta)\omega)}{\sinh(\pi\omega)\sinh(\pi\gamma\Delta\omega)}\,,\end{aligned} \tag{2.82}$$

where $\Delta=\frac{1}{N}$. This has a WH decomposition given by

$$1-K(\omega)=\frac{1}{G_+(\omega)G_-(\omega)}\,, \tag{2.83}$$

where

$$\begin{aligned} G_+(\omega) &= e^{-2i\beta\omega}\sqrt{\frac{\gamma}{(\gamma+1)(1-\Delta)}}\frac{\Gamma(1-i(1-\Delta)\omega)\Gamma(1-i(\gamma+1)\Delta\omega)}{\Gamma(1-i\omega)\Gamma(1-i\gamma\Delta\omega)} \\ &= e^{-2i\beta\omega}\left(\frac{\gamma}{(\gamma+1)(1-\Delta)}\right)^{-\frac{1}{2}}\frac{B(-i\Delta\omega,-i(1-\Delta)\omega)}{B(-i\Delta\omega,-i\gamma\Delta\omega)} \end{aligned} \tag{2.84}$$

and $G_-(\omega) = G_+(-\omega)$. To ensure $G_+(\omega)$ is analytic on the UHP, we are assuming that $1+\gamma > 0$. Again, demanding that $G_+(\omega)$ has polynomial series behaviour as $\omega \to i\infty$ fixes

$$\beta = \frac{1}{2}\left(\Delta\left[\gamma\log(\gamma) - (1+\gamma)\log(1+\gamma)\right] + (1-\Delta)\log(1-\Delta) - \Delta\log\Delta\right), \tag{2.85}$$

such that $G_+(2is) \sim 1 + \mathcal{O}(s^{-1})$.

2.4.4 $SU(2)$ bi-Yang-Baxter Model

In the case of the bi-Yang-Baxter (bi-YB) deformation applied to the $SU(2)$ PCM, we are able to make direct contract with the results of Fateev [130] in which two parameter deformations of the $O(4)$ σ-model (i.e. the non-linear σ model with S^3 target equivalent to the $SU(2)$ PCM) are constructed. This two parameter deformation can be equated to the corresponding $SU(2)$ bi-YB, where we recall we had introduced the deformation parameters η and ζ. The two parameters p_1, p_2 of the Fateev [130] model are related, after some algebra, to ones entering the bi-YB theory with

$$p_1 = \frac{2\pi}{\mathsf{t}\zeta}, \quad p_2 = \frac{2\pi}{\mathsf{t}\eta}. \tag{2.86}$$

In [130] the S-matrix of this theory was determined to be the product of two Sine-Gordon S-matrices given in Equation (2.63)

$$S_{p_1,p_2}(\theta) = S^{SG}_{\gamma=p_1}(\theta)\otimes S^{SG}_{\gamma=p_2}(\theta). \tag{2.87}$$

This is entirely natural; just as the principal chiral model has an S-matrix containing the product of two SU(N) invariant factors reflecting the $SU(N)\times SU(N)$ global symmetry, here the two sine-Gordon factors reflect the anticipated $\mathscr{U}_{q_L}(\mathfrak{g})\times\mathscr{U}_{q_R}(\mathfrak{g})$ quantum group symmetry described in Section 2.4.5. Of course, the relation between the p_i in the S-matrix and the classical Lagrangian parameters could be modified by quantum effects - a reasonable assumption is that one should perturbatively find corrections of p_1 such that it remains an RG invariant at higher loops.

The scattering kernel yields

$$1 - K(\omega) = \frac{1}{2}\tanh(\pi\omega/2)\frac{\sinh(\pi(p_1+p_2)\omega/2)}{\sinh(p_1\pi\omega/2)\sinh(p_2\pi\omega/2)}. \tag{2.88}$$

Equation (2.88) has a Wiener-Hopf factorisation

$$1 - K(\omega) = \frac{1}{G_+(\omega)G_-(\omega)}\,, \tag{2.89}$$

where $G_-(\omega) = G_+(-\omega)$ and

$$G_+(\omega) = e^{\alpha\omega}\left(\frac{p_1+p_2}{2p_1p_2}\right)^{\frac{1}{2}} \frac{B(\frac{-i\omega}{2},\frac{-i\omega}{2})}{B(\frac{-ip_1\omega}{2},\frac{-ip_2\omega}{2}))}\,. \tag{2.90}$$

2.4.5 $SU(N)$ Bi-Yang-Baxter Model

The SG model is to the $SU(2)$ bi-Yang-Baxter model what the $A(N)$ Toda models is to the $SU(N)$ bi-Yang-Baxter model. That is, to construct the $SU(N)$ bi-Yang-Baxter S-matrix, we take two copies of the $A(N)$ Toda S-matrix given by (2.81) with different deformation paramters

$$S_{p,q}(\theta) = \chi(\theta)S_{\gamma=p}(\theta) \times S_{\gamma=q}(\theta)\,. \tag{2.91}$$

Here, $\chi(\theta)$ is a dressing factor introduced by hand with the purpose to cancel any double zeroes that arise in the physical strip after taking the square of the Toda S-matrix. The physical strip is the region where $0 \leq \mathrm{Im}(\theta) \leq \pi$. A critical point here is that any zeros that depend on γ do not become double zeroes.[13] The only double zero on the physical strip is located at $x = -\Delta$.

Here we have a puzzle, when the dressing factor is chosen to be the inverse of of the PCM model Equation (2.69) (i.e. $\chi(\theta) = (\chi_{1,1}(\theta))^{-1}$) we use Equation (2.80) to find the kernel

$$K(\omega) = \frac{1}{\sinh(\pi\omega)}\Bigg[\sinh(\pi\Delta\omega)\left(\frac{\sinh((p\Delta+\Delta-1)\pi\omega}{\sinh(p\pi\Delta\omega)} + \frac{\sinh((q\Delta+\Delta-1)\pi\omega}{\sinh(q\pi\Delta\omega)}\right) + \sinh(\pi(1-2\Delta))\Bigg]\,, \tag{2.92}$$

or

$$1 - K(\omega) = \frac{\sinh((p+q)\pi\Delta\omega)\sinh(\pi\Delta\omega)\sinh((1-\Delta)\pi\omega)}{\sinh(\pi\omega)\sinh(p\pi\Delta\omega)\sinh(q\pi\Delta\omega)}\,. \tag{2.93}$$

This passes two strong consistency checks: first it agrees with the $SU(2)$ bi-Yang-Baxter kernel (2.88) for $\Delta = 1/2$, second if we take $p, q \to \infty$, we recover the $SU(N)$ PCM kernel (2.71).

However, this choice of dressing factor is curious from the point of view of zeros of the S-matrix. The S-matrix provided by $\mathcal{S}_{\gamma=p}(\theta) \times \mathcal{S}_{\gamma=q}(\theta)$ without the dressing factor has a selection of zeros that at generic choices of $p \neq q \in \mathbb{R}$ are simple. Ignoring such

[13] Some subtleties may occur when $p = q$ as the roots of the functions will thence collide, which we will not worry about here.

factors that cannot contribute in general double zeros, we have that

$$\mathcal{S}_{\gamma=p}(\theta) \times \mathcal{S}_{\gamma=q}(\theta) = \frac{\Gamma(1+x)\Gamma(1-x-\Delta)}{\Gamma(1-x)\Gamma(1+x-\Delta)} \times \prod \dots$$

The remaining p, q independent factor also has no double poles or zeros on the physical strip. From this perspective there is no immediate motivation for the introduction of *any* dressing factor. In contrast to the PCM case in which $\chi_{1,1}(\theta))$ was introduced to convert a double zero at $x = -\Delta$ to a single zero, here we are dressing with $\chi_{1,1}(\theta))^{-1}$ to create a single zero at $x = -\Delta$ where previously there was none.

The kernel (2.93) has the WH-decomposition

$$1 - K(\omega) = \frac{1}{G_+(\omega)G_-(\omega)}\,, \tag{2.94}$$

with

$$G_+(\omega) = e^{-2i\beta\omega}\sqrt{\frac{(p+q)(1-\Delta)}{pq}}\,\frac{B(-i\Delta\omega, -i(1-\Delta)\omega)}{B(-ip\Delta\omega, -iq\Delta\omega)} \tag{2.95}$$

and $G_-(\omega) = G_+(-\omega)$. The constant β is fixed by demanding that the function has polynomial series behaviour as $\omega \to \infty$,

$$\beta = \frac{1}{2}\Big(\Delta(p\log p + q\log q) - \Delta(p+q)\log(p+q) - (1-\Delta)\log(1-\Delta) - \Delta\log\Delta\Big)\,. \tag{2.96}$$

2.4.6 λ-Model

The S-matrix of the λ-model was given in [106] for the $SU(2)$ case and conjectured in general for the $SU(N)$ case by [139] as the rank k representation of an $SU(N)$ spin chain [140]. A Restricted-Solid-On-Solid (RSOS) piece [14] features in the decomposition of the S-matrix for λ-deformed model [140, 145, 146]. In the $SU(2)$ case this means that there are kinks going between $k+1$ vacua labelled by the highest weight vector. In the general case, it is explained in [145] how to take a certain *middle anti-symmetric* highest weight vector $\omega_{N/2}$. We will later introduce a chemical potential such that only the state corresponding to the vector $\omega_{N/2}$ will condense. It was remarked [145] that this particular state does not form bound states with other asymptotic states. On an intuitive level, other positively charged states should thus be repelled from condensing into the ground state.

In summary, we will thus only be considering scattering between particular identical

[14] RSOS models are integrable models with integer variables at square lattice sites. The "restricted" nature derives from an adaptation made by [141–143] to limit the integer to maximum "height". A similar procedure was performed by [144] in a lattice calculation of the Sine-Gordon model. They obtained an S-matrix after transforming a vertex interaction to an interaction-round-vertices (IRF) and reducing the phase space from an SOS to an RSOS model. This S-matrix is relevant currently.

states. Its scattering kernel is then given by [145].

$$1 - K(\omega) = \frac{\sinh^2(\pi\omega/2)}{\sinh(\pi\omega)\sinh(k\pi\omega\Delta)} \exp(k\Delta\pi\omega)\,, \tag{2.97}$$

where $\Delta = \frac{1}{N}$. This has a WH decomposition given by[15]

$$\begin{aligned} 1 - K(\omega) &= \frac{1}{G_+(\omega)G_-(\omega)}\,, \\ G_+(\omega) &= \sqrt{4\kappa}\frac{\Gamma(1 - i\omega/2)^2}{\Gamma(1 - i\omega)\Gamma(1 - i\kappa\omega)} \exp\left(ib\omega - i\kappa\omega\log(-i\omega)\right)\,, \end{aligned} \tag{2.98}$$

and $G_-(\omega) = G_+(-\omega)$ and we defined $\kappa = k\Delta$. The constant b is fixed by demanding series behaviour as $\omega \to \infty$ yielding

$$b = \kappa(1 - \log(\kappa)) - \log(2)\,. \tag{2.99}$$

[15] Interestingly, for any complex value of κ, rather than just the physical region $\kappa \in \mathbb{R}_{>0}$, Equation (4.71) is a good decomposition, i.e. $G_+(\omega)$ is holomorphic in the UHP.

Chapter 3

Resurgence in the Bi-Yang-Baxter Model

Our main focus in this chapter is to understand how the ideas of resurgence can be applied in quantum field theories. To retain a degree of control we choose to work in the setting of 1+1 dimensional field theories, that happen to be integrable (although in this work integrability will not be employed in a crucial fashion). The overall aim here is to expose the interrelation between the asymptotic nature of perturbation theory and the non-perturbative sector. With a direct study of the large order QFT using Feynman diagrams not viable there are two directions one could follow here. First one could exploit the exact integrability of these models and study the resurgent properties of the TBA system as in [1, 147, 148] further explored in Chapter 4. A second approach, first used by [46] and the one we adopt here, is to consider a reduction of the system to a quantum mechanical system where a large order perturbative expansion can be carried out directly. In this approach, adiabaticity, achieved essentially by including a twist in the reduction, is used to argue that the lower dimensional theory still encapsulates the key feature of the higher dimensional one. Following this approach, it is possible to identify two-dimensional non-perturbative field configurations (so called unitons rather than instantons in the cases we study) as the origin of the objects that give rise to factorial behaviour in the reduced QM. This is a crucial first step in establishing the resurgent nature of the QFT.

In this work we shall specialise to a particular QFT, called the bi-Yang-Baxter (bYB) model. This theory, introduced by Klimčik [95], deforms the principal chiral model (PCM) on a group manifold G with two deformation parameters, denoted by η and ζ, whilst the underlying integrability is preserved. When $G = SU(2)$, which will be our specific concern here, it was shown in [104] that the theory is equivalent to one already introduced by Fateev [130]. There are a few motivations for studying this particular scenario. First from a resurgence perspective it offers access to having multiple parameters that can be dialled to expose interesting features. Second, we shall see very

explicitly that resurgent structure will require consideration of saddle configurations in a complexified field space. Third, when the two deformation parameters are set equal to each other, $\eta = \zeta = \varkappa$ which we call the critical line, the deformed $SU(2)$ theory is equivalent [104] to the so-called η-deformation of S^3 viewed as a coset $SO(4)/SO(3)$. This provides an entry point to consider similar deformations of $AdS_5 \times S^5$ [97, 98, 101] which are of interest since they are thought to encode quantum group deformations in holography. A resurgence perspective was given in [47] for the case with only one parameter, i.e. $\zeta = 0$. Here we find whilst some features remain, the inclusion of a further deformation parameter enriches the story quite considerably.

Let us briefly summarise the findings of our study:

- The bi-Yang-Baxter model admits finite action field configurations that generalise the uniton configurations introduced for the PCM by Uhlenbeck [149] and whose role in resurgence was expounded in [46, 47]. In addition there are finite action field configurations that take values in the complexified target space (i.e. consist of complexified field configurations).

- Upon a certain twisted S^1 reduction these configurations are seen, in specific regimes of their moduli space, to break up, or fractionate, into distinct lumps that resemble instanton-anti-instanton pairs or complex instanton configurations.

- The twisted spatial reduction of the model results in a quantum mechanics with a potential consisting of Jacobi elliptic functions $\mathrm{sd}^2(w|m)$ and $\mathrm{sn}^2(w|m)$

$$V(w) = \mathrm{sd}^2(w|m)(1 + (\zeta - \eta)^2 \mathrm{sn}^2(w|m)) \,, \tag{3.1}$$

  with a modular parameter $m = \frac{4\eta\zeta}{1+(\eta+\zeta)^2}$. Taking one of the parameters to zero, the Whittaker-Hill potential studied in [47] is recovered. Moreover, along the critical line $\eta = \zeta = \kappa$, the potential reduces to that studied by [41]. Looking at the co-critical line $\eta = -\zeta$, we recover the potential studied by [35]. This new system thus interpolates between already known systems.

- The large order behaviour of the perturbation theory of the ground state energy gives rise, using a Borel-Padé transformation, to poles in the Borel plane that are located precisely at the values of the action for the above uniton configurations. Commensurate to this we find Stokes rays in the $\vartheta = 0, \pi$ directions of the Borel plane, and these are reflected as flip mutations of the corresponding Stokes graph.

- The $\zeta = \eta = \varkappa$ critical line is distinguished by a discontinuous jump in which the Borel pole associated to the one-complex uniton disappears and instead the leading pole in the $\vartheta = \pi$ ray corresponds to a two-complex uniton. At the special point $\varkappa = \frac{1}{2}$, which corresponds to an enhanced $\mathbb{Z}_2$ symmetry, the real uniton and two-complex uniton have actions of equal modulus indicating a perfect cancellation in which the perturbative ground state energy becomes a series in g^4 rather than

g^2. This provides a nice field theory example of resonate behaviour in resurgence[1].

- The WKB quadratic differential corresponding to the potential in Equation (3.1) can be equated to the quadratic differential of $\mathcal{N} = 2$ gauge theories in two realisations. First as the elliptic $SU(2) \times SU(2)$ quiver with one of the gauge couplings sent to infinity and with the relative Coloumb branch parameter set to zero. Second as the $SU(2)$ $N_f = 4$ theory with pairwise equal flavour masses. In both cases, the masses are described by the quantum-group parameters of the bi-Yang-Baxter model.

The structure of this Chapter is as follows: in Section 3.1 we provide a summary of the model under consideration before identifying the uniton configurations. We perform the reduction to quantum mechanics in Section 3.2 and perform a detailed perturbative analysis of this in Section 3.3. We end the story by establishing the linkage to the $\mathcal{N} = 2$ gauge theory in Section 3.4. We close with a discussion of a number of possible future directions.

3.1 Uniton Solutions

We now study non-perturbative field configurations, i.e. exact classical solutions of the Euclidean theory with finite action, analogous to instantons. At first sight this may seem counter intuitive since there is no obvious topological protection (recall that $\pi_2(G) = 0$) and it is far from obvious that these are good vacua to expand around in a Quantum Field Theory. However in a seminal early work by Uhlenbeck [149], classes of such solutions were found and classified for the principal chiral model. These solutions are known as *unitons* due to the additional constraint $g^2 = -\mathrm{Id}$ and have played a prominent role in recent attempts [46, 47] to elucidate the resurgent quantum structure of two-dimensional quantum field theories.

In this Section we shall study uniton solution of the deformed $SU(2)$ sigma model, but it is interesting to note that solutions have later been found on more general deformed group manifold by [150]. In particular, they construct on the critical line $\eta = \zeta$ a Weyl operator which reproduces the complex uniton. In general, they show the power of using Hodge theory to study the classical dynamics of sigma model – see also [151].

3.1.1 Real Unitons

Let us briefly recall some basics of the bi-Yang-Baxter deformed model discussed in Section 2.2. We introduced an action

$$S_{\zeta,\eta} = \frac{1}{2\pi \mathfrak{t}} \int d^2\sigma \, \mathscr{L}[g] \,, \quad \mathscr{L}[g] = \mathrm{Tr}\left(g^{-1}\partial_+ g \frac{1}{1 - \eta R - \zeta R^g} g^{-1}\partial_- g \right) , \tag{3.2}$$

[1]The potential Equation (3.1) at the critical line was indeed used as an proto-typical example to study such resonances in a 0-dimensional toy example in [43].

where g is a function of the world-sheet valued in the target-space group manifold G. We defined the adjoint operator $\mathrm{Ad}_g(u) = gug^{-1}$ and we defined $R^g = \mathrm{Ad}_{g^{-1}} \circ R \circ \mathrm{Ad}_g$, where R is a solution to the modified Yang-Baxter Equation (2.13). η and ζ are the deformation parameters. Sending them to 0 bring us back to the PCM.

We will specialise to the $G = SU(2)$ case and use Equation (2.15) as the solution of the modified Yang-Baxter Equation. In the $SU(2)$ case, which is geometrically an S^3, we used the Hopf angle fibration of the group manifold

$$g = \begin{pmatrix} \cos(\theta)e^{i\phi_1} & i\sin(\theta)e^{i\phi_2} \\ i\sin(\theta)e^{-i\phi_2} & \cos(\theta)e^{-i\phi_1} \end{pmatrix}, \tag{3.3}$$

In terms of the Hopf angles ϕ_1, ϕ_2, θ, we find a solution to the Euclidean equations of motions (2.19) given by

$$\phi_1 = \frac{\pi}{2}, \qquad \phi_2 = \pi + \frac{i}{2}\log\left(\frac{f}{\overline{f}}\right), \qquad \theta(f,\overline{f}) = \theta(|f|^2), \tag{3.4a}$$

$$\sin(\theta(|f|^2))^2 = \frac{4|f|^2}{(1+|f|^2)^2 + (\eta-\zeta)^2(1-|f|^2)^2} =: P(|f|^2)\,, \tag{3.4b}$$

with $f(z)$ any holomorhpic function of the Euclidean coordinate $z = x+ti$. Interestingly, the solution can be obtained simply from that of the single deformed case constructed in [47] by substituting $\eta^2 \to (\eta-\zeta)^2$, although this change is not at all apparent from the equations of motion. The peculiarity of the critical line $\eta = \zeta = \varkappa$ is apparent already at this level: in this situation the uniton solution does not depend on the deformation parameter at all (although the on-shell value of the action will of course depend on $\varkappa$).

Usually, the topological classification of saddle points in non-linear sigma models with target space M depends on $\pi_2(M)$. However, in the present case we have that $\pi_2(SU(2)) = \pi_2(S^3) = 0$. From the uniton solutions (3.4a), we see that the uniton is the embedding of a Riemann sphere into a particular $S^2 \subset SU(2)$. The discretisation of the uniton action can be connected to the homotopy group $\pi_1(\mathcal{M})$ of the field space $\mathcal{M} = \{g : S^2 \to SU(2)\}$. Therefore, the unitons are classified by $\pi_1(\mathcal{M}) = \pi_3(SU(2)) = \mathbb{Z}$, see also [152]. Here this quantisation is reflected in the order of the polynomial $f(z)$.

In Figure 3.1, we illustrate the Lagrangian density of this uniton configuration, for the case that k, the degree of $f(z)$, is one. That is, we take

$$f(z) = \lambda_0 + \lambda_1 z\,, \tag{3.5}$$

where λ_i are some moduli that become significant later. The uniton solution appears as a lump of localised Lagranian density. The deformation parameters induce some additional structure, qualitatively described by punching a depression and flattening out the lump.

Whilst this uniton is not a bona-fide BPS protected solution, for the reasons de-

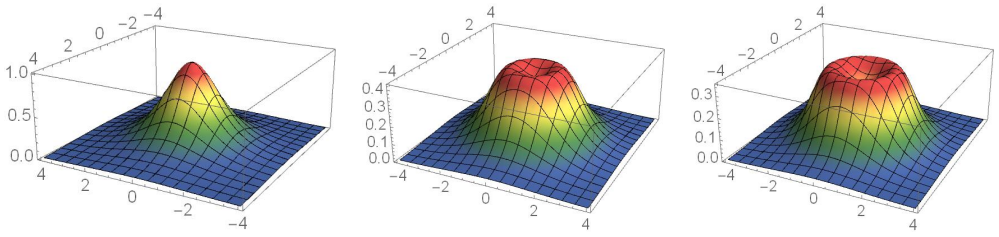

(a) $\eta = 0, \zeta = 0$ (b) $\eta = 0.8, \zeta = 0$ (c) $\eta = 0.8, \zeta = 0.8$

Figure 3.1: A plot of the Lagrangian density of the $k = 1$ real uniton on $\mathbb{R}^2$ illustrating the flattening out as the deformation paramaters are tuned up. The moduli in Equation (3.5) are fixed in these plots such that the uniton is centered at the origin: $\lambda_0 = 0$, while $\lambda_1 = 1/2$.

scribed above, the solution does satisfy a first order ODE pseudo-BPS condition

$$4x^2(\theta'(x))^2 = \sin^2\theta(x) + (\eta - \zeta)^2 \sin^4\theta(x), \quad x = |f|^2. \tag{3.6}$$

By substituting the uniton solution into the action (2.16), we find

$$S = \frac{2}{\pi \mathsf{t}} \int d^2z \frac{|f(z)|^2 |f'(z)|^2 (\theta'(|f(z)|^2))^2}{1 + \eta^2 + \zeta^2 + 2\eta\zeta \cos 2\theta(|f(z)|^2)} \,. \tag{3.7}$$

To proceed, the integration coordinate is switched from z to $w = f(z)$. The order k of the polynomial $f(z)$ appears as it revolves k times around its integration domain. We can integrate over the argument of w, which yields 2π. By changing the integration variable to $\theta(|w|^2)$, and by making use of Equation (3.6) the action evaluates to

$$S = \frac{2k}{\mathsf{t}(1 + \chi_+^2)} S_I \,, \tag{3.8}$$

with[2]

$$S_I = \frac{2}{m} \left(\chi_+ \text{arctan}\chi_+ - \chi_- \text{arctan}\chi_- \right) \,, \tag{3.9}$$

where we recall that $\chi_\pm = \zeta \pm \eta$, and we have defined

$$m = \frac{4\eta\zeta}{1 + (\eta + \zeta)^2} \,, \tag{3.10}$$

the significance of which will become clear later. Similarly, we have rather artificially extracted a factor of $1 + \chi_+^2$ from the action for reasons that will follow later. Observe that S_I is real and positive if η and ζ are real and positive.

Moreover, note that in this formulation, S_I reduces to $1 + (\eta + \eta^{-1}) \arctan(\eta)$ in the single deformation limit $\zeta \to 0$, matching the result of [47].

Another way of describing the solution is through a projector Π obeying $\Pi^2 = \Pi$.

[2]The notation S_I is perhaps confusing, we have chosen this to be in keeping with other works in the field in which the subscript I is meant to invoke instantons.

We let

$$g = i(2\Pi - \mathrm{Id})\,, \qquad \Longrightarrow \qquad g^2 = -\mathrm{Id}\,, \tag{3.11}$$

and Π given by

$$\Pi = \frac{v^\dagger \otimes v}{v^\dagger \cdot v}\,, \quad v = \begin{pmatrix} 1 \\ \sqrt{\frac{\bar{f}}{f}}\frac{1+\sqrt{P(|f|^2)}}{\sqrt{1-P(|f|^2)}} \end{pmatrix}\,, \tag{3.12}$$

where $P(|f|^2)$ is as in Equation (3.4b). This approach might be more amenable to higher rank generalisations since it does not require an explicit choice of Hopf coordinates.

3.1.2 Complex Unitons

An important feature of this model is the existence of a second solution to the equations of motion which lives in the complexified target space. We shall thus refer to this configuration as a *complex uniton*, and, by contrast, the uniton discussed above shall be referred to as the *real uniton*. For the complex uniton, the configuration of the fields ϕ_i shall be the same as for the real uniton given by Equation (3.4a). For $\theta(|f|^2)$, we obtain

$$\theta(|f|^2) = \frac{\pi}{2} + i\,\mathrm{arctanh}\left(\frac{1}{2}\left(|f| + \frac{1}{|f|}\right)\sqrt{\chi_-^2 + 1}\right)\,. \tag{3.13}$$

When this is substituted into the action we obtain

$$S = \frac{2k}{\mathsf{t}(1+\chi_+^2)} S_{CI}\,, \tag{3.14}$$

with

$$S_{CI} = \frac{2}{m}\left(\chi_- \mathrm{arccot}\chi_- - \chi_+ \mathrm{arccot}\chi_+\right)\,, \tag{3.15}$$

$\chi_\pm = \zeta \pm \eta$ and m is as in (3.10). Interestingly, the action of the real uniton and the complex uniton arise as the integral of the same function. This leads to a surprising connection

$$S_{CI}(\zeta,\eta) - S_I(\zeta,\eta) = \frac{\pi(1+(\zeta+\eta)^2)}{4\zeta\eta}\left(|\zeta-\eta| - |\zeta+\eta|\right)\,, \tag{3.16}$$

which is explained further in Appendix 3.A. Observe that S_{CI} is real and negative if η and ζ are real and positive.

Readers familiar with the undeformed PCM [46] might wonder why such complex uniton configurations played no role there. The answer is simple: although it is still a solution to the field equations, its action diverges and plays no important role.

In Figure 3.2, we show the (real part) of the Lagrange density of these complex uniton lumps. This reveals a peculiar behaviour across the critical line of deformation parameters. At generic values of deformation parameters, there is a secondary valley in the Lagrangian density. This structure however disappears discontinuously across the critical line.

Similarly discontinuous behaviour is visible directly in the value of the complex

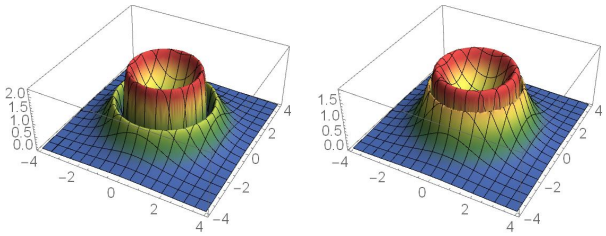

(a) $\eta = 0.2, \zeta = 0.1$ (b) $\eta = 0.2, \zeta = 0.19$

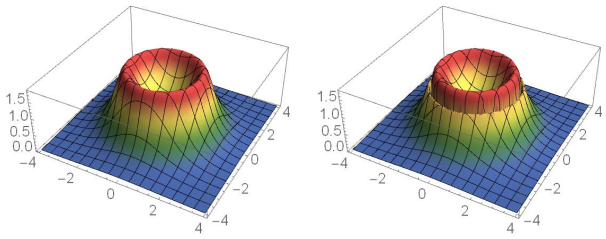

(c) $\eta = 0.2, \zeta = 0.2$ (d) $\eta = 0.2, \zeta = 0.21$

Figure 3.2: A plot of (the real part of) the Lagrangian density of the $k = 1$ complex uniton on $\mathbb{R}^2$ as the deformation parameters are tuned to cross the critical line. In (a) there is a clear concentric valley structure which is removed precisely at the critical line in (c). The moduli are fixed in these plots at $\lambda_0 = 0$, $\lambda_1 = 1/2$.

uniton action eq. (3.15) which exhibits a cusp across the critical line as can be seen from

$$\left(\lim_{\eta \to \zeta^+} - \lim_{\eta \to \zeta^-} \right) \partial_\eta S_{CI} = -\frac{4\pi\zeta^2}{1 + 4\zeta^2} \,. \tag{3.17}$$

This a strong early hint for a feature that we will later see in detail, namely that the quantum behaviour away from the critical line is rather different from that exactly on the critical line.

3.1.3 Uniton Dominance Regimes

Whilst discussing the classical aspects of these solutions, let us preempt a little of what is to follow. We have in the complex and real unitons two types of classical saddles, and one should anticipate that both are important to define the full quantum theory. However, which (classical) saddle is most important will depend on where we are in (classical) parameter space. Because the configuration with the lowest action yields the biggest contribution in perturbation theory, we divide the parameter space spanned by η and ζ into different regions, based on inequalities among the actions (3.9) and (3.15). This is displayed in Figure 3.3 where one can see that there are demarcations between regimes when the absolute value of the real and complex uniton actions become equal or integer multiples of each other. One should anticipate that perturbation theory will behave differently in different regimes, and this will indeed be the case as will be seen in Section 3.3.

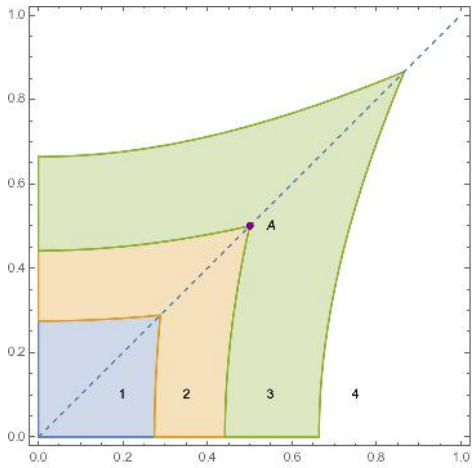

Figure 3.3: A plot in the $\eta - \zeta$ plane indicating the hierarchy of the various non-perturbative configurations. In region 1 (blue) $|2S_I| < |S_{CI}|$; in region 2 (yellow) $|S_I| < |S_{CI}| < |2S_I|$; in region 3 (green) $|S_{CI}| < |S_I| < |2S_{CI}|$ and finally in region 4 (white) $|2S_{CI}| < |S_I|$. The dashed line indicates the critical line $\varkappa := \eta = \zeta$ and the point A is where $\varkappa = \frac{1}{2}$ and $S_I = -S_{CI} = \pi$ and will be shown to exhibit interesting behaviour. The critical line crosses from region 1 to 2 at $\varkappa = \frac{1}{2\sqrt{3}}$, where $2S_I = -S_{CI} = \frac{8\pi}{4\sqrt{3}}$. It crosses from region 3 to 4 at $\varkappa = \sqrt{3}/2$ where $S_I = -2S_{CI} = \frac{8\pi}{4\sqrt{3}}$.

3.2 Compactification and Fractionation

Our primary goal is to expose the quantum resurgent structure of these theories. We shall do so in a slightly indirect fashion following the arguments proposed in [46], to reduce the problem from a full 1+1 dimensional quantum field theory to a tractable quantum mechanics. This is achieved by performing an adiabatic reduction on a spatial S^1 with a twisted boundary condition of the form[3]

$$g(t, x + L) = e^{iH_L} g(t, x) e^{-iH_R} . \tag{3.18}$$

However, it is more practical, instead, to work with a periodic boundary condition by defining

$$\tilde{g}(t, x) = e^{-iH_L x/L} g e^{iH_R x/L} \quad \Longrightarrow \quad \tilde{g}(t, x + L) = \tilde{g}(t, x). \tag{3.19}$$

Introducing a nonzero H_L and H_R is like turning on an effective background gauge field in the untwisted theory with periodic boundary conditions. This can be subdivided in a contribution from a vectorial twist and an axial twist $H_{V,A} = \frac{1}{L}(H_L \pm H_R)$.

By an adiabatic compactification, we mean that we are looking for a compactification that has no phase transition as we send the compactification radius L of the S^1 from large to small. The contribution of [46] is the precise analysis of two compactifications: one thermal and one spatial. It is shown that the thermal compactification has a phase transition, whereas the spatial compactification under some additional constraints does

[3] It should be clear from the context if L refers to the compactification radius or if it serves as a label for the left symmetry group, in contrast to R for the right symmetry group.

not. The nature of the phase transition is measured by $\mathcal{F}/N^2$ in the $N \to \infty$ limit, where $\mathcal{F}$ is the free energy. This quantity has a sharp transition from $\mathcal{O}(1)$ to 0 for thermal compactification as we go from large L to small L, whereas for the spatial compactification it tends to 0 in the limit for all L. Of course here we are at finite N (the target space is $SU(2)$) rendering some of this discussion moot in point but we retain the strategy employed at large N with some post-hoc justification.

It was shown in [46] that to achieve adiabatic continuity one must impose two things. Firstly, we need to set $H_A = 0$. Secondly, one must minimise the contributions of the Wilson line for the background gauge field, $\Omega = \exp(i \oint dx H_V) = \exp(iLH_V)$, to the free energy which occurs when

$$\Omega = e^{\frac{\nu i\pi}{N}} \operatorname{diag}\left(1, e^{\frac{2i\pi}{N}}, \ldots, e^{\frac{2i\pi(N-1)}{N}}\right), \qquad \nu = 0, 1 \text{ if } N = \text{odd, even}. \tag{3.20}$$

For the $SU(2)$ case this means we require

$$LH_V = H_L = H_R = \frac{\pi}{2}\begin{pmatrix} 1 & 0 \\ 0 & -1 \end{pmatrix}. \tag{3.21}$$

We will paramterise the effective gauge field as

$$H_L = H_R = \begin{pmatrix} \xi & 0 \\ 0 & -\xi \end{pmatrix}, \tag{3.22}$$

so the maximal twist (3.21) is given by $\xi = \pi/2$.

The idea here is that this simplifies the theory considerably, retaining only a small selection of modes from the full theory, but does so in a way that retains the salient perturbative structure. Whilst this approximation is evidently not complete (for instance the role of the renormalisation in the quantum field theory is somewhat obscured), rather remarkably we will find that we can relate the features of perturbation theory in the resultant quantum mechanics obtained after shrinking the S^1 to the non-perturbative saddles found in the full 1+1 dimensional theory.

To understand the twisted Lagrangian $\mathscr{L}[\tilde{g}]$, we shall consider the currents under both the right and the left acting symmetries $g \to e^{i\alpha_L\sigma_3} g e^{-i\alpha_R\sigma_3}$ of the untwisted Lagrangian studied in Section 2.2.4. The Minkowkian current are given by Equation (2.28). In terms of these currents, the twisted Lagrangian obtained by substituting the field (3.19) with $H_{L/R}$ given by (3.22) into the lagrangian (2.16) is given by

$$\mathscr{L}[\tilde{g}] = \mathscr{L}[g] + \frac{\xi}{L}(\mathrm{j}_L^3 + \mathrm{j}_R^3) + \frac{8\xi^2}{L^2\Delta(\theta)} \sin^2(\theta)[(\zeta - \eta)^2 \sin^2(\theta) + 1], \tag{3.23}$$

where we recall $\Delta(\theta) = 1 + \zeta^2 + \eta^2 + 2\zeta\eta\cos(2\theta)$.

We will now perform a Kaluza-Klein reduction and discard all the spatial dependence. Moreover, we will eliminate all total derivatives. In particular, this means the contribution linear in currents $\mathrm{j}^3_{L/R}$ vanishes. In the resulting Lagrangian, the fields

ϕ_i become non-dynamic, and thus we can focus on the low energy effective theory by setting all momenta in these directions to zero.

Following this procedure we thus obtain the reduced Lagrangian

$$\mathscr{L} = \frac{1}{\mathsf{t}} \frac{\dot{\theta}^2 - \frac{8\xi^2}{L^2} \sin^2(\theta)[(\zeta-\eta)^2 \sin^2(\theta)+1]])}{\Delta(\theta)} \,. \tag{3.24}$$

To put the kinetic term into canonical form it is necessary to redefine variables such that the denominator factor $\Delta(\theta)$ can be absorbed. This is achieved by defining

$$\tilde{\theta} = F(\theta|m) \,, \tag{3.25}$$

where $F(\theta|m)$ is the elliptic integral of the first kind. The modulus m was foreshadowed by Equation (3.10). Employing Jacobi elliptic functions[4], the Hamiltonian of the quantum mechanics takes the following form

$$H = \frac{g^2}{4} p_{\tilde{\theta}}^2 + \frac{1}{g^2} V(\tilde{\theta}) \,, \tag{3.26}$$

with

$$V(\tilde{\theta}) = \frac{4\xi^2}{L^2} \mathrm{sd}^2(\tilde{\theta})(1 + \chi_-^2 \mathrm{sn}^2(\tilde{\theta})) \,, \tag{3.27}$$

where $g^2 = \mathsf{t}(1+\chi_+^2)$[5]. Notice in the $\zeta \to 0$ limit, we have that $m \to 0$, which implies that $\mathrm{am}(u) \to u$, so $\mathrm{sn}(u) \to \sin u$ and $\mathrm{dn}(u) \to 1$ such that the potential degenerates to a Whitaker–Hill type found for the single deformation in [47].

The approach to UV fixed lines, $\eta - \zeta = i$ and $\eta + \zeta = i$ in the complex plane displays further striking behaviour. In elliptic variables these limits correspond to sending $m \to 1$ and $m \to \infty$ respectively. Using the the elliptic variables, when we set $\eta - \zeta = \pm i$, the potential becomes $\tanh^2(\theta)$. Up to a shift, this is a Pöschl-Teller potential which has an exactly solvable discrete spectrum in terms of Legendre polynomials. The $m \to \infty$ limit is better understood without going to elliptic variables, indeed setting $\eta = \zeta = \frac{i}{2}$ we see that $\Delta(\theta) \to \sin^2\theta$ such that the Lagrangian (3.24) describes a free particle. In both cases, one should not anticipate any asymptotic behaviour to be exhibited. However, any small deformation away from these points will induce a non-trivial potential and a rich resurgent structure will become manifest. This is rather reminiscent of the Cheshire cat resurgence [27, 40, 153], as we obtain a theory that has energy eigenvalues that are not asymptotic in g^2, but rather are exact. It would certainly be interesting to understand this directly at the two-dimensional level for which the fixed point is understood as a $SU(1,1)/U(1)+U(1)$ gauged WZW CFT.

For the remainder of the Chapter, we shall be studying a quantum mechanical system

[4]The Jacobi amplitude $\mathrm{am}(u|m) = \phi$ is the function such that ϕ satisfies $u = F(\phi|m) \equiv \int_0^\phi d\theta \, (1 - m\sin^2\theta)^{-\frac{1}{2}}$. We shall generally drop the argument m, unless it is unclear. The Jacobi elliptic sine is $\mathrm{sn}(u) = \sin\phi$. The delta amplitude is $\mathrm{dn}^2(u) = 1 - m\,\mathrm{sn}^2(u)$ and we make use of $\mathrm{sd}(u) = \frac{\mathrm{sn}(u)}{\mathrm{dn}(u)}$.

[5]Notice a similar rescaling was applied in Equations (3.8) and (3.14).

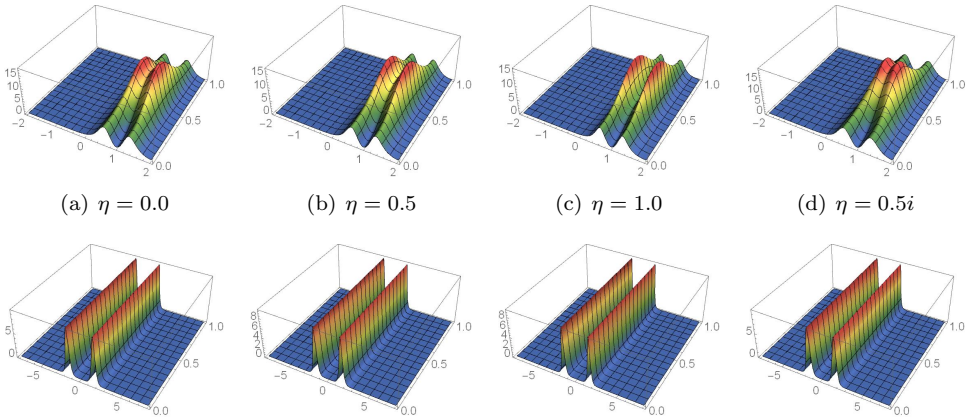

(a) $\eta = 0.0$ (b) $\eta = 0.5$ (c) $\eta = 1.0$ (d) $\eta = 0.5i$

(e) $\eta = 0.0$ (f) $\eta = 0.5$ (g) $\eta = 1.0$ (h) $\eta = 0.5i$

Figure 3.4: The Lagrangian density of the real uniton on $\mathbb{R} \times S^1$ with twisted periodic boundary conditions. We have set $\zeta = 0.5$ everywhere. In the top row, $\lambda_0 = e^2$ and $\lambda_1 = e^{-4}$ and we cannot see a clear fractionation. In the bottom row we consider $\lambda_0 = \lambda_1 = e^{-5}$ and there is a clear fractionation.

with potential (3.27). Before doing so, let us remark on the fate of the uniton (real and complex) under this twisted reduction. The first point to remark is that it is straightforward to modify the uniton solutions to accommodate the twisted boundary condition, this is done by simply by replacing the holomorphic function $f(z)$ entering in the minimal unitons (i.e. $k = 1$) on $\mathbb{R}^2$ with a twisted version $f(z) = \lambda_0 e^{-\pi z/L} + \lambda_1 e^{\pi z/L}$.

Recall that on $\mathbb{R}^2$ the unitons formed localised lumps of Lagrangian density (with some non-trivial profile induced by the deformation parameters) and this is true across the moduli space parameterised by $\{\lambda_0, \lambda_1\}$. In contrast, on the twisted cylinder a different behaviour emerges; there are regions of moduli space for which the real uniton breaks up (or fractionates) into well separated and clearly distinct lumps of Lagrangian density (see Figure 3.4). In this way we anticipate that a single real uniton makes a contribution to the dimensionally reduced theory much like an instanton anti-instanton pair. The complex uniton exhibits a similar fractionation (see Figure 3.5), but in addition we observe a strange phenomenon around the critical line: the additional valley in the uniton density discontinuously vanishes.

3.3 WKB and Resurgence

In this section we study a Schrödinger Equation

$$\left(g^4 \frac{\partial^2}{\partial \theta^2} - V(\theta) + g^2 E \right) \Psi(\theta) = 0 \,, \tag{3.28}$$

with potential (to ease notation we now drop the tilde accent on θ)

$$V(\theta) = \mathrm{sd}^2(\theta)(1 + \chi_-^2 \mathrm{sn}^2(\theta)) \tag{3.29}$$

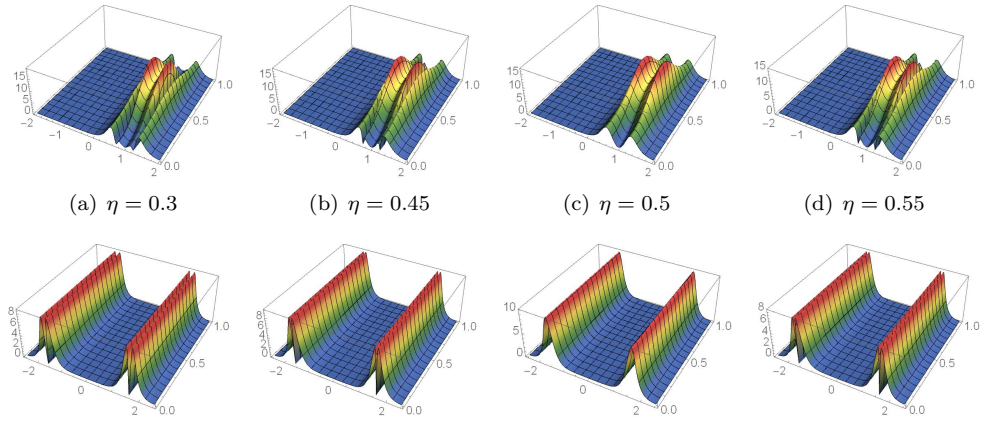

(a) $\eta = 0.3$ (b) $\eta = 0.45$ (c) $\eta = 0.5$ (d) $\eta = 0.55$

(e) $\eta = 0.3$ (f) $\eta = 0.45$ (g) $\eta = 0.5$ (h) $\eta = 0.55$

Figure 3.5: The Lagrangian density of the complex uniton on $\mathbb{R} \times S^1$ with twisted periodic boundary conditions. Here we have set $\zeta = 0.5$ and zoomed in to study the behaviour around the critical line $\eta = \zeta$. In the top row, we show $\lambda_0 = e^2$ and $\lambda_1 = e^{-4}$, which should be contrasted with the bottom row where $\lambda_0 = \lambda_1 = e^{-5}$ and fractionation is clearly evident. In both rows we clearly see, in (c) and (g), a sharp change in the profile as the critical line is reached.

and $g^2 = \mathtt{t}(1 + \chi_+^2)$. We employ the WKB method to obtain an expansion in $g^2 \to 0$. We make an ansatz similar to Equation (1.29)

$$\Psi(\theta) = \exp\left(\frac{i}{g^2}\int_{\theta_0}^{\theta} d\theta\, S(\theta)\right), \tag{3.30}$$

in which, $S(\theta)$ is a function that still depends of g^2. This will solve the Schrödinger Equation (3.28) if the function $S(\theta, g^2)$ satisfies the Ricatti Equation (1.30)

$$S^2(\theta) - ig^2 S'(\theta) = p^2(\theta)\,, \tag{3.31}$$

where $p(\theta) = \sqrt{g^2 E - V(\theta)}$ is the classical momentum, as usual. We assume a power series ansatz for $S(\theta)$

$$S(\theta) = \sum_{n=0} g^{2n} S_n(\theta)\,, \tag{3.32}$$

for which there exists a recursive solution widely available in the literature [23, 43, 44]. At the same time we make a power series ansatz

$$E = \sum_{n\geq 0} a_n g^{2n}\,. \tag{3.33}$$

Here, a_n of course still depends on the parameters η and ζ.

In this section we will compute this perturbative series to a very high order. For explanatory purposes, will mostly restrict our investigation to the behaviour along two trajectories: along the critical line $\varkappa = \eta = \zeta$ and along the line $\zeta = 1/5$. We will study

how the behaviour transitions as we cross the different regions shown in Figure 3.3. Along these trajectories, we compute the Borel-Padé approximant. We show how its pole structure suggests branch points that precisely match the value of the uniton actions (3.9) and (3.15). By looking at the Stokes lines of the quadratic form associated to this potential, we see that these contributions can be associated with saddle trajectories for real values of the coupling.

Next, we use the uniform WKB ansatz [15] to find an asymptotic form for the perturbative expansion. We show that the perturbative series converges rapidly to its asymptotic form. This asymptotic form, however, depends on which regions of the parameter space we analyse, as different unitons are dominant across the different regions of Figure 3.3.

3.3.1 Borel Transform

We use the BenderWu package [81] to compute WKB expansion so that we obtain a perturbative asymptotic expansion of the ground state energy (we will not consider higher level states in this Chapter). Unfortunately, the script runs too slow for general η and ζ so for most of the asymptomatic analysis to come we will be working with explicit values for the deformation parameters. For specified values of η and ζ, we could typically obtain 300 order of perturbation theory in 30 minutes on a desktop computer. The first terms for the deformed model in the expansion come out as

$$\begin{aligned}
E &= 1 - \frac{1}{4}g^2 - \frac{1}{16}g^4 - \frac{3}{64}g^6 + \mathcal{O}(g^8), && \eta = 0,\ \zeta = 0\,, \\
E &= 1 - \frac{1}{16}g^2 - \frac{61}{256}g^4 + \frac{777}{4096}g^6 + \mathcal{O}(g^8), && \eta = \frac{1}{2},\ \zeta = 0\,, \\
E &= 1 - \frac{69}{1600}g^2 - \frac{360357}{2560000}g^4 + \mathcal{O}(g^6), && \eta = \frac{1}{2},\ \zeta = \frac{1}{4}\,, \\
E &= 1 - \frac{3}{32}g^4 - \frac{39}{2048}g^8 + \mathcal{O}(g^{12}), && \eta = \zeta = \frac{1}{2}\,,
\end{aligned} \tag{3.34}$$

The fact that at $\eta = \zeta = 1/2$ we obtain a perturbative series in g^4 is very specific to this point as is explained further in Figure 3.15. In essence, it is due to a perfect cancellation of an alternating and a non-alternating series. This can be traced back to the equality $S_I = -S_{CI} = \pi$, as can be explained through resonance, see also Figure 3.3.

Mimicking Section 1.1, we compute the Borel transform

$$\hat{E} = \sum_{n\geq 0} \frac{a_n}{n!}\hat{g}^{2n} \tag{3.35}$$

of this series. We would like to understand something about the singularity and branch cut structure of the $\hat{g}^2$-plane, which is also called the Borel plane. We will sometimes use $z = g^2$, while $s = \hat{g}^2$ is the variable in the Borel plane. When the Laplace transformation can be done un-ambiguously this results in a finite re-summed value for the original series. However, in many interesting cases $\hat{E}(s)$ has poles along the integration path

$s \in [0, \infty]$ defining the Laplace transformation. As discussed in Section 1.1.2, to give meaning to the integration one can instead deform the integration contour and define the lateral resummation in the direction ϑ as

$$\mathcal{S}_\vartheta E(z) = \frac{1}{z} \int_0^{e^{i\vartheta}\infty} ds\, e^{-s/z} \hat{E}(s)\,. \tag{3.36}$$

A ray, $\vartheta = \vartheta_0$, is said to be a Stokes direction if $\hat{E}(s)$ has singularities along that ray. One can then define two lateral summations $\mathcal{S}_{\vartheta_0+\epsilon}E(z)$ and $\mathcal{S}_{\vartheta_0-\epsilon}E(z)$ which have the same perturbative expansion but differ by non-perturbative contributions, a change known as a Stokes jump. The crucial idea of the resurgence paradigm in the quantum mechanical context, going back to [12, 72, 73] is that the inherent ambiguity between these two perturbative resummations is precisely cancelled by a similarly ambiguous contribution from the fluctuations around an appropriate non-perturbative configurations in the same topological sector. For instance, in quantum mechanic the path integral over the quasi-zero mode separation between an instanton anti-instanton pair has an ambiguous imaginary contribution that cancels that of the ground state energy ambiguity. The first test of this programme is then that the location of the poles in the Borel plane should be in accordance with the values of the on-shell action for non-perturbative field configurations. When performing a numerical calculation, the summation defining the Borel transformation has to be cut off at the order to which the perturbative expansion was performed. Hence $\hat{E}(z)$ becomes a simple polynomial which has no poles. For this reason, we employ the Padé approximant, which was introduced in Remark 7, which is an approximation of the function by the ratio of two polynomials, where the coefficients are determined by demanding that the Taylor series matches the original. By calculating the roots of the denominator of the Padé approximant, we find its poles in the $\hat{g}^2$-plane. These are called the (Borel-)Padé poles. An accumulation of Padé poles suggests a branch point in the Borel plane. These methods are expanded upon further in [43, 44, 154, 155].

Critically, we find that those branch points can be identified precisely with the finite action configurations found previously by the real and complex unitons (3.9) and (3.15)! This is illustrated in Figures 3.6 and 3.7 demonstrating the behaviour across the critical line and along it. We are thus able to relate non-perturbative contributions with these instanton configuration. It is important to emphasise that what we have done is to take a two-dimensional QFT and truncated to a particular quantum mechanics, but the relevant non-perturbative saddles are coming from finite action solutions in the full two-dimensional theory.

Beyond the headline matching of poles to non-perturbative saddles lies a more intricate structure. In Figure 3.6 we show that for generic real values of η and ζ, the Borel-Padé approximation suggests the existence of two Stokes rays. The first is at $\arg(s) = 0$ for which we see evidence of a branch cut terminating at the value of the real 1-uniton action. The second is the $\arg(s) = \pi$ ray and with a cut terminating at the complex 1-uniton action. However, as the parameters are tuned to the critical line

$\eta = \zeta$ (see Figure 3.6 (c)) the location of the cut in the $\arg(s) = \pi$ direction jumps from the complex 1-uniton to the complex 2-uniton action. Figure 3.6 confirms that all along the critical $\zeta = \eta = \varkappa$ line that $\arg(s) = \pi$ branch cut terminates at the complex 2-uniton action. This implies that for the entire range $0 < \varkappa < \frac{1}{2}$ the leading pole (the one nearest to the origin) continues to be that along $\arg(s) = 0$ at the location of the real 1-uniton action. At $\varkappa = \frac{1}{2}$ (see Figure 3.7 (c)), the action of the complex 2-uniton coincides with that of the real 1-uniton; this is the non-perturbative feature corresponding to the fact that the perturbative series in eq. (3.34) discontinuously jumps to being a series in g^4 rather than g^2 when $\varkappa = \frac{1}{2}$ – see Equation (3.34).

Having established that it is essential to consider complexified field configurations to understand the Borel pole structure, it is natural to now analytically continue the deformation parameters η and ζ themselves into the complex plane.

Generically, as indicated in Figure 3.8, the branch cuts continue to match to the values of the uniton actions, and now lie along angles governed by the phase of the uniton action. In Figure 3.9 we show what happens as the phase of the critical parameter $\varkappa$ is rotated; again we see that the direction of the branch cuts track the phases of the unitons. These plots also hint, although the numerics are limited, at the existence of a tower of poles located at multiples of the complex 2-uniton action.

Finally, we study the potential as it approaches the point $\eta = \zeta = \frac{i}{2}$ which corresponds to the RG fixed point. Here, m has a pole, so the elliptic potential is not well-defined (but recall that this is a consequence of the Jacobi variables; in the original Euler angle variables this point was simply a free theory). The actions (3.9) and (3.15) tend to zero[6], as do the elliptic periods of the potential. As discussed in the previous section, though a different change of variable this point can be associated to a free theory.

Firstly, we consider the behaviour as we rotate around $\eta = \zeta = \frac{i}{2}$ on the critical line by looking at

$$\varkappa = \eta = \zeta = \frac{i}{2} + \epsilon e^{i\theta} \,. \tag{3.37}$$

We find that there is an infinite tower of branch points located at

$$2S_{CI} + 2n(S_I - S_{CI}), \qquad n \in \mathbb{Z} \,. \tag{3.38}$$

In particular, for $n = 1$ and $n = 0$ there are branch poles at the real and complex uniton actions respectively. This is consistent with the previous analyses.

In addition we consider the behaviour as we rotate around $\eta = \zeta = i/2$ slightly off the critical line, that is, let

$$\eta = \frac{i}{2}, \quad \zeta = \frac{i}{2} + \epsilon e^{i\theta} \,. \tag{3.39}$$

[6] In general, we have chosen the branch cuts in the Borel plane to run from $2S_I$ to $+\infty$ and from $2S_{CI}$ to $-\infty$; here however a more natural choice would be to take a cut from $2S_I$ to $2S_{CI}$ such that cut is removed entirely as the free theory point is approached. For this interpretation to make sense it is necessary that the branch points at $2S_I$ and $2S_{CI}$ display the same behaviour - which they do (see Equation (3.53)).

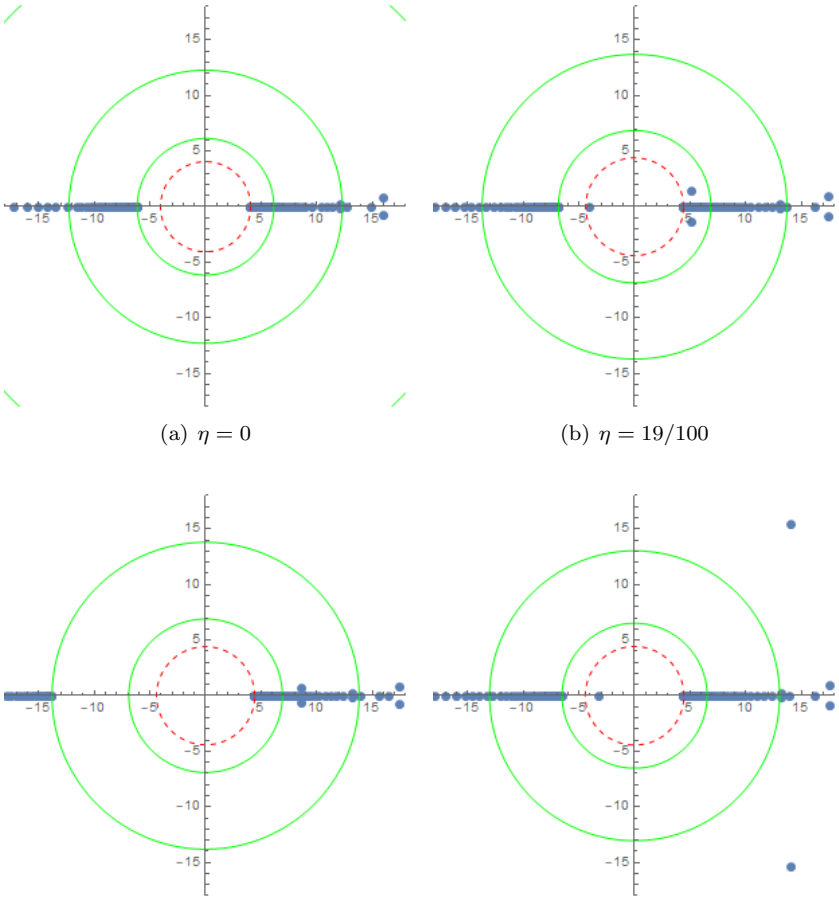

(a) $\eta = 0$ (b) $\eta = 19/100$

(c) $\eta = 20/100 = 1/5$ (d) $\eta = 21/100$

Figure 3.6: The complex Borel s-plane for $\zeta = \frac{1}{5}$ at different values of η with blue dots indicating poles of the Borel-Padé approximation obtained from 300 orders of perturbation theory in g^2 (hence we computed a total of 150 poles). Accumulations of poles are anticipated to encode branch cuts in the full Borel transform, and isolated poles are expected to be residuals of the numerical approximation. The red dashed circle indicates the magnitude of the the real uniton action located at $|s| = 2S_I$. The green dashed circles indicate the magnitude of the complex 1- and 2-uniton actions located at $|s| = |S_{CI}|, |2S_{CI}|$ respectively. For η and ζ real, the real and complex instanton action have an complex argument of 0 and π respectively. We see a clear match to the location of expected branch points with these values. At the critical line $\eta = \zeta$, we observe a curious discontinuous jump; the accumulation of poles at the 1-complex uniton disappears entirely and instead, we get an accumulation point at the complex 2-uniton action $s = 2S_{CI}$.

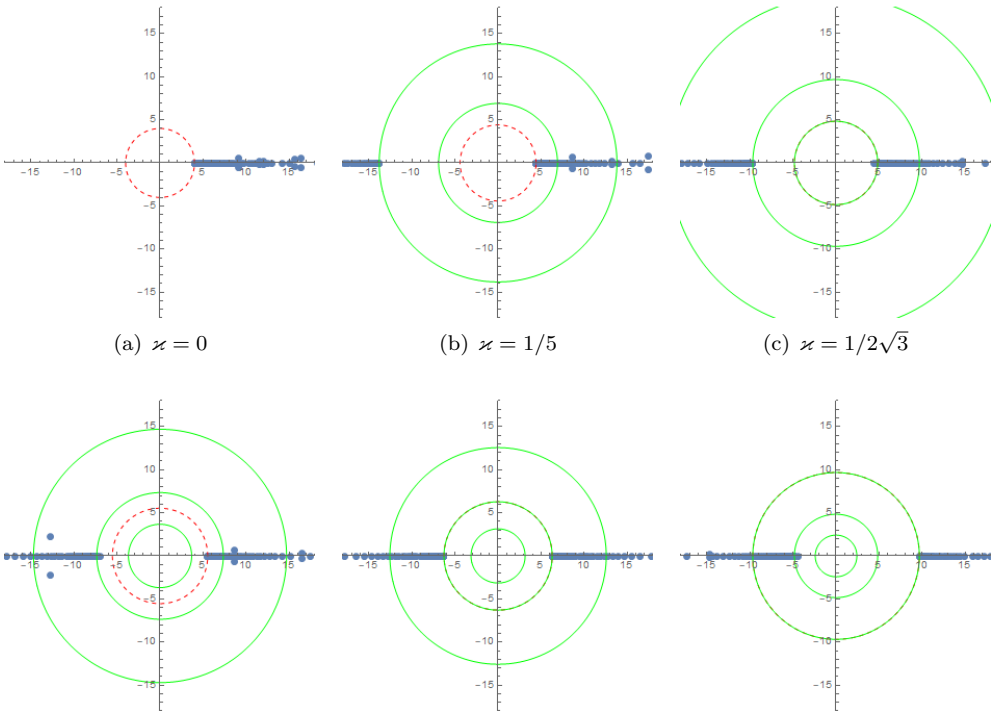

(a) $\varkappa = 0$ (b) $\varkappa = 1/5$ (c) $\varkappa = 1/2\sqrt{3}$

(d) $\varkappa = 2/5$ (e) $\varkappa = 1/2$ (f) $\varkappa = \sqrt{3}/2$

Figure 3.7: The complex Borel s-plane along the $\zeta = \eta = \varkappa$ critical line as we cross different region of Figure 3.3. Colours, key, and numerical approximation as per Figure 3.6, but we have also plotted the action of the complex 4-uniton $|s| = |4S_{CI}|$ as a green circle. In the undeformed model $\varkappa = 0$ there is not complex uniton [46] since it has infinite action. When $\varkappa = 1/5$, we are in region 1. At $\varkappa = 1/2\sqrt{3}$, we have $2S_I = -S_{CI}$ and cross from region 1 to 2. Notice that a dashed red circles coincides with the inner green circle. For $\varkappa = 2/5$, we are in region 2. When $\varkappa = 1/2$ we cross into region 3 and $S_I = -S_{CI}$. If $\varkappa = \sqrt{3}/2$ we cross from into 4 where $S_I = -2S_{CI}$. Consistent we the results of Figure 3.6, we note that along the critical line, the branch points along the negative real axis accumulate at $2S_{CI}$, not at S_{CI}.

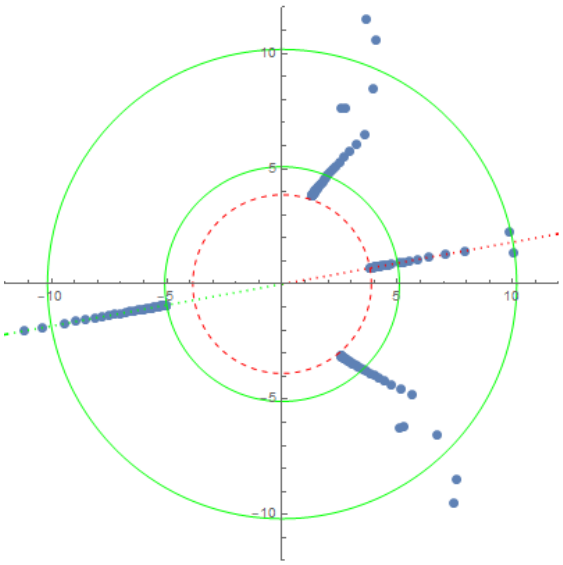

Figure 3.8: The complex s Borel plane for $\zeta = 1/5$, $\eta = 2i/5$. Colours, key, and numerical approximation as per Figure 3.6 with in addition the argument of the real (complex) uniton indicated by a red (green) dotted ray. The accumulation points still gravitate towards the uniton actions and are direct with an argument matching precisely that of the relevant uniton action. In this particular case, because $\mathrm{Re}(\eta) = \mathrm{Im}(\zeta) = 0$, we have that $\chi_+ = \overline{\chi_-}$ and therefore the ratio of the actions is real and negative. This explains why the angle between the dotted rays is precisely π. We were unable to explain the phases of the secondary branch point that have an absolute value equal to that of the real uniton action.

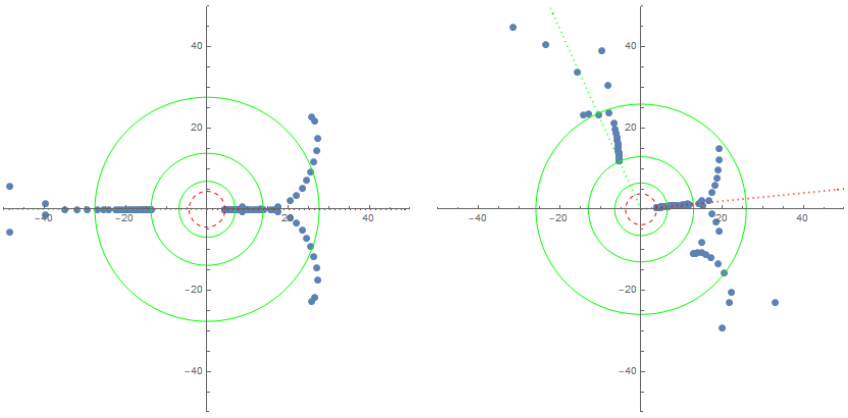

(a) $\theta = 0$ (b) $\theta = \pi/3$

(c) $\theta = 9\pi/20$ (d) $\theta = \pi/2$

Figure 3.9: Here, we consider the critical line $\varkappa = \eta = \zeta$ and compute 300 order of perturbation theory. We keep $|\varkappa| = 1/5$ fixed, but vary $\theta = \arg(\varkappa)$. We suspect that the tails splitting into 2 ends is due to numerics and could be resolved by going to higher orders. Interestingly, it appears we can see towers of higher order states more easily when η and ζ are analytically continued.

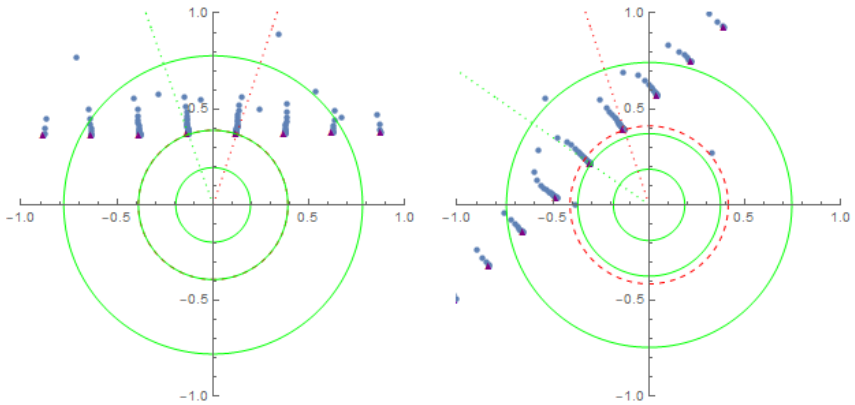

(a) $\theta = 0$ (b) $\theta = \pi/4$

(c) $\theta = 2\pi/4$ (d) $\theta = 3\pi/4$

Figure 3.10: Here, we look at the behaviour around the special point $\varkappa = \frac{i}{2}$, paramatrised by Equation (3.37) with $\epsilon = 0.01$. We observe that the branch poles, indicated by purple triangles, are given precisely by Equations (3.38). Note also that we have zoomed relative to other Borel plots shown since both the real and the complex uniton action tend to 0 as $\varkappa \to \frac{i}{2}$.

In this case we find a tower of branch points located at

$$S_{CI} + 2n(S_I - S_{CI}), \qquad n \in \mathbb{Z}\,. \tag{3.40}$$

This in particular reproduces the the branch point at S_{CI} for $n = 0$, which is consistent with off-critical line behaviour. There are also hints off branch point of the tower given by Equation (3.38), but the numerics are not as clean.

The relevant Borel plots are shown in Figures 3.10 and 3.11. We emphasise that perturbations of the form $\epsilon e^{i\theta}$ are not relevant for generic values of η and ζ. Only at $\varkappa = i/2$ do these have a substantial effect on the Borel poles.

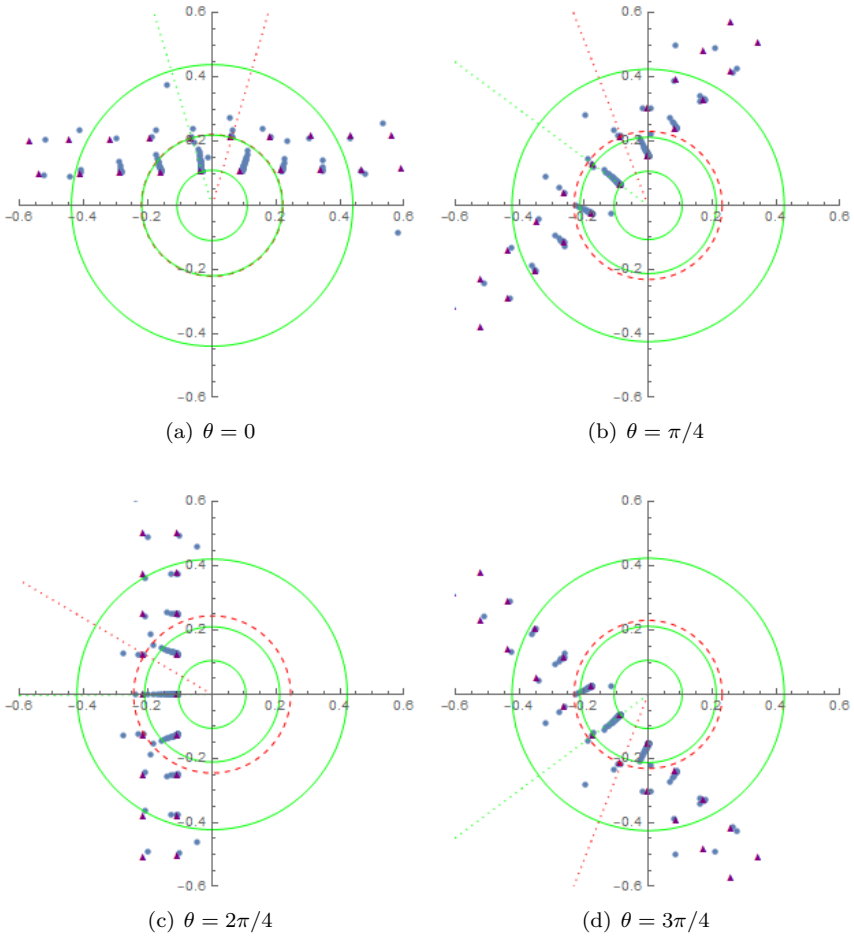

(a) $\theta = 0$ (b) $\theta = \pi/4$

(c) $\theta = 2\pi/4$ (d) $\theta = 3\pi/4$

Figure 3.11: Here, we look at the behaviour around the special point $\eta = \zeta = \frac{i}{2}$, paramatrised by Equation (3.39) with $\epsilon = 0.01$. We find a very clear set of inner branch point given by Equations (3.40). In addition, there are traces of the outer tower given by Equation (3.38).

3.3.2 Asymptotic Analysis

We now have the ingredients to investigate the asymptotic behaviour of the perturbative series for the ground state energy. Let us first split the behaviour into three contributions

$$E_n \sim E_n^{S_I} + E_n^{S_{CI}} + E_n^{2S_{CI}} + \dots , \tag{3.41}$$

where $E_n^{kS_{(C)I}}$ is a contribution due to the (complex) k-uniton. To give an idea, for the real uniton, this contribution will look like $E_n^{kS} \propto (2kS)^{-n}\Gamma(n+a)$. We emphasise that we cannot concretely decompose the perturbative coefficients. Rather, our objective is to identify large order behaviour in different areas of the moduli space spanned by the parameters (η, ζ) (recall figure 3.3). These different contributions to the large order behaviour are what we try to sketch in Equation (3.41). We calculate Stokes discontinuities of these large order behaviours more carefully in Section 3.3.3.

We use the uniform WKB-method in Section 1.3. This will be in particular useful into giving the form of the $E_n^{S_I}$ contribution. However, also on the critical line, we can argue what $E_n^{2S_{CI}}$ should look like. Our motivation for $E_n^{S_{CI}}$ shall be of empirical nature. We use the ansatz (1.72) and expand the energy $\mathcal{E}$ and the function $u(\theta)$ and as power series in g^2:

$$u(\theta) = \sum_{n=0} g^{2n} u_n(\theta), \qquad \mathcal{E}(B) = \sum_{n=0} g^{2n} \mathcal{E}_n(B)\,, \qquad B = \nu + \frac{1}{2} \tag{3.42}$$

They will now satisfy a slightly modified Ricatti Equation (1.60) which can be solved perturbatively. Integration constants are determined by demanding that $u(\theta)$ is regular around $\theta = 0$. $\mathcal{E}_n(B)$ is a polynomial of order n in B of definite parity: $\mathcal{E}_n(B) = (-1)^{n+1}\mathcal{E}_n(-B)$. Of course, in our problem, it also depends on η and ζ. For $u_0(\theta)$, we find

$$\begin{aligned}(u_0(\theta))^2 &= 4\int_0^\theta d\theta\, \sqrt{V(\theta)} \\ &= \frac{4}{m}\left(\chi_+ \arctan(\chi_+) - \chi_+ \arctan\left(\frac{\chi_+ \mathrm{cn}(\theta)}{\sqrt{\chi_-^2 \mathrm{sn}(\theta)^2 + 1}}\right) + \right. \\ &\left. i\chi_- \left(\log(1+i\chi_-) - \log\left(\sqrt{\chi_-^2 \mathrm{sn}(\theta)^2 + 1} + i\chi_- \mathrm{cn}(\theta)\right)\right)\right),\end{aligned} \tag{3.43}$$

where $\chi_\pm = \zeta \pm \eta$. For $n > 0$, we use a power series ansatz of $u_n(\theta)$ in θ which results

in the following coefficients for the expansion of the energy at level B

$$\begin{aligned}
\mathcal{E}_0 &= 2B\,, \\
\mathcal{E}_1 &= \frac{\left(4B^2+1\right)\left(-1+\chi_-^2+\chi_+^2+3\chi_-^2\chi_+^2\right)}{8(1+\chi_+^2)}\,, \\
\mathcal{E}_2 &= \frac{-1}{8}B^3\left(17\chi_-^4+16m\chi_-^2+2\chi_-^2+1\right)-\frac{B}{32}\left(8m(1-m+7\chi_-^2)+67\chi_-^4+22\chi_-^2+3\right)\,,
\end{aligned} \tag{3.44}$$

where we recall m is given by Equation (3.10). We also found $\mathcal{E}_3$, but the expression is too long to be displayed usefully. As a consistency check, we note coefficients match up perfectly with [47] upon setting $\zeta = 0$. We impose a Bloch quantisation condition (1.68) around the midway point. In the potential (3.29), this would be the half period $\theta_{\text{midpoint}} = \mathbb{K}(m)$. We shall therefore need to compute $u(\theta_{\text{midpoint}})$. By using the periodicities of the Jacobi elliptic functions we find[7]

$$u_0(\theta_{\text{midpoint}}) = \sqrt{2S_I}\,, \tag{3.45}$$

and

$$u_1(\theta_{\text{midpoint}}) = \frac{\log[S_I(1+\chi_-^2)/4]}{\sqrt{2S_I}}\,, \tag{3.46}$$

where S_I is given by (3.9). This is our first evidence that the 2d uniton solutions have a role to play in the reduced quantum mechanics that are studied in this Section.

The resulting asymptotic expansion from the uniform WKB method are as in Equation (1.72). In the regime where $|S_I| < |S_{CI}|$, the perturbative energy coefficients are dominated by the following behaviour

$$E_n^{S_I} \approx A(\eta,\zeta)\left(\frac{1}{2S_I}\right)^{n+1}\Gamma(n+1)\left(1+a_I^1(\eta,\zeta)\frac{2S_I}{n}+\mathcal{O}\left(\frac{1}{n^2}\right)\right)\,, \tag{3.47}$$

where

$$A(\eta,\zeta) = -\frac{1}{\pi}\frac{16}{1+\chi_-^2}\,. \tag{3.48}$$

Because Equation (3.46) is an $\eta \to \eta - \zeta$ substitution compared to the single deformation case, the same follows for Equation (3.48). Working in higher order in the wave function allows a determination of the sub-leading contributions. E.g. $a_I^1(\eta,\zeta)$, which is a correction due to an instanton-anti-instanton $[I\bar{I}]$ event, is determined from $u_2(\theta_{\text{midpoint}})$, which did not however prove easy to analytically evaluate.

Furthermore, from our numerical analysis, we predict that the 1-complex uniton and

[7] Note that because the Jacobi functions appear squared in the potential, we need not worry about the fact that Jacobi functions are strictly speaking *anti*-periodic across the interval $2K(m)$.

the 2-complex uniton behave as

$$E_n^{S_{CI}} \approx B(\eta,\zeta)\left(\frac{1}{S_{CI}}\right)^{n+1/2}\Gamma(n+1/2)(1+a^1_{CI}(\eta,\zeta)\frac{2S_{CI}}{n}+\mathcal{O}(n^{-2}))\,, \tag{3.49a}$$

$$E_n^{2S_{CI}} \approx -A(\eta,\zeta)\left(\frac{1}{2S_{CI}}\right)^{n+1}\Gamma(n+1)(1+a^1_{2CI}(\eta,\zeta)\frac{4S_{CI}}{n}+\mathcal{O}(n^{-2}))\,, \tag{3.49b}$$

where

$$B(\eta,\zeta) = -\frac{\sqrt{A(\eta,\zeta)}}{\pi} = \frac{-4i}{\sqrt{\pi^3(1+\chi_-^2)}}\,. \tag{3.50}$$

We emphasise that these predictions for the asymptotic behaviour are not derivable from any conventional uniform WKB for generic η and ζ, but are based on empirical evidence.

However, on the critical line we can argue using the uniform WKB the validity of the asymptotic expansion $E_n^{2S_{CI}}$ Equation (3.49b). As established by Figure 3.6, there is no complex 1-uniton contribution along the critical line and the $E_n^{S_{CI}}$ contribution (3.49a) vanishes. We can use the ellipticity of the potential and argue a second global boundary condition along the secondary period of the potential. When evaluating $u_0(\theta)$ and $u_1(\theta)$ at the complex midpoint $i\mathbb{K}(1-m)$, we obtain precisely Equation (3.45) and (3.46) only with S_{CI} instead of S_I. Carrying through the argument of uniform WKB, one arrives precisely at (3.49b).

This analysis is consistent with the results from [41] where the system along the critical line is studied. It is observed that the potential respect a symmetry that sends $m \to m'$, $g^2 \to -g^2$ and $\theta \to i\theta$. This $\mathbb{Z}_2$ duality interchanges the real and the complex instanton solutions and therefore also interchanges their actions. It follows that $m = \frac{1}{2}$ is the fixed point of the duality, which can be traced back to $\varkappa = \frac{1}{2}$. We can also reformulate the $m \to m'$ transformation in terms of $\varkappa$ by sending $\varkappa \to \frac{1}{4\varkappa}$. Note that the asymptotic expansion of the energy (3.41), (3.47), (3.49), respects this symmetry only if we ignore the $E_n^{S_{CI}}$ contribution, which is precisely what happens on the critical line. Moreover, at the fixed point $m = \frac{1}{2}$, or $\varkappa = \frac{1}{2}$, we have that $E_n^{S_I}$ and $E_n^{S_{2CI}}$ contribute equally. Finally, understanding the interchanging of the two periods of the potential as interchanging complex and real instantons, it is clear why we should expect an expansion for the asymptotic energy of to the complex instanton when performing uniform WKB along the imaginary axis.

That on the critical line we get a sudden disappearance of the complex 1-uniton is odd when looking at the asymptotic formula (3.49b) as one might expect that $B(\eta=\zeta)=0$. However, this is *not* the case. That we have sudden vanishing of the complex 1-uniton action should however be clear from the Borel-Padé Figure 3.6. Possibly another way to study this might be through quantum periods in exact WKB. It will be observed in Section 3.3.4 that there are certain turning points that disappear on the critical line, together with associated saddle trajectories. One might thus speculate that the discontinuous shift in the value of the leading asymptotic instanton action is due to a

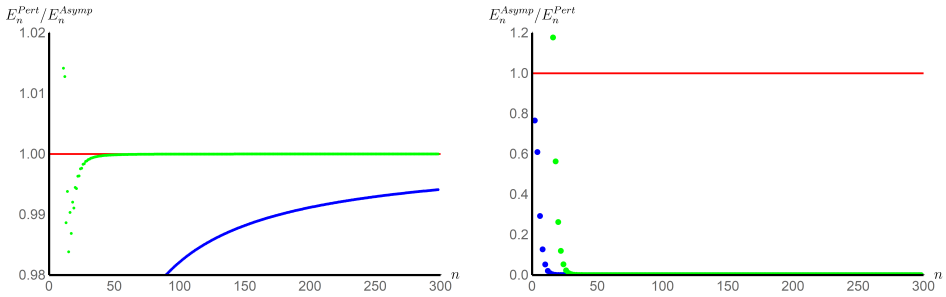

Figure 3.12: Here we study the convergence of the perturbative coefficients to the asymptotic prediction (3.47). Their ratio is given by the blue dots. To accelerate the convergence we employ the second Richardson Transformation, here given in green. In both plots we follow the trajectory where $\zeta = 1/5$. In the left plot $\eta = 19/100$, we obtain virtually the same results for $\eta = 1/5$. Here, we are in the first region of Figure 3.3 where $|2S_I| < |S_{CI}|$. Therefore, the real uniton is dominant, both on and off the critical line. In the right plot we show $\eta = 2/5$, which is in region 2. Using the same asymptotic expansion, we see that the approximation fails, because the real uniton is not dominant anymore.

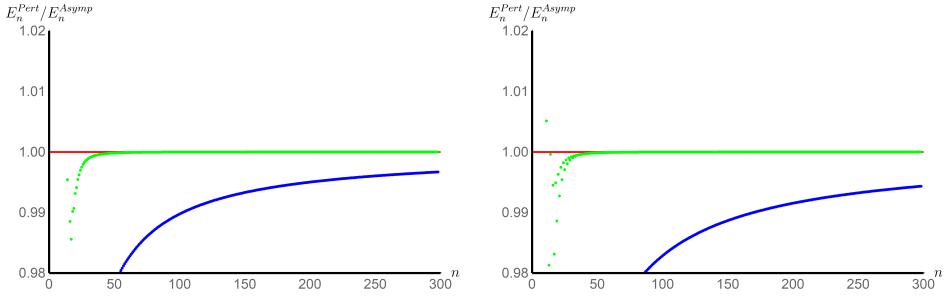

Figure 3.13: Colours are as in Figure 3.12. We follow the critical line $\varkappa = \zeta = \eta$. In the first plot $\varkappa = 1/2\sqrt{3}$, which is on the border of regions 1 and 2 of Figure 3.3 where $S_I = -S_{CI} = 8\pi/3\sqrt{3}$. In the second plot $\varkappa = 2/5$, which is firmly in region 2. In both cases $|S_I| < |2S_{CI}|$. Because along the critical line there is no complex 1-uniton contribution, the real uniton is dominant.

different Stokes graph structure. This could also lead to a different instanton action.

In Figures 3.12, 3.13, 3.14 and 3.15 we compare the asymptotic expression $E_n^{S_I}$ from Equation (3.47) with the actual values E_n^{pert} obtained from the perturbative calculation with the BenderWu package. We plot the ratio and study its convergence to 1. Doing so in Figure 3.12, we numerically verify Equation (3.47). The convergence of the raw data (shown in blue in Figure 3.12) is somewhat slow – a situation that could be improved by determining $a_I^1(\eta, \zeta)$.

However, convergence can be improved spectacularly by using a Richardson transform (see e.g. [43, 44]). Indeed, with just the second Richardson transform (shown in green in Figure 3.12) we see convergence between the 300^{th} order perturbative data and asymptotic predictions with a typical accuracy of between $4 \cdot 10^{-7}$ and $9 \cdot 10^{-7}$. This is an impressive agreement approaching the theoretical uncertainty resulting from using

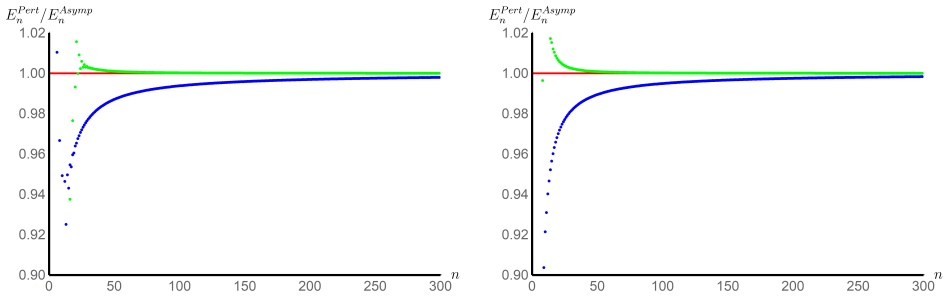

Figure 3.14: Colours are as in Figure 3.12. In both plots we follow the trajectory where $\zeta = 1/5$. In the first plot $\eta = 2/5$, in the second plot $\eta = 1/2$. We are thus in the second and third region of Figure 3.3. Because $|2S_I| > |S_{CI}|$, the complex uniton is dominant.

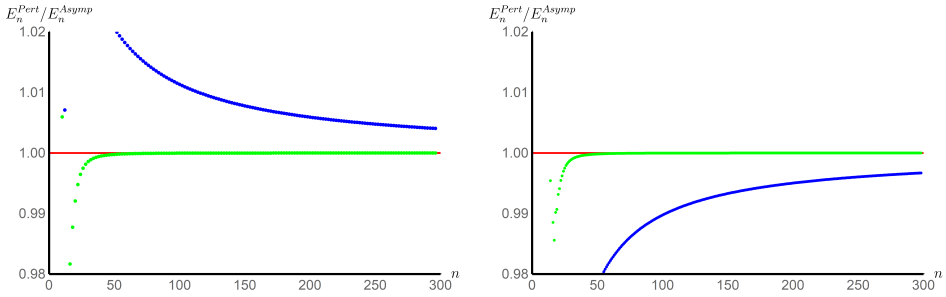

Figure 3.15: Colours are as in Figure 3.12. Here, we study the behaviour along the critical line $\varkappa = \eta = \zeta$. In the first plot, $\varkappa = 1/2$, the second plot $\varkappa = 2/\sqrt{3}$. We know that in regions 3 and 4 of Figure 3.3 along the critical line the complex 2-uniton is dominant. This is verified by the second figure. However, $\varkappa = 1/2$ is a very special point indeed as it acquires equal contributions from the complex 2-uniton and the real uniton. Because $S_I = -S_{CI} = \pi$, the only difference is that these contributions are non-alternating and alternating respectively. These precisely cancel out, leading to a series in g^4, as already foreshadowed in Equation (3.34).

the second Richardson transformation (results should be accurate to $O(1/n^3)$, hence for $n = 300$ this is $1/300^3 \approx 4 \cdot 10^{-8}$). Further theoretical uncertainty arises from the undetermined sub-leading terms in the asymptotic prediction. For the single deformed potential in [47] we have $a_I^1(\eta, \zeta = 0) = \frac{1}{24}\left(-23 + 77\eta^2 + \frac{8}{1+\eta^2}\right)$. Under the assumption that $a_I^1(\eta, \zeta)$ is of the same order as $a_I^1(\eta, 0)$, we can estimate the magnitude of this uncertainty, which also matches well with the measured accuracy[8].

As an additional remark, in Figure 3.6 we saw that the single complex instanton contribution disappears at the critical line $\eta = \zeta$. We suspect that a consequence of this is that the 1-uniton behaviour of Equation (3.47) remains dominant until $|2S_I| < |2S_{CI}|$ if $\eta = \zeta$. Therefore, the real uniton is dominant not only in region 1 of Figure 3.3, but also in region 2 along the critical line. This is corroborated by the numerical analysis displayed in Figure 3.13.

[8] To give an impression of the magnitude of this discrepancy, $a_I^1(0,0) = -15$, $a_I^1(1/5,0) \approx -12.2$, $a_I^1(1/2,0) = 2.65$ and $a_I^1(1,0) = 58$.

The computations that support the predictions given by Equation (3.49) are exhibited in Figures 3.14 and 3.15. Here, we investigate the regimes in which the 1- and 2-complex unitons are dominant. This corresponds to regions 3 and 4 and region 2 off the critical line of Figure 3.3.

At the boundary between region 1 and 2 in Figure 3.3, we would expect from the asymptotic expansions (3.47) and (3.49) that the real 1-uniton and the complex 1-uniton interact approximately at the same order. For example, the point $\zeta = 0$, $\eta_c = 0.274$, considered in [47], belongs to this family. However, because the asymptotic expansions do not precisely match, there is not a perfect cancellation of alternating and non-alternating terms like there is at $\varkappa = \eta = \zeta = 1/2$. The perturbative series along this border is thus in g^2 and not in g^4.

We can also explain this scenario in terms of resonance. Generically, one speaks of resonance phenomena when there are two tunable instanton actions at play, say S_1 and S_2 such that they are linearly dependent over the integers [43], i.e. $nS_1 + mS_2 = 0$ for some $n, m \in \mathbb{Z}$. In this case the n-instanton with action S_1 and the m-instanton with action S_2 operate at the same non-perturbative level. In our setting this is most clearly seen on the critical line at $\varkappa = \frac{1}{2}$. In this case, the complex 2-uniton and the real instanton have precisely opposite action. This results in a conspiracy where the non-alternating and alternating large-order behaviour precisely cancel in the odd terms of the odd expansion. This is the reason that the energy is an expansion in g^4 rather than g^2.

Combining all the information in the analyses of Equations (3.47) and (3.49) and Figures 3.12, 3.13, 3.14 and 3.15, we thus arrive at the following picture: across the $\zeta = 1/5$ trajectory, varying η, we find that the real uniton is dominant in region 1 of 3.3, while the complex 1-uniton is dominant in regions 2, 3, and 4. Along the critical line, there is no 1-complex uniton, thus the real uniton is dominant in regions 1 and 2, while the complex 2-uniton is dominant in regions 3 and 4.

Lastly, let us compare the perturbative calculation with the asymptotic expansion (3.47) to say something about $a_I^1(\eta, \zeta)$. Equating the predicted asymptotic to the perturbative expansion and rearranging implies that

$$\frac{(2S_I)^{n+1}}{\Gamma(n+1)A(\eta,\zeta)} E_n^{\text{pert}} - 1 \approx a_I^1(\eta,\zeta)\frac{2S_I}{n}\,. \tag{3.51}$$

By performing a Richardson transformation on the left hand side we can make predictions about $a_I^1(\eta, \zeta)$ in the regime where the real uniton dominates. The same can be done for $a_{CI}^1(\eta, \zeta)$. Example results are given in Tables 3.1 and 3.2. In addition, we can predict a_{2CI}^1 along the critical line for $\varkappa > 1/2$. For example, we expect $a_{2CI}^1 = -0.0581325$ for $\varkappa = \sqrt{3}/2$. Whilst the $a_I^1(\eta, \zeta)$ can in principle be determined from uniform WKB, there is not yet a systematic understanding of how to determine the a_{CI}^1 and a_{2CI}^1 .

η	$a_I^1(1/5,\eta)$
0	-0.509487
1/100	-0.497592
1/20	-0.444087
1/5	-0.157644

Table 3.1: Numerical predictions for $a_I^1(1/5,\eta)$ for selected values of η and ζ. We used the 10th Richardson transform and 300 perturbative coefficients. The $\eta = 0$ result agrees with the exact result from [47].

η	$a_{CI}^1(0.4,\eta)$
0.2	0.204395
0.38	7.20539
0.39	14.9317
0.395	34.06471
0.4	431.158
0.41	15.3672

Table 3.2: Numerical predictions for $a_{CI}^1(0.4,\eta)$ for selected values of η and ζ. We used the 10th Richardson transform and 150 perturbative coefficients. Notice the sudden jump at the Critical point $\eta = \zeta$, because the 1-uniton approximation brakes down at this point. Had we used the E_I approximation, we would have obtained $a_I^1(0.4, 0.4) = 54.9459$. This might suggest the coefficients a_I^1 and a_{CI}^1 have a simple pole at $\eta = \zeta$. However, it should be noted the numerics are quite unstable around the critical point as the asymptotic series approximates the perturbative series much slower.

3.3.3 Stokes Discontinuities

In this section we will make a schematic attempt to show the significance of our results and how this might be implemented to expose the resurgent structure of the system. We make a simplification to further explain the significance of the coefficients A and B in the asymptotic forms in Equations (3.47) and (3.49). Let us consider new asymptotic expansions in $z = g^2$ whose coefficients $E_n^{S_I}$, $E_n^{S_{CI}}$ and $E_n^{S_{2CI}}$ are, for all n and not just large enough n, given by the leading behaviour of Equations (3.47) and (3.49) (the sub-leading behaviour will be discussed later):

$$\tilde{E}_I(z) = \sum_{n=0}^{\infty} E_n^{S_I} z^n\,, \quad \tilde{E}_{CI}(z) = \sum_{n=0}^{\infty} E_n^{S_{CI}} z^n\,, \quad \tilde{E}_{2CI}(z) = \sum_{n=0}^{\infty} E_n^{S_{2CI}} z^n\,. \tag{3.52}$$

Their Borel transforms, using Equation (3.35) with $s = \hat{g}^2$, are given by

$$\hat{E}_I(s) = \frac{A(\eta,\zeta)}{2S_I - s}\,, \quad \hat{E}_{2CI}(s) = \frac{-A(\eta,\zeta)}{2S_{CI} - s}\,, \quad \hat{E}_{CI}(s) \quad = \frac{B(\eta,\zeta)\sqrt{\pi}}{\sqrt{S_{CI} - s}}\,. \tag{3.53}$$

We remind the reader that S_{CI} is a negative real number if η and ζ are real whereas S_I will be positive real, thus explaining the locations of the Borel poles in our preceding Borel analysis.

Recalling the re-summation, discussed in Section 1.1.2, in a direction ϑ of a series $\tilde{\psi}(z)$ is given by

$$\mathcal{S}_\vartheta \tilde{\psi}(z) = \frac{1}{z}\int_0^{e^{i\vartheta}\infty} ds\, e^{-s/z}\hat{\psi}(s)\,, \tag{3.54}$$

we can also see that the Borel resummation of $\tilde{E}_I$ is singular only along the positive real axis (i.e. there is a Stokes ray along $\vartheta = 0$), whilst the Borel resummations of $\tilde{E}_{CI}$ and $\tilde{E}_{2CI}$ are singular only along the negative real axis (i.e. a Stokes ray along $\vartheta = \pi$). Resummations along these rays are inherently ambiguous. To study these ambiguities we adopt lateral Borel resummations $\mathcal{S}_{\vartheta\pm}\tilde{\psi}(z) = \mathcal{S}_{\vartheta\pm\epsilon}\tilde{\psi}(z)$. We thus compute that non-perturbative ambiguity due to the 1-uniton is[9]

$$(\mathcal{S}_{0^+} - \mathcal{S}_{0^-})\tilde{E}_I(z) = -\frac{2\pi i}{z}\text{Res}_{s=2S_I}\left[e^{-s/z}\frac{A(\eta,\zeta)}{2S_I - s}\right] = \frac{2\pi i}{z}A(\eta,\zeta)e^{-2S_I/z}. \tag{3.55}$$

The sign after the first equality is due to the clockwise integration contour. Similarly

$$(\mathcal{S}_{\pi^+} - \mathcal{S}_{\pi^-})\tilde{E}_{2CI}(z) = -\frac{2\pi i A(\eta,\zeta)}{z}e^{-2S_{CI}/z}. \tag{3.56}$$

To resum $\hat{E}_{CI}(z)$, we choose the branch cut to go from $z = S_{CI}$ to negative infinity. (Hence the branch cut of the square root function lies along the positive real axis). The integral from 0 to S_{CI} does not contribute. For the remaining bit, we switch to an integration variable $x = S_{CI} - s$, and solve the integral. Performing the outlined procedure then gives

$$(\mathcal{S}_{\pi^+} - \mathcal{S}_{\pi^-})\tilde{E}_{CI}(z) = \frac{1}{z}\int_\gamma ds\, e^{-s/z}\frac{B(\eta,\zeta)\sqrt{\pi}}{\sqrt{S_{CI}-s}} = \frac{2B(\eta,\zeta)\sqrt{\pi}}{\sqrt{z}}e^{-S_{CI}/z} \tag{3.57}$$

The reason we are interested in computing quantities such as $(\mathcal{S}_{\vartheta^+} - \mathcal{S}_{\vartheta^-})\tilde{E}(z)$ is that this might shed light on the nature of the Stokes automorphism $\mathfrak{S}_\vartheta$, introduced in Section 1.1.3, which is defined by

$$\mathcal{S}_{\vartheta^+} - \mathcal{S}_{\vartheta^-} = -\mathcal{S}_{\vartheta^-}\circ \text{Disc}_\vartheta = \mathcal{S}_{\vartheta^-}\circ(\mathfrak{S}_\vartheta - \text{Id}). \tag{3.58}$$

The Stokes automorphism describes the analytic structure of the ambiguities as a Stokes ray is crossed [34, 44]. From Equations (3.55), (3.56) and (3.57), we can see that $A(\eta,\zeta)$ and $B(\eta,\zeta)$ are directly related to the Stokes coefficients.

For the undeformed model [46], it was conjectured that the Stokes automorphism of the perturbative sector is due to a contribution $\mathcal{E}_{[I\bar{I}]}(z)$ of the intantin-anti-instanton sector. This means there would be some expansion around a secondary saddle point that impacts the perturbative series $E_{[0]}(z)$ of the perturbative sector [0] which was calculated above. This intricate interplay of sectors from different saddle points is part of the rich study of resurgence as it is the starting point of establishing large-order

[9] We should emphasise here that we consider the ambiguity of the found large order behaviour in certain regimes, not for the perturbative series itself which we do not know completely.

relations.

On the field theory side, different contributions are ascribed to the fractons which constitute the unitons. Although typically these contributions are combined in sectors classified by π_2, we re-emphasise that for the $SU(2)$ PCM this group is trivial. Instead we classify the sectors through π_3. It is expected within the resurgence paradigm [12, 34, 43, 44, 46, 72, 73] that ambiguities should cancel within each sector. That means that the fracton-anti-fracton event should carry an ambiguity that matches the ambiguity obtained by resumming the perturbative sector given by Equation (3.55).

The contributions due to discontinuities along individual (branch) singularities w are often described in terms of Alien derivatives Δ_w, as introduced in Section 1.A.1. The alien derivative is then expected [46] to look like

$$\Delta_{2S_I} E_{[0]}(z) = s_1 E_{[I\bar{I}]}(z), \tag{3.59}$$

where s_1 is a Stokes constant.

3.3.4 Stokes Graphs

Stokes graphs provide a graphical method to understand the Borel resummability and jumping phenomena associated to the WKB solutions of a Schrödinger equation as encoded by the DDP forumla [19] for the behaviour of Voros symbols [17] across Stokes rays. As parameters in the Schrodinger potential are varied, the Stokes graph can undergo topology changes, or mutations, which have a rich mathematical structure [22, 23] and are captured by the Stokes automorphism (3.58) described above. From a physics perspective, the seminal work [156] showed that the mutations of Stokes graphs are intimately related to BPS spectrum of $\mathcal{N} = 2$ four-dimensional gauge theory, where the Stokes automorphism describes wall-crossing phenomena.

Let us review some terminology that was introduced in Section 1.2 required to explain what is meant by Stokes graphs. We consider a Schrödinger equation defined over a Riemann surface Σ with local coordinate w,

$$\left(\frac{d}{dw^2} - \frac{1}{g^4} Q(w, g^2)\right) \Psi(w) = 0\,, \tag{3.60}$$

where g^2 is a small parameter in which we construct formal perturbative expansions. In a general theory $Q(w, g^2)$ itself can be expanded in g, though we are interested here in the case where $Q(w, g^2) \equiv Q_0(w)$ is given by the classical momentum $p(w) = \sqrt{E - V(w)}$. Under coordinate transformations $w \to \tilde{w}(w)$, Q_0 transforms holomophically with weight 2 and thus defines a meromorphic quadratic differential

$$\phi_{Sch} = p(w)^2 dw \otimes dw\,. \tag{3.61}$$

Trajectories of ϕ_{Sch} are defined as curves γ of constant phase in the sense that if ∂_t is

tangent to γ then $\lambda \cdot \partial_t = e^{i\vartheta}$ where $\phi_{Sch} = \lambda \otimes \lambda$. Equivalently they can be defined by

$$\mathrm{Im}\left[\int^w dw\, p(w)\right] = \text{constant}\,, \tag{3.62}$$

and these provide a foliation of Σ. Generically these trajectories will start and end at poles of $p(w)$, but a special role is played by *Stokes trajectories* satisfying

$$\mathrm{Im}\left[\int^w dw\, p(w)\right] = 0\,, \tag{3.63}$$

which have at least one end point at a zero of $p(w)$, which is also called a turning point. A Stokes trajectory is a *saddle* if both end points are located at zeros. It is *regular* if these zeros are different and it is *degenerate* if it is a loop. Given $\phi_{Sch}(w)$, we define the associated *Stokes graph*, $G[\phi_{Sch}]$, as a graph with vertices comprised of zeros and poles of ϕ_{Sch} and edges comprised of Stokes trajectories.

It is useful to consider the effect on the Stokes graph of rotating g^2 into the complex plane. An equivalent way to see this is to define the Stokes graph in a direction ϑ, $G_\vartheta[\phi_{Sch}] = G[e^{2i\vartheta}\phi_{Sch}]$ whose edges satisfy

$$\mathrm{Im}\left[e^{i\vartheta}\int_a^w dw\, p(w)\right] = 0\,, \tag{3.64}$$

where a is a zero of $p(w)$. The crucial linkage is that, if G_ϑ has no saddles, then the formal WKB solutions to the Schrodinger system are Borel summable in the direction ϑ in the sense of Equation (3.54) (this is explained for general surfaces Σ in [23] reporting on a result attributed to Koike and Schäfke [157]). Along Stokes rays, however, a saddle will emerge. As ϑ is varied across the ray, the topology of G_ϑ will undergo a transition (known as a flip for a regular saddle or a pop for a degenerate saddle).

Let us sketch the schematic structure of the Stokes graphs applied to the case at hand for which we have

$$p(w)^2 = E - \mathrm{sd}^2(w)(1 + \chi_-^2\,\mathrm{sn}^2(w))\,. \tag{3.65}$$

Because $p(w)$ is an elliptic function with periodic identification $w \sim w + 2\mathbb{K}(m) \sim w + 2i\mathbb{K}(m')$, it will suffice to study it in its fundamental domain. For $\eta \neq \zeta$ there are two distinct poles located at $w = i\mathbb{K}(m')$ and $w = \mathbb{K}(m) + i\mathbb{K}(m')$. For $E \neq 0$ and $\eta \neq \zeta$ there are generically four zero's which are given by solutions of

$$r^4(\zeta - \eta) + r^2(1 + mE) - E = 0\,, \quad r = \mathrm{sn}(w \mid m)\,. \tag{3.66}$$

In the range[10] $0 < E < E_c = 1 + (\eta + \zeta)^2$, two of these zeros are located along the $\mathrm{Im}(w) = 0$ axis symmetrically distribute about the half period $w = \mathbb{K}(m)$, with the two remaining zeros in the $\mathrm{Re}(w) = 0$ axis symmetrically distributed about $w = i\mathbb{K}(m')$.

[10] Here we view E as a parameter that can be continuously varied, and we find taking a small positive E helps in regulating the diagrams.

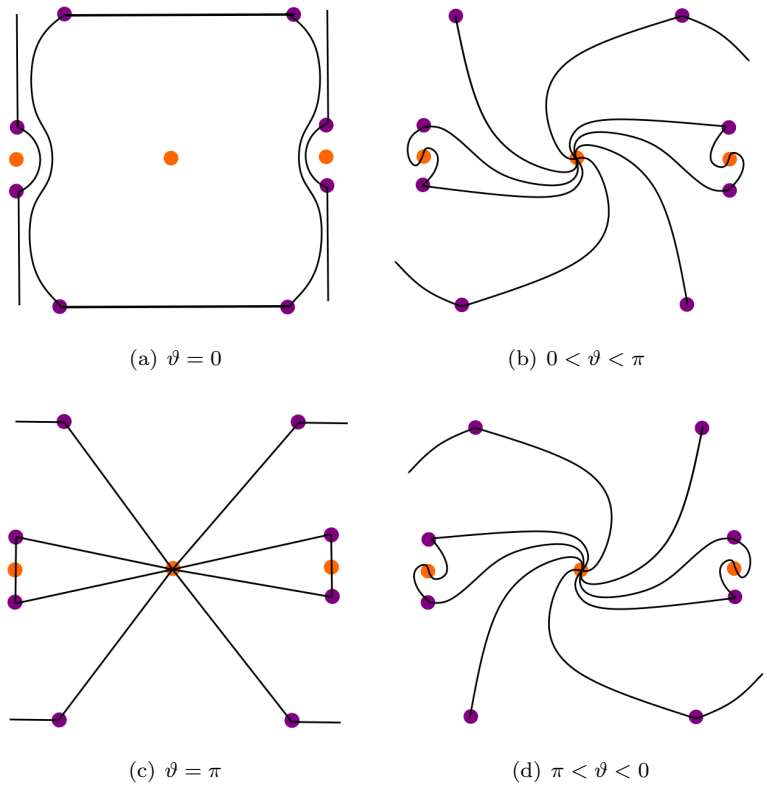

(a) $\vartheta = 0$ (b) $0 < \vartheta < \pi$

(c) $\vartheta = \pi$ (d) $\pi < \vartheta < 0$

Figure 3.16: Sketches of the directional Stokes graphs for generic values $\eta \neq \zeta$ with $0 < E < E_c$. Poles and are shown in orange and zeros in purple. We have shown one fundamental domain per Figure, but note that the trajectories can of course cross into neighbouring domains. In particular, in (a) and (c), horizontal and vertical trajectories form saddles with the images of zero in the next domain.

When $E = 1 + (\eta + \zeta)^2$, the two reals zeros coalesce at $w = \mathbb{K}(m)$ and if the energy increases still further this single zero proceeds to acquire an imaginary part and approach the pole at $\mathbb{K}(m) + i\mathbb{K}(m')$

Looking at $E < E_c$ we sketch the directional Stokes graphs in Figure 3.16 and 3.17. In complete agreement with the discussion of the Borel pole structure, we see two directions $\vartheta = 0, \pi$ for which the graphs contain saddles and over which the graphs undergo flip transitions.

In the critical case of $\eta = \zeta$ an important modifications occurs. The two zeros on the imaginary axis coincide at, and annihilate against, the pole at $w = i\mathbb{K}(m')$ leaving just two remaining zeros situated on the real axis (for $E < E_c$) and the double pole at the centre of the fundamental domain. This topology change is the graphical reason behind the jump in critical line behaviour such that the complex 1-uniton makes no contribution. In this case however still saddles persist in the two directions $\vartheta = 0, \pi$ as shown in Figure 3.18.

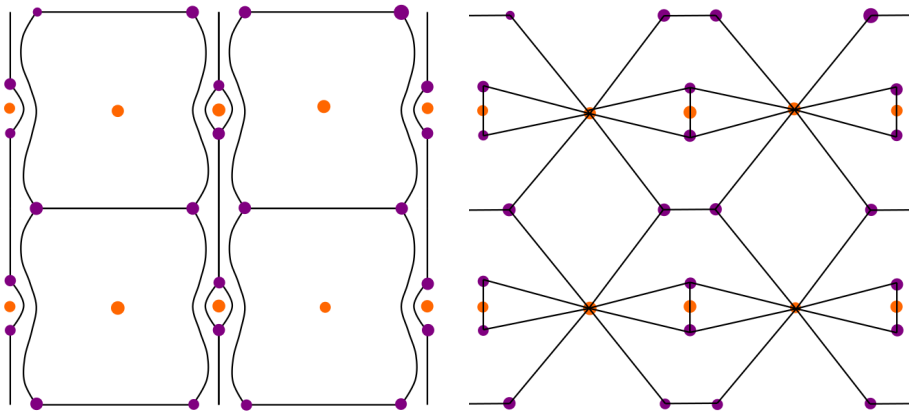

Figure 3.17: The lattice formed in 4 fundamental domains by saddles in the Stokes graph with $\eta \neq \zeta$ with $0 < E < E_c$ for $\vartheta = 0$ (left) and $\vartheta = \pi$ (right).

3.4 Connection to $\mathcal{N} = 2$ Seiberg-Witten Theory

From the WKB treatment above we saw that Stokes graphs are a elegant way of visualising the structure of the Borel plane. In a seminal work, Gaiotto, Moore and Neitzke [24, 25] explained how the same structure plays a crucial role in the spectrum of BPS states of $d = 4, \mathcal{N} = 2$ gauge theories. The essential idea (going back to the construction of Klemm et al [158] for $SU(2)$ theories that will be relevant here) is that BPS states on the Coulomb branch associated with M2 branes stretched on a curve γ between sheets of the M5 brane carry charge $Z = \frac{1}{\pi}\int_\gamma \lambda_{SW}$ but have mass given given by $M = \frac{1}{\pi}\int_\gamma |\lambda_{SW}|$. The BPS bounds is saturated providing that λ_{SW} has constant phase along the curve, i.e. $\lambda_{SW} \cdot \partial_t = e^{i\vartheta}$. For certain values of ϑ these Stokes curves become finite and start and end at the zero's of λ_{SW} and the BPS state, in this case a hypermultiplet, has finite mass.

It is natural to wonder if the integrable theories we consider here have an analogue description in gauge theory. Stated more precisely, we are led to ask if there is a gauge theory for which the quadratic differential obtained as the square of the Seiberg Witten differential, $\phi_{SW} = \lambda_{SW} \otimes \lambda_{SW}$, matches that defined by the quantum mechanics arising from the reduction of the two-dimensional non-linear sigma model we consider.

This has been shown to be the case first for the undeformed PCM on S^3. The corresponding quantum mechanics had a trigonometric Mathieu potential [46] and for which the corresponding gauge theory is $SU(2)$, $N_f = 0$. The resurgent structure of the Schrödinger equation corresponding to this quadratic differential was studied in [34]. An interesting connection with the TBA equations of the corresponding integrable SG field theory was made by [159].

For the single parameter η-deformed theory it was shown in [47] that the quantum mechanics has a Whittaker-Hill (or double sine-Gordon) potential and the corresponding gauge theory is $SU(2)$, $N_f = 2$ (in the first realisation of [156]) with equal masses for

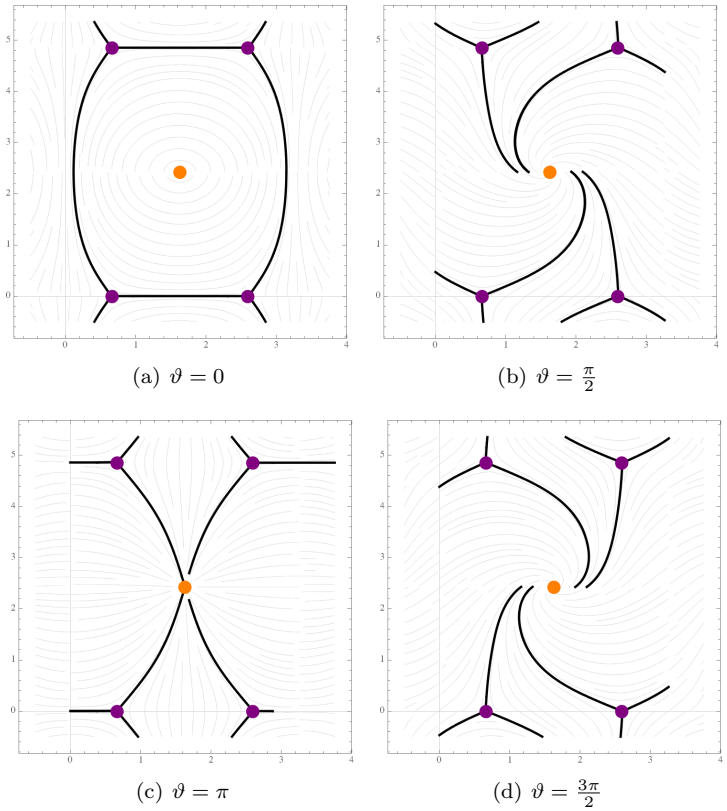

(a) $\vartheta = 0$ (b) $\vartheta = \frac{\pi}{2}$

(c) $\vartheta = \pi$ (d) $\vartheta = \frac{3\pi}{2}$

Figure 3.18: Here we plot the Stokes graphs in the directions $\vartheta = 0, \frac{\pi}{2}, \pi, \frac{3\pi}{2}$. Here we display the critical line $\varkappa = 0.2$ and we set $E = 0.4$. Poles are shown in orange and zeros in purple. As the direction crosses $\vartheta = 0, \pi$ saddles manifest themselves and a flip mutation is seen.

the flavours. In this scenario an interesting connection is made between the masses of the flavours and the RG invariant combination of tension and deformation parameter parameter, namely that $M = m_1 = m_2 \propto \sigma_\eta = \frac{1}{t\eta}$.

Here we shall provide a similar correspondence for the potential with two deformation parameters. We shall do so in two related ways, first linking to an $SU(2) \times SU(2)$ quiver theory and secondly linking to $SU(2)$ $N_f = 4$ theory. To begin it is convenient to understand the form of the potential of the quantum mechanics considered above as a generalised Lamé potential.

3.4.1 The Generalised Lamé Potential

First, we will rewrite the potential, $V(w)$, in terms of Weierstrass functions $\wp(z)$. We shall denote the periods of the Weierstrass function as $2\omega_1$ and $2\omega_2$. The elliptic invariants are given by g_2, g_3 and the constants e_i denote the roots of corresponding cubic.

The modular parameter of the torus $\tau = \omega_2/\omega_1$ is given by

$$\tau = \frac{i\mathbb{K}(m')}{\mathbb{K}(m)}\,, \tag{3.67}$$

where $m = \frac{e_2-e_3}{e_1-e_3}$ is the Jacobi elliptic parameter and $m' = 1-m$. They are related to the invariant cross-ratio as

$$\omega = \frac{(e_3-e_1)^2 - 9e_2^2}{(e_3-e_1)^2} = 4mm'\,. \tag{3.68}$$

In terms of[11] $w = z\sqrt{e_1-e_3}$, the potential can then be rewritten as

$$V(z) = (e_1-e_3)\frac{\frac{1}{3}((e_1-e_2)(e_1-e_3)-3e_1)+\wp(z)}{(e_2-\wp(z))(e_3-\wp(z))}\,, \tag{3.69}$$

when the elliptic moduli are fixed by

$$e_1 = \frac{2-m}{m'}(1+\chi_-^2)\,,\quad e_2 = \frac{2m-1}{m'}(1+\chi_-^2)\,,\quad e_3 = -\frac{1+m}{m'}(1+\chi_-^2)\,. \tag{3.70}$$

In particular, this means a relation between the z and w coordinate

$$w = z\sqrt{(1+\chi_+^2)}\,. \tag{3.71}$$

We can further rewrite Equation (3.69) as a generalised Lamé potential

$$V(z) = h + \sum_{i=0}^{3} c_i \wp(z+\omega_i)\,, \tag{3.72}$$

where

$$\begin{aligned} h &= \frac{(e_3-e_1)\left(e_1^2-3e_1+2e_2e_3\right)}{3\,(e_2-e_3)^{\,2}} \\ c_0 &= c_1 = 0 \\ c_2 &= \frac{(e_1-e_3)\,(-e_1+e_3+3)}{3\,(e_2-e_3)^{\,2}} \\ c_3 &= \frac{(e_1-e_2-3)\,(e_3-e_1)}{3\,(e_2-e_3)^{\,2}}\,, \end{aligned} \tag{3.73}$$

and $\omega_3 = \omega_1+\omega_2$ and $\omega_0 = 0$.

The Weierstrass form of the potential is also revealing about the nature of the $(\eta,\zeta)\to(-\eta,\zeta)$ transformation, which was given an interpretation in the PCM context in Equation (2.42). From Equation (3.70) it is clear that in the Weierstrass description this corresponds to interchanging $e_2 \leftrightarrow e_3$. This has the effect of rescaling the coordinate by $z \to \sqrt{\frac{e_1-e_3}{e_1-e_2}}z$ and an overall scaling of the potential $V \to \frac{e_1-e_2}{e_1-e_3}V$. Such transformations are easily absorbed in a rescaling of the coupling constant and do not

[11] At this point we are using z as a coordinate on the torus which we trust will not be confused with the earlier usage as g^2.

alter the physics.

Let us study two special cases in this formulation. First, the critical line $\eta = \zeta \equiv \varkappa$ corresponds to $e_1 - e_2 - 3 = 0$, which implies that $c_3 = 0$. In this situation, equation (3.69) simplifies to

$$V(z) = \frac{e_1 - e_3}{\wp(z) - e_2}. \tag{3.74}$$

We can also think about a co-critical point where $\eta = -\zeta$. In this situation the potential reduces to

$$V(z) = \frac{1}{3} - \frac{1}{12\eta^2}(1 - \wp(z)), \tag{3.75}$$

which is similar to the Lamé potential studied in [35], identifying $-4\eta^2 = k^2$. We know that this potential governs the WKB curve of the vacuum structure of $SU(2)$ $\mathcal{N} = 2^*$ Seiberg-Witten theory, which is a mass deformation of an $\mathcal{N} = 4$ theory [160].

The $\zeta \to 0$ limit is quite delicate in this description as can immediately be seen from the fact that the Jacobi elliptic parameter $m \to 0$ and correspondingly the modular parameter diverges as $\tau \to i\infty$. In particular, in this regime not all e_i are distinct which is forbidden in the generic Weierstrass setting, because the determinant

$$\Delta = g_2^3 - 27g_3^2 = 11664(1 + \chi_+^2)^2(1 + \chi_-^2)^2(\chi_-^2 - \chi_+^2)^2 \tag{3.76}$$

of the polynomial $4t^3 - g_2 t - g_3$ vanishes. However, if we consider the case in which we blow up one of the periods $\omega_2 \to \infty$, we see that

$$\begin{aligned} g_2 &= 2 \times 60 \sum_{n=1}^{\infty} \frac{1}{(n\omega_1)^4} = \frac{4\pi^4}{3\omega_1^4}, \\ g_3 &= 2 \times 140 \sum_{n=1}^{\infty} \frac{1}{(n\omega_1)^6} = \frac{8\pi^6}{27\omega_1^6}, \end{aligned} \tag{3.77}$$

where we have used that the Riemann ζ-functions takes the following values: $\zeta(4) = \frac{\pi^4}{90}$ and $\zeta(6) = \frac{\pi^6}{945}$. This leads to $\Delta = 0$, thus we may identify the two limits. To conclude, in this regime, $\omega_2 \to \infty$ and we break the finite double periodicity, i.e. the length of one side of the torus has a pole. Moreover, e_2 and e_3 are not distinct anymore. In particular this leads to a pole in c, c_2 and c_3.

3.4.2 $N_f = 2$ Elliptic $SU(2) \times SU(2)$ Quiver Theory

We now consider the $SU(2) \times SU(2)$ quiver gauge theory with two flavours. To extract the relevant differential, we employ Witten's string theory construction of the Seiberg-Witten theories [161, 162]. On the M-theory side, we compactify along the x^6 and the x^{10} direction which creates a base torus E with modular parameter τ which is the base Riemann surface. Let z be a coordinate on the torus. The Seiberg-Witten curve takes the form [162]

$$F(v, z) = (v - v_1(z))(v - v_2(z)) \equiv 0\,, \tag{3.78}$$

in which roots in v are the locations of the D4-branes. Let the locations z_1 and z_2 of the 2 NS5-branes be marked points on the base torus. We require that $v_i(z)$ has a pole at z_i with residue m_i parametrising the masses of the hypermultiplets. In addition, we allow a fibration of the v-space over the base torus E around $z = 0$

$$z \to z + 2\pi R, \qquad v \to v + m_1 + m_2\,. \tag{3.79}$$

Using the double periodicity and the singularity structure of $v_i(z)$, we can completely fix the form of the coefficients:

$$\begin{aligned} v_1(z) + v_2(z) &= m_1\zeta(z - z_1) + m_2\zeta(z - z_2) - (m_1 + m_2)\zeta(z) + c_0 \\ v_1(z)v_2(z) &= \frac{1}{4}(m_1 + m_2)^2\wp(z) + B(\zeta(z - z_1) - \zeta(z - z_2)) + C, \end{aligned} \tag{3.80}$$

where B, C and c_0 are some moduli and $\zeta(z)$ is the quasiperiodic Weierstrass function defined by $\zeta'(z) = -\wp(z)$ such that the combination $\sum_i a_i\zeta(z' - z_i') = 0$ is doubly periodic if $\sum_i a_i = 0$ and has a simple pole around $z = 0$ with a residue of 1.

The Seiberg-Witten differential is given by

$$\lambda_{SW} = \hat{v}dz\,, \tag{3.81}$$

in which

$$\hat{v} = v - \frac{1}{2}(v_1(z) + v_2(z))\,. \tag{3.82}$$

We can now use the definition of the curve equation (3.78) to determine that

$$\hat{v}^2 = \frac{m_1^2}{4}\wp(z - z_1) + \frac{m_2^2}{4}\wp(z - z_2) + u_-(\zeta(z - z_1) - \zeta(z - z_2)) + u_+, \tag{3.83}$$

where

$$u_\pm = \langle \mathrm{Tr}\Phi_1^2 \pm \mathrm{Tr}\Phi_2^2 \rangle. \tag{3.84}$$

are Coulomb branch moduli.

We would like to match the quadratic differential

$$\phi_{SW} = \lambda_{SW} \otimes \lambda_{SW} \tag{3.85}$$

to that of Schrödinger system given in Eq. (3.61).

By inspection this identification is achieved when the coordinates z and w are related exactly as described in Equation (3.71) and when the Coulomb branch parameter $u_- = 0$ with the locations of the five branes are fixed to the half-periods $z_1 = \omega_2$ and $z_2 = \omega_3$. To complete the identification we must match the hypermultiplet masses to the parameters of the Schrödinger the system and the result is quite striking; we find that they are directly given by the parameters that control the underlying quantum group symmetry

of the YB deformed PCM

$$\sigma_\eta = \frac{m_1 + m_2}{2\nu} \,, \quad \sigma_\zeta = \frac{m_1 - m_2}{2\nu} \,, \tag{3.86}$$

in which we have reinstated chemical potential and compactification radius in the combination $\nu^2 = \frac{4\xi^2}{L^2}$. The final Coulomb branch parameter, u_+, is related linearly to the energy of the Schrödinger system (the exact coefficients do not appear very insightful at this stage).

The two gauge couplings of the quiver are given in terms of the torus modular parameter by [160]

$$\begin{aligned} z_1 - z_2 = \tau_1 &= \frac{4\pi i}{g_1^2} + \frac{\theta_1}{2\pi} \,, \\ \tau - (z_1 - z_2) = \tau_2 &= \frac{4\pi i}{g_2^2} + \frac{\theta_2}{2\pi} \,. \end{aligned} \tag{3.87}$$

Now since the roots of the elliptic curve are all real, and the five branes are located at the half periods we concluded that $z_1 - z_2 = \omega_1 \in \mathbb{R}$ and that τ is pure imaginary. As a result we see that the coupling $g_1 \to \infty$ with $\frac{4\pi i}{g_2^2} = \tau$ finite whist the theta angles obey $\theta_1 = -\theta_2 = 2\pi\omega_1$. In this language the critical line is approached in the limit that the mass $m_2 \to 0$.

3.4.3 $N_f = 4$ $SU(2)$ Theory

In [71, 163], Ta-Sheng Tai recovers curves with the form (3.72) in some SW curve setting via a duality to the Heun equation. We will now show how one obtains the appropriate SW curve.

Let us now connect the Schrödinger system obtained above to the quadratic differential for the Seiberg-Witten curve of 4d $\mathcal{N} = 2$ supersymmetric Yang-Mills with $SU(2)$ gauge group and $N_f = 4$ flavours. The theory is specified by a Coulomb branch parameter u, the four flavour masses m_i and the marginal coupling $\tau_{YM} = \frac{4\pi i}{g_{YM}^2} + \frac{\theta}{2\pi}$. The UV curve of the theory is given by

$$F(t, v) = t^2(v - m_1)(v - m_2) + b(v^2 - u)t + c(v - m_3)(v - m_4) = 0 \,, \tag{3.88}$$

in which the parameters b and c are related to the elliptic invariants $g_2 = \frac{1}{12}\left(b^2 - 3c\right)$ and $g_3 = \frac{1}{432}\left(9bc - 2b^3\right)$ and moreover the roots of the polynomial $(c + bt + t^2) = (t - t_+)(t - t_-)$ can be understood as relating to the M-theory lifting of the NS5 branes in the IIA picture. The SW differential is obtained as

$$\lambda_{SW} = \hat{v}\frac{dt}{t} \,, \quad \hat{v} = v - \frac{c(m_3 + m_4) + (m_1 + m_2)t^2}{2(c + bt + t^2)} \,, \tag{3.89}$$

in which the shifted quantity $\tilde{v}$ is used to factor out the overall U(1) degree of freedom.

We can define a change of coordinates

$$t = 4\wp(z) - \frac{b}{3}\,, \tag{3.90}$$

by which we can bring the quadratic differential to the form

$$\phi_{SW} = \lambda_{SW} \otimes \lambda_{SW} = \left[h + \sum_{i=0}^{3} c_i \wp(z - w_i)\right] dz \otimes dz\,, \tag{3.91}$$

where w_i with $i = 1 \ldots 3$ are the half-periods and $w_0 = 0$. The coefficients c_i in this expression are slightly unedifying expressions depending to $t_\pm$, the mass parameters and for h also on u, but in particular $c_0 = (m_1 - m_2)^2$ and $c_1 = (m_3 - m_4)^2$.

We would like to match this to Schrödinger system of eq. (3.61).

Using the relation between coordinates z and w given by eq. (3.71), we find that the matching is achieved with setting the flavor masses pairwise equal

$$m_1 = m_2 = M\,, \quad m_3 = m_4 = \tilde{M}\,, \tag{3.92}$$

and relating them to the bi-Yang-Baxter parameters according to

$$\sigma_\eta = \frac{2}{\nu}\left(\tilde{M} - M\right)\,, \quad \sigma_\zeta = \frac{2}{\nu}\left(\tilde{M} + M\right)\frac{1+m'}{m}\,. \tag{3.93}$$

To complete the matching we also need to relate the parameter on the Coulomb branch to the energy of the Schrödinger system which is achieved with

$$E = \frac{\nu^2(1+m')(M^2-u)}{M^2(1+m'+m'^2) + 2m'M\tilde{M} - m'\tilde{M}^2}\,. \tag{3.94}$$

To close this section let us remark that along the critical line, parametrised by $\varkappa = \eta = \zeta$, we find very particular behaviour in the matching. First we can note that the masses are related via $\tilde{M} = -(1+4\varkappa^2)M$, Using (3.67), we find that the elliptic modulus of the torus is $\tau = i\mathbb{K}(\frac{1}{1+4\varkappa^2})/\mathbb{K}(\frac{4\varkappa^2}{1+4\varkappa^2})$. When $\varkappa = \frac{1}{2\sqrt{3}}$ we encounter a point for which the complex uniton action has exactly twice the magnitude as the real uniton action, and at this point we have a relation between the masses $\tilde{M} = -\frac{4}{3}M$. At this point we have the $\tau = i\mathbb{K}(\frac{3}{4})/\mathbb{K}(\frac{1}{4})$. Continuing to increase the deformation we arrive at $\varkappa = \frac{1}{2}$ when the complex uniton has the same magnitude as the real uniton for which we find $\tau = i$ and $\tilde{M} = -2M$. At $\varkappa = \frac{\sqrt{3}}{2}$, for which $|S_I| = 2|S_{CI}|$, we have $\tilde{M} = -4M$ and $\tau = i\mathbb{K}(\frac{1}{4})/\mathbb{K}(\frac{3}{4})$.

We remark that the previously discussed duality in [41] that sends $m \to m'$, results in an S-duality sending $\tau \to \frac{-1}{\tau}$. In addition we observe that $\varkappa = \frac{1}{2\sqrt{3}}$ and $\varkappa = \frac{\sqrt{3}}{2}$ are dual under this transformations, whereas $\varkappa = \frac{1}{2}$, corresponding to $\tau = i$, is self-dual.

3.5 Conclusion and Outlook

We thus conclude our study of the bi-Yang-Baxter deformed $SU(2)$ PCM. We have seen that the model harbours two types of solutions which we have dubbed the real and the complex uniton, both with a quantised finite action. By employing an adiabatic compactification [46, 47] we obtained a reduced quantum mechanics whose non-perturbative behaviour is dominated by finite action configuration derived from the unitons. Moreover, we were able to find an $\mathcal{N} = 2$ Seiberg-Witten theory that gives rise to the same WKB curve as that of our reduced quantum mechanics. By introducing a new example into the framework of resurgence, we hope to expand the non-perturbative discourse. In particular, we believe the complex saddle point in our system might elucidate more advanced structures of resurgence. Possible future directions of study could include:

- In [15], Equation (108), it was observed that the following relation holds for both the double well and the Sine-Gordon quantum mechanics

$$\frac{\partial E}{\partial B} = -\frac{g^2}{S_I}\left(2B + g^2\frac{\partial A}{\partial g^2}\right). \tag{3.95}$$

  $A(B, g^2)$ is a function that appears in the global boundary conditions of the uniform WKB and is determined by $u(\theta_{\text{midpoint}})$. It was first introduced by [72, 73] and for the Sine-Gordon model it reads

$$A_{SG}(B, g^2) = \frac{4}{g^2} - \frac{g^2}{2}\left(B^2 + \frac{1}{4}\right) - \frac{g^4}{8}\left(B^3 + \frac{B}{4}\right) + \mathcal{O}(g^6) \tag{3.96}$$

  It was shown in [35] that this relation in the undeformed limit is a consequence of a generalised Matone's relation [164] on the gauge theory side. In addition, [15] attribute a great deal of importance to this relation as it explain a lot of the resurgent behaviour. However, in the compactified Yang-Baxter deformed models studied in this Chapter, there does not appear to be a related identity. It would be interesting to understand how the relation (3.95) can be modified in systems with a real and a complex saddle point.

- One concrete such avenue might be through further developing the uniform WKB techniques [15] introduced in Section 1.3. A crucial ingredient were the Bloch quantisation conditions that were inherited from the periodicity of the potential. Is it possible to leverage the double periodicity of the elliptic potential studied in this Chapter to study systems with a complex saddle more completely?

- In Figures 3.4 and 3.5 we observed that the uniton with twisted boundary conditions fractionates into 2 separate lumps. In the undeformed model [46], it was shown how solutions for these individual constituent fractons can be constructed. These are not exact solutions to the equations of motions, but are rather *quasi*-solutions, meaning that the equations of motion can be satisfied with parametrically good accuracy in some limit of the moduli λ_i. Critically, it was shown

that the amplitude of a fracton-anti-fracton event carries an ambiguity that precisely cancels the Borel-resummation ambiguity of the perturbative sector given by Equation (3.55). It would be an impressive check for the resurgence programme to extent this analysis to the YB-deformed PCM which also harbours a complex uniton fractionation.

- The Thermodynamic Bethe Ansatz (TBA) is a powerful technique to study integrable field theories that exploits the exact scattering matrix of the model, which will be a central character of Chapter 4. It was shown that the resurgent structure of the Sine-Gordon quantum mechanics can be reinterpreted in terms of TBA equations [159]. It would be very interesting to generalise these ideas to the QM found by reducing the bi-YB deformed PCM.

3.A Evaluating Uniton Actions

Here, we dwell upon the following observation. When integrating the action, in both the real and the complex uniton we switch to $w = f(z)$ coordinates. We transition to polar coordinates $w = re^{i\theta}$. Because there is no θ-dependence we integrate it out. When considering the real uniton we make the substition $\rho = r^2 - 1$, for the complex uniton we substitute $\rho = -r^2 - 1$. Remarkably, in both cases we obtain the following integrand:

$$g(\rho) = \frac{-2(2+\rho)^2}{(4+4\rho+(1+(\zeta+\eta)^2)\rho^2)(4+4\rho+(1+(\zeta-\eta)^2)\rho^2)}\,, \tag{3.97}$$

with the only difference that for the real uniton we integrate ρ from positive infinity to -1, for the complex uniton, we integrate ρ from -1 to negative infinity.

On the interval $(-1, \infty)$, we can construct a continuous (i.e. without branch cuts) anti-derivative:

$$\frac{(\zeta+\eta)\text{arctan}(\frac{(\zeta+\eta)\rho}{2+\rho}) - (\zeta-\eta)\text{arctan}(\frac{(\zeta-\eta)\rho}{2+\rho})}{4\zeta\eta}\,. \tag{3.98}$$

This can be used to evaluate the real uniton action (3.9). It cannot be used to compute the complex uniton action because it is in particular discontinuous at $\rho = -2$. On the interval $(-\infty, -1)$, we can use

$$\frac{(\zeta+\eta)\text{arccot}(\frac{(\zeta+\eta)\rho}{2+\rho}) - (\zeta-\eta)\text{arcot}(\frac{(\zeta-\eta)\rho}{2+\rho})}{4\zeta\eta} \tag{3.99}$$

as an antiderivative to compute the complex uniton action.

Jointly, they can be used to reconstruct $\int_{-\infty}^{\infty} g(\rho)d\rho$. This integral can be easily computed using the Cauchy residue theorem. The integrand vanishes in all direction at infinity, and it has 4 poles, two in the upper half plane and two in the lower half plane. This yields (for $\eta, \zeta \in \mathbb{R}$)

$$\int_{-\infty}^{\infty} g(\rho)d\rho = \frac{\pi}{4\zeta\eta}(|\zeta-\eta| - |\zeta+\eta|)\,. \tag{3.100}$$

Via the above explanation or by using the identity $2\,x\arctan(x) + 2\,x\,\mathrm{arccot}(x) = \pi|x|$, we thus obtain the following relation between the complex and the real uniton actions for $\eta, \zeta \in \mathbb{R}$

$$S_{CI}(\zeta,\eta) - S_I(\zeta,\eta) = \frac{\pi(1+(\zeta+\eta)^2)}{4\zeta\eta}(|\zeta-\eta| - |\zeta+\eta|)\,. \tag{3.101}$$

Chapter 4

Resurgence from TBA Equations

4.1 Introduction

The calculation of the mass gap in QFT is notoriously a difficult puzzle. In fact, proving its existence in a general non-abelian 4d Yang-Mills theory has been named as one of the seven millenium problems posed by the Clay Institute [165, 166]. However, in 2d integrable models, powerful techniques have been developed to solve the puzzle in many examples [167–174]. We shall give more details on these computation in Section 4.1.1.

Although in this Chapter we shall not be attempting to calculate mas gaps of new theories, we shall be using and developing the same techniques. Our goal shall be to study the system in a particular thermodynamic limit with a chemical potential and calculate a perturbative series for some observable. Such a perturbative series shall enable us to employ the machinery developed in Chapter 1 which will uncover information about the non-perturbative effects in such theories.

At the heart of the techniques developed by [167–174] is the so-called *Thermodynamic Bethe Ansatz* (TBA). We shall introduce these techniques in Section 4.1.3. The resulting integrable equation, the TBA system, unfortunately, is still technically challenging to solve. To write the TBA equations for a particular model, the key ingredient that is needed is its scattering kernel which was introduced in Section 2.4.

One way to make the situation more tractable, is to consider a model with just one type of particle in the presence of a chemical potential h. All particles carry the same charge under the chemical potential, which means we adapt the Hamiltonian by $H \to H - hQ$, where Q is the charge of the particles under the chemical potential. We might imagine that this charge arises in association with a global $U(1)$ conserved current. By turning on a background gauge field we can implement this charge as a chemical potential. When dealing with a specific QFT we will specify more carefully exactly which current is being used as it determines which states are dominant in the

ensemble at large h, for now however we keep our considerations generic and assume that there is a single type of particle carrying charge under this $U(1)$.

That we can reduce the TBA system to involve just one species of particle from the fundamental representation singled out by the applied chemical potential is of course an assumption that makes the problem readily tractable. One anticipates that states of higher mass and higher charge are energetically disfavoured, but properly speaking this assumption ought to be proven starting from a complete nested TBA system (which we do not attempt here).

In the regime of large chemical potential, the new techniques pioneered by [1, 2, 48, 52] (see also [50, 51, 53–59]) make it possible to recover a perturbative series and compute the mass gap for finite N. In Section 4.2, we will explain how this new method works. We will then reproduce known results for the $SU(N)$ PCM, and apply the same methods to the λ-deformed sigma model.

The choice of studying the λ-model (discussed in more detail in Section 2.3) is motivated by the desire to understand how integrable deformations are reflected in resurgent structures, which is the central line of the thesis. There is however another more profound reason for the study of the resurgence in the λ-model: all previous investigations into resurgent structures in integrable 2d QFTs have considered asymptotically free theories. Whilst such models mimic 4d non-Abelian gauge theory, there is another appealing RG trajectory in which the UV consist not of a free theory but of an interacting Conformal Field Theory (CFT). The λ-model provides exactly such an RG flow as in the far UV it is described by a relevant deformation away from the WZW CFT. One might even suspect that such a UV completion puts significant constraints into the structure of UV renormalon poles in the Borel plane. To put it snappily, by investigating the resurgent behaviour of the λ model, we are examining "asymptotic behaviour in an asymptotically CFT".

We obtain a novel perturbative series for the λ-model, which we will study extensively in Section 4.2.5. The series grows factorially, implying there is resurgent behaviour at work. We can construct an asymptotic form which allows us to uncover the Borel-structure of the expansion. We will give a concrete formula for the ambiguity of the large-order behaviour of the asymptotic expansions we find.

Further developments, that encapsulate this information in more general transseries [49], allows the computation of this ambiguity on a more fundamental footing. These techniques are presented in Section 4.3 and applied to the λ-deformed model. We show that this ambiguity matches the one found from the perturbative computation.

The headline of our findings, which are confirmed both by the analysis of the perturbative expansion in Section 4.2 and the transseries setting in Section 4.3, is the existence of certain non-perturbative objects. These seem to match the renormalons posited by the Parisi-'t Hooft conjecture [175–177][1]. This is contrast to the studies [2, 49], where in e.g. the Gross-Neveu context, renormalons are found that do *not* fit into the framework of Parisi-'t Hooft. However, one striking feature of our analysis is that the leading

[1]We thank M Mariño and T Reis for illuminating us on this point.

renormalon vanishes when the WZW level k divides the rank of the symmetry group N. We finish with ideas for future research in Section 4.4.

4.1.1 Mass Gap

As mentioned, the integrable models under consideration have mass gaps. To introduce this, let us assume a usual β-function of an asymptotically free theory given by

$$\mu \frac{dg}{d\mu} = \beta(g) = -\beta_1 g^3 - \beta_2 g^5 - \dots \tag{4.1}$$

In general the β-function coefficients may depend on the renormalisation scheme. However, the first two coefficients are scheme-independent [9] and the methods outlined below heavily depend on them. This equation can be solved by [173]

$$\frac{1}{g^2} = 2\beta_1 \ln \frac{\mu}{\Lambda} + \frac{\beta_2}{2\beta_1} \ln \ln \frac{\mu}{\Lambda} + \mathcal{O}\left(\ln \ln \frac{\mu}{\Lambda} / \ln \frac{\mu}{\Lambda}\right) . \tag{4.2}$$

Here, Λ is the scheme-dependent cut-off scale which appears as a constant of integration in solving Equation (4.1). Λ further dynamically generates the scale of the mass gap.

We can also formulate these relations in terms of $\alpha = g^2$, in that case we get

$$\mu \frac{d\alpha}{d\mu} = -2\beta_1 \alpha^2 - 2\beta_2 \alpha^3 - \dots \tag{4.3}$$

This Equation is solved by a relation

$$\frac{1}{\alpha} = 2\beta_1 \ln(\mu/\Lambda) + \frac{\beta_2}{\beta_1} \ln \ln(\mu/\Lambda) + \dots , \tag{4.4}$$

This is equivalent to

$$\frac{1}{\alpha} + \frac{\beta_2}{\beta_1} \log \alpha = 2\beta_1 \log \frac{\mu}{\Lambda} . \tag{4.5}$$

From this it is easy to determine that

$$\Lambda = \mu \alpha^{\beta_2/2\beta_1^2} e^{-1/2\beta_1 \alpha} (1 + \mathcal{O}(\alpha)) \tag{4.6}$$

In terms of the β-function it is given by

$$\Lambda = \mu \exp\left(- \int^{g[\mu]} \frac{dg}{\beta[g]} \right) . \tag{4.7}$$

Λ is the only relevant mass scale of these theories, it thus stands to reason that the mass gap of these theories is proportional to Λ as

$$m = c\Lambda . \tag{4.8}$$

Note that, because Λ is scheme dependent, the mass gap is also scheme dependent.

The exact constant of proportionality between the mass gap was unknown for a long time. Hasenfratz, Niedermayer and Maggiore [167, 168] showed in 1990 that it is possible to calculate this constant in integrable models. By performing a perturbative calculation of the free energy, the answer in naturally given in terms of Λ/h. However, when using the TBA methods, the answer is given in terms of m/h. Hence by comparing the expression, the proportionality constant can be given. This computation was intially performed for the $O(N)$ model [167, 168], but was later also completed for Gross-Neveu models [169, 170] and PCM models [171, 172]. A more concrete sketch of this computation is given by [173].

4.1.2 Free Energy

As a brief interlude, let us call to the stage the key observables that we will be calculating for the remainder of this Chapter. We recall that all models we are considering have some symmetry group and we can consider their symmetry currents. We have introduced an external field h coupled to such a charge Q. When the value of the external field exceeds that of the mass gap, we get a finite density of particles ρ. When the external field is strong, we are in a perturbative regime. If we know the free energy density $\mathcal{F}(h)$, we can reconstruct the energy density $e(\rho)$ through

$$e(\rho) = \min_h(\mathcal{F}(h) + \rho h)\,, \tag{4.9}$$

or vice versa, from an energy density, we can reconstruct a free energy density:

$$\mathcal{F}(h) = \min_\rho(e(\rho) - h\rho)\,. \tag{4.10}$$

We note that while $\mathcal{F}$ is a function of h, its Legendre transform e, is a function of ρ. Their relation is given by

$$\begin{aligned} \rho &= -\mathcal{F}'(h) \\ \mathcal{F}(h) - \mathcal{F}(0) &= e(\rho) - \rho h\,. \end{aligned} \tag{4.11}$$

Polyakov and Wiegmann [178–180] showed in the 80s that it is possible to compute the free energy of an integrable system with a chemical potential turned on using a thermodynamic Bethe ansatz (TBA) technique. The procedure relies on knowledge of the exact S-matrix and its factorisation. In the next section we will explain how to obtain the system of equations that governs this model. Such a computation was done in the large N limit of the Principal Chiral model by [181].

4.1.3 TBA Equations

To motivate the TBA equations, we begin not in QFT but with a collection of N identical, bosonic, quantum mechanical particles on circle with length L. The continuum TBA limit will be subsequent achieved by taking $L \to \infty$ and $N \to \infty$. Each particle,

labelled by a number $\alpha = 1, \ldots, N$, carries a rapidity θ_α, as was defined in Equation (2.55), such that the wave-function of the system can be written as $\psi(\theta_1, \ldots, \theta_N)$. We demand that the wavefunction be periodic under translations, infinitesimally generated by p_1. As a specific particle α is translated about this circle, it picks up a scattering phase $S(\theta_\alpha - \theta_\beta) = \exp i\phi(\theta_\alpha - \theta_\beta)$ each time it meets another particle β. This periodicity is achieved by demanding that

$$\exp(imL \sinh \theta_\alpha) \prod_{\beta \neq \alpha} S(\theta_\alpha - \theta_\beta) = 1 \,. \tag{4.12}$$

Let us take the logarithm of this equation which yields

$$imL \sinh \theta_\alpha + \sum_{\beta \neq \alpha} \log S(\theta_\alpha - \theta_\beta) = 2\pi i k_\alpha \,. \tag{4.13}$$

Here $k_\alpha \in \mathbb{Z}$ is a set of integers that describe on which branch cut the equation is. The possible values of k_α parametrise the possible states of the system.

In the continuum limit k_α defines a density distribution $\chi(\theta)$ of possible states. We will split this into a density of occupied states $f(\theta)$ and a density of holes $f_h(\theta)$, subject to the constraint

$$\chi(\theta) = f(\theta) + f_h(\theta) \,. \tag{4.14}$$

The limit is taken by making the substitutions

$$\frac{1}{L}\delta k_\alpha \to \chi(\theta) d\theta \,, \qquad \frac{1}{L}\sum_{n=1}^{N} \to \int_{-\infty}^{\infty} d\theta f(\theta) \,. \tag{4.15}$$

When taking the θ-derivative of Equation (4.13), we obtain

$$\frac{m}{2\pi} \cosh \theta = \chi(\theta) - \int_{-\infty}^{\infty} K(\theta - \theta') f(\theta') d\theta' \,, \tag{4.16}$$

where, as we did in Equation (2.57), we have defined the scattering kernel as

$$K(\theta) = \frac{1}{2\pi i} \frac{d}{d\theta} \log S(\theta) \,. \tag{4.17}$$

The total charge and energy densities are given by

$$\begin{aligned} \rho &= \frac{N}{L} = \int_{-\infty}^{\infty} d\theta f(\theta) \,, \\ e &= \int_{-\infty}^{\infty} d\theta f(\theta) m \cosh \theta \,. \end{aligned} \tag{4.18}$$

The free energy density is given by

$$F = \mathcal{F}/L = e - h\rho = \int_{-\infty}^{\infty} d\theta f(\theta)(m \cosh \theta - h) \,. \tag{4.19}$$

We assume that the free energy is minimised by configurations in which the support of particle excitations, $f(\theta)$, has rapidity bounded by a Fermi surface $\theta \in [-B, B]$. The support of $f_h(\theta)$ lies in the complement so that for $\theta \in [-B, B]$ the density of possible states $\chi(\theta)$ coincides with the density of occupied states $f(\theta)$. We will rescale $\tilde{\chi}(\theta) = 2\pi\chi(\theta)$, and then with abuse of notation drop the tildes, such that the TBA system becomes

$$\begin{aligned} m\cosh(\theta) &= \chi(\theta) - \int_{-B}^{B} K(\theta-\theta')\chi(\theta')d\theta' \,, \qquad \theta^2 < B^2 \,, \\ e &= m\int_{B}^{-B} \chi(\theta)\cosh(\theta)\frac{d\theta}{2\pi} \,, \\ \rho &= \int_{B}^{-B} \chi(\theta)\frac{d\theta}{2\pi} \,. \end{aligned} \tag{4.20}$$

There is a dual set of TBA equations to this form, which moves towards an equation for a pseudo-energy density that determines the free energy density (rather than the total energy as done above). This approach also explains how to achieve the minimisation from Equation (4.10). The details are given in appendix 4.A. More comprehensive introductions to the TBA equations can be found in [182, 183].

4.2 Perturbative Series from TBA Methods

In this section we will show how the thermodynamic Bethe ansatz can be used to compute the free energy of thermodynamic systems. We shall focus towards the recent developments pioneered by [1, 2, 48–50, 52, 53]. These techniques will be introduced in Sections 4.2.1 - 4.2.3, after which we will reproduce these results in Section 4.2.4 for a simple model: the PCM. In Section 4.2.5, we shall present new results for the λ-deformed model.

4.2.1 Resolvent

It will prove useful to recast the integral equation that determines $\chi(\theta)$ in terms of a resolvent function that is defined by

$$R(\theta) = \int_{-B}^{B} \frac{\chi(\theta')}{\theta-\theta'}d\theta'. \tag{4.21}$$

The resolvent is analytical everywhere except around the interval $[-B, B]$ where it has an ambiguity given by

$$\chi(\theta) = -\frac{1}{2\pi i}\left(R^{+}(\theta) - R^{-}(\theta)\right) \,, \tag{4.22}$$

where we use the short hand notation $R^{\pm}(\theta) = R(\theta \pm i\epsilon)$. This statement is proven simply by using the residue theorem.

It is natural to express the average particle density ρ in terms of the resolvent,

as we shall now explain. If we try to compute the residue of the resolvent, given by Equation (4.21), at infinity, we can move the residue operator through the integral. Using, $\text{res}_{z=\infty}\frac{1}{z-a} = -1$, it follows from Equation (4.20) that

$$\rho = -\frac{1}{2\pi}\text{Res}_{\theta=\infty}R(\theta)\,. \tag{4.23}$$

Let us introduce a shift operation $\mathsf{D} = \exp(i\pi\partial_\theta)$, and let us use the formal definition that $[f(\theta)]^{\mathsf{D}} = \exp(\mathsf{D}\log([f(\theta)])$. In particular that means that $\theta^{\mathsf{D}} = \theta + i\pi$ justifying the name of the operator. Furthermore, we will use a power series to formally define inversions such as $\frac{1}{1-\mathsf{D}} = \sum_{n=0}^{\infty}\mathsf{D}^n$.

Another useful way to encode the structure of the Kernel is through the shift operator formalism as was done by [1, 48]. Although it will not be critical for the remainder of the thesis, it can be used as a parallel method to [2] to verify the form of the edge ansatz, which will be introduced in the next Section, for a specific model. We present it for future reference. Let us write

$$K(\theta) = \frac{1}{2\pi i}\mathsf{O}\frac{1}{\theta}\,, \tag{4.24}$$

in such a way that O is given as a rational combination of shift operators D. Using Equations (4.22) and (4.20) we recast the integral equation as

$$R^+(\theta) - R^-(\theta) + \mathsf{O}R(\theta) = -2\pi i m\cosh\theta\,. \tag{4.25}$$

4.2.2 Edge and Bulk Expansions

Our aim is to solve the above TBA systems in a "weak coupling" limit in which B is large (and accordingly h is large). This will in general produce a perturbative evaluation of e and ρ in $\frac{1}{B}$ and $\log B$. A breakthrough was achieved by Volin [1, 48] using a clever procedure of matched asymptotic expansions [184–187]. The idea is to analyse the TBA equations in two different regimes, the *bulk* and the *edge*, in which they take a simplified form. In each regime an ansatz for the resolvent can be given and partially solved leaving some unknown coefficients. By subsequently matching the bulk and edge ansätze all remaining coefficients are fully determined.

Edge limit

We begin first with the edge limit in which the weak coupling limit $B \to \infty$ is taken whilst holding $z = 2(\theta - B)$ fixed and small. This evidently scales to large θ and hence probes the properties of $\chi(\theta)$ around the vicinity of the Fermi energy, B.

This edge limit is best expressed in Laplace transformed variables,

$$R[z] = \int_0^\infty \hat{R}[s]e^{-sz}ds\,, \qquad \hat{R}[s] = \frac{1}{2\pi i}\int_{-i\infty+\delta}^{i\infty+\delta} e^{sz}R[z]dz\,. \tag{4.26}$$

We will typically use s for the variable before the (forward) Laplace transform, and z for the transformed functions. Notice that, under the Laplace transformation, the shift operator is realised as $D \mapsto e^{-2\pi i s}$. The factor of 2 comes from the Jacobian going between θ and z variable. Crucial to the method is that a small z expansion corresponds to a large s expansion of the Laplace transformed quantities (i.e. the Lapalace transform of $z^n \propto s^{-(n+1)}$).

The density of roots has the following expansion[2] around $z \approx 0$

$$\chi(z) = \chi_0 + \chi_1 z + \chi_2 z^2, \dots . \tag{4.27}$$

which, by virtue of the the discontinuity relation (4.22), has a resolvent given by

$$R(z) = -\log(z)\left(\chi_0 + \frac{z}{2}\chi_1 + \frac{z^2}{4}\chi_2 + \dots\right) . \tag{4.28}$$

By using an analytic continuation of the Laplace transform[3] , we arrive at a large s expansion for the inverse Laplace transform of the resolvent:

$$\widehat{R}(s) = \frac{\chi_0}{s} - \frac{\chi_1}{s^2} + \frac{\chi_2}{s^3} - \dots . \tag{4.30}$$

The analytical structure of $\widehat{R}(s)$ can be more precisely established using the shift operator formalism applied to Equation (4.25) as was done by Volin [1, 48]. More expediently, it was realised by [2, 52] that this analysis can be reproduced more generally using a Wiener-Hopf method. The usage of Wiener-Hopf techniques was crucial in the original calculation of the mass gap of integrable models [167, 168].

The Wiener-Hopf method refers to factorisation of the Fourier transform of the scattering kernel. This was foreshadowed in Equation (2.60) and (2.61), but we shall re-state them here. We have that the Fourier-Transform

$$K(\omega) = \int_{-\infty}^{\infty} d\theta e^{i\omega\theta} K(\theta) , \tag{4.31}$$

can be expressed as

$$1 - K(\omega) = \frac{1}{G_+(\omega) G_-(\omega)} , \tag{4.32}$$

such that $G_+(\omega)$ and $G_-(\omega)$ are analytic in the upper half plane (UHP) and the lower half plane (LHP) respectively. Moreover, we require $G_-(\omega) = G_+(-\omega)$. It will become clear later in what way this factorisation is useful. The key result of [2, 52] is that in

[2] This is a consequence of the TBA integral equations and the analyticity of $K(\theta)$ on the real axis.

[3] Concretely, [52, 188] tell us what to do:

$$s^{-n} \leftrightarrow \frac{(-1)^n}{(n-1)!} \log(z) z^{n-1} . \tag{4.29}$$

the edge limit the resolvent has the following form

$$\widehat{R}(s) = me^B A\Phi(s)\left(\frac{1}{s+1/2} + Q(s)\right), \tag{4.33}$$

where

$$\Phi(s) = G_+(2is), \qquad A = \frac{G_+(i)}{2}, \tag{4.34}$$

and $Q(s)$ is a series in large s and a perturbative expansion in $\frac{1}{B}$ in the form

$$Q(s) = \frac{1}{Bs}\sum_{m,n=0}^{\infty}\frac{Q_{n,m}}{B^{m+n}s^n}. \tag{4.35}$$

It should be noted that the coefficients $Q_{n,m}$ may still depend on $\log B$. Because the new approach based on the Wiener-Hopf method is more general, it can readily be applied to many different theories. Moreover, the Wiener-Hopf composition of many scattering kernels are well-known.

Let us now re-express the particle and energy densitities from Equation (4.20) using the techonology of resolvents. We will work in a large B limit, and suppress terms exponentially small in B. This means that we approximate $\cosh(B) \approx e^B/2$. Because the integral is symmetric in $\theta \to -\theta$, we can write

$$\begin{aligned} e &= \frac{m}{2\pi}\int_B^{-B}\chi(\theta)\cosh(\theta)d\theta \\ &\approx \frac{m}{2\pi}\int_0^{-B}\chi(\theta)e^{\theta}d\theta \\ &= \frac{m}{4\pi}\int_{-B/2}^{0}\chi(z)e^{B+z/2}dz \end{aligned} \tag{4.36}$$

where we have switched the integration variable by $\theta = B + z/2$. As we take B large let us pull the integration domain to $(-\infty, 0)$. By using the discontinuity formula (4.22), we compute that

$$\begin{aligned} e &\approx \frac{me^B}{4\pi}\int_{-\infty}^{0}\chi(z)e^{z/2}dz \\ &= -\frac{me^B}{4\pi}\int_{-\infty}^{0}\frac{1}{2\pi i}\left[R^+(\theta) - R^-(\theta)\right]e^{z/2}dz \\ &= -\frac{me^B}{4\pi}\int_{\mathcal{C}}\frac{1}{2\pi i}R(z)e^{z/2}dz\,, \end{aligned} \tag{4.37}$$

where $\mathcal{C}$ is the contour that goes $\int_{-\infty+i\epsilon}^{i\epsilon}dz + \int_{-i\epsilon}^{-\infty-i\epsilon}dz$. This contour can be transformed into the contour of the inverse Laplace transform. By using Equation (4.26), we

can thus write

$$\begin{aligned} e &= \frac{me^B}{4\pi}\widehat{R}(1/2) \\ &= \frac{m^2A^2e^{2B}}{2\pi}\left[1+Q\left(\frac{1}{2},B\right)\right], \end{aligned} \tag{4.38}$$

where in the second equality we used Equations (4.33) and (4.34).

Bulk limit

In the "bulk" limit we let $B \to \infty$ and $\theta \to \infty$ but we keep $u = \theta/B$ fixed, we are hence studying the regime where θ is in the bulk, between 0 and B. The rest of computation is based on writing an ansatz for $R(\theta)$ in the bulk regime. By re-expanding this edge ansatz in the bulk regime, we can recursively fix all the coefficients $Q_{n,m}$ as well as the unknown coefficients in the bulk regime through a careful matching procedure. Because the bulk ansatz is different depending on the theory under consideration, we shall give more details about the bulk ansatz when we discuss the individual theories.

For example, for the Principal Chiral Model (and also the $O(N)$ model) we take a bulk ansatz with the following form

$$R(\theta) = \sum_{n,m=0}^{\infty}\sum_{k=0}^{m+n}\frac{2A\sqrt{B}c_{n,m,k}(\theta/B)^{e(k)}}{B^{m-n}(\theta^2-B^2)^{n+1/2}}\left[\log\frac{\theta-B}{\theta+B}\right]^k, \tag{4.39}$$

where $e(k)$ is 0 if k is even and 1 if k is odd. This bulk ansatz is best understood as a perturbative expansion in the bulk parameter $u = \frac{\theta}{B}$.

$$R(u) = \sum_{n,m=0}^{\infty}\sum_{k=0}^{m+n}\frac{\sqrt{B}c_{n,m,k}(u)^{e(k)}}{B^{m+n+1}(u^2-1)^{n+1/2}}\left[\log\frac{u-1}{u+1}\right]^k. \tag{4.40}$$

Let us take a moment to review the analytic properties of the bulk ansatz (4.39). In particular, notice that for $\theta \in [-B, B]$, there is a branch cut. This is expected because Equation (4.22) tells us that the discontinuity of $R(\theta)$ across this interval is given by $\chi(\theta)$. Let us study the dummy functions

$$f(x) = \log\frac{x-B}{x+B}, \quad g(x) = \frac{1}{\sqrt{x^2-B^2}}. \tag{4.41}$$

Notice that the argument of the logarithm and the the argument of the square-root function are both negative on the real line precisely when $x \in (-B, B)$. This means that in both cases there is a branch cut running from $x = -B$ to $x = B$. The discontinuity

across this branch cut is given by[4]

$$\begin{aligned} f(x+i\epsilon) - f(x-i\epsilon) &= 2\pi i + \mathcal{O}(\epsilon)\,, \\ g(x+i\epsilon) - g(x-i\epsilon) &= \frac{-2i}{\sqrt{B^2-x^2}} + \mathcal{O}(\epsilon)\,. \end{aligned} \tag{4.42}$$

However, these functions area analytic outside the interval $[-B, B]$. This is precisely the analytic structure that was demanded when discussing Equations (4.21) and (4.22). For a more detailed analysis of the bulk solution, see [188].

4.2.3 Matching and Determination of e/ρ^2

If we re-expand the bulk ansatz (4.39) in an edge regime where $z = 2(\theta - B)$ is fixed, we should recover the expansion in the edge regime given by (4.33). Here miraculous feature occurs: upon comparing expansions order by order in large B, then order by order in large z (which is small s) and then in $\log(z)$, we can solve for all the coefficients $c_{n,m,k}$ and $Q_{n,m}$.

Once this procedure is completed, we compute e and ρ. Using equations (4.38) and (4.33) we can express e in terms of the coefficients by

$$e = \frac{m^2 e^{2B} A^2}{2\pi}\left[1 + \sum_{m=1}^{\infty} \frac{1}{B^m} \sum_{n=0}^{m-1} 2^{n+1} Q_{n,m-1-n}\right]. \tag{4.43}$$

We can do the same for ρ using Equations (4.23) and (4.39)

$$\rho = \frac{A\sqrt{B}}{\pi}\left(c_{0,0,0} + \sum_{m=1}^{\infty} \frac{c_{0,m,0} - 2c_{0,m,1}}{B^m}\right). \tag{4.44}$$

The last step is to calculate the quantity $\frac{e}{\rho^2}$ as an expansion in B. Because $c_{n,m,k}$ and $Q_{n,m}$ in general depend also on $\log(B)$, it is convenient [1, 48] to define a new effective coupling α in terms of which the perturbative expansion is free from logarithms as we shall now illustrate for the PCM.

4.2.4 PCM Model

To illustrate the techniques in this Section 4.2, we first will consider the Principal Chiral Model on $SU(N)$. This model we serve as an example to show consistency with the literature [2].

[4] We use the formulas $\log(-a \pm i\epsilon) = \log(a) \pm i\pi + \mathcal{O}(\epsilon)$ and $\sqrt{-a \pm i\epsilon} = \pm i\sqrt{a} + \mathcal{O}(\epsilon)$ for $a, \epsilon \in \mathbb{R}_{>0}$.

Kernel and Matching Procedure

The scattering matrix of the $SU(N)$ PCM model was discussed in Section 2.4.2. It has a WH-decomposition with a $G_+(\omega)$ given by

$$G_+(\omega) = \frac{e^{i\omega((1-\Delta)\log(1-\Delta)+\Delta\log(\Delta))}\Gamma(1-i(1-\Delta)\omega)\Gamma(1-i\Delta\omega)}{\sqrt{2\pi(1-\Delta)\Delta}\sqrt{-i\omega}\Gamma(1-i\omega)}\,, \tag{4.45}$$

where $\Delta = \frac{1}{N}$. We can now use the techniques laid out in Section 4.2 to compute a perturbative series for $\frac{e}{\rho^2}$. We calculate the quantity $\Phi(s)$ from Equation (4.34) using (4.45) and obtain

$$\Phi(s) = G_+(2is) = \frac{e^{-2s((1-\Delta)\log(1-\Delta)+\Delta\log(\Delta))}\Gamma(2s(1-\Delta)+1)\Gamma(2s\Delta+1)}{2\sqrt{\pi(1-\Delta)\Delta}\sqrt{s}\Gamma(2s+1)} \tag{4.46}$$

Notice that this function has an expansion in small s with terms that look like $s^{n-1/2}$, for $n = 0, 1, 2, \ldots$. Notably there are no $\log s$ terms.

For the matching procedure, we employ a bulk ansatz of the form (4.39), which we re-expand in an edge regime as a power-series in large B. At any fixed order of B we encounter a finite number of "divergent" terms $z^{n+1/2}, z^{n-1/2}, \ldots$ and then an expansion in $1/z$. The expansion in $1/z$ is truncated and compared against the edge ansatz in the following way.

Because the Laplace transform of s^n is $\frac{\Gamma(n+1)}{z^n+1}$ we argue that the large z expansion must arise as the Laplace transform of a small s expansion. At every order of $\frac{1}{B}$, we thus perform a small s expansion of the edge-ansatz (4.33) with $\Phi(s)$ given by (4.46). After the Laplace transform becomes a large z expansion. The edge and bulk ansatz are compared order by order in large B and then z. The resulting equations fix all the coefficients $c_{n,m,k}$ and $Q_{n,m}$. The coefficients $c_{n,m,k}$ are all proportional to me^{-B}, but neither the coefficients $c_{n,m,k}$ nor $Q_{n,m}$ depend on $\log B$ for this model. As a result, when we calculate $\frac{e}{\rho^2}$, a pure series in B is obtained.

Let us contrast this procedure against its counterpart for the $O(N)$ model and the GN model. Although in the former case we use the same bulk ansatz (4.39), in the latter case we use

$$R(\theta) = \sum_{m=1}^{\infty}\frac{A}{B^m}\sum_{n=1}^{m}\sum_{k=0}^{m} c_{n,m-n,k}\frac{(\theta/B)^{e(k+1)}}{(\theta^2/B^2-1)^n}\left[\log\frac{\theta-B}{\theta+B}\right]^k\,. \tag{4.47}$$

This reflects the fact that the small s expansion in of the edge ansatz of the GN model does not have square roots. i.e. at every order of $\frac{1}{B}$ there are are a number of divergent terms $s^{-n}, s^{-n+1}, \ldots$ but otherwise it is a series in s.

One main difference between the $O(N)$ and GN model on the one side and the $SU(N)$ PCM on the other, is the fact that the former models contain series in $\log(s)$ as well as in s in the small s expansion of their edge ansatz. In should be noted here that the order of the $\log(s)^k$ terms is never higher than s^n, i.e. $k \leq n$ in a certain term. The

$SU(N)$ PCM does not have $\log(s)^k$ terms for any $k > 0$. This results in the coefficients $c_{n,m,k}$ vanishing for $k > 0$ in the PCM model.

Another difference between the $O(N)$ and GN model on the one side and the $SU(N)$ PCM on the other is the discarding of divergent terms in the matching procedure. In the GN model this means that we ignore all terms with z^k and $k > 0$. At order z^0 we perform matching for the term with $\log(z)$, but the term that is constant in z is ignored[5]. For the $O(N)$ model, we do not consider the terms with $k \geq \frac{3}{2}$. The "softest" divergent term, with $k = \frac{1}{2}$ is still matched at any order of $\log(z)$ and B.[6]

As an illustration the first few coefficients determined in this fashion for the $SU(N)$ PCM are

$$\begin{gathered} c_{0,0,0} = X\,, \quad c_{1,0,0} = -X(1+\Upsilon)\,, \quad c_{0,1,0} = -\frac{1}{16}X(3+4\Upsilon) \\ Q_{0,0} = \frac{1}{8}\,, \quad Q_{0,1} = \frac{9}{128} + \frac{\Upsilon}{8}\,, \quad Q_{1,0} = \frac{9}{256} \end{gathered} \tag{4.48}$$

where $X = e^B m(\Delta(1-\Delta))^{-\frac{1}{2}}$ and $\Upsilon = \Delta\log\Delta + (1-\Delta)\log(1-\Delta)$. Because the expansion of $\Phi(s)$ does not contain any terms with $\log(s)$ (whereas it does in the $O(N)$ model), the expansion in fact simplify quite a lot. In fact, we have that $c_{n,m,k} = 0$ for all $k \neq 0$. Accordingly we have that

$$\frac{e}{\rho^2} = \frac{1}{B} + (1-\Upsilon)\frac{1}{B^2} + \mathcal{O}(B^{-3})\,. \tag{4.49}$$

Coupling Constant Redefinitions

Notably in the series (4.49) there are no $\log(B)$ terms that we are compelled to remove through a redefinition of the coupling (as was done $O(N)$-sigma model [167, 168, 189] in which a coupling γ was introduced such that the quantity $\frac{e}{\rho^2}$ was a pure power series in γ).

Nonetheless in keeping with conventions elsewhere, we shall perform a coupling constant redefinition. Let us motivate our choice starting from the coupling α which has an RG-flow determined by

$$\mu\frac{d\alpha}{d\mu} = -\beta(\alpha) = -\beta_1\alpha^2 - \beta_2\alpha^3 + \dots\,, \tag{4.50}$$

where

$$\beta_1 = \frac{1}{16\pi\Delta}, \qquad \beta_2 = \frac{1}{256\pi^2\Delta^2} \tag{4.51}$$

such that $\xi = \frac{\beta_2}{2\beta_1^2} = \frac{1}{2}$.

It turns out that the Free energy of the PCM (as well other bosonic models) has the

[5] At order B^0 this term is matched for free, but at higher order in $\frac{1}{B}$ it is ignored

[6] A more sophisticated explanation of the discarding of divergent terms can be done through the lens explained in [188] Section 6.2.4. There the importance of $\frac{z}{B} \to 0$ in the matching limit is explained. Because z appears in the bulk only in the form $\frac{z}{B}$, taking $z \to \infty$ can be practically achieved by taking $z \to 0$. Using this perspective results in a series in large B and z without any terms of the form z^k with $k \geq 1$.

form[172]

$$\Delta F(h) = -h^2(c_{-1}\frac{1}{\alpha} + c_0 + c_1\alpha + \dots)\,, \tag{4.52}$$

for some determinable coefficients c_n. Because $\rho = -\frac{\partial \Delta F}{\partial h}$, we get that $\rho = \frac{2hc_{-1}}{\alpha} + \mathcal{O}(\alpha^0)$. It follows that $\frac{e}{\rho^2} = \frac{\alpha}{4c_{-1}} + \mathcal{O}(\alpha^2)$.

Instead of thinking of the coupling parameter as a function of μ (evaluated at the scale $\mu = h$), we will think of it as a function of ρ. This dependence is fixed by the relation[7] $h = \frac{\alpha\rho}{2c_{-1}} + \mathcal{O}(\alpha^2)$, which gives that [8]

$$\rho\frac{\partial\alpha(h(\rho))}{\partial\rho} = -\tilde{\beta}_1\alpha^2 - \tilde{\beta}_2\alpha^3 - \dots\,, \tag{4.53}$$

where

$$\tilde{\beta}_1 = \beta_1\,, \qquad \tilde{\beta}_2 = \beta_2 - \beta_1^2\,. \tag{4.54}$$

The RG-equation (4.53) can be solved to leading orders by

$$\frac{1}{\alpha} + c_1\log\alpha = c_2\log(c_3\rho)\,, \tag{4.55}$$

if

$$c_1 = \frac{\tilde{\beta}_2}{\tilde{\beta}_1} = \frac{\beta_2}{\beta_1} - \beta_1\,, \qquad c_2 = \tilde{\beta}_1 = \beta_1\,, \tag{4.56}$$

where we used Equations (4.54). c_3 appears as a constant of integration. Dividing the entire equation by β_1, and scaling $\alpha' = \beta_1\alpha$ gives

$$\frac{1}{\alpha'} + (\xi - 1)\log\alpha' = \log(c_3\rho) + (\xi-1)\log\beta_1 = \log(c_4\rho)\,. \tag{4.57}$$

In the last part we define c_4 to absorb the constant of integration c_3 and the other term and the quantity ξ is given by[9]

$$\xi = \frac{\beta_2}{\beta_1^2}\,. \tag{4.58}$$

The final coupling chosen is

$$\frac{1}{\gamma} + (\xi-1)\log\gamma = \log\left(\frac{\rho}{2\mathcal{A}\beta_1\Lambda}\right)\,, \tag{4.59}$$

[7] In principle, there will be additional terms in such as $\frac{\partial\alpha}{\partial\rho}$, but these are subleading and can be omitted in this discussion.

[8] To prove this relation, we first use $h = \frac{\alpha\rho}{2c_{-1}}$ to calculate

$$\frac{\partial h}{\partial\rho} = \frac{\alpha}{2c_{-1}} + \frac{\partial\alpha}{\partial\rho}\frac{\rho}{2c_{-1}} = \frac{\alpha}{2c_{-1}} + \frac{\partial\alpha}{\partial h}\frac{\partial h}{\partial\rho}\frac{\rho}{2c_{-1}}\,,$$

which is solved for $\frac{\partial h}{\partial\rho}$. This is used to calculate $\rho\frac{\partial\alpha}{\partial\rho} = \rho\frac{\partial\alpha}{\partial h}\frac{\partial h}{\partial\rho}$, after which we use the RG-equation for h and perform a small α expansion.

This computation can be generalised to higher order. However, we should keep in mind that the coefficients $\beta_3, \beta_4, \dots$ are no longer scheme independent. Moreover, the equations that determine $\tilde{\beta}_3, \tilde{\beta}_4, \dots$ in terms of β_i will also depend on the coefficients c_n.

[9] [2] uses g^2 in places of α with a β-function $\beta(g) = -\hat{\beta}_0 g^3 - \hat{\beta}_1 g^5$. Comparing with this language gives $2\hat{\beta}_0 = \beta_1$ and $2\hat{\beta}_1 = 2\beta_2$ and $\xi = \frac{\hat{\beta}_2}{2\hat{\beta}_1^2}$.

and $\mathcal{A} = 4$. The added benefit is here that this eliminates many logarithms of π, Δ or 2 and products thereof from the expression.

Using the leading expansion of ρ:

$$\rho = \frac{me^B\sqrt{B}(1-\Delta)^{-1+\Delta}\Delta^{-\Delta}}{4\sqrt{2\pi}\sin(\pi\Delta)}\left[1+\frac{1}{8}(4\Upsilon-3)\frac{1}{B}+\mathcal{O}\left(\frac{1}{B^2}\right)\right], \tag{4.60}$$

we can perform the reversion of Equation (4.59) to obtain

$$\frac{1}{B} = \gamma + \gamma^2\left(\log c - \Upsilon + \log\frac{\Delta\sqrt{\pi}}{\sqrt{8}\sin\pi\Delta}\right) + \mathcal{O}(\gamma^3), \tag{4.61}$$

in which $c = m/\Lambda$. We now determined the expansion of e/ρ^2 in terms of the new coupling

$$\frac{e}{\rho^2} = 2\pi(1-\Delta)\Delta\left[\gamma + \left(1+\log\frac{c\sqrt{\pi}\Delta}{\sqrt{8}\sin\pi\Delta}\right)\gamma^2 + \mathcal{O}(\gamma^3)\right] \tag{4.62}$$

We now note that the term of order γ^2 simplifies when we fix the mass gap ratio to be

$$c = \sqrt{\frac{8}{e\pi\Delta^2}}\sin(\pi\Delta), \tag{4.63}$$

in precise agreement with the value found by [171]. However, in this derivation there is no strict necessity for this mass-gap as we are not comparing the mass to a concrete cut-off scale. The choice of c in this derivation is thus strictly speaking aesthetic.

To check our methodology and implementation we calculate the next few orders

$$\frac{e}{\rho^2} = 2\pi(1-\Delta)\Delta\left[\gamma+\frac{1}{2}\gamma^2+\frac{1}{4}\gamma^3+\frac{1}{16}(5+6(\Delta-1)\Delta\zeta(3))\gamma^4+\mathcal{O}(\gamma^5)\right], \tag{4.64}$$

which do indeed agree with the results obtained in [2].

It was found by [1, 2, 48] that this perturbative series has IR-renormalons for finite N. That is, at finite N, the Borel transform of (4.64) has singularities on the positive real axis. It was argued by David in the 80s [190–192] that the PCM-model has these IR renormalons due to ambiguities of the condensates of the operator

$$\mathcal{O} = \mathrm{Tr}\,\partial_\mu g\partial^\mu g^{-1}, \tag{4.65}$$

where g is the field as in Equation (2.2). The map between the location of these renormalons and those of the series (4.64) was made more precise by [2]. However, the theory also exhibits a UV renormalon (that is a Borel singularity on the negative real axis), which is not so well understood.

The $N = 3$ and $N = 4$ cases were studied more in depth by [54] and [57–59]. In those models, they respectively computed an astounding 336 and 2000 order of perturbation theory for these models and were thus able to identify higher order renormalons than previously known.

4.2.5 λ-Model

In Section 2.3, we constructed the λ-deformed model with WZW level k and a PCM model with coupling r^2 on an $SU(N)$ target space. The deformation parameter was given by (2.48)

$$\lambda = \frac{k}{k + r^2} \,. \tag{4.66}$$

We recall its RG-flow with a β-function at all orders in λ, but to leading order in $\frac{1}{k}$ given by [111–113]

$$\mu \frac{d\lambda}{d\mu} = \beta(\lambda) = -\frac{2N}{k} \left(\frac{\lambda}{1+\lambda} \right)^2 . \tag{4.67}$$

The leading order behaviour is given by

$$\beta(\lambda) = -\beta_1 \lambda^2 - \beta_2 \lambda^3 + \mathcal{O}(\lambda^4) \,, \tag{4.68}$$

with

$$\beta_1 = \frac{2N}{k} \,, \qquad \beta_2 = -\frac{4N}{k} \,, \tag{4.69}$$

and hence

$$\xi = \frac{\beta_2}{\beta_1^2} = -\frac{k}{N} \,. \tag{4.70}$$

In this Section we shall use the techniques from the above Sections to obtain a perturbative series from the TBA equation in the case of the λ-model. It was explained in [145] that the vector symmetry of the λ-model can be gauged. By fixing this gauge field to a certain charge operator with a chemical potential, we can isolate a certain state to condense. We chose a certain state associated to the anti-symmetric highest-weight vector $\omega_{N/2}$. Scattering between such states has a (Fourier-transformed) kernel with a WH-decomposition given by (2.98).

$$G_+(\omega) = \sqrt{4\kappa} \frac{\Gamma(1 - i\omega/2)^2}{\Gamma(1 - i\omega)\Gamma(1 - i\kappa\omega)} \exp\left(ib\omega - i\kappa\omega \log(-i\omega) \right) \,, \tag{4.71}$$

where $G_-(\omega) = G_+(-\omega)$ and we defined $\kappa = \frac{k}{N}$ and

$$b = \kappa(1 - \log(\kappa)) - \log(2) \,. \tag{4.72}$$

We first observe that for small s, we observe $G_+(is)$ is a series in s and $\log s$. In this regard the λ-model reminds us of the Gross-Neveu model. We shall thus use similar ansätze.

Ansätze and Matching Procedure

The edge ansatz is given by

$$\begin{aligned}\hat{R}(s) &= mAe^{B}\Phi(s)\left(\frac{1}{s+1/2}+Q(s)\right),\\ Q(s) &= \frac{1}{Bs}\sum_{m=1}^{\infty}\sum_{n=0}^{\infty}Q_{nm}\frac{1}{B^{m+n}s^{n}},\\ \Phi(s) &= G_{+}(2is),\\ A &= \frac{\Phi(1/2)}{2}.\end{aligned} \tag{4.73}$$

The bulk ansatz is the same as for the Gross-Neveu model and is given by

$$R(\theta)=\sum_{n=1}^{\infty}\sum_{m=0}^{\infty}\sum_{k=0}^{n+m}c_{nmk}\frac{(\theta/B)^{e(k+1)}}{B^{m-n}(\theta^2-B^2)^n}\left[\log\frac{\theta-B}{\theta+B}\right]^k. \tag{4.74}$$

Just like in the Gross-Neveu model, we expand the edge ansatz in small s and take the Laplace transform. We compare this against the bulk ansatz at large $z=2(\theta-B)$. We compare order by order in large B all the convergent terms, i.e. those with non-negative exponents of $\frac{1}{z}$. This procedure fixes all the coefficients c_{nmk} and Q_{nm}. It is important to note that these coefficients still depend on $\log(B)$ as well as on κ.

Comparison to Mass Gap Calculation

In this section we recover the expansion found by [193] which determines the mass gap of this theory. Using standard TBA techniques, they find an expansion for the free energy given by

$$\begin{aligned}\mathcal{F}(h)-\mathcal{F}(0) = -\frac{2h^2\kappa}{\pi}\Big\{&1-2\kappa\alpha+2\kappa\alpha^2\left[2+\kappa+\log 4++2\kappa\log\kappa+2\kappa\log\alpha\right]\\ &-8\kappa^2\alpha^3\left[(-2+2\kappa+\log 4)+2\kappa\log(\kappa)\log(\alpha)+\kappa\log(\alpha)^2\right]+\mathcal{O}(\alpha^3)\Big\}.\end{aligned} \tag{4.75}$$

The coupling α is here defined by

$$\frac{1}{\alpha}=2\log\left(\frac{8h\Delta}{m}\sqrt{\frac{2k\Delta}{\pi}}\right). \tag{4.76}$$

By using the Legendre transformation (4.11) we can compute the total energy e[10]. Doing so, we obtain the expression

$$\begin{aligned}\frac{8k\Delta}{\pi}\frac{e}{\rho^2} =& 1 + 2\alpha\Delta k - 2\alpha^2(\Delta k(2\Delta k\log(\alpha\Delta k) - \Delta k - 2 + \log(4))) \\ &+ 4\alpha^3\Delta^2k^2(2\log(\alpha)(\Delta k\log(\alpha) - 2 + \log(4)) \\ &+ 4\Delta k(\log(\alpha) - 1)\log(\Delta k) + 4 - 4\log(2)) + O\left(\alpha^4\right)\end{aligned} \tag{4.77}$$

We now perform a computation analogous to Section 4.2.3. From Equation (4.9), it follows that to leading order $\frac{e}{\rho^2} = \chi_0 + \mathcal{O}(\alpha)$ where $\chi_0 = \frac{\pi}{8k\Delta}$. Therefore $h = \frac{\partial e}{\partial \rho} = 2\chi_0\rho$, which leads to

$$\rho = \frac{4hk\Delta}{\pi}\,. \tag{4.78}$$

Therefore, we might be inspired to define a coupling by

$$\frac{1}{\alpha} = 2\log\left(\frac{\rho}{m}\sqrt{\frac{2\pi}{k\Delta}}\right)\,. \tag{4.79}$$

Using this coupling after our matching procedure recovers precisely the expansion (4.77). This is an important consistency check for our programme, as we find the same expansion that was was obtained from a different method.

A key result from [193] is obtained by comparing the series (4.77) against an expansion in terms of $\log\frac{h}{\Lambda}$. The expansions are shown to be equivalent if the mass gap is given by

$$m = c\Lambda\,, \qquad c = e^{3/2}\Delta^{1/2}\,. \tag{4.80}$$

Log-free Perturbative Expansion

In this section we take inspiration from the Gross-Neveu treatment of [2] to create a series expansions for $\frac{e}{\rho^2}$. This is appropriate because we have that to leading order $\Delta F \sim -h^2 + \mathcal{O}(\alpha)$, which leads to a coupling defined by[11]

$$\frac{1}{\gamma} + \xi\log\gamma = \log\frac{2\pi\rho}{m/c}\,, \tag{4.81}$$

where ξ is given by Equation (4.70). We could have chosen the right hand side to be $\log\frac{2\pi\rho}{\Lambda_{MS}}$, where Λ_{MS} is the cut-off in the minimal subtraction scheme. This would then be related to the mass gap by $c\Lambda_{MS} = m$. However, we shall leave the re-normalisation

[10] Because the free energy has the form $\delta\mathcal{F}(h) = -h^2 f(z)$, we can understand the Legendre transform quite concretely. Firstly, we have that $\rho = -\mathcal{F}'(h) = 2hf(z)$ and therefore

$$e(\rho) = \delta\mathcal{F}(h) + \rho h = h^2 f(z)\,,$$

and hence

$$\frac{e(\rho)^2}{\rho^2} = \frac{h^2 f(z)}{\rho^2} = \frac{1}{4f(z)} = -\frac{h^2}{4\delta\mathcal{F}}\,.$$

[11] This is in contrast to the PCM calculation where the free energy has a structure $\Delta F \sim -\frac{h^2}{\alpha} + \mathcal{O}(\alpha^0)$, which leads to a coupling $\frac{1}{\gamma} + (\xi - 1)\log\gamma \sim \log\rho$.

scheme unspecified and instead choose some "pseudo-mass gap" c of our own choosing. A choice of c that simplifies the expression considerably is

$$c = \frac{2^{-\kappa}\Gamma(\kappa)}{\pi}\,. \tag{4.82}$$

This leads to an expansion that is log-free in the coupling, given by

$$\begin{aligned}\frac{8\kappa}{\pi}\frac{e}{\rho^2} =& 1 + \kappa\gamma + \frac{\kappa}{2}(2-\kappa)\gamma^2 + \frac{\kappa}{2}\left[3 - 5\kappa + 2\kappa^2\right]\gamma^3 \\ &+ \frac{\kappa}{8}\left[3(8-\zeta(3)) - 61\kappa + 52\kappa^2 - 15\kappa^3\right]\gamma^4 \\ &+ \frac{\kappa}{12}[46\kappa^4 - 203\kappa^3 + 355\kappa^2 + \kappa(33\zeta(3) - 288) - 18\zeta(3) + 90]\gamma^5 + \mathcal{O}(\gamma^6)\,.\end{aligned} \tag{4.83}$$

It is important to note that other choices of c exists which retain the property that the series is log-free. Let us write in general

$$\frac{8\kappa}{\pi}\frac{e}{\rho^2} = \sum_{n=0} a_n(\kappa)\gamma^n\,, \tag{4.84}$$

where $a_n(\kappa)$ is a polynomial in the variable κ. We have obtained this polynomial up to $n = 38$ using computations in a Mathematica notebook over the course of several days of running time on a desktop PC.

Let us meander a moment on some empirical observations of the polynomial $a_n(\kappa)$. Firstly, $a_n(\kappa)$ is a polynomial of degree n, so that we can write it as

$$a_n(\kappa) = \sum_{m=0}^{n} a_n^{(m)}\kappa^k\,. \tag{4.85}$$

Although in the next section we shall analyse $a_n(\kappa)$ for various values of κ, it is interesting to remember that these are simply polynomials with known numerical coefficients. These coefficients form an aesthetically pleasing curve, forming the basis of the cover of this thesis - See Figure 4.1. We finish with some last observations:

1. The polynomial $a_n(\kappa)$ has no constant part, unless $n = 0$, i.e. $a_n^{(0)} = 0$. In other words, there is a root $a_{n>0}(0) = 0$.

2. $a_n(\kappa)$ has no degenerate roots, i.e. it has precisely n unique roots over the complex numbers.

3. We now consider the roots of $a_n(\kappa)$ over the real numbers. If n is odd and $n \neq 3$, then $\kappa = 0$ is the only real root of the polynomial. For $n = 3$, there are 3 real roots. Lastly, if n is even and positive, the polynomial only has one additional root over the reals, other than $\kappa = 0$. This secondary root decreases strictly as n increases.

4. The coefficients of $a_n^{(m)}$ depend on $\zeta(k)$ in the following way. Given a positive

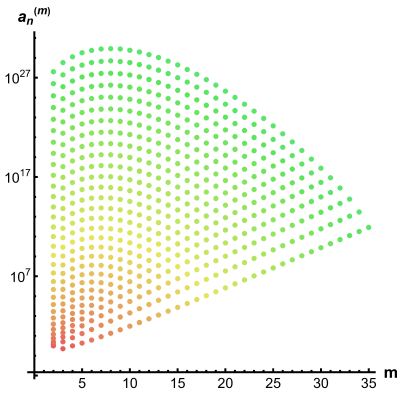

Figure 4.1: We plot the numerical values $|a_n^{(m)}|$, introduced in Equation (4.85), logarithmically for each value of m. Each value of n is represented by its own colour, ranging from the red $n = 1$ near the origin, to the green $n = 34$ away from the origin.

integer M we let

$$OP(M) = \{(m_1, m_2, \ldots, m_i) \Big| \sum_{j=1}^{i} m_j \leq M\,, \quad m_j \geq 3\,, \quad m_j \text{ is odd}\,, \quad m_j \leq m_{j+1}\}\,.$$

In other words, $OP(M)$ is the set of (ordered) partitions of at most M such that all constituent parts are odd and at least 3. We allow duplicates in the partitioning. For example, $OP(8) = \{(3), (5), (7), (3,3), (3,5)\}$. We then observe that for $m > 0$ the coefficients take the form

$$a_n^{(m)} = f_{n,m} + \sum_{\mathbf{x}=(x_1,\ldots,x_i)\in OP(n-m)} f_{n,m,\mathbf{x}} \prod_{s=1}^{i} \zeta(x_s)\,,$$

and the numbers $f_{n,m}$ and $f_{n,m,x}$ are all rational. To illustrate an example, we have[12]

$$\begin{aligned} a_{10}^{(2)} = &-\frac{574461}{16} + \frac{381915\zeta(3)}{32} + \frac{380511\zeta(5)}{64} + \frac{1129383\zeta(7)}{512} \\ &- \frac{23679}{16}\zeta(3)^2 - \frac{46197}{64}\zeta(5)\zeta(3)\,. \end{aligned}$$

Asymptotic Analysis

In this Section we will analyse the 38 orders of Perturbation series obtained in the previous Section in a more quantitative way. The goal shall be to compute an asymptotic formula for the growth of the coefficients as a function of κ. After obtaining such a formula, we can compute its ambiguity, which can later be compared against an ambiguity of a transseries. However, before we commence this more quantitative study,

[12] The fact that all the denominators are powers of 2 is not a generic feature. However, it does appear to be true for the coefficients $a_n^{(2)}$ and $a_n^{(1)}$.

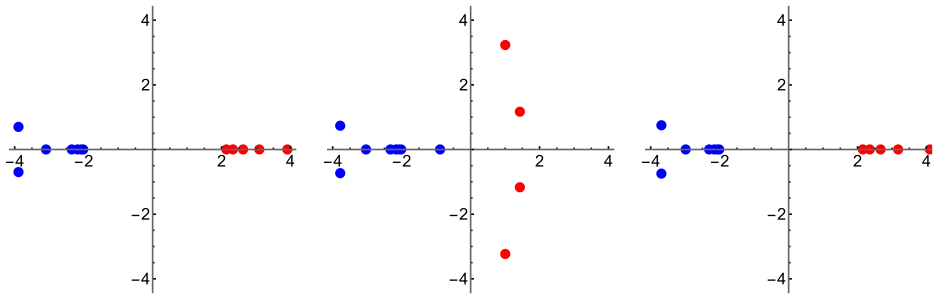

Figure 4.2: In these Figures we give the Borel-Padé poles for $\kappa = 0.95, 1.0, 1.05$ from left to right. We can see two unmoving Borel-poles at $\zeta = \pm 2$ on the outside Figures. For $\kappa = 1$, the $\zeta = 2$ pole disappears.

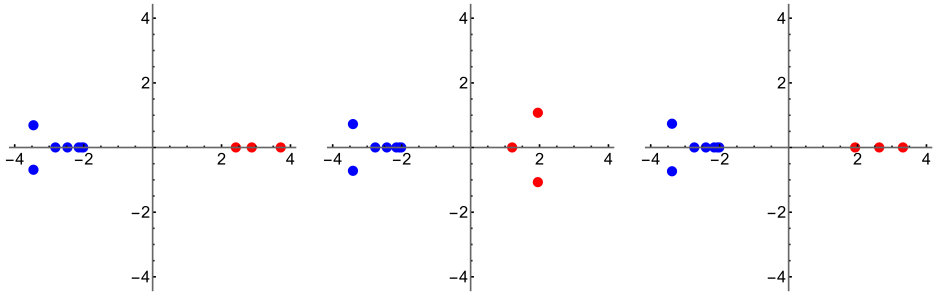

Figure 4.3: In these Figures we give the Borel-Padé poles for $\kappa = 1.95, 2.0, 2.05$. We can see two unmoving Borel-poles at $\zeta = \pm 2$ on the outside Figures. For $\kappa = 2$, the $\zeta = 2$ pole disappears.

let us start with a brief qualitative study of the Borel-Padé poles of the expansion.

Firstly, we will compute the Borel transform of the series (4.84) and then compute its diagonal Padé-approximant. We compute the poles of this approximant by setting the denominator to 0. An accumulation of Borel-Padé poles indicates a branch cut-singularity of the Borel transform. As such, the poles of the Borel-Padé approximant should give a good indication of the pole discontinuity structure of the Borel-transform. We compute the Borel-Padé poles for a number of different values of κ. Our findings are given in Figures 4.2 and 4.3.

In general, the Borel-Padé analysis seems to indicate that generically there are at least two Borel branch points located at $\zeta = \pm 2$. However, for integer values of κ, the positive pole at $\zeta = 2$ disappears. We will support these claims more quantitatively below.

Although the Padé analysis is relatively sound for small values of κ (including negative ones), the radius of convergence of the Borel-series shrinks to less than 2 around $\kappa = 3$, which makes the analysis less reliable for large κ. This is shown in Figure 4.4. The unreliability of large κ analysis will be explained at a further stage.

In general, the non-alternating poles on the positive real axis will also be referred to as *IR renormalons* ans they correspond non-resummability of the series for positive

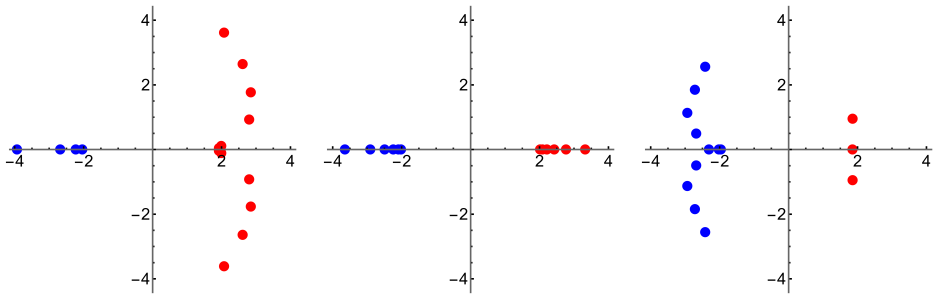

Figure 4.4: In these Figures we give the Borel-Padé poles for $\kappa = -1.2, 0.01, 4.5$. We can clearly see two unmoving Borel-poles at $\zeta = \pm 2$ on the first two figures. In the first Figure, the fact that κ is negative seems to correlate with the fact that pole on the positive axis is more pronounced than the one on the negative axis. The second Figure shows the analysis works perfectly well for very small values of κ. In the last Figure, the radius of convergence of the Borel-transform appears to be shrinking, which spoils our analysis.

coupling constant. The alternating poles on the negative axis will be referred to as *UV renormalons*. We will return to these renormalons in Section 4.3.4.

We now turn to a more quantitative analysis of the perturbative coefficients. The central goal is to find a general large n-asymptotic formula for the coefficients, as a function of κ. The general approach shall be to keep in mind a certain ansatz and define an auxiliary series that can determine certain parameters of the ansatz. Initally, we do this for fixed values of κ, but by considering many different values, we can extrapolate and find a functional form of the κ-dependence of the parameters. After we have determined all the parameters, we can compare the asymptotic formula to the actual coefficients and verify that they agree.

The first task is to compute the location of the Borel branch points. From the analysis of Borel-Padé poles it looked like there were poles at $\zeta = \pm 2$. We will now verify this. If we assume the coefficients grow as

$$a_n \sim A_+ \Gamma(n+1)/A^n + A_- \Gamma(n+1)/(-A)^n \,,$$

we can consider the series

$$\begin{aligned} f_{\text{even},n} \sim a_{2n} &= \frac{A_+ + A_-}{A^{2n}} \Gamma(2n+1) \,, \\ f_{\text{odd},n} \sim a_{2n+1} &= \frac{A_+ - A_-}{A^{2n-1}} \Gamma(2n) \,. \end{aligned} \tag{4.86}$$

We then find that

$$g_{+,n} := \frac{f_{\text{even},n}}{2n(2n-1) f_{\text{even},n-1}} \sim \frac{1}{A^2} \,, \qquad g_{-,n} := \frac{f_{\text{odd},n+1}}{2n(2n+1) f_{\text{odd},n}} \sim \frac{1}{A^2} \,. \tag{4.87}$$

By computing the series $g_{\pm,n}$ from our perturbative coefficients (4.84), we can thus find the locations of our Borel branch points. We find that the series $g_{\pm,n}$ converge to $\frac{1}{4}$,

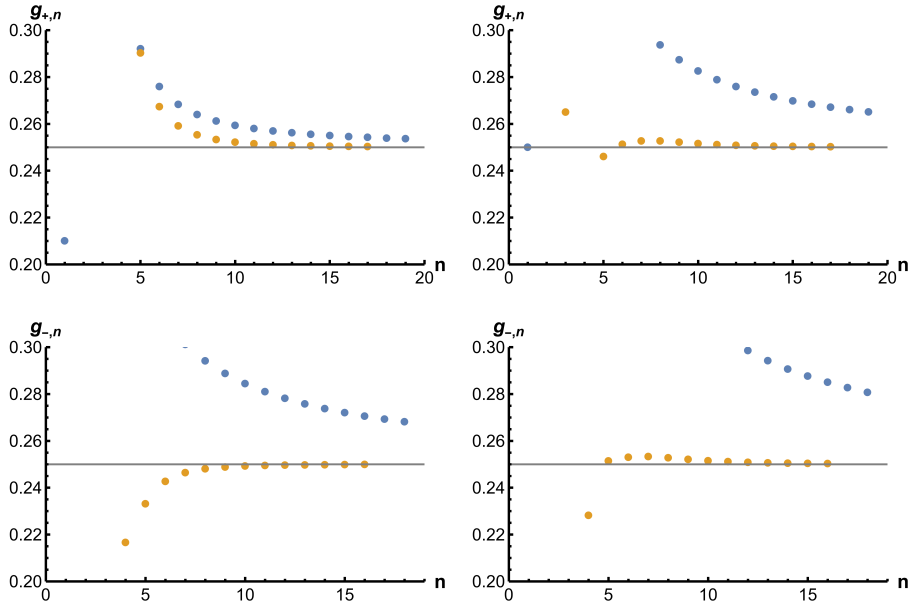

Figure 4.5: In these Figures, we consider the series $g_{\pm,n}$ from Equation (4.87). On the top line we consider the even coefficients $g_{+,n}$, on the bottom, we consider $g_{-,n}$. Both are are represented by the blue points, while in orange we give its second Richardson Transformation. On the left we set $\kappa = 0.6$, on the right $\kappa = 1.0$. In all cases it is evident that the series converges to $\frac{1}{4}$, given in grey. The second Richardson Transform differs from this guess by 0.11%, 0.098%, 0.046% and 0.12%.

independent of κ. Therefore, we have poles at $\zeta = \pm 2$. The numerics are shown in Figure 4.5.

We now know that the perturbative series does indeed have Borel singularities at $\zeta = \pm 2$. This allows us to move forward towards a more general asymptotic formula to fill in more details. Such a more general asymptotic formula for the perturbative series is of the following form

$$a_n \sim A_+ \frac{\Gamma(n+a_+)}{2^n}\left(1+\sum_{k=1}^{\infty}\frac{\beta_k^+}{n^k}\right) + A_- \frac{\Gamma(n+a_-)}{(-2)^n}\left(1+\sum_{k=1}^{\infty}\frac{\beta_k^-}{n^k}\right), \tag{4.88}$$

or

$$a_n \sim \frac{A_+}{2^n}\sum_{k=0}^{\infty}\tilde{\beta}_k^+\Gamma(n+a_+-k) + \frac{A_-}{(-2)^n}\sum_{k=0}^{\infty}\tilde{\beta}_k^-\Gamma(n+a_--k), \tag{4.89}$$

where the parameters $\tilde{\beta}_k^{\pm}$ are determined in terms of the parameters $\beta_k^{\pm}$ by the large n

asymptotics. For the first few coefficients

$$\begin{aligned}
\tilde{\beta}_0^{\pm} &= 1\,, \\
\tilde{\beta}_1^{\pm} &= \beta_1^{\pm}\,, \\
\tilde{\beta}_2^{\pm} &= \beta_1^{\pm}(a_{\pm}-1)+\beta_2^{\pm}\,, \\
\tilde{\beta}_3^{\pm} &= \beta_1^{\pm}(a_{\pm}^2-3a_{\pm}+2)+\beta_2^{\pm}(2a_{\pm}-3)+\beta_3^{\pm}\,.
\end{aligned} \tag{4.90}$$

Our central claim can be summarised by stating that the perturbative series has coefficients that grow as in (4.89), where the parameters $a_{\pm}, A_{\pm}, \beta_n^{\pm}$ are given below. In the rest of this Section, we support these result with numerical tools.

$$\begin{aligned}
a_+ &= -2\kappa \\
a_- &= +2\kappa \\
A_+ &= -\frac{8}{\pi}\sin\pi\kappa\frac{\Gamma(\kappa)}{\Gamma(-\kappa)} = -\frac{8}{\Gamma(-\kappa)\Gamma(1-\kappa)} \\
A_- &= \frac{1}{8\pi}\sin(\pi\kappa)\frac{\Gamma(-\kappa)}{\Gamma(\kappa)} = -\frac{1}{8}\frac{1}{\Gamma(\kappa)\Gamma(\kappa+1)} \\
\tilde{\beta}_1^- &= -4\kappa \\
\tilde{\beta}_2^- &= 4\kappa
\end{aligned} \tag{4.91}$$

To support these claims, we will introduce auxiliary series that will determine the coefficients $a_{\pm}$, $A_{\pm}$ and $\beta_k^{\pm}$ for fixed κ of the asymptotic series (4.89). By computing the parameters for many values of κ, we can extract a functional form. We shall define the auxiliary series

$$c_n = \frac{2^n}{\Gamma(n+1)}a_n\,, \tag{4.92}$$

which, assuming the ansatz (4.89), has large n asymptotics given by[13]

$$c_n = \left(A_+ n^{a_+-1} + (-1)^n A_- n^{a_--1}\right)\left(1+\mathcal{O}\left(\frac{1}{n}\right)\right). \tag{4.93}$$

Contributions from $\beta_k^{\pm}$ would appear as sub-leading corrections to these asymptotics. We project to the alternating and non-alternating parts of the series by considering

$$f_k^{\pm} = c_{2k} \pm c_{2k-1}\,, \tag{4.94}$$

which have asymptotics

$$f_n^{\pm} = 2A_{\pm}(2n)^{a_{\pm}-1}\left(1+\mathcal{O}\left(\frac{1}{n}\right)\right). \tag{4.95}$$

[13] We use that $\frac{\Gamma(n+b)}{\Gamma(n)} = n^b\left(1+\mathcal{O}\left(\frac{1}{n}\right)\right)$

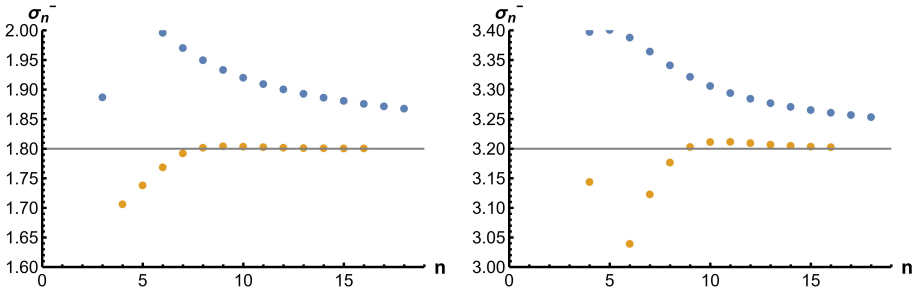

Figure 4.6: We compute σ_k^- using (4.96) and take the limit (4.97). The convergence of this series is given by the blue points, whereas the orange points depict the second Richardson transform of the sequence. On the left we have taken $\kappa = 0.9$. On the right, we take $\kappa = 1.6$. We can clearly see that the sequences converge to the expected value of $a_- = 2\kappa$. The final error of the second Richardson Transforms are 0.012% and 0.073%

By defining a final auxiliary sequence

$$\sigma_n^{\pm} = 1 + n \log \frac{f_{n+1}^{\pm}}{f_n^{\pm}}\,, \tag{4.96}$$

we can find $a_\pm$ by taking the limit

$$\underset{n\to\infty}{\text{Lim}}\, \sigma_n^{\pm} = a_\pm\,. \tag{4.97}$$

When we know $a_\pm$, we can use this to find $A_\pm$ by computing

$$\underset{n\to\infty}{\text{Lim}}\, \frac{f_n^{\pm}}{2(2n)^{a_\pm - 1}} = A_\pm\,. \tag{4.98}$$

However, from empirical observation we notice that this can only be done effectively when the series is sufficiently leading. For example, we can only compute $A_\pm$ if $a_\pm$ is (sufficiently) larger than $a_\mp$. After determining the leading term, however, we can subtract it from the main series a_n and repeat the process to find a sub-leading term.

We will use the methods above and calculate the auxiliary sequences $c_k, f_k^{\pm}, \sigma_n^{\pm}$ defined by (4.92), (4.94), (4.96). These are used to compute $A_\pm$ and $a_\pm$ using the limits (4.97) and (4.98). The limiting procedure of taking $n \to \infty$ is accelerated by using Richardson accelerations.

The result for the non-alternating series (A_+, a_+, β_1^+) can only be verified in a $\kappa < 1$ regime. However, we will present other evidence to support the claim for higher values of κ at a later stage. Moreover, we will be able to motivate why the analysis works less well for large values of κ.

In the first stage, we focus on the alternating part of the series. We compute a_-, and show that the sequences converge in figure 4.6. Using this result we can compute A_-, which are given in figure 4.7.

The next stage is to subtract the now known alternating series from the total per-

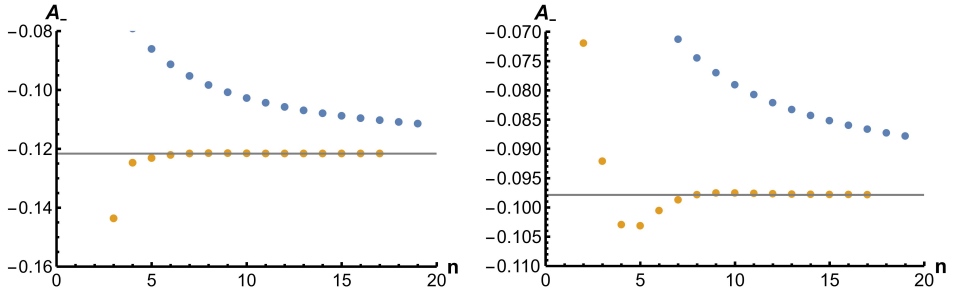

Figure 4.7: We take the limit (4.98). The convergence of this series is given by the blue points, whereas the orange points depict the second Richardson transform of the sequence. On the left we have taken $\kappa = 0.9$. On the right, we take $\kappa = 1.6$. We can clearly see that the sequences converge to the expected value of $A_- = -\frac{1}{8}\frac{1}{\Gamma(\kappa)\Gamma(\kappa+1)}$ indicated by the black line. The final discrepancies between the second Richardson Transform and the expected result are 0.015% and 0.032%.

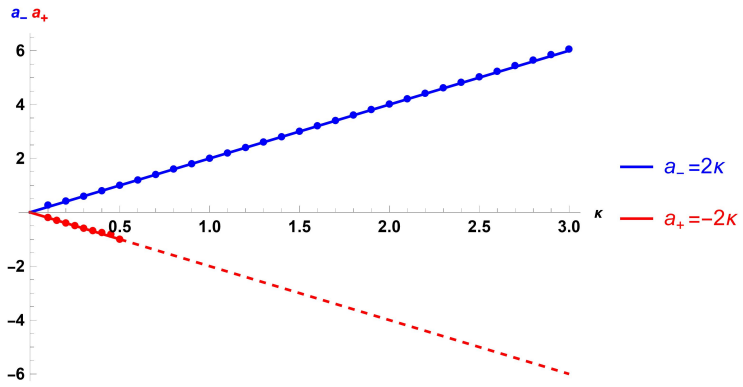

Figure 4.8: We performed a second Richardson transformation of the sequence (4.97) to determine $a_\pm$ for various values of κ, put on the horizontal axis. The best estimates for the alternating (non-alternating) pieces are given by the red (blue) points. Our claimed analytic formula $a_\pm = \mp 2\kappa$ is drawn as well and perfectly matches the predictions.

turbative series. This will give us more accurate results for a_+ and A_+. Because a_+ is numerically smaller these terms are otherwise sub-leading, which is why it is important to do the subtraction. After this procedure, we can calculate a_+ and A_+ using the same techniques as those for a_- and A_-.

By using these techniques for various values of κ we were able to claim the analytic form of $A_\pm$ and $a_\pm$. The data to support those claims is presented in Figure 4.8 and 4.9. Due to the sub-leading nature of the non-alternating parts, even after subtracting leading and sub-leading alternating parts, the non-alternating parts can only be analysed for small values of κ.

Because we now know both the leading alternating and leading non-alternating asymptotics, we can start studying the sub-leading asymptotics. We construct a new series $\tilde{a}_n$ by subtracting the leading alternating and non-alternating terms. We proceed

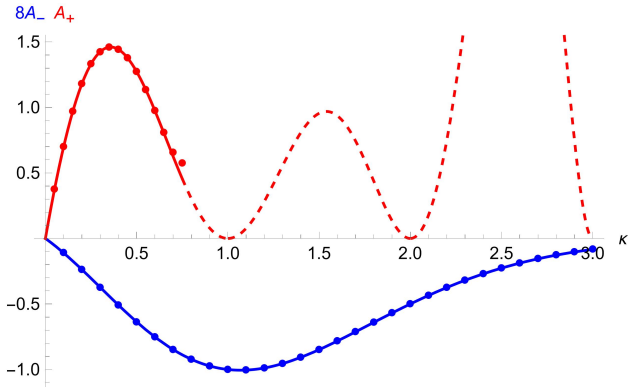

Figure 4.9: Using the result $a_\pm = \mp 2\kappa$, obtained in Figure 4.8, we performed a second Richardson transformation of the sequence (4.98). This gives estimates of $A_\pm$ for various values of κ, put on the horizontal axis. The best estimates for the alternating (non-alternating) pieces are given by the red (blue) points. Our claimed analytic formulas for $A_\pm$ in Equation (4.91) is drawn as well and perfectly matches the predictions.

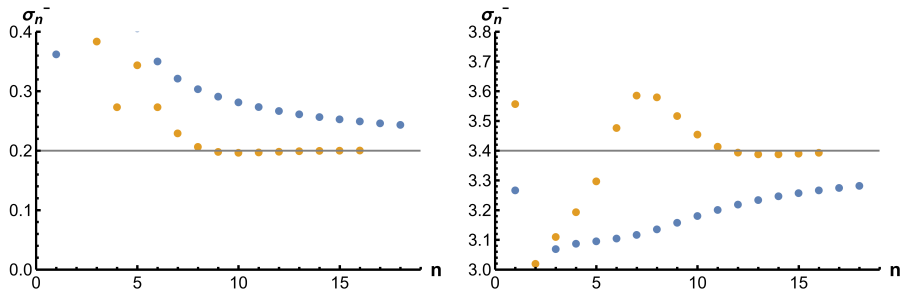

Figure 4.10: We take the limit (4.97) after subtracting the leading alternating and non-alternating asymptotics. The convergence of this series is given by the blue points, whereas the orange points depict the second Richardson transform of the sequence. On the left we have taken $\kappa = 0.6$. On the right, we take $\kappa = 2.2$. We can clearly see that the sequences converge to the expected value of $\tilde{a}_- = a_- - 1 = 2\kappa - 1$ indicated by the black line. The discrepancies are 0.034% and 0.2% respectively.

as before and calculate the auxiliary series $\tilde{c}_n$, $\tilde{f}_n$ and $\tilde{\sigma}_n$ using Equations (4.92), (4.94) and (4.96). By taking the limits (4.97) and (4.98) we access $\tilde{a}_\pm$ and $\tilde{A}_\pm$. However, as this is expected to be the subleading behaviour in Equation (4.89), we should have that $\tilde{a}_\pm = a_\pm - 1$ and $\tilde{A}_\pm = A_\pm \tilde{\beta}_1^\pm$.

Unfortunately, we find that this analysis only works well for the non-alternating series. We show these convergences at fixed κ in Figures 4.10 and 4.11. We extrapolate to all values of κ in Figure 4.12. With this information in hand, we can go a step further and use the same techniques outlined above, but now also subtract the sub-leading alternating asymptotics. This allows us to access β_2^- - see Figure 4.13.

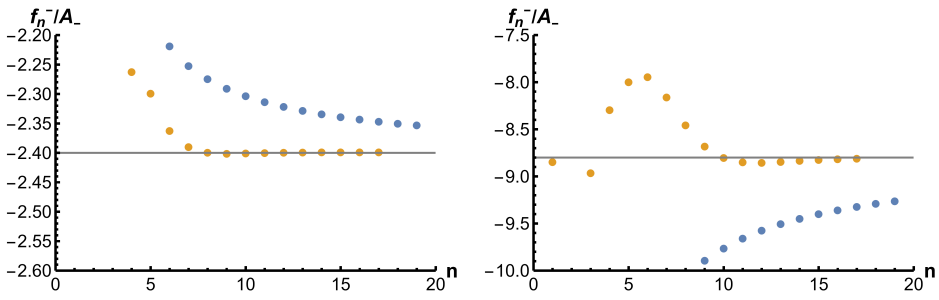

Figure 4.11: We take the limit (4.98) after subtracting the leading alternating and non-alternating asymptotics, and we divide the result by A_-. The convergence of this series is given by the blue points, whereas the orange points depict the second Richardson transform of the sequence. On the left we have taken $\kappa = 0.6$. On the right, we take $\kappa = 2.2$. We can clearly see that the sequences converge to the expected value of $\tilde{\beta}_1^- = -4\kappa$ indicated by the black line, with discrepancies of 0.022% and 0.15%.

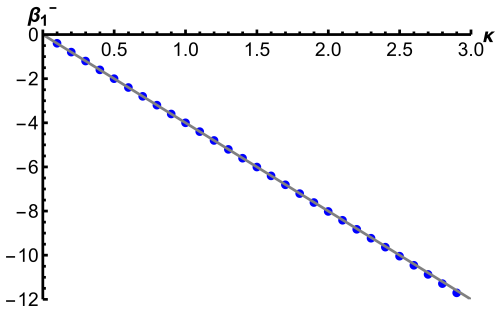

Figure 4.12: We use the same method as in Figure 4.11, but now apply the second Richardson Transformation to many values of κ, all represented as the blue points. The grey line is the expected value $\tilde{\beta}_1^- = -4\kappa$

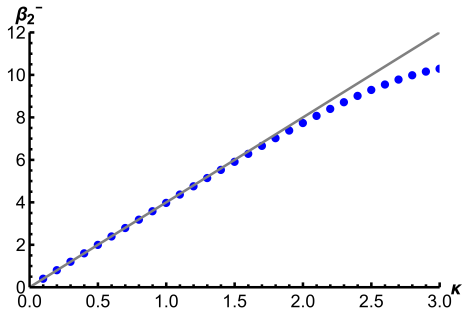

Figure 4.13: After subtracting leading alternating and non-alternating analytics, as well as the sub-leading alternating analytics, we take the limit (4.98). We divide the result by A_- and take the second Richardson Transformation. By performing this analysis for many values of κ, we can extract a functional form for $\tilde{\beta}_2$, given by the blue points. The grey line is the expected value $\tilde{\beta}_2^- = +4\kappa$. We can see that the analysis falls off for larger values of κ.

Large κ Asymptotics

Although the current non-alternating analysis does not extend to higher values of κ, there is additional evidence to support our claim that $A_+ = \frac{8}{\pi}\sin\pi\kappa\frac{\Gamma(\kappa)}{\Gamma(-\kappa)}$: we notice that A_+ vanishes if κ is an integer, which is the reason that there are no Borel-Padé poles on the positive real axis for these values of κ. This was already seen in Figures 4.2 and 4.3.

By studying the asymptotics of (4.89) with parameters (4.91), we can also explain why our asymptotic analysis is bad for large κ, but good for small κ. The critical observation lies in the large n expansion (4.88). We recall this relies on parameters $\beta_k^{\pm}$, which are related to $\tilde{\beta}_k^{\pm}$ by the dictionary in Equation (4.90). In particular, notice that $\beta_2^+ = 8\kappa^2$. We might then postulate that in general, the sub-leading coefficients $\beta_n^{\pm}$ scale with κ^n. In either case, the sub-leading terms β_1^+ and β_2^+ become more dominant as κ becomes larger. To compensate for this, one would have to go to higher order of perturbation theory.

Another curiosity from the large κ limit can be found by taking the limit at the level of the perturbation coefficients $a_n(\kappa)$ in Equation (4.83) and (4.84). As mentioned, the coefficients $a_n(\kappa)$ are polynomials in κ of order n. Let us for a moment take the large κ limit by discarding all terms in a_n, except the n^{th}-order monomial. As an example, let us apply this procedure for the first few coefficients given is Equation (4.83). In terms of a new coupling $\tilde{\gamma} = \kappa\gamma$ this gives

$$\frac{8\kappa}{\pi}\frac{e}{\rho^2} = 1 + \kappa\gamma - \frac{1}{2}(\kappa\gamma)^2 + (\kappa\gamma)^3 - \frac{15}{8}(\kappa\gamma)^4 + \frac{23}{6}(\kappa\gamma)^5 + \mathcal{O}(\kappa^6) = \sum_{n=1}^{\infty}\tilde{a}_n\tilde{\gamma}^n\,, \quad (4.99)$$

where $\tilde{a}_n = a_n^{(n)}$ in the language of Equation (4.85). The first observations are that the coefficients are all rational numbers (i.e. they do not depend on $\zeta(n)$) and that they are alternating[14].

As a first analysis, we can consider the Padé-poles of this new series, given in Figure 4.14. The presence of an accumulation point of these poles indicates that the series has a finite radius of convergence. In other words, there is no factorial growth. This can also be seen by computing the ratios of the numbers $b_n = \frac{\tilde{a}_n}{\tilde{a}_{n-1}}$ – see Figure 4.15. It is observed that the ratios converge to some number $\alpha = -2.678$. This indicates that an asymptotic formula should contain a factor of α^n, which explains the location of the singular point $1/\alpha = -0.3733$ in Figure 4.14. In general, the asymptotic formula

[14] If one looks at these rational numbers a bit more closely, one finds a strange pattern when looking at their prime number factorisation. The denominators seem to contain factors of $n!$, whereas the numerators typically contain large prime numbers. As an example, consider

$$\begin{aligned}\tilde{a}_{34} &= -\frac{1162400759590144333924690390484056829950082081}{13860389764408548091111271833600000}\\ &= \frac{2^{36}\times 3^9\times 5^5\times 7^4\times 11^2\times 13^2\times 17\times 19\times 23\times 29\times 31}{872251\times 216332159958569981\times 6160178867635064734351}\\ &= \frac{2^5\times 3^{-5}\times 5^{-2}\times 32!}{872251\times 216332159958569981\times 6160178867635064734351}\end{aligned}$$

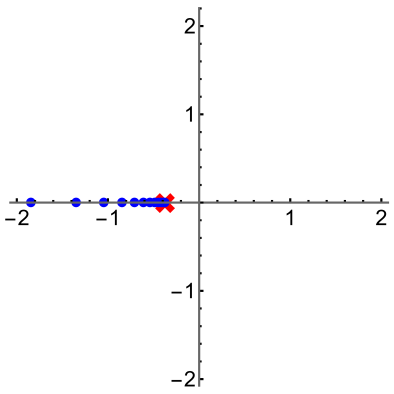

Figure 4.14: We consider the Padé approximant of the series (4.99) and compute its Padé poles in the $\tilde{\gamma}$-plane. We see a single branch point around $\tilde{\gamma} = -0.3733$ (the red cross) on the negative axis.

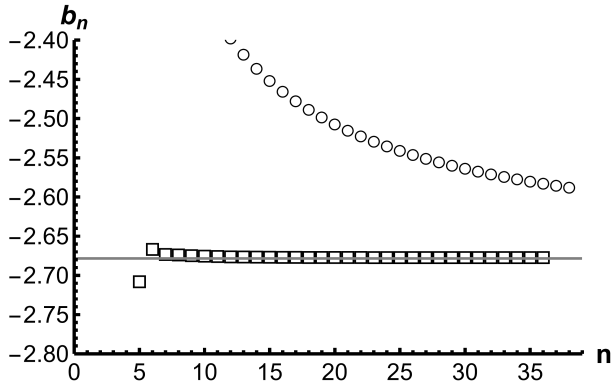

Figure 4.15: In this Figure, we consider the series $b_n = \frac{\tilde{a}_n}{\tilde{a}_{n-1}}$ given with circles, and its second Richardson Transformation, with squares. It converges to about $\alpha = -2.678378$, drawn in grey. The last and the second to last element of the sequence differ only in the sixth decimal place.

could look something like $a_n^{\text{asymp}} = B\alpha^n n^\beta$. In Figure 4.16, we show that the sequence $c_n = n \log \frac{\tilde{a}_n}{\alpha \tilde{a}_{n-1}}$ converges to $-\frac{4}{3}$, indicating that $\beta = -\frac{4}{3}$. Lastly, in Figure 4.17, it is shown that the proportionality constant is given by $B = -0.265$.

Ambiguity

In this Section, we return to the full formula for the asymptotic expansion given in Equation (4.89) with parameters given by Equation (4.91), which now have been motivated numerically. Our goal shall be to understand the Borel-structure of this abstract series so that we can compute its Stokes ambiguity. This ambiguity will then later be compared against a transseries computation.

Instead of analysing the Borel-structure of the full series (4.89), we start with a simpler example. We will then build out from this to the full series. For Borel-resummation

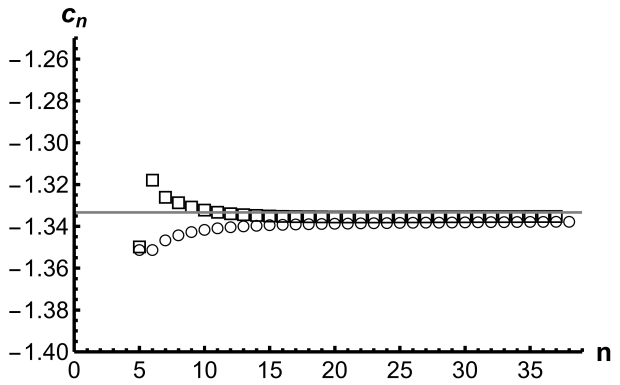

Figure 4.16: In this figure, we consider the series $c_n = n \log \frac{\tilde{a}_n}{\alpha \tilde{a}_{n-1}}$, given by the circles, and its second Richardson Transformation, with squares. It converges to $\beta = -\frac{4}{3}$, drawn in grey, from which the last elements of the sequence differs by 0.18%.

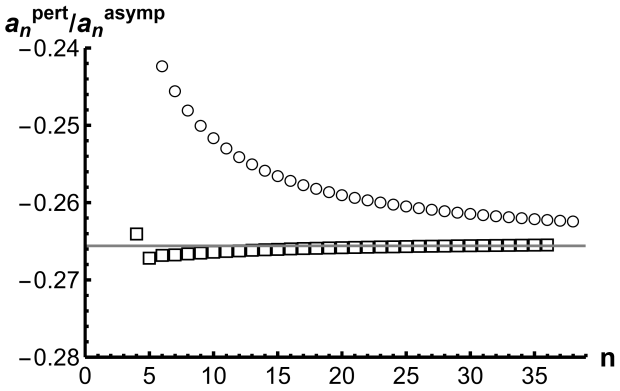

Figure 4.17: In this figure, we consider the series $\frac{\tilde{a}_n}{\tilde{a}_n^{\text{asymp}}}$, given by the circles, and its second Richardson Transformation, with squares. We take $\tilde{a}_n^{\text{asymp}} = \alpha^n n^\beta$, with $\alpha = -2.678$ and $\beta = -\frac{4}{3}$. The sequence converges to $B = -0.265$, drawn in grey. The last two elements of the sequence of the second Richardson transformation only differ in the fourth decimal.

techniques, we choose the conventions

$$\begin{aligned}\phi(\gamma) &= \sum_{n=0}^{\infty} a_n \gamma^n \,, \\ \hat{\phi}(\zeta) = \mathcal{B}[\phi] &= \sum_{n=0}^{\infty} \frac{a_n}{\Gamma(n+1)} \zeta^n \,, \\ \mathcal{S}_\theta[\phi] &= \frac{1}{\gamma} \int_0^{\infty e^{i\theta}} d\zeta \mathcal{B}[\phi] e^{-\zeta/\gamma} \,.\end{aligned} \tag{4.100}$$

These are good conventions because re-expansion of the resummation gives $\mathcal{S}_0[\phi] = \sum_{n=0}^{\infty} a_n \gamma^n$. We can break down the asymptotic expansion 4.89 by decomposing it as a sum of asymptotic expansions with coefficients $a_n \sim \frac{1}{(\pm 2)^n}\Gamma(n + a_\pm - k)$. These asymptotic expansions were discussed in Examples 4 and 5, albeit with a slightly different convention for the asymptotic expansion, and we shall import their results here, adapted to the conventions (4.100). We will be specialising to the case $A = 2$ and $a = a_\pm - k$. The discontinuity around the positive real axis of (4.89) is hence given by

$$\begin{aligned}(S_+ - S_-)\tilde{\phi}(\gamma) &= 2\pi i A_+ \Big(\frac{2}{\gamma}\Big)^{a_+} e^{-2/\gamma} \sum_{k=0}^{\infty} \tilde{\beta}_k^+ \Big(\frac{\gamma}{2}\Big)^k \\ &= -\frac{16\pi i}{\Gamma(-\kappa)\Gamma(1-\kappa)} \Big(\frac{\gamma}{2}\Big)^{2\kappa} e^{-2/\gamma}[1 + \mathcal{O}(\gamma)] \,.\end{aligned} \tag{4.101}$$

We hence see that the corrections $\beta_k^\pm$ correspond to fluctuations around the transseries. Across the negative real axis we find an ambiguity given by

$$\begin{aligned}(S_{\pi+\epsilon} - S_{\pi-\epsilon})\tilde{\phi}(\gamma) &= 2\pi i A_- \Big(-\frac{2}{\gamma}\Big)^{a_-} e^{2/\gamma} \sum_{k=0}^{\infty} \tilde{\beta}_k^- \Big(-\frac{z}{2}\Big)^k \\ &= -\frac{\pi i}{4\Gamma(\kappa)\Gamma(1+\kappa)} \Big(-\frac{\gamma}{2}\Big)^{-2\kappa} e^{2/\gamma}[1 + \mathcal{O}(\gamma)] \,.\end{aligned} \tag{4.102}$$

In the next section we shall develop techniques to calculate these ambiguities using a very different approach.

4.3 Analytic Transseries

In this section we use techniques developed by [49] to compute an analytic transseries which will decode the analytic structure of the discontinuities of the perturbative expansion. In particular, we make a prediction of the Stokes coefficient.

Firstly, we review Wiener-Hopf techniques to re-write the TBA equations. We will then specialise to the case where $G_+(0)$ is finite, which is the situation in Sine-Gordon, Gross-Neveu and λ-deformed models.

After re-writing the integral equation we can solve them iteratively in both a perturbative and non-perturbative parameter up to an ambiguity. Because we are tracking perturbative and non-perturbative corrections separately, this computation ultimately

yields a transseries solution. We will show that the ambiguity of the non-perturbative part will precisely match the ambiguity of the Borel-re-summed perturbative series.

4.3.1 Wiener-Hopf Techniques

In this section we will be using the "free energy TBA" system, which was related to the "total energy TBA" system in Appendix 4.A. The derivation in this Section is not new [167–169, 171], but serves to flesh out some of the steps motivating our transformed integral Equations. For $\theta \in I = [-B, B]$, we have that $\epsilon(\theta)$ is determined by the equations

$$\begin{aligned} &\epsilon(\theta) - \int_{-B}^{B} d\theta' K(\theta - \theta')\epsilon(\theta') = h - m\cosh\theta \\ &\Delta F(h) = F(h) - F(h=0) = -\frac{m}{2\pi}\int_{-B}^{B} d\theta \cosh(\theta)\epsilon(\theta) \\ &\epsilon(\pm B) = 0\,. \end{aligned} \tag{4.103}$$

It is convenient to analyse this system in Fourier space[15] where Wiener-Hopf factorisation techniques can be deployed [167–169, 171]. To perform the Fourier transform we need to extend the limits on the convolution integral to $\pm\infty$ which we do by first letting $\epsilon(\theta)$ extend to the zero function outside of $I = [-B, B]$.[16] To soak up the remaining contributions of the convolution outside of this domain we let

$$\epsilon(\theta) - \int_{-\infty}^{\infty} d\theta' K(\theta - \theta')\epsilon(\theta') = g(\theta) + Y(\theta - B) + Y(-\theta - B)\,, \tag{4.104}$$

now valid for $\theta \in \mathbb{R}$ with Y unknown and $g(\theta)$ chosen such that it agrees with $h - m\cosh\theta$ on I. This can now be Fourier transformed

$$\frac{1}{G_+(\omega)G_-(\omega)}\tilde{\epsilon}(\omega) = \tilde{g}(\omega) + e^{i\omega B}\tilde{Y}(\omega) + e^{-i\omega B}\tilde{Y}(-\omega)\,, \tag{4.105}$$

in which we used the Wiener-Hopf factorisation of the kernel

$$1 - K(\omega) = \frac{1}{G_+(\omega)G_-(\omega)}\,, \tag{4.106}$$

where G_+ is analytic in the UHP, G_- analytic in the LHP and $G_-(\omega) = G_+(-\omega)$ is assumed. In what follows for a function $f(\omega)$ we define its analytic projections into the UHP and LHP as

$$[f]_\pm = \pm\frac{1}{2\pi i}\int_{-\infty}^{\infty} d\omega' \frac{f(\omega')}{\omega' - \omega \mp i\delta}\,, \tag{4.107}$$

[15] We use the Fourier transform conventions

$$\tilde{f}(\omega) = \int_{-\infty}^{\infty} d\theta e^{i\omega\theta} f(\theta)\,.$$

[16] This is not unlike the function $\epsilon^+(\theta)$ which appears in Appendix 4.A.

such that $f = [f]_+ + [f]_-$ and $[[f]_+]_- = 0$ and $[[f]_+]_+ = [f]_+$. Furthermore, it is useful to employ the definitions

$$g_\pm(\omega) = e^{\pm iB\omega}\tilde{g}(\omega)\,, \quad \epsilon_\pm(\omega) = e^{\pm iB\omega}\tilde{\epsilon}(\omega)\,, \quad \sigma(\omega) = \frac{G_-(\omega)}{G_+(\omega)}\,, \tag{4.108}$$

$$Q_+(\omega) = G_+(\omega)\tilde{Y}(\omega)\,, \quad Q_-(\omega) = Q_+(-\omega) = G_-(\omega)\tilde{Y}(-\omega)\,. \tag{4.109}$$

We now take the equation (4.105) and multiply by $e^{i\omega B}G_-(\omega)$ to give

$$\begin{aligned}\frac{1}{G_+(\omega)}\epsilon_+(\omega) &= G_-(\omega)g_+(\omega) + e^{2i\omega B}G_-(\omega)\tilde{Y}(\omega) + G_-(\omega)\tilde{Y}(-\omega) \\ &= G_-(\omega)g_+(\omega) + e^{2i\omega B}\sigma(\omega)Q_+(\omega) + Q_-(\omega)\,.\end{aligned} \tag{4.110}$$

Taking the WH projections yields two equations:

$$0 = [G_-g_+]_- + [e^{2i\omega B}\sigma Q_+]_- + Q_-\,, \tag{4.111}$$

$$\tfrac{\epsilon_+}{G_+} = [G_-g_+]_+ + [e^{2i\omega B}\sigma Q_+]_+\,. \tag{4.112}$$

The first can be solved for Q (in principle, but of course not in general in closed form), which seeds the second equation to determine $\epsilon_+(\omega)$ and hence the free energy at finite density[17]. The relation between B and h is determined by the boundary conditions that $\epsilon(\pm B) = 0$.

In the case where $G_+(0)$ is finite the analysis can be further streamlined by rephrasing eq. (4.105) as

$$\tilde{\epsilon}(\omega) = e^{i\omega B}\tilde{V}(\omega)G_-(\omega) + e^{-i\omega B}\tilde{V}(-\omega)G_+(\omega)\,. \tag{4.113}$$

This is achieved by making using of the explicit form

$$\tilde{g}(\omega) = e^{iB\omega}\left(-\frac{ih}{\omega} + \frac{ime^B}{2}\frac{1}{\omega - i}\right) + e^{-iB\omega}\left(\frac{ih}{\omega} - \frac{ime^B}{2}\frac{1}{\omega + i}\right)\,. \tag{4.114}$$

to relate $\tilde{V}(\omega)$ and $\tilde{Y}(\omega)$ as

$$\tilde{V}(\omega) = G_+(\omega)\left(\tilde{Y}(\omega) - \frac{hi}{\omega} - \frac{ime^B}{2}\frac{1}{i - \omega}\right)\,. \tag{4.115}$$

This implies in particular that $\tilde{V}(\omega)$ is not analytic in UHP, instead it has poles at $\omega = i$ and $\omega = i0$. Consequently, $[\tilde{V}(-\omega)]_- \neq \tilde{V}(-\omega)$ but rather

$$[\tilde{V}(-\omega)]_- = \tilde{V}(-\omega) + \frac{hiG_-(0)}{\omega + i\delta} - \frac{ime^BG_+(i)}{2}\frac{1}{\omega + i}\,. \tag{4.116}$$

We could proceed to carry out the WH evaluation directly in terms of this function $\tilde{V}$, however it is more elegant to remove the pole at $\omega = i$ by defining $\tilde{U}(\omega) = (1 + i\omega)\tilde{V}(\omega)$.

[17] infinite volume and zero temperature.

Multiplying eq.(4.113) by $(1-i\omega)e^{iB\omega}/G_+(\omega)$ yields

$$(1-i\omega)\frac{\epsilon_+(\omega)}{G_+(\omega)} = e^{2i\omega B}\tilde{U}(\omega)\varrho(\omega) + \tilde{U}(-\omega)\,. \tag{4.117}$$

in which

$$\varrho(\omega) = \frac{1-i\omega}{1+i\omega}\frac{G_-(\omega)}{G_+(\omega)}\,. \tag{4.118}$$

Now the WH projections read

$$\begin{aligned} 0 &= [e^{2i\omega B}\tilde{U}(\omega)\varrho(\omega)]_- + \tilde{U}(-\omega) + \frac{ihG_-(0)}{\omega+i\delta} \\ (1-i\omega)\frac{\epsilon_+(\omega)}{G_+(\omega)} &= [e^{2i\omega B}\tilde{U}(\omega)\varrho(\omega)]_+ - \frac{ihG_-(0)}{\omega+i\delta}\,. \end{aligned} \tag{4.119}$$

We further refine by rescaling $\tilde{U}(\omega) = hG_-(0)u(\omega)$ so that

$$u(\omega) = \frac{i}{\omega-i\delta} + \frac{1}{2\pi i}\int d\omega' \frac{e^{2i\omega' B}u(\omega')\varrho(\omega')}{\omega'+\omega+i\delta} \tag{4.120}$$

From the second of Equation (4.119) we have

$$(1-i\omega)\frac{\epsilon_+(\omega)}{G_+(\omega)} = +hG_-(0)\frac{1}{2\pi i}\int d\omega' \frac{1}{\omega'-\omega-i\delta}e^{2i\omega' B}u(\omega')\varrho(\omega') - \frac{ihG_-(0)}{\omega+i\delta}\,.$$

Evaluating this at $\omega = i$ gives

$$\epsilon_+(i) = \frac{h}{2}G_+(i)G_-(0)\left(1 - \frac{1}{2\pi i}\int d\omega' \frac{1}{\omega'-i}e^{2i\omega' B}u(\omega')\varrho(\omega')\right)\,.$$

We can therefore compute the free energy

$$\begin{aligned} \Delta F(h) &= -\frac{1}{2\pi}me^B\epsilon_+(i) \\ &= -\frac{1}{2\pi}h^2u(i)G_-(0)^2\left(1 - \frac{1}{2\pi i}\int_{-\infty}^{\infty} d\omega' \frac{e^{2i\omega' B}u(\omega')\varrho(\omega')}{\omega'-i}\right)\,, \end{aligned} \tag{4.121}$$

in the last step we invoked that the boundary condition $\epsilon(\pm B) = 0$ can be reformulated as

$$u(i) = \frac{m}{2h}e^B\frac{G_+(i)}{G_+(0)}\,. \tag{4.122}$$

It shall than be the goal of the coming section to solve the integral equation

$$u(\omega) = \frac{i}{\omega} + \frac{1}{2\pi i}\int_{-\infty}^{\infty} d\omega' \frac{e^{2iB\omega'}\varrho(\omega')u(\omega')}{\omega'+\omega+i\delta}\,. \tag{4.123}$$

4.3.2 Recursive Solution

We will now present the techniques pioneered by [49] and adapt them so that it can be applied to the λ-deformed model. The goal is to solve Equation (4.123), which will be

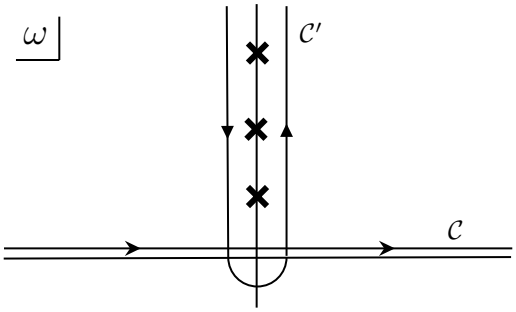

Figure 4.18: The contour $\mathcal{C} = (-\infty, \infty)$ is deformed into $\mathcal{C}'$ and as such picks up the residues indicated by crosses.

done by a clever deformation of the contour. The resulting equation can be recursively solved order by order in a perturbative parameter and a non-perturbative parameter.

Before jumping into the more difficult case which will apply to the λ-deformed model, we consider a simpler case. For a moment, let us assume the function $\varrho(\omega)$ has just simple poles, but no branch cuts, located at $x_1 < x_2 < x_3 < \dots$ with residues $\text{res}_{\omega=ix_n}\varrho(\omega) = \varrho_n$. In this case, closing the contour in Equation (4.123) around the UHP (see Figure 4.18) thus pick up the residues as given by

$$u(ix) = \frac{1}{x} + \sum_n \frac{e^{-2Bx_n} u(ix_n)\varrho_n}{x_n + x} \,. \tag{4.124}$$

Letting $u_n \equiv u(ix_n)$ we would obtain a set of algebraic equations

$$u_m = \frac{1}{x_m} + \sum_n \frac{e^{-2Bx_n} u_n \varrho_n}{x_n + x_m} \,. \tag{4.125}$$

This scenario applies to the Sine-Gordon model and it is studied by [194] who found its mass gap.

However, more generally, $\varrho(ix)$ will have both poles and a branch cut across the positive real axis. This is the case in the λ-deformed model. The idea is to move the cut to the ray $C_\pm = \{\xi e^{i\theta} | \theta = \frac{\pi}{2} \pm \delta\}$. We can then pull the deformed contour around this cut - see Figure 4.19. We let $\varrho_{n,\pm}$ be the residues at $x = x_n$ with the cut moved to $C_\pm$. In this case we have that Equation (4.123) becomes

$$u(ix) = \frac{1}{x} + \frac{1}{2\pi i}\int_0^{\infty e^{\pm i\epsilon}} dx' \, \frac{e^{-2Bx'} u(ix')\delta\varrho(ix')}{x' + x} + \sum_n \frac{e^{-2Bx_n} u_n \varrho_{n,\pm}}{x_n + x} \,, \tag{4.126}$$

where $u_n \equiv u(ix_n)$. For the discontinuity function, we use the convention

$$\delta\rho(\omega) = \rho(\omega(1 - i\epsilon) - \rho(\omega(1 + i\epsilon)) \,. \tag{4.127}$$

For $x \in \mathbb{R}_{>0}$, we can also write this as $\delta\varrho(ix) = \varrho(ix + \epsilon) - \varrho(ix - \epsilon)$. Notice that the residues, as drawn in Figure 4.19, are sensitive to the choice of branch cut deformation.

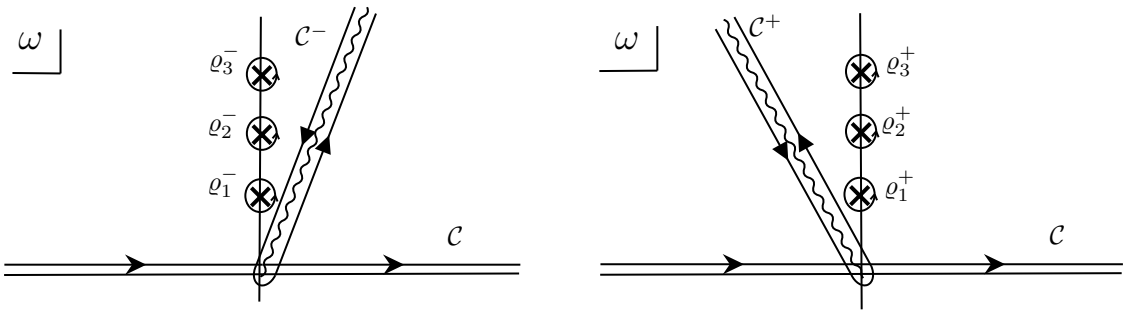

Figure 4.19: The contour $\mathcal{C} = (-\infty, \infty)$ is deformed into either of two ways. The branch cut, represented by the curvy line is moved to either the ray C_+ or C_-. In those cases respectively, the contour is deformed into $\mathcal{C}^+$ or $\mathcal{C}^-$. In both cases we pick up the residues $\varrho_n^\pm$, but their values differ by the branch cut discontinuity.

That means we defined

$$\varrho_{n,\pm} = \mathrm{Res}_{x=x_n \mp i\epsilon} \varrho(ix)\,. \tag{4.128}$$

This procedure should be non-ambiguous so in particular

$$0 = \frac{1}{2\pi i}\int_{C_+ - C_-} \frac{e^{-2Bx'} u(ix')\delta\varrho(ix')}{x' + x} + \sum_n \frac{e^{-2Bx_n} u_n(\varrho_{n,+} - \varrho_{n,-})}{x_n + x}\,. \tag{4.129}$$

This is demanding that the residues of the discontinuity function are the same as the discontituities of the residues. Schematically we have $\mathrm{Res}_{x=x_n}\delta\varrho(ix) = (\varrho_{n,+} - \varrho_{n,-})$.

We define the function $P(\eta, v)$ by

$$e^{-2Bx}\delta\varrho(ix) = -2ive^{-\eta}P(\eta, v)\,, \tag{4.130}$$

with a change of variables $(x, B) \to (\eta, v)$ given by

$$\frac{1}{v} + a\log v = 2B \quad x = v\eta\,. \tag{4.131}$$

Here, a is a constant determined by demanding that $P(\eta, v)$ is regular in v. In particular, we need to remove any dependence on $\log(v)$. Typically, we have that $\delta\varrho(ix) \propto e^{\tilde{a}x\log x}\sum d_n x^n$, in which case this determines $\tilde{a} = a$. In the Gross-Neveu model, we have $a = -2\Delta$, whereas in the lambda-deformed model we have $a = -2k\Delta$. In general we have that

$$P(\eta, v) = d_{1,0}\eta + v\eta^2(d_{2,0} + d_{2,1}\log(\eta)) + \mathcal{O}(v^2)\,. \tag{4.132}$$

In the new coordinates, Equation (4.126) becomes

$$u(\eta) = \frac{1}{v\eta} - \frac{v}{\pi}\int_0^{\infty e^{\pm i\epsilon}} d\eta' \frac{e^{-\eta'}P(\eta', v)u(\eta')}{\eta + \eta'} + \frac{1}{v}\sum_n \frac{e^{-2Bx_n}u_n\varrho_{n,\pm}}{\eta_n + \eta} \tag{4.133}$$

in which we abuse notation $u(\eta) = u(i\eta v)$ and we define $x_n = v\eta_n$. Following [49], we

define the integral operator

$$\mathcal{I}[f](\eta) = -\frac{v}{\pi}\int_0^{\infty e^{\pi i\epsilon}} d\eta' \frac{e^{-\eta'}P(\eta', v)f(\eta')}{\eta + \eta'} \tag{4.134}$$

such that Equation (4.133) can be re-written as

$$u(\eta) = \frac{1}{v\eta} + \mathcal{I}[u](\eta) + \frac{1}{v}\sum_n \frac{e^{-2Bv\eta_n}u_n\varrho_{n,\pm}}{\eta_n + \eta}\,. \tag{4.135}$$

We shall here make a slight adaptation compared to [49] to suit our own model. We shall assume that the residue locations are distributed $x_n = \mu n$ (later we shall set $\mu = 2$), whereas previously $x_n = \frac{2n+1}{\Upsilon}$ was considered for some constant Υ. We will then evaluate Equation (4.135) at $\eta = \eta_n = \mu n/v$ and define $\mathcal{I}_n[f] \equiv \mathcal{I}[f](\eta = \eta_n)$ such that we obtain

$$u_n = \frac{1}{\mu n} + \mathcal{I}_n[u] + \frac{1}{\mu}\sum_m \frac{e^{-2Bv\eta_n}u_m\varrho_{m,\pm}}{m + n}\,. \tag{4.136}$$

Let us now solve this equation. We define the seed of the equation as

$$\mathfrak{u}(\eta) = \frac{1}{v\eta} + \frac{1}{v}\sum_n \frac{e^{-2Bv\eta_n}u_n\varrho_{n,\pm}}{\eta_n + \eta}\,. \tag{4.137}$$

We can write Equation (4.135) as

$$u(\eta) = \mathfrak{u}(\eta) + \mathcal{I}[u](\eta) \tag{4.138}$$

which has a formal recurrence solution

$$u(\eta) = \sum_{l=0}^{\infty}\mathcal{I}^l\mathfrak{u}](\eta) \equiv \mathcal{J}[\mathfrak{u}](\eta) \tag{4.139}$$

Supposing that the poles are regularly distributed we can tidy up the residue term. We recall that $x_n = \mu n$ and introduce the small parameter

$$q = e^{-2B\mu} = e^{-\mu/v}v^{-\mu a}\,. \tag{4.140}$$

We will expand our solution as a series in q and solve it order by order. Firstly, we write the residues as

$$u_n = \sum_{s=0} u_n^{(s)}q^s\,.$$

If we write the seed as a power series

$$\mathfrak{u}(\eta) = \sum_{s=1}\mathfrak{u}^{(s)}(\eta)q^s\,,$$

we can compute its first terms[18] using (4.137)

$$\mathfrak{u}^{(0)} = \frac{1}{v\eta}\,, \quad \mathfrak{u}^{(1)} = \frac{\varrho_{1,\pm} u_1^{(0)}}{v\eta+\mu}\,, \quad \mathfrak{u}^{(2)} = \frac{\varrho_{1,\pm} u_1^{(1)}}{v\eta+\mu} + \frac{\varrho_{2,\pm} u_2^{(0)}}{v\eta+2\mu}\,. \tag{4.142}$$

We write the full solutions (4.139) as

$$u(\eta) = \sum u^{(s)}(\eta) q^s\,, \quad u^{(s)}(\eta) = \mathcal{J}[\mathfrak{u}^{(s)}](\eta)\,,$$

as the operator $\mathcal{J}$ crucially does not introduce factors of q. For the first terms of Equation (4.142), at $\eta = \eta_n$, we thus have that

$$u_n^{(0)} = \mathcal{J}[\mathfrak{u}^{(0)}](\eta_n) = \frac{1}{\mu n} + \mathcal{I}_n[\mathcal{J}[\frac{1}{v\eta}]]\,, \tag{4.143}$$

$$u_n^{(1)} = \mathcal{I}_n[\mathcal{J}[\frac{\varrho_{1,\pm} u_1^{(0)}}{v\eta+\mu}]] + \frac{1}{\mu}\frac{\varrho_{1,\pm} u_1^{(0)}}{1+n}\,. \tag{4.144}$$

Let us assume, and return later if not, that $\varrho_{1,\pm} \neq 0$, such that these two expressions are governing the leading behaviour.

Suppose now we work formally to leading order in v and leading order in q (i.e. ignoring that q is exponentially smaller than higher order polynomial terms in v). Because each application of $\mathcal{I}$ carries a factor v, to leading order it is sufficient to consider only the identity operator $\mathcal{J} = 1 + \dots$ which results in[19]

$$u_n^{(0)} = \frac{1}{\mu n} - \frac{v}{n\pi\mu} d_{1,0} + \mathcal{O}(v^2) \tag{4.145}$$

$$u_n^{(1)} = \frac{\varrho_{1,\pm}}{\mu^2(n+1)} - \frac{d_{1,0}\varrho_{1,\pm}}{\mu^2\pi(n+1)} v + \mathcal{O}(v^2) \tag{4.146}$$

To compute $u(\eta)$ to leading orders we takes

$$\begin{aligned} u(\eta) &= \left[\mathfrak{u}^{(0)} + \mathcal{I}[\mathfrak{u}^{(0)}] + \mathcal{O}(v)\right] + q\left[\mathfrak{u}^{(1)} + \mathcal{I}[\mathfrak{u}^{(1)}] + \mathcal{O}(v^2)\right] + \mathcal{O}(q^2) \\ &= \left[\frac{1}{v\eta} - \frac{e^\eta d_{1,0}\Gamma(0,\eta)}{\pi} + \mathcal{O}(v)\right] \\ &\quad + \frac{q\varrho_{1,\pm}}{\mu^2}\left[1 - \frac{v}{\pi\mu}(\pi\eta + 2\mu d_{1,0} - e^\eta \eta\mu d_{1,0}\Gamma(0,\eta))\right] + \mathcal{O}(q^2)\,, \end{aligned} \tag{4.147}$$

where $\Gamma(0,x) = \int_x^\infty dt\, \frac{e^{-t}}{t}$ is the incomplete Γ-function. To implement the boundary

[18] For $n \geq 1$, we have in general

$$\mathfrak{u}^{(n)}(\eta) = \sum_{m=1}^{n} \frac{\varrho_{m,\pm} u_m^{(n-m)}}{v\eta + \mu m}\,. \tag{4.141}$$

[19] the small v limit has to be taken also in the integral:

$$\mathcal{I}\left[\frac{1}{v\eta}\right](\eta_n) = -\frac{v}{\pi}\int_0^\infty \frac{e^{\eta'} d_{1,0}\eta}{v\eta' + n\mu} = -\frac{v}{\pi}\int_0^\infty \left(\frac{e^{\eta'} d_{1,0}}{n\mu} + \mathcal{O}(v)\right) = -\frac{v d_{1,0}}{n\pi\mu} + \mathcal{O}(v^2)\,.$$

condition we need to compute

$$u(i) = u\left(\eta = \frac{1}{v}\right) = \left[1 - \frac{d_{1,0}}{\pi}v + \mathcal{O}(v^2)\right] + \frac{q\varrho_{1,\pm}}{\mu(1+\mu)}\left[1 - \frac{d_{1,0}v}{\pi} + \mathcal{O}(v^2)\right] + \mathcal{O}(q^2), \tag{4.148}$$

where we use that $e^{1/v}\Gamma(0, 1/v) = v + \mathcal{O}(v^2)$.

We are now in a position to compute the free energy given by (4.121). We shall use the same technique as when going from Equation (4.123) to Equation (4.126). We deform the contour and write the integral over ω as an integral over a discontinuity plus the contributions from the residues. This results in

$$\begin{aligned}\Delta F(h) = -\frac{h^2}{2\pi}u(i)G_+(0)^2\Bigg(1 + \frac{v^2}{\pi}\int \frac{e^{-\eta}P(\eta, v)u(\eta)}{\eta v - 1}d\eta \\ - e^{-2B}\varrho(i \pm \epsilon)u(i) - \sum_{n\geq 1}\frac{q^n\varrho_{n,\pm}u_n}{\mu n - 1}\Bigg)\end{aligned} \tag{4.149}$$

We can evaluate the integral after making a small v expansion, which yields

$$\begin{aligned}\Delta F(h) = -\frac{h^2}{2\pi}G_+(0)^2\left(1 - \frac{2d_{1,0}v}{\pi} + \mathcal{O}(v^2)\right) \\ \times\left(1 - \varrho(i \pm \epsilon)q^{\frac{1}{\mu}} + \frac{2\varrho_{1,\pm}}{\mu(1-\mu^2)}q - \frac{2\varrho_{1,\pm}\varrho(i \pm \epsilon)}{\mu(1+\mu)}q^{1+\frac{1}{\mu}} + \mathcal{O}(q^2)\right)\end{aligned} \tag{4.150}$$

At this stage it is better to specialise for the model we are interested in. There are two main reasons for this. Firstly, we need to fix μ in order to compare things like $q^{2/\mu}$ to q. The second reason is that we wish to define a new coupling to compare with the perturbation result. However, the definition of the coupling is model-dependent.

4.3.3 UV Renormalons

In the above section we are working with a transseries in a transseries parameter $q = e^{-\mu/v}v^{\mu a}$. Although the calculation is not fully finished until a new coupling parameter has been introduced, we can foreshadow that the transseries in the parameter q are due to Borel singularities on the positive real axis. Currently, we can only say this would be on the positive real axis of the Borel plane of v, but after the coupling parameter redefinition, this will stay on the positive real axis of that parameter. Singularities on the positive real axis are associated with IR renormalons. In this Section, we shall slightly modify the method above to obtain a transseries than explains singularities on the negative real axis in the Borel plane, which are associated with UV renormalons.

The calcuation above relies on moving the contour in Equation (4.123) into the UHP leading to Equation (4.126) which picks up the discontinuity and singularities of ϱ in the UHP. In this Section we strengthen the hypothesis of [49] that the UV renormalons come from the singularities and discontinuities of ϱ is the LHP. To this end, we move

the contour of (4.123) into the LHP which leads to[20]

$$u(-ix) = -\frac{1}{x} + \frac{1}{2\pi i}\int_0^{\infty e^{\pm i\epsilon}} dx' \, \frac{e^{2Bx'}u(-ix')\delta\varrho(-ix')}{x'+x} - \sum_n \frac{e^{2Bx_n^{UV}}u_n^{UV}\varrho_{n,\pm}^{UV}}{x_n+x} \quad (4.151)$$

Here, $\varrho_{n,\pm}^{UV}$ are the residue at $x = x_n^{UV} > 0$ of $\varrho(-ix)$ for $n = 1, 2, \ldots$.[21] The convention (4.118) now prescribes we use $\delta\varrho(-ix) = \rho(-ix-\epsilon) - \rho(-ix+\epsilon)$.

Analogous to the coordinates η, v we introduce coordinates η, w given by

$$-\frac{1}{w} + a\log w = 2B\,, \qquad x = w\eta\,. \quad (4.152)$$

We typically have that $\delta\varrho^{IR}(ix) = f(x)e^{ax\log x}$ and that $\delta\varrho^{UV}(-ix) = f(-x)e^{-ax\log x}$. It then follows from Equation (4.130) that

$$e^{2Bx}\delta\varrho^{UV}(-ix) = 2iwe^{-\eta}P(\eta, -w)\,. \quad (4.153)$$

We will implement this in (4.151) leading to

$$u(-iw\eta) = -\frac{1}{w\eta} + \frac{w}{\pi}\int_0^{\infty e^{\pm i\epsilon}} \frac{e^{-\eta'}P(\eta', -w)u(-iw\eta')}{\eta+\eta'} - \sum_{n\geq 1}\frac{q_{UV}^{x_n^{UV}}\varrho_n^{UV}u_n^{UV}}{w\eta + x_n^{UV}}\,, \quad (4.154)$$

where[22]

$$q_{UV} = e^{2B} = e^{-1/w}w^a\,. \quad (4.155)$$

This integral equation can be solved with the same techniques as those from Section 4.3.2.

However, notice that we cannot use (4.154) to calculate $u(i)$. Instead, we must go back to (4.123) and deform the contour down. This pick up an additional residue at $\omega = -i$ leading to

$$u(i) = 1 + \frac{w}{\pi}\int_0^{\infty e^{\pm i\epsilon}} d\eta' \frac{e^{\eta'}P(\eta, -w)u(-iw\eta')}{\eta' - 1/w} - \sum_{n\geq 1}\frac{q_{UV}^{x_n^{UV}}\varrho_n^{UV}u_n^{UV}}{x_n^{UV}-1} + e^{2B}\varrho(-i\mp\epsilon)u(-i)\,. \quad (4.156)$$

The value $u(-i)$, however, can be calculated from (4.154) by setting $\eta = \frac{1}{w}$ which leads at leading order in q_{UV} to

$$u(-i) = -1 - \frac{d_{1,0}}{\pi}w + \mathcal{O}(w^2) + \mathcal{O}(q_{UV}^{x_1^{UV}})\,. \quad (4.157)$$

[20] The sign in front of the residue term is different from [49]. However, we believe this to be correct, as the contour is now traversed clockwise.

[21] We require the residue locations to be ordered $x_n^{UV} > x_{n-1}^{UV}$. In both the GN and λ-model we have $x_n^{UV} = 2n+1$.

[22] This convention is slightly different compared to $q_{IR} = q^{-2B_\mu}$.

We can therefore calculate

$$u(i) = \left(1 + \frac{d_{1,0}}{\pi} w + \mathcal{O}(w^2)\right)\left(1 - q_{UV}\,\varrho(-i \mp \epsilon) + \mathcal{O}(q_{UV}^2)\right), \tag{4.158}$$

where the assumption is that $x_1^{UV} > 1$. Just like in the IR case, to take the computation further, we must specialise to a specific model so we can write down a new coupling. Moreover, we will need to make more assumption as to locations of the residues x_n^{UV}.

Let us deform the contour of the free energy in (4.121) equation around the negative imaginary axis, like we did with $u(\omega)$. Notice that in the IR calculation above, we picked up a residue at $\omega = i$. This is not picked up now and hence we find

$$\Delta F = -\frac{h^2}{2\pi} u(i) G_-(0)^2 \left(1 + \frac{w^2}{\pi} \int_0^{\infty e^{\pm i\epsilon}} \frac{e^{-\eta'} P(\eta', -w) u(-iw\eta')}{-x' - 1} + \sum_n \frac{e^{2Bx_n^{UV}} u_n^{UV} \rho_{n,\pm}^{UV}}{-x_n^{UV} - 1}\right). \tag{4.159}$$

Plugging in the solution gives

$$\Delta F = \frac{h^2}{2\pi} u(i) G_-(0)^2 \left(1 - \frac{d_{1,0}}{\pi} w + \mathcal{O}(w^2) + \mathcal{O}(q_{UV}^{x_1^{UV}})\right). \tag{4.160}$$

4.3.4 λ-Model

In this section we specialise the solution of the previous Section to the λ-model. We first collect the analytic data required before defining a new coupling in which we will re-expand the Legendre-transformed free energy. We will compare the transseries ambiguity with that obtained from the perturbative analysis and show that they match.

Analytic Data

Let us recall the kernel (4.71) for the λ model in chemical potential

$$G_+(\omega) = \sqrt{4\kappa} \frac{\Gamma(1 - i\omega/2)^2}{\Gamma(1 - i\omega)\Gamma(1 - i\kappa\omega)} \exp\left(ib\omega - i\kappa\omega \log(-i\omega)\right), \tag{4.161}$$

where we defined b by (4.72). The case above where $G_+(0)$ is finite applies, as we now have that $G_+(0) = 2\sqrt{\kappa}$. We will define $\varrho(\omega)$ by Equation (4.118), which, using (4.161), is explicitly given by

$$\varrho(\omega) = -\frac{\omega + i}{\omega - i} \frac{\Gamma\left(\frac{i\omega}{2} + 1\right)^2 \Gamma(1 - i\omega)\Gamma(1 - i\kappa\omega)}{\Gamma\left(1 - \frac{i\omega}{2}\right)^2 \Gamma(i\omega + 1)\Gamma(i\kappa\omega + 1)} e^{-2ib\omega} e^{i\kappa\omega(\log(i\omega) + \log(-i\omega))} \tag{4.162}$$

Noting that the reciprocal Gamma-function is entire, we conclude the only possible location of poles in the UHP comes from the numerator term $\Gamma(1 - x/2)^2$, i.e. at $x = x_n = 2n$ with n a positive integer. The factor $\Gamma(1 - x)$ in the denominator reduces these double poles to single poles. The pole structure of $\varrho(ix)$ is hence determined by

the combination of Gamma functions

$$\frac{\Gamma(1-x/2)^2}{\Gamma(1-x)\Gamma(1-\kappa x)}\,.$$

However, it can be the case that some of these would-be simple poles at $x = x_n = 2n$ are removed if they coincide with poles of $\Gamma(1-\kappa x)$. This pole removal happens when κ is rational. Suppose we express $\kappa \equiv \frac{k}{N} = p/q$ as a reduced fraction with p, q coprime integers (i.e. $q = N/\gcd(N,k)$), then the set of poles are located at $x \in 2\mathbb{Z} \setminus q\mathbb{Z}$. In particular, when k is an integer multiple of a half, i.e. $q = 1$ or $q = 2$, all poles are removed entirely.

The residue at these poles is found to be[23]

$$\varrho_n^{(\pm)} = \operatorname*{Res}_{x=x_n\pm i\epsilon} \varrho(ix) = -2ie^{2n(2b\pm i\pi\kappa-2\kappa\log(2n))}n\frac{2n+1}{2n-1}\frac{((2n)!)^2}{(n!)^4}\frac{\Gamma(1+2n\kappa)}{\Gamma(1-2n\kappa)} \tag{4.163}$$

The expression for ϱ_n evaluates to zero if $2n \in 2\mathbb{Z} \cap q\mathbb{Z}$, and hence in the manipulations that follow we can simply consider the full set of $\{x_n\} = 2\mathbb{Z}$, with ϱ_n only contributing at non-removed poles. However, an important observation is that if $\varrho_1 = 0$, then $\varrho_n = 0$ for all n. Because ϱ_1 will cause the leading contribution, and we will only do computations to this leading order, we only need to consider two cases: Either, $q = 1$ or 2, and all residues vanish, or $q > 2$, and the leading residue ϱ_1 is non-zero.

In terms of the language of the previous Section, it means that we have $\mu = 2$ for the λ-model.

The ambiguity of the residue is given by

$$\varrho_n^{(+)} - \varrho_n^{(-)} = 4n^{1-4\kappa n}e^{4n(b-\kappa\log 2)}\frac{2n+1}{2n-1}\frac{((2n)!)^2}{(n!)^4}\frac{\Gamma(1+2n\kappa)}{\Gamma(1-2n\kappa)}\sin(2n\pi\kappa)$$

Notice that this vanishes if κ is half-integer.

We employ the convention that $\delta f(\omega) = f(\omega(1-i0)) - f(\omega(1+i0))$. Hence, the discontinuity function is given by[24]

[23] The term that gives the poles has residues

$$\operatorname*{Res}_{x=x_n}\frac{\Gamma(1-x/2)^2}{\Gamma(1-x)} = \frac{4\Gamma(2n)}{\Gamma(n)^2} = 2^{n+1}\frac{(2n-1)!!}{\Gamma(n)} = 2^{2n+1}\frac{\Gamma(n+\frac{1}{2})}{\Gamma(\frac{1}{2})\Gamma(n)}$$

[24] To calculate the discontinuity of $\varrho(\omega)$ across the branch cut, which is located along the ray $\mathrm{Arg}(\omega) = \frac{\pi}{2}$, we will isolate the discontinuous part and define a toy function

$$g(\omega) = \exp\left[i\kappa\omega(\log(i\omega) + \log(-i\omega))\right] \tag{4.164}$$

We choose a new coordinate $x = i\omega$ so that the branch cut is now at positive real x. If x is positive and real we have $\log(-x \pm i\epsilon) = \log(x) \pm i\pi$, this leads to a discontinuity

$$\begin{aligned}\delta g(ix) &= g(ix+\epsilon x) - g(ix-\epsilon x)\\ &= \exp\left(-2\kappa x\log x\right)\left[\exp(-i\pi\kappa x) - \exp(i\pi\kappa x)\right]\\ &= -2i\exp\left(-2\kappa x\log x\right)\sin(\kappa\pi x)\,.\end{aligned} \tag{4.165}$$

$$\delta\varrho(ix) = 2i\frac{x+1}{x-1}e^{2bx}e^{-2\kappa x\log x}\sin(\kappa\pi x)\frac{\Gamma(1-x/2)^2\Gamma(1+x)\Gamma(1+\kappa x)}{\Gamma(1+x/2)^2\Gamma(1-x)\Gamma(1-\kappa x)}\,. \tag{4.166}$$

Notice this has simple poles at $x = 2n$, which have residues that vanish for κ half-integer. This is precisely the behaviour that we saw from the residues which is needed to make this analysis non-ambiguous. Lastly we need the data

$$\varrho(i\pm 0) = 8e^{2b\mp i\pi\kappa}\frac{\Gamma(1+\kappa)}{\Gamma(1-\kappa)} = \frac{8}{\pi\kappa}e^{2b\mp i\pi\kappa}\Gamma(1+\kappa)^2\sin(\pi\kappa)\,. \tag{4.167}$$

This quantity is zero if and only if $\kappa = 1, 2, 3, \ldots$.

We define the function

$$P(\eta) = -e^{-2Bx+\eta}\delta\varrho(ix)\frac{1}{2iv}\,, \tag{4.168}$$

which in the coordinates

$$\frac{1}{v} - 2\kappa\log(v) = 2B\,, \qquad x = v\eta \tag{4.169}$$

is given by

$$P(\eta) = -e^{2v\eta\kappa\log v}\delta\varrho(iv\eta)\frac{1}{2iv}\,. \tag{4.170}$$

Notice that $\delta\varrho(ix)$ contains a $e^{-2\kappa x\log x}$ part. Splitting this into a $\log v$ and $\log\eta$ contribution, we see that the former is anihilated by the construction (4.170), whereas the latter term survives. This explains why $P(\eta)$ has an expansion of the form

$$P(\eta) = \sum_{n=1}^{\infty}\sum_{m=0}^{n-1} d_{n,m}(\eta v)^n v^{-1}(\log\eta)^m\,. \tag{4.171}$$

The coefficients $d_{n,m}$ are easily computable and the first few are given by

$$d_{1,0} = \pi\kappa\,, \quad d_{2,0} = 2\pi\kappa(1+b-\gamma_E\kappa)\,, \quad d_{2,1} = -2\pi\kappa^2\,. \tag{4.172}$$

We found that $\varrho(ix)$ has poles at $x = x_n = 2n$ with $n = 1, 2, 3, \ldots$, i.e. $\mu = 2$. We define an exponentially small parameter using the variable as in (4.140) using $a = -2\kappa$ giving

$$q = e^{-2B\mu} = v^{4\kappa}e^{-2/v}\,. \tag{4.173}$$

Coupling Re-definition

The goal shall now be to define the coupling used in the perturbative expansion. We will do the Legendre transform to calculate $\frac{e}{\rho^2}$ from ΔF. This can then be used to compare

against the perturbative calculation (4.81), namely

$$\frac{1}{\gamma} - \kappa \log \gamma = \log \frac{2\pi\rho}{m/c}\,, \tag{4.174}$$

where the pseudo-mass gap c is given by (4.82). Because $\rho \propto h$ in the models we are considering, we have that this coupling is leading order the same as the previous: $\gamma = \tilde{\gamma} + \mathcal{O}(\tilde{\gamma}^2)$.

First we calculate

$$\begin{aligned} -\rho = \frac{d\Delta F}{dh} &= \frac{\partial \Delta F}{\partial h} + \frac{\partial B}{\partial h}\frac{\partial \Delta F}{\partial B} + \frac{\partial v}{\partial h}\frac{\partial \Delta F}{\partial v} \\ &= \frac{\partial \Delta F}{\partial h} + \left(\frac{\partial B}{\partial v}\frac{\partial \Delta F}{\partial B} + \frac{\partial \Delta F}{\partial v}\right)\frac{\partial v}{\partial h}\,. \end{aligned} \tag{4.175}$$

To calculate $\frac{\partial v}{\partial h}$ we use the boundary condition (4.122),

$$\frac{\partial h}{\partial v} = \frac{\partial}{\partial v}\left(\frac{me^B}{2u(i)}\frac{G_+(i)}{G_+(0)}\right)\,, \tag{4.176}$$

and we evaluate $u(i)$ using (4.148). Similarly, we use the boundary condition (4.122) to substitute h in favour of as series in v and q. This gives

$$\rho = \frac{G_+(i)G_+(0)m}{12\pi^2}\Big(\pi - d_{1,0}v + \mathcal{O}(v^2)\Big)\Big(q^{-1/4} + \rho_1 q^{3/4} + \mathcal{O}(q^{7/4})\Big)\,. \tag{4.177}$$

We can then use this result to compute $\frac{e}{\rho^2}$ as a series in v and q given by

$$\frac{e}{\rho^2} = \frac{\Delta F + \rho h}{\rho^2} = \frac{6}{G_+(0)^2}\Big(\pi + 2d_{1,0}v + \mathcal{O}(v^2)\Big)\Big(3 + 3\rho(i)q^{1/2} + \rho_1 q + \mathcal{O}(q^{3/2})\Big)\,. \tag{4.178}$$

We introduce the perturbative coupling γ by substituting (4.177) back into the definition of the perturbative coupling (4.174). Let us introduce a parameter exponentially small in γ, analogous to q being exponentially small in v, given by $q_\gamma = e^{-4/\gamma}(\gamma/2)^{4\kappa}$. We assume an ansatz

$$v = a_1\gamma + a_2\gamma^2 + \mathcal{O}(\gamma^3) + b_1 q_\gamma(1 + \mathcal{O}(\gamma)) + \mathcal{O}(q_\gamma^2)$$

The coefficients a_1 and b_1 are consequently fixed by enforcing (4.174) at appropriate orders. Using this expression for v and for $q = q(v)$ we arrive at

$$\begin{aligned} \frac{8\kappa}{\pi}\frac{e}{\rho^2} =& \Big(1 + \kappa\gamma + \mathcal{O}(\gamma^2)\Big) - 8e^{\mp i\pi\kappa}\frac{\Gamma(\kappa)}{\Gamma(-\kappa)}q_\gamma^{1/2}(1 + \mathcal{O}(\gamma)) \\ &+ 2^{3-4\kappa}e^{\mp 2i\pi\kappa}\frac{\Gamma(2\kappa)}{\Gamma(-2\kappa)}q_\gamma(1 + \mathcal{O}(\gamma)) \end{aligned} \tag{4.179}$$

We see that the first two coefficient of the perturbative series match precisely (4.83).

The presence of transseries parameters $q_\gamma = e^{-4/\gamma}(\gamma/2)^{4\kappa}$ provides concrete predictions of the resurgent structure of the perturbative series.

We can make some initial observation. Firstly, we see that the leading transseries series term with $q_\gamma^{1/2}$ has a coefficient that vanishes if $\kappa = 1, 2, 3, \ldots$. This behaviour confirms our observation that the leading IR Borel-Padé singularity vansishes for $\kappa \in \mathbb{Z}_{>0}$.

This is slightly more restrictive than the general coefficients which also depend on the residues (4.163). These vanish if κ is half-integer, in which case the renormalon structure already simplifies. However, if κ is integer we predict that the theory is IR-renormalon free.

Let us now compute the ambiguity of the transseries (4.179) due to the difference in result if the branch cut is to left of or right of the poles. To leading order in q_γ and γ, it is given by

$$\begin{aligned}\frac{8\kappa}{\pi}\left[\left(\frac{e}{\rho^2}\right)_- - \left(\frac{e}{\rho^2}\right)_+\right] &= 8\frac{\Gamma(\kappa)}{\Gamma(-\kappa)} q_\gamma^{1/2}\left(e^{i\pi\kappa} - e^{-i\pi\kappa}\right) \\ &= \frac{16\pi i}{\Gamma(-\kappa)\Gamma(1-\kappa)}\left(\frac{\gamma}{2}\right)^{2\kappa} e^{-2/\gamma}\end{aligned} \tag{4.180}$$

This is exactly the same ambiguity as obtained through the asymptotic analysis of our perturbative calculation - see Equation (4.101). We thus observe that our Borel-ambiguity of the perturbative sector can be cancelled precisely by a transseries ambiguity. Therefore, the large order non-perturbative behaviour is unambiguous up to the order considered. This is the fabled Zinn-Justin ambiguity cancellation [13, 72, 73].

UV Renormalons

To calculate UV-renormalons we require the information

$$\delta\varrho(-ix) = -2i\frac{1-x}{x+1}e^{-2bx}e^{2\kappa x\log x}\sin(\kappa\pi x)\frac{\Gamma(1+x/2)^2\Gamma(1-x)\Gamma(1-\kappa x)}{\Gamma(1-x/2)^2\Gamma(1+x)\Gamma(1+\kappa x)}\,. \tag{4.181}$$

Moreover, $\varrho(-ix)$ has poles in the LHP at $x_n^{UV} = 2n+1$ for $n = 1, 2, \ldots$. However, just as in the case above, this will turn out to be subleading.

However, there is another set of residues located at $\tilde{x}_n^{UV} := \frac{n}{\kappa}$, for $n = 1, 2, 3, \ldots$. Its residue is given by

$$\tilde{\varrho}_n^{UV} = \operatorname*{Res}_{x=\tilde{x}_n^{UV}} \varrho(-ix) = -i\left(\frac{n}{\kappa}\right)^{1+2n}\frac{e^{-\frac{2bn}{\kappa}}}{(n!)^2}\frac{\Gamma(2-\frac{n}{\kappa})\Gamma(1+\frac{n}{2\kappa})^2}{\Gamma(1-\frac{n}{2\kappa})^2\Gamma(2+\frac{n}{\kappa})} \tag{4.182}$$

If κ is a reciprocal even number number, or n is even and κ is a reciprocal odd number, the residue vanishes. It diverges if n is odd and κ is the reciprocal of an odd number number, except if $n = \kappa = 1$, in which case the residue is finite. If κ is half-integer, and n is a multiple of 2κ, the residue vanishes.

In particular the leading residue $\tilde{\varrho}_1^{UV}$ diverges if κ is a reciprocal odd number bigger

than 1, while $\tilde{\varrho}_1^{UV}$ vanishes if κ is a reciprocal even number. In all other cases, $\tilde{\varrho}_1^{UV}$ is finite and non-zero.

However, we also observe that the residues $\tilde{\varrho}_n^{UV}$ do not have an ambiguity. This can also be seen from the fact that $\delta\varrho(-ix)$ from Equation (4.181) is regular at $x = \tilde{x}_n^{UV} = \frac{n}{\kappa}$.

Notice that this does not violates the mantra that $\delta\text{Res} = \text{Res}\delta$ (both sides are 0) which was explained in Equation (4.129). This means that $\tilde{\varrho}_n^{UV}$ are not residues of real interest as they will not cause ambiguities later on. This is further motivated by the fact that these residues would cause leading Borel-Padé singularities for $\kappa > 1$. However, no such poles were visible.

We will also need

$$\varrho(-i \pm \epsilon) = -e^{-2b \mp i\pi\kappa} \frac{\Gamma(-\kappa)}{8\Gamma(\kappa)} \,. \tag{4.183}$$

We see that for generic positive κ this never vanishes. However, if κ is integer, this turns into a residue

$$\text{res}_{\omega=-i}\varrho(\omega)|_{\kappa=1,2,\ldots} = -\frac{ie^{-2b}}{8(\kappa!)^2} \,. \tag{4.184}$$

Notice that the ambiguity in the residue disappears in this case. However, a better way to think about this as conspiracy leading to the observation that $\delta\varrho(-i)$ is regular at $\kappa \in \mathbb{Z}$. We should therefore consider

$$\varrho(-(i+\epsilon)) - \varrho(-(i-\epsilon)) = -ie^{-2b}\sin(\pi\kappa)\frac{\Gamma(-\kappa)}{4\Gamma(\kappa)} \,, \tag{4.185}$$

which is finite and non-zero at $\kappa = 1, 2, \ldots$.

We choose a coupling given by

$$\frac{1}{\gamma} - \kappa \log|\gamma| = \log\frac{2\pi\rho}{m/c} \,, \tag{4.186}$$

which is an extension for negative γ of the coupling (4.81). We will again use the boundary condition to determine h in terms of q and w which will allow us to perform the Legendre transform. Putting this together, we arrive at

$$\frac{8\kappa}{\pi}\frac{e}{\rho^2} = (1 + \mathcal{O}(\gamma)) + q_\gamma^{\text{UV}}(1 + \mathcal{O}(\gamma))e^{\pm i\pi\kappa}\frac{\Gamma(-\kappa)}{8\Gamma(\kappa)} \,, \tag{4.187}$$

where $q_\gamma^{UV} = e^{2/\gamma}\left(-\frac{\gamma}{2}\right)^{2\kappa}$ is the transseries parameter. The ambiguity of the first transmonomial is given by

$$q_\gamma^{\text{UV}}\frac{\Gamma(-\kappa)}{8\Gamma(\kappa)}\left(e^{+i\pi\kappa} - e^{-i\pi\kappa}\right) = -\frac{\pi i}{4\Gamma(\kappa)\Gamma(1+\kappa)}\left(-\frac{\gamma}{2}\right)^{-2\kappa} e^{2/\gamma} \,. \tag{4.188}$$

This precisely matches the ambiguity found in the asymptotic form of the perturbative coefficients - see Equation (4.102). This ambiguity matching in the IR mirrors the ambiguity matching we found in the IR in Equation (4.180). We thus have ambiguity cancellation not only in the IR, but also in the UV. This means that up to this order

the large order behaviour of the perturbative series in non-ambiguous.

4.4 Outlook

In this Chapter we have studied the λ-model and brought it into the fold of resurgent analysis of [1, 2, 49]. The model is particularly interesting, because, distinct from previously considered models, has a CFT fixed point in the UV.

We have found a perturbative series in Section 4.2 with an asymptotic form which generates an ambiguity in both the IR and the UV. This ambiguity has been carefully matched by a transseries solution in Section 4.3. Of particular note is that the IR renormalon vanishes for $\kappa \in \mathbb{Z}_{>0}$, i.e. when the WZW level k divides the rank N of the gauge group $SU(N)$.

Let us finish with some questions to ponder following the analysis of the λ-model in this Chapter.

- In the λ-model, when we choose integer κ, all poles and residues disappear. The resulting $\rho(\omega)$ only has a branch cut. Analysing such a system might be interesting, as it might be easier than the the most general version of the current system. This would be the reverse image of systems like the Sine-Gordon or the bi-Yang-Baxter deformed PCM, which have residues, but no branch cuts. A deformation away from such a special special point that creates new non-perturbative contributions is reminiscent of Cheshire-cat resurgence [27, 40, 153] – see also [65] for similar behaviour of disappearing singularities of integer values of a parameter connected to quantum-mechanical reduction of a WZW model.

- Why is it that this analysis is sensitive to renormalon ambiguities but not uniton ambiguities? Can we be more concrete, like [2] is, as to which operator condensates lie behind the renormalons? On a more general note, traditionally, the renormalons come from a perturbative calculation involving Feynman diagrams. In [53, 195] it was shown how to construct a series on diagrams which source the renormalon ambiguities in $1/N$ expansion of the $O(N)$ vector model, the GN and the $SU(N)$ PCM. It would be interesting to investigate if there are diagrams that are responsible for the ambiguities in the λ-models.

- What role is played by any level-rank dualities this system might exhibit? In the small $\kappa = \frac{k}{N}$ limit, in which our analysis in well-behaved, we are probing the small k regime which corresponds to the WZW side of the deformation parameter. Level-rank dualities exchange $SU(N)_k$ and $SU(k)_N$ WZW models according to [196]. They also studied this for $U(N)_k$ [197]. In our language, however, level-rank dualities send $\kappa \leftrightarrow \frac{1}{\kappa}$.

- Are there ways in which we can better explore the large κ regimes? The large κ limit is particularly interesting because the λ-deformed model becomes the non-abelian T-dual of the PCM model. It would be interesting to make contact with

the asymptotic series obtained for the PCM model obtained by [2] in this large κ limit.

- Under a $\kappa \leftrightarrow -\kappa$ transformation, the parameters of (4.91) act as $a_+ \leftrightarrow a_-$ and $8A_- \leftrightarrow \frac{A_+}{8}$. This seems to hint that this transformation interchanges the UV and IR regimes. Can this be understood better? We also observe that $A_+A_- = -\frac{\sin^2(\pi\kappa)}{\pi^2}$, is this a coincidence?

- In the matched asymptotics approach of Section 4.2, the bulk and edge ansätze are based on analytic arguments resulting in certain type of constraint series behaviour in those regimes. Is it possible to enhance those ansätze to include transseries terms resulting in a matching procedure for transseries rather than perturbative series? Such an approach might form an alternative to the transseries computation of Section 4.3.

Further to this, we can pose some question regarding more generally the application and interpretation of the techniques discussed in this Chapter.

- At the quantum level, the parameter λ dimensionally transmutes into the mass gap. If would be interesting to explore if it is possible to do a dimensional reduction as in Section 3.2 with twisted boundary conditions for the λ-model. This compactification should be adiabatically connected to the original theory. What is the fate of λ under the dimensional reduction?

- It was found by [49] that the UHP and LHP of $\rho(\omega)$ control the IR and UV behaviour of the model respectively. This was confirmed in the analysis in this Chapter. Is it possible to construct a first principles understanding of why this behaviour can be expected?

- Is it possible to perform this analysis when multiple deformation parameters are involved? Or, perhaps we can do this analysis for λ-deformed co-set models. Such models were studied in [118, 198–200].

- The S-matrix is constrained by a number of analyticity constraints discussed in Section 2.4. Is it possible to translate these constraints more directly to analyticity constraints of $\hat{K}(\omega)$ and $G_+(\omega)$? Put more concretely, can one read from an S-matrix more directly whether the WH function will have a branch cut, or where its poles will be? Even more ambitiously, is it possible to extract, from these analytic properties, through the TBA, an analytic structure of the ambiguities, without the explicit solution discussed in Section 4.3?

- In [145], the authors constructed the λ-models as a continuum limit of a Heisenberg spin-chain. The WZW-model can be constructed as an XXX spin chain, but to generalise to the λ-model we need to introduce in-homogeneities. The WZW-level k is corresponds to the representation of the of spin chain, whereas the group of the

WZW-model is the group of the spin chain. The parameter that governs the inhomogeneity becomes a mass. Although the ground state of the system is quite a complicated Fermi sea, one can identify holes as certain particle excitations. After taking the continuum limit, one can obtain a TBA system for the spin chain. The question is whether a resurgent structure can be found in the spin chain without taking a continuum limit.

It was attempted to do TBA analysis of the scattering kernel of the bi-Yang-Baxter deformed PCM (2.93). However, the attempts were thwarted as we were not able to establish an adequate bulk ansatz. On a technical level, the small s expansion of the WH-decomposition $G_+(2is)$ in (2.95) is pure in s. In particular, there are no terms such as $s^{n+1/2}$ or $\log(s)$. However, this leads us to consider Laplace transforms of the form (4.29), which introduces terms linear in $\log(z)$ (but no further $\log(z)^k$). This makes the kernel of the bi-Yang-Baxter deformed $SU(N)$ PCM unique from previously discussed kernels in [1, 2, 48]. It should also be noted that $G_+(\omega)$ (and hence also $\varrho(\omega)$) has no branch cuts which makes it similar to the SG model. A transseries analysis might thus be relatively simple and enlightening.

4.A TBA for the Free Energy

In this appendix we will discuss a common restructuring of the TBA equations. Instead of writing an integral for the total energy density, we write an integral equation for the free energy density. This will feature a more explicit dependence of the chemical potential h, and we will motivate why the free energy is minimised.

The literature often makes use of the definition $K(\theta) = \delta(\theta) - \mathcal{R}(\theta)$ where $\delta(\theta)$ is the dirac-delta functional such that the TBA system given by Equation (4.16) can be re-written as

$$\frac{m}{2\pi}\cosh\theta = f_h(\theta) + \int_{-\infty}^{\infty} \mathcal{R}(\theta-\theta')f(\theta')d\theta' \,. \tag{4.189}$$

We will introduce the pseudo-energies $\epsilon_+(\theta) > 0$ and $\epsilon_-(\theta) < 0$ of holes and particles respectively, which satisfy

$$\delta F = \int_{-\infty}^{\infty} d\theta \left[\delta f_h(\theta)\epsilon_+(\theta) - \delta f(\theta)\epsilon_-(\theta)\right] . \tag{4.190}$$

We assume that the Fermi see is filled in the area $\theta \in [-B, B]$ and empty outside. This means that we assume $\epsilon_+(\theta)$ and $f(\theta)$ have support precisely inside this interval, whereas $\epsilon_-(\theta)$ and $f_h(\theta)$ have support outside that interval. This is another way of saying that we work at zero temperature. Conversely, we can say the Fermi density is defined by the value of B such that $\epsilon_\pm(\pm B) = 0$. These constraints guarantee indeed that the free energy is minimised because the right-hand side of Equation (4.190) now vanishes.

It follows by varying Equation (4.189) that

$$f_h(\theta) = -\int_{-\infty}^{\infty} \mathcal{R}(\theta - \theta') f(\theta') d\theta' \,. \tag{4.191}$$

Plugging this into (4.190) gives

$$\delta F = -\int_{-\infty}^{\infty} d\theta \left[\int_{-\infty}^{\infty} d\theta' \epsilon^+(\theta') \mathcal{R}(\theta' - \theta) \delta\rho(\theta) + \epsilon^-(\theta) \delta\rho(\theta) \right] . \tag{4.192}$$

We compare this against the variation of the free energy given by Equation (4.19)

$$\delta F = \int_{-\infty}^{\infty} d\theta \, \delta f(\theta) (m \cosh\theta - h) \,, \tag{4.193}$$

which gives

$$\begin{aligned} h - m\cosh\theta &= \epsilon^-(\theta') + \int_{-\infty}^{\infty} d\theta' \epsilon^+(\theta') \mathcal{R}(\theta' - \theta) \\ &= \epsilon^-(\theta') + \int_{-\infty}^{\infty} d\theta' \epsilon^+(\theta') \mathcal{R}(\theta - \theta') \\ &= \epsilon(\theta) - \int_{-B}^{B} \epsilon(\theta') K(\theta - \theta') d\theta' \,, \end{aligned} \tag{4.194}$$

where we have used that $\mathcal{R}(\theta)$ is a symmetric function because $S(-\theta) = S(\theta)^{-1}$.

Using the minimisation constraints decribed above, we can evaluate the free energy as

$$\begin{aligned} F &= \int_{\infty}^{\infty} f(\theta)(m\cosh\theta - h) \\ &= -\int_{\infty}^{\infty} f(\theta) \left[\epsilon^-(\theta') + \int_{-\infty}^{\infty} d\theta' \epsilon^+(\theta') \mathcal{R}(\theta - \theta') \right] \\ &= -\int_{\infty}^{\infty} d\theta \epsilon^+(\theta) \int_{\infty}^{\infty} d\theta' \mathcal{R}(\theta - \theta') f(\theta') \\ &= -\int_{\infty}^{\infty} d\theta \epsilon^+(\theta) \left[\frac{m}{2\pi} \cosh\theta - f_h(\theta) \right] \\ &= -\frac{m}{2\pi} \int_{-B}^{B} \cosh(\theta) \epsilon(\theta) \,. \end{aligned} \tag{4.195}$$

In the first step, we used (4.194), then we used the minimisation constraints and relabels the dummy variables. We used (4.189), before using the minimisation constraints again in the last step.

To summarise, we find the following TBA equations

$$\begin{aligned} &h - m\cosh\theta = \epsilon(\theta) - \int_{-B}^{B} \epsilon(\theta')K(\theta-\theta')d\theta' \\ &\epsilon(\pm B) = 0 \\ &F = -\frac{m}{2\pi}\int_{-B}^{B}\cosh(\theta)\epsilon(\theta)\,. \end{aligned} \tag{4.196}$$

Chapter 5

Summary

This thesis has shown how ideas of resurgence can be applied to deformed integrable models. We have done so for bi-Yang-Baxter models in the context of an adiabatic reduction with twisted boundary conditions and for λ-models in the context of TBA equations. In both cases, we see some signs on an ambiguity cancellation. In the bi-Yang-Baxter case, the uniton solutions appear to play the role of an instanton-like solution that causes non-perturbative effects. In the TBA context, the origin of the renormalon is not as clear, but we do see a mathematical ambiguity cancellation in a transseries approach and an asymptotic series approach. Both these result reinforce the idea that resurgence is a necessary ingredient to give a complete understanding of asymptotic expansions and non-perturbative effects in two-dimensional integrable models.

As a coda to this thesis we consider some large-scale questions of possible future enquiry that go beyond the analyses in either those of Chapters 3 and 4, but straddle both Chapters or make connections to other recent developments.

The apparent connection between the reduction of the 2d integrable theory and the $\mathcal{N} = 2$ gauge theories, explored in Section 3.4, provokes a number of questions. First, is this simply coincidental? If not, is there a more fundamental way to make this connection we find (that doesn't required picking particular coordinate, adiabatic reduction etc.)? Second, what significance do dualities exhibited on the gauge theory side hold for the integrable models? Third, how do the integrable Hitchin systems associated to the gauge theory [160] compare to the integrable structures of the PCM (e.g. Maillet-brackets and twist functions) and its deformations? If such a connection can be made it seems likely it is via the use of affine Gaudin models [201, 202]. A final intriguing question here is to understand if the wall-crossing phenomena seen in the gauge theory has an interpretation and implication for the two-dimensional deformed sigma-model considered in this paper.

It was shown by a series of papers [103, 119–122] that the non-abelian T-dual (more precisely, an analytic continuation of a Poisson-Lie dual) of the λ-model is the η-model. A natural question is how the non-abelian T-duality is manifested in the asymptotic

series studied in this thesis. This question can be explored through either the TBA techniques of Chapter 4, or the adiabatic reduction techniques in Chapter 3. Of particular interest are the λ-deformed $AdS_5 \times S^5$ [101] and the η-deformed $AdS_5 \times S^5$, whose S-matrix was constructed by [203], as these models are deformations of a super-string background. Its Lagrangian and target space descriptions were studied by [98, 100].

The papers [46, 47, 149] and Section 3.1 established certain uniton solutions of the (Yang-Baxter deformed) PCM. Is it possible to consider a TBA system which has these unitons scattering? The (bi)-Yang-Baxter models also involved complex unitons. Is it possible to isolate these individually?

At the quantum level, the parameter λ dimensionally transmutes into the mass gap. If would be interesting to explore if it is possible to do a dimensional reduction as in Section 3.2 with twisted boundary conditions for the λ-model. This compactification should be adiabatically connected to the original theory. What is the fate of λ under the dimensional reduction?

Lastly, in a recent series of papers [204–206], it was shown how one can construct 2d integrable field theories from a certain four-dimensional holomorphic Chern-Simons type theory. It was later shown by [207] that Yang-Baxter deformations and the λ-deformations can also be incorporated in this framework. A direct question is to understand the more general resurgent structure of integrable 2d field theories from the perspective of this 4d gauge theory. A rather concrete first question would be to understand the significance of the uniton, and its cousin in complex field space, within the gauge theory. A potential route here would be to exploit the connection with affine Gaudin models established by [208]. Other in-roads to the integrable structures of these models were made by [202, 209].

Bibliography

[1] Dmytro Volin. 'From the mass gap in $O(N)$ to the non-Borel-summability in $O(3)$ and $O(4)$ sigma-models'. *Phys. Rev. D* 81 (2010), p. 105008. DOI: 10.1103/PhysRevD.81.105008. arXiv: 0904.2744 [hep-th].

[2] Marcos Mariño and Tomás Reis. 'Renormalons in integrable field theories'. *JHEP* 04 (2020), p. 160. DOI: 10.1007/JHEP04(2020)160. arXiv: 1909.12134 [hep-th].

[3] D. Hanneke, S. Fogwell and G. Gabrielse. 'New Measurement of the Electron Magnetic Moment and the Fine Structure Constant'. *Phys. Rev. Lett.* 100 (2008), p. 120801. DOI: 10.1103/PhysRevLett.100.120801. arXiv: 0801.1134 [physics.atom-ph].

[4] Tatsumi Aoyama, Toichiro Kinoshita and Makiko Nio. 'Revised and Improved Value of the QED Tenth-Order Electron Anomalous Magnetic Moment'. *Phys. Rev. D* 97.3 (2018), p. 036001. DOI: 10.1103/PhysRevD.97.036001. arXiv: 1712.06060 [hep-ph].

[5] Freeman J Dyson. 'Divergence of perturbation theory in quantum electrodynamics'. *Physical Review* 85.4 (1952), p. 631.

[6] Carl M. Bender and Tai Tsun WU. 'Large order behavior of Perturbation theory'. *Phys. Rev. Lett.* 27 (1971), p. 461. DOI: 10.1103/PhysRevLett.27.461.

[7] E. Brezin, J.C. Le lou and Jean Zinn-Justin. 'Perturbation Theory at Large Order. 1. The ϕ^{2N} Interaction'. *Phys. Rev. D* 15 (1977), pp. 1544–1557. DOI: 10.1103/PhysRevD.15.1544.

[8] J.C. Le Guillou and Jean Zinn-Justin, eds. *Large order behavior of perturbation theory*. North Holland, 1990.

[9] M. Beneke. 'Renormalons'. *Phys. Rept.* 317 (1999), pp. 1–142. DOI: 10.1016/S0370-1573(98)00130-6. arXiv: hep-ph/9807443.

[10] Mithat Ünsal. 'TQFT at work for IR-renormalons, resurgence and Lefschetz decomposition' (June 2021). arXiv: 2106.14971 [hep-th].

[11] Robert B Dingle. *Asymptotic expansions: their derivation and interpretation*. Academic Press, 1973.

[12] EB Bogomolny. 'Calculation of instanton-anti-instanton contributions in quantum mechanics'. *Physics Letters B* 91.3-4 (1980), pp. 431–435.

[13] Jean Zinn-Justin. 'Perturbation Series at Large Orders in Quantum Mechanics and Field Theories: Application to the Problem of Resummation'. *Phys. Rept.* 70 (1981), p. 109. DOI: 10.1016/0370-1573(81)90016-8.

[14] Gerald V Dunne and Mithat Ünsal. 'Resurgence and trans-series in Quantum Field Theory: the $\mathbb{CP}^{N-1}$ model'. *JHEP* 11 (2012), p. 170. DOI: 10.1007/JHEP11(2012)170. arXiv: 1210.2423 [hep-th].

[15] Gerald V. Dunne and Mithat Ünsal. 'Uniform WKB, Multi-instantons, and Resurgent Trans-Series'. *Phys. Rev. D* 89.10 (2014), p. 105009. DOI: 10.1103/PhysRevD.89.105009. arXiv: 1401.5202 [hep-th].

[16] Carl M Bender and Tai Tsun Wu. 'Anharmonic oscillator'. *Physical Review* 184.5 (1969), p. 1231.

[17] André Voros. 'The return of the quartic oscillator. The complex WKB method'. *Annales de l'IHP Physique théorique*. Vol. 39. 1983, pp. 211–338.

[18] Harris J Silverstone. 'JWKB connection-formula problem revisited via Borel summation'. *Physical review letters* 55.23 (1985), p. 2523.

[19] H. Dillinger, E. Delabaere and Frédéric Pham. 'Résurgence de Voros et périodes des courbes hyperelliptiques'. fr. *Annales de l'Institut Fourier* 43.1 (1993), pp. 163–199. DOI: 10.5802/aif.1326. URL: aif.centre-mersenne.org/item/AIF_1993__43_1_163_0/.

[20] Eric Delabaere, Hervé Dillinger and Frédéric Pham. 'Exact semiclassical expansions for one-dimensional quantum oscillators'. *Journal of Mathematical Physics* 38.12 (1997), pp. 6126–6184.

[21] Eric Delabaere and Frédéric Pham. 'Resurgent methods in semi-classical asymptotics'. *Annales de l'IHP Physique théorique* 71.1 (1999), pp. 1–94.

[22] Tom Bridgeland and Ivan Smith. 'Quadratic differentials as stability conditions'. *Publications mathématiques de l'IHÉS* 121.1 (2015), p. 155. DOI: 10.1007/s10240-014-0066-5. arXiv: 1302.7030 [math.AG].

[23] Kohei Iwaki and Tomoki Nakanishi. 'Exact WKB analysis and cluster algebras'. *Journal of Physics A: Mathematical and Theoretical* 47.47 (2014), p. 474009. arXiv: 1401.7094 [math.CA].

[24] Davide Gaiotto, Gregory W. Moore and Andrew Neitzke. 'Four-dimensional wall-crossing via three-dimensional field theory'. *Commun. Math. Phys.* 299 (2010), pp. 163–224. DOI: 10.1007/s00220-010-1071-2. arXiv: 0807.4723 [hep-th].

[25] Davide Gaiotto, Gregory W Moore and Andrew Neitzke. 'Wall-crossing, Hitchin systems, and the WKB approximation'. *Advances in Mathematics* 234 (2013), pp. 239–403. arXiv: 0907.3987 [hep-th].

[26] Maxim Kontsevich and Yan Soibelman. 'Analyticity and resurgence in wall-crossing formulas' (May 2020). arXiv: 2005.10651 [math.AG].

[27] Daniele Dorigoni and Philip Glass. 'Picard-Lefschetz decomposition and Cheshire Cat resurgence in 3D $\mathcal{N} = 2$ field theories'. *Journal of High Energy Physics* 2019.12 (2019), pp. 1–40.

[28] Daniele Dorigoni and Axel Kleinschmidt. 'Resurgent expansion of Lambert series and iterated Eisenstein integrals'. *Commun. Num. Theor. Phys.* 15.1 (2021), pp. 1–57. DOI: 10.4310/CNTP.2021.v15.n1.a1. arXiv: 2001.11035 [hep-th].

[29] Davide Gaiotto, Ji Hoon Lee, Benoît Vicedo and Jingxiang Wu. 'Kondo line defects and affine Gaudin models'. *JHEP* 01 (2022), p. 175. DOI: 10.1007/JHEP01(2022)175. arXiv: 2010.07325 [hep-th].

[30] Davide Gaiotto, Ji Hoon Lee and Jingxiang Wu. 'Integrable Kondo problems'. *JHEP* 04 (2021), p. 268. DOI: 10.1007/JHEP04(2021)268. arXiv: 2003.06694 [hep-th].

[31] Igor Krichever and Nikita Nekrasov. 'Towards Lefschetz Thimbles in Sigma Models, I'. *J. Exp. Theor. Phys.* 132.4 (2021), pp. 734–751. DOI: 10.1134/S1063776121040129. arXiv: 2010.15575 [hep-th].

[32] Inês Aniceto and Michał Spaliński. 'Resurgence in Extended Hydrodynamics'. *Phys. Rev. D* 93.8 (2016), p. 085008. DOI: 10.1103/PhysRevD.93.085008. arXiv: 1511.06358 [hep-th].

[33] Gökçe Başar and Gerald V Dunne. 'Hydrodynamics, resurgence, and transasymptotics'. *Physical Review D* 92.12 (2015), p. 125011.

[34] Gerald V. Dunne and Mithat Ünsal. 'WKB and Resurgence in the Mathieu Equation'. Mar. 2016. arXiv: 1603.04924 [math-ph].

[35] Gökçe Başar and Gerald V Dunne. 'Resurgence and the Nekrasov-Shatashvili limit: connecting weak and strong coupling in the Mathieu and Lamé systems'. *JHEP* 02 (2015), p. 160. DOI: 10.1007/JHEP02(2015)160. arXiv: 1501.05671 [hep-th].

[36] Inês Aniceto, Ricardo Schiappa and Marcel Vonk. 'The Resurgence of Instantons in String Theory'. *Commun. Num. Theor. Phys.* 6 (2012), pp. 339–496. DOI: 10.4310/CNTP.2012.v6.n2.a3. arXiv: 1106.5922 [hep-th].

[37] Inês Aniceto and Michał Spaliński. 'Resurgence in extended hydrodynamics'. *Phys. Rev. D* 93.8 (2016), p. 085008. DOI: 10.1103/PhysRevD.93.085008. arXiv: 1511.06358 [hep-th].

[38] Marcos Mariño, Ricardo Schiappa and Marlene Weiss. 'Nonperturbative Effects and the Large-Order Behavior of Matrix Models and Topological Strings'. *Commun. Num. Theor. Phys.* 2 (2008), pp. 349–419. DOI: 10.4310/CNTP.2008.v2.n2.a3. arXiv: 0711.1954 [hep-th].

[39] Marcos Mariño. 'Nonperturbative effects and nonperturbative definitions in matrix models and topological strings'. *JHEP* 12 (2008), p. 114. DOI: 10.1088/1126-6708/2008/12/114. arXiv: 0805.3033 [hep-th].

[40] Daniele Dorigoni and Philip Glass. 'The grin of Cheshire cat resurgence from supersymmetric localization'. *SciPost Physics* 4.2 (2018), p. 012.

[41] Gökçe Başar, Gerald V Dunne and Mithat Ünsal. 'Resurgence theory, ghost-instantons, and analytic continuation of path integrals'. *JHEP* 10 (2013), p. 041. DOI: 10.1007/JHEP10(2013)041. arXiv: 1308.1108 [hep-th].

[42] Daniele Dorigoni. 'An Introduction to Resurgence, Trans-Series and Alien Calculus'. *Annals Phys.* 409 (2019), p. 167914. DOI: 10.1016/j.aop.2019.167914. arXiv: 1411.3585 [hep-th].

[43] Inês Aniceto, Gokçe Başar and Ricardo Schiappa. 'A Primer on Resurgent Transseries and Their Asymptotics'. *Phys. Rept.* 809 (2019), pp. 1–135. DOI: 10.1016/j.physrep.2019.02.003. arXiv: 1802.10441 [hep-th].

[44] Inês Aniceto. 'Asymptotics, ambiguities and resurgence'. *Resurgence, Physics and Numbers*. Springer, 2017, pp. 1–66.

[45] David Sauzin. 'Introduction to 1-summability and resurgence'. *arXiv preprint arXiv:1405.0356* (2014).

[46] Aleksey Cherman, Daniele Dorigoni and Mithat Ünsal. 'Decoding perturbation theory using resurgence: Stokes phenomena, new saddle points and Lefschetz thimbles'. *JHEP* 10 (2015), p. 056. DOI: 10.1007/JHEP10(2015)056. arXiv: 1403.1277 [hep-th].

[47] Saskia Demulder, Daniele Dorigoni and Daniel C. Thompson. 'Resurgence in η-deformed Principal Chiral Models'. *JHEP* 07 (2016), p. 088. DOI: 10.1007/JHEP07(2016)088. arXiv: 1604.07851 [hep-th].

[48] Dmytro Volin. 'Quantum integrability and functional equations: Applications to the spectral problem of AdS/CFT and two-dimensional sigma models'. *Journal of Physics A: Mathematical and Theoretical* 44.12 (2011), p. 124003. arXiv: 1003.4725 [hep-th].

[49] Marcos Mariño, Ramon Miravitllas and Tomas Reis. 'New renormalons from analytic trans-series' (Nov. 2021). arXiv: 2111.11951 [hep-th].

[50] Marcos Mariño and Tomás Reis. 'A new renormalon in two dimensions'. *JHEP* 07 (2020), p. 216. DOI: 10.1007/JHEP07(2020)216. arXiv: 1912.06228 [hep-th].

[51] Zoltan Bajnok, Janos Balog and Istvan Vona. 'The full analytic trans-series in integrable field theories' (Dec. 2022). arXiv: 2212.09416 [hep-th].

[52] Marcos Mariño and Tomás Reis. 'Resurgence for superconductors' (May 2019). DOI: 10.1088/1742-5468/ab4802. arXiv: 1905.09569 [hep-th].

[53] Marcos Mariño, Ramon Miravitllas and Tomas Reis. 'Testing the Bethe ansatz with large N renormalons'. *Eur. Phys. J. ST* 230.12-13 (2021), pp. 2641–2666. DOI: 10.1140/epjs/s11734-021-00252-4. arXiv: 2102.03078 [hep-th].

[54] Zoltan Bajnok, Janos Balog, Arpad Hegedus and Istvan Vona. 'Instanton effects vs resurgence in the O(3) sigma model'. *Phys. Lett. B* 829 (2022), p. 137073. DOI: 10.1016/j.physletb.2022.137073. arXiv: 2112.11741 [hep-th].

[55] Zoltan Bajnok and Romuald A. Janik. 'OPE coefficients and the mass-gap from the integrable scattering description of 2D CFT's'. *JHEP* 11 (2022), p. 128. DOI: 10.1007/JHEP11(2022)128. arXiv: 2209.10393 [hep-th].

[56] Zoltan Bajnok, Janos Balog, Arpad Hegedus and Istvan Vona. 'Running coupling and non-perturbative corrections for O(N) free energy and for disk capacitor'. *JHEP* 09 (2022), p. 001. DOI: 10.1007/JHEP09(2022)001. arXiv: 2204.13365 [hep-th].

[57] Zoltán Bajnok, János Balog and István Vona. 'Analytic resurgence in the O(4) model'. *JHEP* 04 (2022), p. 043. DOI: 10.1007/JHEP04(2022)043. arXiv: 2111.15390 [hep-th].

[58] Michael C. Abbott, Zoltán Bajnok, János Balog, Árpád Hegedús and Saeedeh Sadeghian. 'Resurgence in the O(4) sigma model'. *JHEP* 05 (2021), p. 253. DOI: 10.1007/JHEP05(2021)253. arXiv: 2011.12254 [hep-th].

[59] Michael C. Abbott, Zoltán Bajnok, János Balog and Árpád Hegedús. 'From perturbative to non-perturbative in the O (4) sigma model'. *Phys. Lett. B* 818 (2021), p. 136369. DOI: 10.1016/j.physletb.2021.136369. arXiv: 2011.09897 [hep-th].

[60] Lucas Schepers and Daniel C. Thompson. 'Resurgence in the bi-Yang-Baxter model'. *Nucl. Phys. B* 964 (2021), p. 115308. DOI: 10.1016/j.nuclphysb.2021.115308. arXiv: 2007.03683 [hep-th].

[61] Lucas Schepers and Daniel C. Thompson. 'Asymptotics in an Asymptotic CFT' (Jan. 2023). arXiv: 2301.11803 [hep-th].

[62] Émile Borel. 'Mémoire sur les séries divergentes'. *Annales scientifiques de l'École Normale Supérieure*. Vol. 16. 1899, pp. 9–131.

[63] David Sauzin. 'Resurgent functions and splitting problems'. *arXiv:0706.0137* (2007).

[64] E. Cavalcanti. 'Renormalons beyond the Borel Plane'. *arXiv:2011.11175* (2020).

[65] Syo Kamata, Tatsuhiro Misumi, Naohisa Sueishi and Mithat Ünsal. 'Exact-WKB analysis for SUSY and quantum deformed potentials: Quantum mechanics with Grassmann fields and Wess-Zumino terms' (Nov. 2021). arXiv: 2111.05922 [hep-th].

[66] MV Berry and CJ Howls. 'Hyperasymptotics'. *Proceedings of the Royal Society of London. Series A: Mathematical and Physical Sciences* 430.1880 (1990), pp. 653–668.

[67] TM Cherry. 'Expansions in terms of parabolic cylinder functions'. *Proceedings of the Edinburgh Mathematical Society* 8.2 (1948), pp. 50–65.

[68] AB Olde Daalhuis and FWJ Olver. 'Hyperasymptotic solutions of second-order linear differential equations I'. *Methods and Applications of Analysis* 2.2 (1995), pp. 173–197.

[69] Rudolph E Langer. 'The asymptotic solutions of certain linear ordinary differential equations of the second order'. *Transactions of the American Mathematical Society* 36.1 (1934), pp. 90–106.

[70] Stanley C Miller Jr and RH Good Jr. 'A WKB-type approximation to the Schrödinger equation'. *Physical Review* 91.1 (1953), p. 174.

[71] Ta-Sheng Tai. 'Uniformization, Calogero-Moser/Heun duality and Sutherland/-bubbling pants'. *JHEP* 10 (2010), p. 107. DOI: 10.1007/JHEP10(2010)107. arXiv: 1008.4332 [hep-th].

[72] J. Zinn-Justin and U.D. Jentschura. 'Multi-instantons and exact results I: Conjectures, WKB expansions, and instanton interactions'. *Annals Phys.* 313 (2004), pp. 197–267. DOI: 10.1016/j.aop.2004.04.004. arXiv: quant-ph/0501136.

[73] J. Zinn-Justin and U.D. Jentschura. 'Multi-instantons and exact results II: Specific cases, higher-order effects, and numerical calculations'. *Annals Phys.* 313 (2004), pp. 269–325. DOI: 10.1016/j.aop.2004.04.003. arXiv: quant-ph/0501137.

[74] Jose Luis Alvarez-Perez. 'A convergent expansion of the Airy's integral with incomplete Gamma functions'. *arXiv preprint arXiv:1909.13394* (2019).

[75] N. S. Manton. *ASYMPTOTIC METHODS*. http://www.damtp.cam.ac.uk/user/gold/pdfs/teaching/AsymptoticMethods.pdf. Last visited on 27 September 2022. 2012.

[76] Edward Witten. 'A New Look At The Path Integral Of Quantum Mechanics' (Sept. 2010). arXiv: 1009.6032 [hep-th].

[77] George Biddell Airy et al. 'On the intensity of light in the neighbourhood of a caustic'. *Transactions of the Cambridge Philosophical Society* 6 (1838), p. 379.

[78] Maxim Kontsevich. 'Intersection theory on the moduli space of curves and the matrix Airy function'. *Communications in Mathematical Physics* 147.1 (1992), pp. 1–23.

[79] Edward Witten. 'Two-dimensional gravity and intersection theory on moduli space'. *Surveys in differential geometry* 1.1 (1990), pp. 243–310.

[80] Edward Witten. 'Algebraic geometry associated with matrix models of two-dimensional gravity'. *Topological methods in modern mathematics (Stony Brook, NY, 1991)* 235 (1993).

[81] Tin Sulejmanpasic and Mithat Ünsal. 'Aspects of Perturbation theory in Quantum Mechanics: The BenderWu Mathematica® package'. *Comput. Phys. Commun.* 228 (2018), pp. 273–289. DOI: 10.1016/j.cpc.2017.11.018. arXiv: 1608.08256 [hep-th].

[82] J. Écalle. 'Les Fonctions Resurgentes, Vols I-III'. *Publ. Math. Orsay* 15 (1981).

[83] Inês Aniceto and Ricardo Schiappa. 'Nonperturbative ambiguities and the reality of resurgent transseries'. *Communications in Mathematical Physics* 335.1 (2015), pp. 183–245.

[84] N Beisert. 'Introduction to Integrability'. *Lecture notes, ETH Zürich, HS16* (2016).

[85] Alessandro Torrielli. 'Lectures on Classical Integrability'. *J. Phys. A* 49.32 (2016), p. 323001. DOI: 10.1088/1751-8113/49/32/323001. arXiv: 1606.02946 [hep-th].

[86] Ana L Retore. 'Introduction to classical and quantum integrability'. *Journal of Physics A: Mathematical and Theoretical* 55.17 (2022), p. 173001.

[87] Ben Hoare. 'Integrable deformations of sigma models'. *J. Phys. A* 55.9 (2022), p. 093001. DOI: 10.1088/1751-8121/ac4a1e. arXiv: 2109.14284 [hep-th].

[88] Daniel C. Thompson. 'An Introduction to Generalised Dualities and their Applications to Holography and Integrability'. *PoS* CORFU2018 (2019). Ed. by Konstantinos Anagnostopoulos et al., p. 099. DOI: 10.22323/1.347.0099. arXiv: 1904.11561 [hep-th].

[89] Abhishek Agarwal. 'Aspects of Integrability in N =4 SYM'. *Mod. Phys. Lett. A* 22 (2007), pp. 2549–2563. DOI: 10.1142/S021773230702542X. arXiv: 0708.2747 [hep-th].

[90] Gregory P Korchemsky. 'Review of AdS/CFT Integrability, Chapter IV. 4: Integrability in QCD and $\mathcal{N} = 4$ SYM'. *Letters in Mathematical Physics* 99.1 (2012), pp. 425–453. arXiv: 1012.4000 [hep-th].

[91] Aleksandr Abramovich Belavin and Vladimir Gershonovich Drinfeld. 'Solutions of the classical Yang–Baxter equation for simple Lie algebras'. *Funktsional'nyi Analiz i ego Prilozheniya* 16.3 (1982), pp. 1–29.

[92] Vyjayanthi Chari, Andrew Pressley et al. *A guide to quantum groups*. Cambridge university press, 1995.

[93] V. G. Drinfeld. 'Hopf algebras and the quantum Yang-Baxter equation'. *Sov. Math. Dokl.* 32 (1985), pp. 254–258.

[94] Michio Jimbo. 'A q difference analog of U(g) and the Yang-Baxter equation'. *Lett. Math. Phys.* 10 (1985), pp. 63–69. DOI: 10.1007/BF00704588.

[95] Ctirad Klimčík. 'Integrability of the bi-Yang-Baxter sigma-model'. *Lett. Math. Phys.* 104 (2014), pp. 1095–1106. DOI: 10.1007/s11005-014-0709-y. arXiv: 1402.2105 [math-ph].

[96] Ctirad Klimčík. 'On integrability of the Yang-Baxter sigma-model'. *J. Math. Phys.* 50 (2009), p. 043508. DOI: 10.1063/1.3116242. arXiv: 0802.3518 [hep-th].

[97] Ben Hoare. 'Towards a two-parameter q-deformation of $AdS_3 \times S^3 \times M^4$ superstrings'. *Nucl. Phys. B* 891 (2015), pp. 259–295. DOI: 10.1016/j.nuclphysb.2014.12.012. arXiv: 1411.1266 [hep-th].

[98] Francois Delduc, Marc Magro and Benoit Vicedo. 'An integrable deformation of the $AdS_5 \times S^5$ superstring action'. *Phys. Rev. Lett.* 112.5 (2014), p. 051601. DOI: 10.1103/PhysRevLett.112.051601. arXiv: 1309.5850 [hep-th].

[99] Io Kawaguchi and Kentaroh Yoshida. 'Hybrid classical integrability in squashed sigma models'. *Phys. Lett. B* 705 (2011), pp. 251–254. DOI: 10.1016/j.physletb.2011.09.117. arXiv: 1107.3662 [hep-th].

[100] Francois Delduc, Marc Magro and Benoit Vicedo. 'On classical q-deformations of integrable sigma-models'. *JHEP* 11 (2013), p. 192. DOI: 10.1007/JHEP11(2013)192. arXiv: 1308.3581 [hep-th].

[101] Timothy J. Hollowood, J.Luis Miramontes and David M. Schmidtt. 'An Integrable Deformation of the $AdS_5 \times S^5$ Superstring'. *J. Phys. A* 47.49 (2014), p. 495402. DOI: 10.1088/1751-8113/47/49/495402. arXiv: 1409.1538 [hep-th].

[102] Konstadinos Sfetsos. 'Integrable interpolations: From exact CFTs to non-Abelian T-duals'. *Nucl. Phys. B* 880 (2014), pp. 225–246. DOI: 10.1016/j.nuclphysb.2014.01.004. arXiv: 1312.4560 [hep-th].

[103] Konstantinos Sfetsos, Konstantinos Siampos and Daniel C. Thompson. 'Generalised integrable λ - and η-deformations and their relation'. *Nucl. Phys. B* 899 (2015), pp. 489–512. DOI: 10.1016/j.nuclphysb.2015.08.015. arXiv: 1506.05784 [hep-th].

[104] B. Hoare, R. Roiban and A.A. Tseytlin. 'On deformations of $AdS_n \times S^n$ supercosets'. *JHEP* 06 (2014), p. 002. DOI: 10.1007/JHEP06(2014)002. arXiv: 1403.5517 [hep-th].

[105] Thiago Araujo, Eoin Ó Colgáin and Hossein Yavartanoo. 'Embedding the modified CYBE in Supergravity'. *Eur. Phys. J.* C78.10 (2018), p. 854. DOI: 10.1140/epjc/s10052-018-6335-6. arXiv: 1806.02602 [hep-th].

[106] Jonathan M. Evans and Timothy J. Hollowood. 'Integrable theories that are asymptotically CFT'. *Nucl. Phys. B* 438 (1995), pp. 469–490. DOI: 10.1016/0550-3213(94)00473-R. arXiv: hep-th/9407113.

[107] J. Balog, P. Forgacs, Z. Horvath and L. Palla. 'A New family of SU(2) symmetric integrable sigma models'. *Phys. Lett. B* 324 (1994). Ed. by D. Lust and G. Weigt, pp. 403–408. DOI: 10.1016/0370-2693(94)90213-5. arXiv: hep-th/9307030.

[108] Konstadinos Sfetsos. 'Gauged WZW models and nonAbelian duality'. *Phys. Rev. D* 50 (1994), pp. 2784–2798. DOI: 10.1103/PhysRevD.50.2784. arXiv: hep-th/9402031.

[109] Timothy J. Hollowood, J. Luis Miramontes and David M. Schmidtt. 'Integrable Deformations of Strings on Symmetric Spaces'. *JHEP* 11 (2014), p. 009. DOI: 10.1007/JHEP11(2014)009. arXiv: 1407.2840 [hep-th].

[110] Timothy J. Hollowood, J. Luis Miramontes and David M. Schmidtt. 'S-Matrices and Quantum Group Symmetry of k-Deformed Sigma Models'. *J. Phys. A* 49.46 (2016), p. 465201. DOI: 10.1088/1751-8113/49/46/465201. arXiv: 1506.06601 [hep-th].

[111] Arkady A. Tseytlin. 'On A 'Universal' class of WZW type conformal models'. *Nucl. Phys. B* 418 (1994), pp. 173–194. DOI: 10.1016/0550-3213(94)90243-7. arXiv: hep-th/9311062.

[112] Calan Appadu and Timothy J. Hollowood. 'Beta function of k deformed $AdS_5 \times S^5$ string theory'. *JHEP* 11 (2015), p. 095. DOI: 10.1007/JHEP11(2015)095. arXiv: 1507.05420 [hep-th].

[113] Konstadinos Sfetsos and Konstadinos Siampos. 'Gauged WZW-type theories and the all-loop anisotropic non-Abelian Thirring model'. *Nucl. Phys. B* 885 (2014), pp. 583–599. DOI: 10.1016/j.nuclphysb.2014.06.012. arXiv: 1405.7803 [hep-th].

[114] Edward Witten. 'Non-abelian bosonization in two dimensions'. *Bosonization*. World Scientific, 1994, pp. 201–218.

[115] Xenia C. de la Ossa and Fernando Quevedo. 'Duality symmetries from nonAbelian isometries in string theory'. *Nucl. Phys. B* 403 (1993), pp. 377–394. DOI: 10.1016/0550-3213(93)90041-M. arXiv: hep-th/9210021.

[116] Yolanda Lozano and Carlos Núñez. 'Field theory aspects of non-Abelian T-duality and $\mathcal{N} = 2$ linear quivers'. *JHEP* 05 (2016), p. 107. DOI: 10.1007/JHEP05(2016)107. arXiv: 1603.04440 [hep-th].

[117] Konstadinos Sfetsos and Daniel C. Thompson. 'On non-abelian T-dual geometries with Ramond fluxes'. *Nucl. Phys. B* 846 (2011), pp. 21–42. DOI: 10.1016/j.nuclphysb.2010.12.013. arXiv: 1012.1320 [hep-th].

[118] Konstantinos Sfetsos and Daniel C. Thompson. 'Spacetimes for λ-deformations'. *JHEP* 12 (2014), p. 164. DOI: 10.1007/JHEP12(2014)164. arXiv: 1410.1886 [hep-th].

[119] Ctirad Klimčík. 'Poisson–Lie T-duals of the bi-Yang–Baxter models'. *Phys. Lett. B* 760 (2016), pp. 345–349. DOI: 10.1016/j.physletb.2016.06.077. arXiv: 1606.03016 [hep-th].

[120] B. Hoare and A. A. Tseytlin. 'On integrable deformations of superstring sigma models related to $AdS_n \times S^n$ supercosets'. *Nucl. Phys. B* 897 (2015), pp. 448–478. DOI: 10.1016/j.nuclphysb.2015.06.001. arXiv: 1504.07213 [hep-th].

[121] Benoit Vicedo. 'Deformed integrable σ-models, classical R-matrices and classical exchange algebra on Drinfel'd doubles'. *J. Phys. A* 48.35 (2015), p. 355203. DOI: 10.1088/1751-8113/48/35/355203. arXiv: 1504.06303 [hep-th].

[122] Ctirad Klimčík. 'η and λ deformations as E -models'. *Nucl. Phys. B* 900 (2015), pp. 259–272. DOI: 10.1016/j.nuclphysb.2015.09.011. arXiv: 1508.05832 [hep-th].

[123] T. H. Buscher. 'Path Integral Derivation of Quantum Duality in Nonlinear Sigma Models'. *Phys. Lett. B* 201 (1988), pp. 466–472. DOI: 10.1016/0370-2693(88)90602-8.

[124] K. Gawedzki and A. Kupiainen. 'G/h Conformal Field Theory from Gauged WZW Model'. *Phys. Lett. B* 215 (1988), pp. 119–123. DOI: 10.1016/0370-2693(88)91081-7.

[125] Edward Witten. 'On Holomorphic factorization of WZW and coset models'. *Commun. Math. Phys.* 144 (1992), pp. 189–212. DOI: 10.1007/BF02099196.

[126] S. F. Hassan and Ashoke Sen. 'Marginal deformations of WZNW and coset models from O(d,d) transformation'. *Nucl. Phys. B* 405 (1993), pp. 143–165. DOI: 10.1016/0550-3213(93)90429-S. arXiv: hep-th/9210121.

[127] Alexander B Zamolodchikov and Alexey B Zamolodchikov. 'Factorized S-matrices in two dimensions as the exact solutions of certain relativistic quantum field theory models'. *Yang-Baxter Equation In Integrable Systems*. World Scientific, 1990, pp. 82–120.

[128] Patrick Dorey. 'Exact S-matrices'. *Conformal field theories and integrable models*. Springer, 1997, pp. 85–125.

[129] Diego Bombardelli. 'S-matrices and integrability'. *J. Phys. A* 49.32 (2016), p. 323003. DOI: 10.1088/1751-8113/49/32/323003. arXiv: 1606.02949 [hep-th].

[130] VA Fateev. 'The sigma model (dual) representation for a two-parameter family of integrable quantum field theories'. *Nuclear Physics B* 473.3 (1996), pp. 509–538.

[131] Sidney R. Coleman. 'The Quantum Sine-Gordon Equation as the Massive Thirring Model'. *Phys. Rev. D* 11 (1975). Ed. by M. Stone, p. 2088. DOI: 10.1103/PhysRevD.11.2088.

[132] S. Mandelstam. 'Soliton Operators for the Quantized Sine-Gordon Equation'. *Phys. Rev. D* 11 (1975). Ed. by M. Stone, p. 3026. DOI: 10.1103/PhysRevD.11.3026.

[133] Denis Bernard and Andre Leclair. 'Quantum group symmetries and nonlocal currents in 2-D QFT'. *Commun. Math. Phys.* 142 (1991), pp. 99–138. DOI: 10.1007/BF02099173.

[134] B. Berg, M. Karowski, P. Weisz and V. Kurak. 'Factorized U(n) Symmetric s Matrices in Two-Dimensions'. *Nucl. Phys. B* 134 (1978), pp. 125–132. DOI: 10.1016/0550-3213(78)90489-3.

[135] B. Berg and P. Weisz. 'Exact S Matrix of the Chiral Invariant SU(N) Thirring Model'. *Nucl. Phys. B* 146 (1978), pp. 205–214. DOI: 10.1016/0550-3213(78)90438-8.

[136] E. Abdalla, B. Berg and P. Weisz. 'More About the S Matrix of the Chiral SU(N) Thirring Model'. *Nucl. Phys. B* 157 (1979), pp. 387–391. DOI: 10.1016/0550-3213(79)90110-X.

[137] PB Wiegmann. 'Exact factorized S-matrix of the chiral field in two dimensions'. *Physics Letters B* 142.3 (1984), pp. 173–176.

[138] Timothy J. Hollowood. 'Quantizing SL(N) solitons and the Hecke algebra'. *Int. J. Mod. Phys. A* 8 (1993), pp. 947–982. DOI: 10.1142/S0217751X93000370. arXiv: hep-th/9203076.

[139] C Ahn, D Bernard and A LeClair. 'Fractional supersymmetries in perturbed coset CFTs and integrable soliton theory'. *Nuclear Physics B* 346.2-3 (1990), pp. 409–439.

[140] Henrik Johannesson. 'The structure of low-lying excitations in a new integrable quantum chain model'. *Nuclear Physics B* 270 (1986), pp. 235–272.

[141] George E Andrews, Rodney J Baxter and Peter J Forrester. 'Eight-vertex SOS model and generalized Rogers-Ramanujan-type identities'. *Journal of Statistical Physics* 35.3 (1984), pp. 193–266.

[142] RJ Baxter. 'The inversion relation method for some two-dimensional exactly solved models in lattice statistics'. *Journal of Statistical Physics* 28.1 (1982), pp. 1–41.

[143] Peter J Forrester and Rodney J Baxter. 'Further exact solutions of the eight-vertex SOS model and generalizations of the Rogers-Ramanujan identities'. *Journal of statistical physics* 38.3 (1985), pp. 435–472.

[144] Andre LeClair. 'Restricted Sine-Gordon Theory and the Minimal Conformal Series'. *Phys. Lett. B* 230 (1989), pp. 103–107. DOI: 10.1016/0370-2693(89)91661-4.

[145] Calan Appadu, Timothy J. Hollowood, Dafydd Price and Daniel C. Thompson. 'Quantum Anisotropic Sigma and Lambda Models as Spin Chains'. *J. Phys. A* 51.40 (2018), p. 405401. DOI: 10.1088/1751-8121/aadc6d. arXiv: 1802.06016 [hep-th].

[146] L. D. Faddeev. 'How algebraic Bethe ansatz works for integrable model'. *Les Houches School of Physics: Astrophysical Sources of Gravitational Radiation*. May 1996, pp. 149–219. arXiv: hep-th/9605187.

[147] Marcos Mariño and Tomás Reis. 'Renormalons in integrable field theories'. *JHEP* 04 (2020), p. 160. DOI: 10.1007/JHEP04(2020)160. arXiv: 1909.12134 [hep-th].

[148] Marcos Mariño and Tomás Reis. 'Resurgence for superconductors' (May 2019). DOI: 10.1088/1742-5468/ab4802. arXiv: 1905.09569 [hep-th].

[149] Karen Uhlenbeck. 'Harmonic maps into Lie groups: classical solutions of the chiral model'. *Journal of Differential Geometry* 30.1 (1989), pp. 1–50.

[150] Thomas W. Grimm and Jeroen Monnee. 'Bi-Yang-Baxter Models and Sl(2)-orbits' (Dec. 2022). arXiv: 2212.03893 [hep-th].

[151] Thomas W. Grimm and Jeroen Monnee. 'Deformed WZW models and Hodge theory. Part I'. *JHEP* 05 (2022), p. 103. DOI: 10.1007/JHEP05(2022)103. arXiv: 2112.00031 [hep-th].

[152] Nicholas Manton and Paul Sutcliffe. *Topological solitons*. Cambridge University Press, 2004.

[153] Can Kozçaz, Tin Sulejmanpasic, Yuya Tanizaki and Mithat Ünsal. 'Cheshire Cat resurgence, Self-resurgence and Quasi-Exact Solvable Systems'. *Commun. Math. Phys.* 364.3 (2018), pp. 835–878. DOI: 10.1007/s00220-018-3281-y. arXiv: 1609.06198 [hep-th].

[154] Ovidiu Costin and Gerald V. Dunne. 'Resurgent extrapolation: rebuilding a function from asymptotic data. Painlevé I'. *J. Phys. A* 52.44 (2019), p. 445205. DOI: 10.1088/1751-8121/ab477b. arXiv: 1904.11593 [hep-th].

[155] Ovidiu Costin and Gerald V. Dunne. 'Physical Resurgent Extrapolation' (Mar. 2020). arXiv: 2003.07451 [hep-th].

[156] Davide Gaiotto. 'Asymptotically free $\mathcal{N} = 2$ theories and irregular conformal blocks'. *J. Phys. Conf. Ser.* 462.1 (2013). Ed. by Sumit R. Das and Alfred D. Shapere, p. 012014. DOI: 10.1088/1742-6596/462/1/012014. arXiv: 0908.0307 [hep-th].

[157] T. Koike and R. Schäfke. 'On the Borel summability of WKB solutions of the Schrödinger equations with polynomial potentials and its application. (In preparation)' ().

[158] Albrecht Klemm, Wolfgang Lerche, Peter Mayr, Cumrun Vafa and Nicholas P. Warner. 'Selfdual strings and N=2 supersymmetric field theory'. *Nucl. Phys. B* 477 (1996), pp. 746–766. DOI: 10.1016/0550-3213(96)00353-7. arXiv: hep-th/9604034.

[159] Alba Grassi, Jie Gu and Marcos Mariño. 'Non-perturbative approaches to the quantum Seiberg–Witten curve' (Aug. 2019). arXiv: 1908.07065 [hep-th].

[160] Nick Dorey, Timothy J Hollowood and S Prem Kumar. 'An exact elliptic superpotential for $\mathcal{N} = 1^*$ deformations of finite $\mathcal{N} = 2$ gauge theories'. *Nucl. Phys. B* 624 (2002), pp. 95–145. DOI: 10.1016/S0550-3213(01)00647-2. arXiv: hep-th/0108221.

[161] N. Seiberg and Edward Witten. 'Electric - magnetic duality, monopole condensation, and confinement in N=2 supersymmetric Yang-Mills theory'. *Nucl. Phys. B* 426 (1994). [Erratum: Nucl.Phys.B 430, 485–486 (1994)], pp. 19–52. DOI: 10.1016/0550-3213(94)90124-4. arXiv: hep-th/9407087.

[162] Edward Witten. 'Solutions of four-dimensional field theories via M theory'. *Nucl. Phys. B* 500 (1997), pp. 3–42. DOI: 10.1016/S0550-3213(97)00416-1. arXiv: hep-th/9703166.

[163] Ta-Sheng Tai. 'Triality in SU(2) Seiberg-Witten theory and Gauss hypergeometric function'. *Phys. Rev. D* 82 (2010), p. 105007. DOI: 10.1103/PhysRevD.82.105007. arXiv: 1006.0471 [hep-th].

[164] Marco Matone. 'Instantons and recursion relations in N=2 SUSY gauge theory'. *Phys. Lett. B* 357 (1995), pp. 342–348. DOI: 10.1016/0370-2693(95)00920-G. arXiv: hep-th/9506102.

[165] Clay Mathematics Institute. *Millennium Problems*. https://www.claymath.org/millennium-problems. [Online; accessed 113-September-2020].

[166] Arthur Jaffe and Edward Witten. 'Quantum yang-mills theory'. *The millennium prize problems* 1 (2006), p. 129.

[167] Peter Hasenfratz, Michele Maggiore and Ferenc Niedermayer. 'The exact mass gap of the $O(3)$ and $O(4)$ non-linear σ-models in $d = 2$'. *Physics Letters B* 245.3-4 (1990), pp. 522–528.

[168] Peter Hasenfratz and Ferenc Niedermayer. 'The exact mass gap of the $O(N)$ σ-model for arbitrary $N \geq 3$ in $d = 2$'. *Physics Letters B* 245.3-4 (1990), pp. 529–532.

[169] P. Forgacs, F. Niedermayer and P. Weisz. 'The Exact mass gap of the Gross-Neveu model. 1. The Thermodynamic Bethe ansatz'. *Nucl. Phys. B* 367 (1991), pp. 123–143. DOI: 10.1016/0550-3213(91)90044-X.

[170] P. Forgacs, F. Niedermayer and P. Weisz. 'The Exact mass gap of the Gross-Neveu model. 2. The 1/N expansion'. *Nucl. Phys. B* 367 (1991), pp. 144–157. DOI: 10.1016/0550-3213(91)90045-Y.

[171] J. Balog, S. Naik, F. Niedermayer and P. Weisz. 'Exact mass gap of the chiral SU(n) x SU(n) model'. *Phys. Rev. Lett.* 69 (1992), pp. 873–876. DOI: 10.1103/PhysRevLett.69.873.

[172] Timothy J. Hollowood. 'The Exact mass gaps of the principal chiral models'. *Phys. Lett. B* 329 (1994), pp. 450–456. DOI: 10.1016/0370-2693(94)91089-8. arXiv: hep-th/9402084.

[173] Jonathan M. Evans and Timothy J. Hollowood. 'Exact results for integrable asymptotically - free field theories'. *Nucl. Phys. B Proc. Suppl.* 45.1 (1996). Ed. by G. Mussardo, S. Randjbar-Daemi and H. Saleur, pp. 130–139. DOI: 10.1016/0920-5632(95)00622-2. arXiv: hep-th/9508141.

[174] Jonathan M. Evans and Timothy J. Hollowood. 'Exact scattering in the SU(n) supersymmetric principal chiral model'. *Nucl. Phys. B* 493 (1997), pp. 517–540. DOI: 10.1016/S0550-3213(97)00077-1. arXiv: hep-th/9603190.

[175] G. Parisi. 'On Infrared Divergences'. *Nucl. Phys. B* 150 (1979), pp. 163–172. DOI: 10.1016/0550-3213(79)90298-0.

[176] G. Parisi. 'Singularities of the Borel Transform in Renormalizable Theories'. *Phys. Lett. B* 76 (1978), pp. 65–66. DOI: 10.1016/0370-2693(78)90101-6.

[177] Gerard 't Hooft. 'Can We Make Sense Out of Quantum Chromodynamics?' *Subnucl. Ser.* 15 (1979). Ed. by Antonino Zichichi, p. 943.

[178] A Polyakov and Paul B Wiegmann. 'Theory of nonabelian Goldstone bosons in two dimensions'. *Physics Letters B* 131.1-3 (1983), pp. 121–126.

[179] Alexander M Polyakov and PB Wiegmann. 'Goldstone fields in two dimensions with multivalued actions'. *Physics Letters B* 141.3-4 (1984), pp. 223–228.

[180] PB Wiegmann. 'Exact solution of the $O(3)$ nonlinear two-dimensional sigma-model'. *JETP Letters* 41.2 (1985), pp. 95–100.

[181] VA Fateev, VA Kazakov and PB Wiegmann. 'Principal chiral field at large N'. *Nuclear Physics B* 424.3 (1994), pp. 505–520.

[182] Fedor Levkovich-Maslyuk. 'The Bethe ansatz'. *J. Phys. A* 49.32 (2016), p. 323004. DOI: 10.1088/1751-8113/49/32/323004. arXiv: 1606.02950 [hep-th].

[183] Stijn J. van Tongeren. 'Introduction to the thermodynamic Bethe ansatz'. *J. Phys. A* 49.32 (2016), p. 323005. DOI: 10.1088/1751-8113/49/32/323005. arXiv: 1606.02951 [hep-th].

[184] V Hutson. 'The circular plate condenser at small separations'. *Mathematical Proceedings of the Cambridge Philosophical Society*. Vol. 59. 1. Cambridge University Press. 1963, pp. 211–224.

[185] Viktor Nikolaevich Popov. 'Theory of one-dimensional Bose gas with point interaction'. *Teoreticheskaya i Matematicheskaya Fizika* 30.3 (1977), pp. 346–352.

[186] Sinya Aoki, Janos Balog, Tetsuya Onogi and Shuichi Yokoyama. 'Bulk reconstruction from a scalar CFT at the boundary by the smearing with the flow equation'. *14th International Workshop on Lie Theory and Its Applications in Physics*. Apr. 2022. arXiv: 2204.01989 [hep-th].

[187] Ines Aniceto, Zoltan Bajnok, Tamas Gombor, Minkyoo Kim and Laszlo Palla. 'On integrable boundaries in the 2 dimensional $O(N)$ σ-models'. *J. Phys. A* 50.36 (2017), p. 364002. DOI: 10.1088/1751-8121/aa8205. arXiv: 1706.05221 [hep-th].

[188] Tomas Reis. 'On the resurgence of renormalons in integrable theories'. PhD thesis. U. Geneva (main), 2022. arXiv: 2209.15386 [hep-th].

[189] Z Bajnok, J Balog, B Basso, GP Korchemsky and L Palla. 'Scaling function in AdS/CFT from the $O(6)$ sigma model'. *Nuclear Physics B* 811.3 (2009), pp. 438–462.

[190] F. David. 'Nonperturbative Effects and Infrared Renormalons Within the $1/N$ Expansion of the O(N) Nonlinear σ Model'. *Nucl. Phys. B* 209 (1982), pp. 433–460. DOI: 10.1016/0550-3213(82)90266-8.

[191] F. David. 'On the Ambiguity of Composite Operators, IR Renormalons and the Status of the Operator Product Expansion'. *Nucl. Phys. B* 234 (1984), pp. 237–251. DOI: 10.1016/0550-3213(84)90235-9.

[192] F. David. 'The Operator Product Expansion and Renormalons: A Comment'. *Nucl. Phys. B* 263 (1986), pp. 637–648. DOI: 10.1016/0550-3213(86)90279-8.

[193] Calan Appadu, Timothy J Hollowood and Dafydd Price. 'Quantum inverse scattering and the lambda deformed principal chiral model'. *Journal of Physics A: Mathematical and Theoretical* 50.30 (2017), p. 305401.

[194] Alexei B. Zamolodchikov. 'Mass scale in the sine-Gordon model and its reductions'. *Int. J. Mod. Phys. A* 10 (1995), pp. 1125–1150. DOI: 10.1142/S0217751X9500053X.

[195] Lorenzo Di Pietro, Marcos Mariño, Giacomo Sberveglieri and Marco Serone. 'Resurgence and 1/N Expansion in Integrable Field Theories'. *JHEP* 10 (2021), p. 166. DOI: 10.1007/JHEP10(2021)166. arXiv: 2108.02647 [hep-th].

[196] Stephen G. Naculich and Howard J. Schnitzer. 'Duality Between $SU(N)_k$ and $SU(k)_N$ WZW Models'. *Nucl. Phys. B* 347 (1990), pp. 687–742. DOI: 10.1016/0550-3213(90)90380-V.

[197] Stephen G. Naculich and Howard J. Schnitzer. 'Level-rank duality of the U(N) WZW model, Chern-Simons theory, and 2-D qYM theory'. *JHEP* 06 (2007), p. 023. DOI: 10.1088/1126-6708/2007/06/023. arXiv: hep-th/0703089.

[198] Dimitrios Katsinis and Pantelis Panopoulos. 'Classical solutions of λ-deformed coset models'. *Eur. Phys. J. C* 82.6 (2022), p. 545. DOI: 10.1140/epjc/s10052-022-10493-9. arXiv: 2111.12446 [hep-th].

[199] Sibylle Driezen, Alexander Sevrin and Daniel C. Thompson. 'Integrable asymmetric λ-deformations'. *JHEP* 04 (2019), p. 094. DOI: 10.1007/JHEP04(2019)094. arXiv: 1902.04142 [hep-th].

[200] Saskia Demulder, Falk Hassler and Daniel C. Thompson. 'Doubled aspects of generalised dualities and integrable deformations'. *JHEP* 02 (2019), p. 189. DOI: 10.1007/JHEP02(2019)189. arXiv: 1810.11446 [hep-th].

[201] Benoit Vicedo. 'On integrable field theories as dihedral affine Gaudin models' (Jan. 2017). arXiv: 1701.04856 [hep-th].

[202] Andrei V. Zotov. '1+1 Gaudin Model'. *SIGMA* 7 (2011), p. 067. DOI: 10.3842/SIGMA.2011.067. arXiv: 1012.1072 [math-ph].

[203] Gleb Arutyunov, Riccardo Borsato and Sergey Frolov. 'S-matrix for strings on η-deformed AdS5 x S5'. *JHEP* 04 (2014), p. 002. DOI: 10.1007/JHEP04(2014)002. arXiv: 1312.3542 [hep-th].

[204] Kevin Costello, Edward Witten and Masahito Yamazaki. 'Gauge Theory and Integrability, I'. *ICCM Not.* 06.1 (2018), pp. 46–119. DOI: 10.4310/ICCM.2018.v6.n1.a6. arXiv: 1709.09993 [hep-th].

[205] Kevin Costello, Edward Witten and Masahito Yamazaki. 'Gauge Theory and Integrability, II'. *ICCM Not.* 06.1 (2018), pp. 120–146. DOI: 10.4310/ICCM.2018.v6.n1.a7. arXiv: 1802.01579 [hep-th].

[206] Kevin Costello and Masahito Yamazaki. 'Gauge Theory And Integrability, III' (Aug. 2019). arXiv: 1908.02289 [hep-th].

[207] Francois Delduc, Sylvain Lacroix, Marc Magro and Benoit Vicedo. 'A unifying 2d Action for integrable σ-models from 4d Chern-Simons Theory' (Sept. 2019). DOI: 10.1007/s11005-020-01268-y. arXiv: 1909.13824 [hep-th].

[208] Benoit Vicedo. 'Holomorphic Chern-Simons theory and affine Gaudin models' (Aug. 2019). arXiv: 1908.07511 [hep-th].

[209] A. Levin, M. Olshanetsky and A. Zotov. '2D Integrable systems, 4D Chern–Simons theory and affine Higgs bundles'. *Eur. Phys. J. C* 82.7 (2022), p. 635. DOI: 10.1140/epjc/s10052-022-10553-0. arXiv: 2202.10106 [hep-th].